

THE INTERACTION BETWEEN UNBURNT HYDROCARBONS AND  
SOOT IN DIESEL EXHAUSTS

BY

CHRISTOPHER RICHARD SEEBOLD B.Sc. (Hons.) G.R.S.C.

A thesis submitted to the Council for National Academic  
Awards in partial fulfilment of the requirement for  
admittance to the degree of:

DOCTOR OF PHILOSOPHY

UNDERTAKEN AT:

POLYTECHNIC SOUTH-WEST  
DEPARTMENT OF MECHANICAL ENGINEERING  
DRAKES CIRCUS  
PLYMOUTH  
DEVON  
U.K.

IN COLLABORATION WITH:

PERKINS TECHNOLOGY BUSINESS  
PETERBOROUGH  
CAMBRIDGESHIRE  
U.K.

SUBMITTED NOVEMBER 1989



COPYRIGHT

Attention is drawn to the fact that the copyright of this thesis rests with the author, and that no quotation from the thesis and information derived from it may be published without prior written consent of the author.

This thesis may be made available for consultation within the Polytechnic of South-West Library and may be photocopied or lent to other libraries for the purpose of consultation.

Signed: *CR Seebdd*.....

## DECLARATIONS

At no time during the registration for the degree of Doctor of Philosophy has the author been registered for any other C.N.A.A. or University award. This study was financed with the aid of a CASE studentship from the Science and Engineering Research Council. The study was undertaken in collaboration with Perkins Technology Business, Peterborough.

A programme of advanced study was undertaken within the Polytechnic which included lecture courses in Computing, courses of instruction on the use of the Scanning Electron Microscope, BET apparatus and Gas Chromatographs.

During the period of registration a number of relevant scientific meetings were attended. A number of conference papers were also presented and three papers were published as listed below:

GLASSON, D.R.; SEEBOLD, C.R.; HORN, N.J. & MILLWARD, G.E. 1988. The microstructures of carbon soots from diesel engine exhausts. In: McEnaney, B. & Mays, T.J. (Eds), Proc. Conf. (Int.) Carbon. Institute of Physics, 34-36. IOP Publishing Ltd.

SEEBOLD, C.R.; GLASSON, D.R.; MILLWARD, G.E. & GRAHAM, M.A. 1989. Diesel particulate characterisation by vacuum microbalance techniques. In: Jayawerra, S.A.A. (Ed), 23rd International Vacuum Microbalance Techniques Conference, Thermochim. Acta., (In Press).

SEEBOLD, C.R.; GLASSON, D.R.; MILLWARD, G.E. & GRAHAM, M.A. 1989. E.G.A. of diesel engine exhaust particles. In: Applications of Evolved Gas Analysis. Thermal Methods Group of the Royal Society of Chemistry, (In Press).

#### CONFERENCES ATTENDED:

- 1) Seminar on Combustion. Plymouth Polytechnic. 11th February 1987.
- 2) Short Course on Diesel Particulates. Leeds University. April 1987.
- 3) Chromatography Seminar. London University. September 1987.
- 4) CRAC/SERC Graduate School. York University. 14-19 July 1988.
- 5) Carbon '88. Newcastle University. 18-23 September 1988.
- 6) 23rd Vacuum Microbalance Techniques Conference, Middlesborough Polytechnic. 31st August - 1st September 1989.
- 7) Applications of Evolved Gas Analysis. Thermal Methods Group Meeting of the Royal Society of Chemistry, London. 15th November 1989.

#### PRESENTATIONS GIVEN:

- 1) Initial Presentation to Perkins Technology Business at Peterborough. 9th September 1986.
- 2) Internal Research Presentation. Plymouth Polytechnic. 2nd December 1987.
- 3) Progress Presentation to Perkins Technology Business at Plymouth. 7th December 1987.
- 4) Tripartite Meeting at Peterborough with Perkins Technology Business and Leeds University Combustion Group. 3rd February 1988.
- 5) Internal Research Presentation. Plymouth Polytechnic. 18th May 1988.
- 6) Transfer Report Presentation to Perkins Technology Business at Plymouth. 10th June 1988.
- 7) Tripartite Meeting at Peterborough with Perkins Technology Business and Leeds University Combustion Group. 21st April 1989.
- 8) Internal Research Presentation. Polytechnic South-West. 1st June 1989.
- 9) Concluding Presentation of Ph.D. Thesis to Perkins Technology Business at Plymouth. 25th September 1989.



## ACKNOWLEDGEMENTS

During the past three years a number of people have assisted me in this work and I wish to thank them for their support. In particular, I would like to thank Dr. G.E. Millward for his continual advice and humour.

I would also like to thank; Professor D.E. Fussey for his direction, Dr. M.M. Rhead for the initial suggestion to carry out this research, Dr. C.T. Trier for 'trail breaking' the Ph.D. route, Mr. J. Clark for much practical advice and Dr. D.R. Glasson for his attention, expertise and confidence.

I would also like to acknowledge Dr. S.P. Petch and Mr. N.J. Horn who have left this establishment. Also the technical staff of the engineering and science departments; Mr. R. Cox, Mr. R. Horn, Mr. D. Ryder, Mr. E. Boles, Mr. I. Doige, Dr. R. Moate and Mr. B. Lakey.

I am also indebted to Perkins Technology Business and the Science and Engineering Research Council for providing the CASE studentship. Very special thanks must go to Dr. M. Graham and Mr. F. Brear for their guidance and specialist knowledge.

Finally I should like to thank my fiancée Miss Penny Keeves, whose encouragement and typewriter were both greatly appreciated.

## ABSTRACT

The potential health risk of diesel particulate (DP) has stimulated research into its physical and chemical composition. Its interaction with unburnt hydrocarbons (UHC) at exhaust temperatures was studied (i.e. composition and microstructure), at varying engine conditions. A hot whole exhaust filtration system was developed to collect DP on Pallflex TX-40 PTFE coated filters (for minimal artefact formation) down the exhaust of a Ricardo E6/T IDI diesel engine.

Electron microscopy (SEM and TEM) and a gravimetric BET method determined particle size, specific surface area (SSA) and pore character. An *in vacuo* gravimetric thermal degassing (TD) apparatus was constructed to extract adsorbed volatiles (filter extractable sample - FES). The volatile FES was trapped and analysed by gas chromatography and identified as fuel and oil derived UHC's. Ultrasonic and soxhlet extraction techniques were employed for comparison studies.

DP are graphitic carbonaceous aggregates of 30-40nm mean particle diameter. Structural analysis indicated that slit-shaped pores (Type II isotherm) were formed between crystallite layers. Highly adsorbed pore-bound FES fractions were identified (fuel in ultramicropores, 0.355-1nm; fuel/oil in supermicropores, 1-2nm), trapped by overlapping crystallite van der Waal's fields. Engine load influenced micropore adsorption and DP SSA. High loads with high combustion temperatures, efficiently pyrolysed fuel, producing DP with little adsorbed FES and SSA's of 100m<sup>2</sup>/g. Low loads with lower in-cylinder temperatures, formed less DP and more fuel survived, producing soots of low SSA (<20m<sup>2</sup>/g). Between aggregated particles, 'ink-bottle' mesopores (2-50nm) were evident (Type IV isotherm) where fuel FES was weakly adsorbed by temperature dependent chemical scavenging as exhaust temperature declined, reducing SSA and increasing particle size.

Thermal degassing was more efficient than soxhlet or ultrasonic extraction methods, because the solvent methods failed to penetrate the smallest pores. TD increased soot SSA, greatest for low load samples (by 200m<sup>2</sup>/g) compared to high load samples (by 50m<sup>2</sup>/g). TD was highly advantageous for DP extraction and allowed progressive removal of volatiles.

A modern DI engine showed structurally similar soots, but the lower DP emissions produced high relative %FES for all engine conditions giving low SSA's.

The research findings are related to cylinder and environmental processes for engineers and environmental scientists to improve control strategies.

## GLOSSARY OF ABBREVIATIONS

During the writing of this thesis numerous abbreviations have been used and are included in this glossary to aid comprehension of this research project.

AC	Aciniform Carbon
AFR	Air/Fuel Ratio
ATDC	After Top Dead Centre
BCF	Box Cassette Filter
BET	BET method for Specific Surface Area Determination
BTDC	Before Top Dead Centre
CRC	Coordinating Research Council
DCM	Dichloromethane
DI	Direct Injection Engine
DOP	Diethyl Phthalate
DP	Diesel Particulate
EEC	European Economic Community
EGA	Evolved Gas Analysis
EM	Electron Microscopy
EPA	Environmental Protection Agency
EUDC	European Extra Urban Driving Cycle
FES	Filter Extracted Sample
GC	Gas Chromatography
HC	Hydrocarbons
ICF	Improved Cassette Filter
IDI	Indirect Injection Engine
OHV	Overhead Valve
PAC	Polyaromatic Compound
PAH	Polyaromatic Hydrocarbon
PTFE	Poly-Tetra-Fluoroethane
RPM	Revolutions per minute
QMA	Quartz Microfibre Filter
SEM	Scanning Electron Microscopy
SOF	Solvent Organic Fraction
SSA	Specific Surface Area
TD	Thermal Degassing
TDCS	Temperature Dependent Chemical Scavenging
TG	Thermogravimetry
TEM	Transmission Electron Microscopy
TES	Tower Extracted Sample
TESSA	Total Exhaust Solvent Scrubbing Apparatus
TLC	Thin Layer Chromatography
TOE	Total Organic Extract
TX-40	TX-40 Pallflex Filter Media
UCM	Unknown Complex Mixture
UDCM	Ultrasonic Extraction Method using DCM
UHC	Unburnt Hydrocarbons
US	United States of America

CONTENTS.	PAGE.
TITLE.	i
COPYRIGHT.	ii
DECLARATIONS.	iii
CONFERENCES ATTENDED.	iv
PRESENTATIONS GIVEN.	iv
ACKNOWLEDGEMENTS.	v
ABSTRACT.	vi
GLOSSARY OF ABBREVIATIONS.	vii
CHAPTER CONTENTS.	viii
FIGURE CONTENTS.	xii
TABLE CONTENTS.	xvi
CHAPTER 1 DIESEL COMBUSTION.	1
CHAPTER 2 DIESEL PARTICULATE FILTRATION.	37
CHAPTER 3 THE CHARACTERISATION OF DIESEL PARTICULATE AND ADSORBED UNBURNT HYDROCARBONS.	80
CHAPTER 4 RESULTS AND DISCUSSION OF EXPERIMENTS UNDERTAKEN.	144
CHAPTER 5 CONCLUSIONS, RECOMMENDATIONS AND FURTHER WORK.	216
REFERENCES.	221
APPENDIX I PUBLISHED WORK	A1

CHAPTER 1 DIESEL COMBUSTION.	PAGE
1.1 PRELIMINARY REMARKS.	1
1.1.1 The Environmental Concerns of Diesel Combustion.	2
1.1.2 Regulation and Control of Diesel Emissions.	5
1.2 DIESEL ENGINES AND COMBUSTION SYSTEMS.	8
1.2.1 Combustion Systems.	11
1.2.2 Soot Formation.	15
1.3 DIESEL EXHAUST EMISSIONS.	21
1.3.1 Unburnt Hydrocarbon Emissions.	21
1.3.2 Diesel Particulate Emissions.	26
1.4 THE PHYSICOCHEMICAL RELATIONSHIP BETWEEN SOOT AND PAH.	31
1.5 OBJECTIVES OF THIS RESEARCH.	36
CHAPTER 2 DIESEL PARTICULATE FILTRATION.	37
2.1 PARTICULATE ARTEFACTS AND FILTRATION SYSTEMS.	39
2.1.1 Diesel Particulate Sampling Systems and Methods.	41
2.1.2 The Dilution Tunnel.	42
2.1.3 Solvent Scrubbing Systems.	44
2.1.4 Hot Whole Exhaust Filtration.	45
2.2 FILTER MEDIA.	46
2.2.1 Rationale for Filter Selection.	50
2.2.2 Filter Handling Procedure.	53
2.3 ENGINE FACILITIES.	54
2.3.1 Research Engine Ricardo E6/T.	54
2.3.2 Research Engine Ford.	56
2.3.3 Ancillary Equipment.	57
2.3.4 Ricardo Emission Maps.	58
2.4 FILTER SYSTEM DESIGN.	64
2.4.1 Mini Cassette Filter.	64
2.4.2 Box Filter System.	66
2.4.3 Box Cassette Filter.	67
2.4.4 Improved Cassette Filter System	71
2.5 PROCEDURES AND VALIDATION OF SYSTEM.	77
2.5.1 Preconditioning.	77
2.5.2 Sample Collection.	78
2.5.3 Conclusions on Sample Integrity in this Study.	79

CHAPTER 3 THE CHARACTERISATION OF DIESEL PARTICULATE AND ADSORBED UNBURNT HYDROCARBONS.	PAGE
3.1 MICROSTRUCTURAL CHARACTERISATION OF DIESEL PARTICULATE USING A NITROGEN ADSORPTION VACUUM MICROBALANCE TECHNIQUE.	84
3.1.1 Series 1A. Extraction of Diesel Particulate for Microstructural Analysis.	84
3.1.2 The Vacuum Microbalance.	86
3.1.3 Theory of Microstructural Analysis and Calculation of Specific Surface Area.	87
3.1.4 Validation of Experimental Method.	98
3.1.5 Discussion of Experimental Errors.	99
3.1.6 Experimental Procedure.	101
3.1.7 Adsorption in Microporous Carbons.	107
3.2 ELECTRON MICROSCOPIC EXAMINATION OF DIESEL SOOTS.	110
3.2.1 Geometric Surface Areas of Diesel Soots.	113
3.3 CHEMICAL ANALYSIS OF UNBURNT HYDROCARBONS.	115
3.3.1 FES Extraction from Filters.	116
3.3.2 The Total Exhaust Solvent Scrubbing Apparatus.	116
3.3.3 UHC Sample Preparation.	118
3.3.4 Open-Column Chromatography.	119
3.3.5 Gas Chromatographic Analysis of Samples.	120
3.3.6 Standards and Identification.	124
3.3.7 Discussion of Sources of Contamination.	127
3.4 EVOLVED GAS ANALYSIS.	129
3.4.1 Thermal Degassing Experiments for the Chemical and Microstructural Characterisation of DP.	132
3.4.2 The EGA System.	133
3.4.3 Experimental Design and Development.	134
3.4.4 Operational Procedure.	139
3.4.5 Additional Experiments.	140



CHAPTER 4	RESULTS AND DISCUSSION OF EXPERIMENTS UNDERTAKEN.	PAGE
4.1	SERIES 1A. DIESEL PARTICULATE MASS EMISSION AND CHARACTERISATION.	147
	4.1.1 Microstructural Analysis of Diesel Particulate.	149
	4.1.2 Electron Microscopic Examination of Series 1A Diesel Soot.	157
4.2	SERIES 1B. FES FROM BCF.	160
	4.2.1 Series 2A. Tower Extractable Sample.	163
4.3	SERIES 1C. TOTAL CHARACTERISATION OF DP.	172
	4.3.1 Microstructural Characterisation of On-Filter DP.	177
	4.3.2 Characterisation of TD FES from On-Filter DP.	181
	4.3.3 Experiment 3A. Comparison Between Extraction Methods on the Microstructure of DP and Adsorbed FES.	182
	4.3.4 Experiment 4A. Comparison of the DP from the Ford DI Engine and the Ricardo IDI Engine.	188
	4.3.5 Experiment 5A. Sequential EGA and Microstructural Characterisation of DP.	192
4.4	SUMMARY OF RESULTS.	207
	4.4.1 The Character of Diesel Particulates.	207
	4.4.2 Identification of Unburnt hydrocarbons in the Exhaust.	208
	4.4.3 The Interaction between Unburnt Hydrocarbons and Diesel Particulate in Diesel Exhausts.	208
CHAPTER 5	CONCLUSIONS, RECOMMENDATIONS AND FURTHER WORK.	216
5.1	CONCLUSIONS.	216
5.2	RECOMMENDATIONS.	218
5.3	FURTHER WORK.	219

LIST OF FIGURES	PAGE	
CHAPTER 1		
1.1	The European Extra Urban Driving Cycle (E.U.D.C.)	6
1.2	A Typical Heat Release Diagram.	10
1.3	A Turbulent Diffusion Flame: Source of Soot and its Oxidation.	14
1.4	Pathways to Soot Formation.	14
1.5	The Mechanism of Soot Particle Formation in Combustion Systems.	16
1.6	Growth from Primary Molecular Species to Soot Aggregates.	16
1.7	A Selection of Polycyclic Aromatic Hydrocarbons (PAH's) Identified in SOF Fractions from Diesel Particulate.	24
1.8	The Structural System of Soot - Showing its Development from Fuel to Soot Aggregate.	28
1.9	Representation of Hexane Soot, with Occluded Substances, as Formed in Flames.	29
1.10	Diesel Particulate Composition. A Simple Model with Extractable Fractions.	32
1.11	Portion of the PAH Adsorbed onto Diesel Particulate as a Function of the Temperature in a Dilution Tunnel.	34
CHAPTER 2		
2.1	The Typical Layout of a Dilution Tunnel.	43
2.2	The Stainless Steel Exhaust Scrubbing Tower (TESSA).	43
2.3	Mechanism of Cake Filtration.	47
2.4	Mechanism of Depth Filtration.	47
2.5	TX-40 Pallflex Filter.	49
2.6	QM-A Whatman Filter.	49
2.7	The Ricardo E6/T Diesel Research Engine with BCF and TESSA.	55
2.8	Ricardo Hydrocarbon Emission Map.	60
2.9	Ricardo Oxides of Nitrogen Emission Map.	61
2.10	Ricardo Carbon Monoxide Emission Map.	62
2.11	Ricardo Bosch Smoke N° Emission Map.	63
2.12	The Mini Cassette Filter with Cassette in View.	65
2.13	The Box Filter Design.	65
2.14	The Box Cassette Filter System.	68
2.15	The Box Cassette Filter (BCF) with sliding Filter Holder.	70
2.16	The Improved Cassette Filter (ICF) with Thermoprobe and Pressure Manometer Fittings.	70
2.17	The Compressed Air Operated Piston Exhaust Valve.	72
2.18	The Improved Cassette Filter (ICF) System with Engine and TESSA.	72
2.19	Graph of Pressure and Temperature During ICF Operation at 1.3m and 4.3m from Exhaust Port.	75



## CHAPTER 3

3.1	The BET Apparatus - A Vacuum Microbalance.	88
3.2	Adsorption/Desorption Isotherms Type I to V Characterised to Different Solid Surfaces.	89
3.3	A BET Plot of Diesel Particulate Extracted by Brushing from a Filter.	92
3.4	Adsorption/Desorption Isotherm Showing Hysteresis Loop for a Brushed Diesel Particulate.	94
3.5	IUPAC Classification of Hysteresis Loops for the Characterisation of Pore Systems.	95
3.6	Graph of Selected Hydrocarbons and Water. A Plot of the Variation in Boiling Point with Pressure.	104
3.7	Graph of Weight Change Against Time for a Particulate Sample During a Full Isotherm Series.	106
3.8	A Model of the Fine Structure of a Microporous Carbon.	108
3.9	Scanning Electron Micrograph of Caked Diesel Particulate.	112
3.10	Transmission Electron Micrograph of Diesel Particulate.	112
3.11	Chromatogram of GROB Standard.	122
3.12	Chromatograms of the Concentrated System Blank and PAH Standards used in the Lee Retention Index.	125
3.13	Chromatograms of Lubricating Oil and Diesel Fuel.	126
3.14	TGA and HFID Results of an Analysed Diesel Particulate.	130
3.15	All Glass Sublimation Apparatus.	130
3.16	Prototype EGA Apparatus Design for Nitrogen Gas.	136
3.17	The Thermal Degassing Apparatus for EGA.	138
3.18	Thermal Desorption Curves of Diesel Particulate and a Doped Diesel Fuel (On-Filter).	141
3.19	Chromatograms of Diesel Fuel and the Thermally Degassed Filter-Doped Diesel Fuel Sample.	142

## CHAPTER 4

4.1	Emissions Graph of the Relationship Between Hydrocarbons, Smoke and Air/Fuel Ratio as a Function of Engine Condition.	145
4.2	Histogram and Pie Graphs of DP Mass Emission and % UDCM Extractable FES with Temperature.	148
4.3	Adsorption/Desorption Isotherms and Hysteresis Loops of a DP Brushed from a Filter Exposed to the Exhaust of the Ricardo IDI Engine.	151
4.4	Adsorption/Desorption Isotherm Showing Hysteresis Loops for a UDCM Extracted Diesel Particulate Before and After Thermal Degassing.	155
4.5	Scanning Electron Micrograph of a Bosch Smoke Filter.	158
4.6	Chromatograms of FES from Series 1B, Extracted by Soxhlet Extraction.	161
4.7	Chromatograms of FES from Series 1B, Extracted by Soxhlet Extraction.	162
4.8	Chromatograms of Unfractionated TES (TESSA).	166
4.9	Chromatograms of the Aromatic Fractions of TES.	167
4.10	Chromatograms of the Aliphatic Fractions of TES.	168
4.11	Reference Chromatograms of Fuel Fractions.	170
4.12	Reference Chromatograms of Lubricating Oil Fractions.	171
4.13	Histograms of the Composition of DP Collected from Different Engine Conditions and Filter Positions.	173
4.14	Adsorption/Desorption Isotherms and Hysteresis Loops of a DP Sample, Before 'A' and After 'B' Thermal Degassing.	178
4.15	Adsorption/Desorption Isotherms and Hysteresis loops of a DP Sample, Before 'A' and After 'B' Thermal Degassing.	179
4.16	Adsorption/Desorption Isotherm of the TX-40 Filter Media.	180
4.17	Chromatograms of FES Extracted by TD from DP.	183
4.18	Chromatograms of FES Extracted by Ultrasonication (UDCM) and TD from DP.	184
4.19	Chromatograms of FES Extracted by Soxhlet and TD from DP.	185
4.20	Adsorption/Desorption Isotherms and Hysteresis Loops of a Ford DI Diesel Engine DP, Before 'A' and After 'B' Thermal Degassing.	189
4.21	Adsorption/Desorption Isotherm and Hysteresis loops of a Ford DI Diesel Engine DP, Before 'A' and After 'B' Thermal Degassing.	190
4.22	Adsorption/Desorption Isotherm and Hysteresis Loop of a DP Sample Determined On-Filter.	197
4.23	Adsorption/Desorption Isotherm and Hysteresis Loop of a TD Extracted (120°C, 1mm Hg) DP Determined On-Filter.	198
4.24	Adsorption/Desorption Isotherm and Hysteresis Loop of a TD Extracted (190°C, 1mm Hg) DP Determined On-Filter.	199

4.25	Adsorption/Desorption Isotherm and Hysteresis Loop of a TD Extracted (290° C, 1mm Hg) DP Determined On-Filter.	200
4.26	Adsorption/Desorption Isotherm and Hysteresis Loop of a TD Extracted (340° C, 1mm Hg) DP Determined On-Filter.	201
4.27	Adsorption/Desorption Isotherm and Hysteresis Loop of a DP Sample Determined On-Filter.	202
4.28	Adsorption/Desorption Isotherm and Hysteresis Loop of a TD Extracted (120° C, 1mm Hg) DP Determined On-Filter.	203
4.29	Adsorption/Desorption Isotherm and Hysteresis Loop of a DP Extracted (190° C, 1mm Hg) DP Determined On-Filter.	204
4.30	Adsorption/Desorption Isotherm and Hysteresis Loop of a TD Extracted (290° C, 1mm Hg) DP Determined On-Filter.	205
4.31	Adsorption/Desorption Isotherm and Hysteresis Loop of a TD Extracted (340° C, 1mm Hg) DP Determined On-Filter.	206
4.32	A Model of DP Formation and Exhaust Processes.	210
4.33	Data Summary of Exhaust Model Showing % FES Mass and DP mass as a Function of Exhaust Temperature for High and Low Load Engine Condition.	212
4.34	Improved Emission Map showing Bosch Smoke Levels, %FES, DP Mass Emission and Sample Temperature. These Samples were gathered at 1.3m from the Engine.	214
4.35	Improved Emission Map showing Bosch Smoke Levels. %FES, DP Mass Emission and Sample Temperature. These Samples were gathered at 3.3m from the Engine.	215

## LIST OF TABLES

### CHAPTER 2

2.1	Technical Data on the Filters used in this Research.	52
2.2	Ricardo Emission Data for Emission Maps.	59
2.3	Pressure Drop Across Filter and Time taken for Engine to Lose 100rpm. Samples taken with BCF.	68
2.4	Maximum Pressure Across ICF Filter and Exhaust Gas Temperature noted during Series 1C.	74

### CHAPTER 3

3.1	Summary of Experiments and Techniques Undertaken in this Research Project.	81
3.2	Boiling Points of Representative Hydrocarbons and Water at Various Pressures used in these Studies.	103
3.3	High Resolution Gas Chromatographic Conditions.	121

### CHAPTER 4

4.1	Emission Map Database for the Ricardo IDI Diesel Engine over the Engine Conditions used during these Studies.	146
4.2	Filter Emission Data from Series 1A (BCF) Showing DP Mass Emission Rate and % UDCM Extracted FES.	146
4.3	Nitrogen Adsorption Specific Surface Area (BET) of UDCM Extracted DP determined after Room Temperature (20°C) 'A' Degassing, and after Thermal Degassing (350°C) 'B'.	153
4.4	Particle Sizes of Soots taken at a Variety of Engine Conditions and Filter Positions with the BCF and Analysed by SEM.	158
4.5	Particulate Mass and TES Mass Emission Rates from the Ricardo Engine and Collected by TESSA.	165
4.6	Tentative Identifications of Compounds in the TES Fractions.	165
4.7	SSA Data from Series 1C Shown with Exhaust Temperature.	174
4.8	Particle Size Evaluation for Different Engine Conditions and Filter Positions Collected by the ICF System.	174
4.9	Variation of SSA with Extraction Method.	186
4.10	Composition Data of Soot Obtained from the Ford DI Engine with the ICF System at 3.3m.	186
4.11	Engine Condition and SSA for Two DP Samples Sequentially Degassed at Successively Higher Temperatures.	196

## CHAPTER 1 DIESEL COMBUSTION

### 1.1 PRELIMINARY REMARKS

Diesel powered vehicles now achieve 20-40% more distance per unit volume of fuel than those vehicles powered by petrol because of their higher fuel efficiencies, and because diesel fuel contains about 15% more energy than an equal volume of petrol (Cuddihy et al, 1984). Diesel vehicles emit 30 to 100 times more soot than petrol engines if lead-free petrol and catalytic traps are employed (Ball, 1984). The combustion of diesel fuel normally results in the emission of four times the mass of particulate matter per unit weight of fuel consumed, when compared to petrol engines using leaded petrol.

The small diesel powered car is now highly competitive and being rapidly developed to overcome ever tightening emission legislation, especially important if the US market is to be cracked by the dominant European manufacturers. Indeed, apart from particulate emission the diesel engine produces less gaseous pollutants than equivalent sized spark ignition engines (Ball, 1984). The predicted growth for diesels is such that by the year 2000, 40% of cars and 90% of heavy duty vehicles, in W.Germany and the US will be diesel driven. Currently, in Britain, 15% of passenger cars and nearly 100% of heavy goods vehicles are diesels.



However, concerns over health and the environmental implications of increasing diesel particulate emission, have also been expressed, especially in the US with its high emission standards. Thus, European manufacturers wish to reduce these emissions, and this project is directed towards the study of the exhaust interactions between diesel particulate (DP) and unburnt hydrocarbons (UHC), both of which are important pollutants.

#### 1.1.1 The Environmental Concerns of Diesel Combustion

The innate products of combustion are water, carbon dioxide, carbon monoxide, oxides of nitrogen and sulphur, hydrocarbons and particulate matter. Carbon Dioxide (CO<sub>2</sub>) has been linked with the 'greenhouse effect'. Nitrous and sulphur oxides are precursors of 'acid rain'. Nitrogen oxides (NO<sub>x</sub>) are also involved in the photochemical reactions with hydrocarbons (HC), producing 'smog' in the lower atmosphere, and contribute to the depletion of ozone in the upper atmosphere (Beer, 1988). Hydrocarbon emissions from the partial combustion of fuel may also include polycyclic aromatic compounds (PAC's) some of which are known mutagens, and may adsorb onto the diesel particulates (DP), which are of a respirable size range (< 0.1µm diameter), and become lodged in lung spaces causing lung tumors (Wolff et al, 1986). Many researchers have identified these

PAC's (Lee et al, 1981; Lee et al, 1983) because of concern that nitrogen and sulphur containing polyaromatic hydrocarbons (PAH's) may be important precursors for direct acting mutagenic nitro-PAH's which have been identified in diesel exhausts (Schuetzle, 1983). Lindskog (1983) showed that PAH may undergo chemical transformations to nitro-PAH and other compounds when exposed to gases such as NO<sub>2</sub>, O<sub>3</sub> and SO<sub>3</sub>. Thus, diesel emissions are considered to be a potential health threat. Other nuisances of diesel combustion include the smell and visible smoke. DP, because of its oily nature, high optical absorbance and small size, has a high relative soiling index of 5.8 (Ball, 1984) which makes it a prominent soiler of buildings.

The health concerns of DP centre on the interaction and bioavailability of PAC's adsorbed on DP. The mass median diameter of atmospheric DP may be as low as 0.1µm and these particles are able to deeply penetrate the respiratory tract. The presence of solid matter may slow the pulmonary clearance mechanism, thus allowing potentially toxic agents to remain in effective contact with susceptible tissues for long periods. Studies on the risks of DP have involved four approaches; chemical characterisation of hydrocarbons, in vitro studies of mutagenicity, epidemiological surveys and whole animal studies (McClellan, 1986). PAC's, extracted by solvent extraction from DP (gives a solvent organic fraction - SOF), have displayed mutagenicity to the Ames Test (Ames et al, 1975).

Nitro-arenes and specifically nitro-pyrene has been identified as mutagenic. Epidemiological surveys suffer from outside influences on survey populations, e.g. smoking, and therefore have been inconclusive. Whole animal studies (Waller, 1986; Mauderly et al, 1986) have shown that DP exposure at street exposure levels, over long periods (2-3 years) have caused lung tumors in rats. Waller (1986), showed that lung tumors were only significantly present in rats exposed to unfiltered exhaust (at levels of exhaust an order of magnitude greater than maximum street level values), compared to filtered exhaust exposed rats, thus linking DP to lung tumour development. Mauderly et al (1986) investigated the site location of DP in lungs and Wolff et al (1986) suggested that tumour formation was due to a combination of factors; non-specific particle effects, release of organics from particles and interaction with lung macro-molecules, and the influence of particles on metabolism and cellular responses, which augments the effects of released organics. However, Stöber (1987) reviewed the whole animal data and concluded that only one animal species (the rat), has shown a cause-effect relationship between diesel soot exposure and lung tumour induction and that this was primarily due to the physical particle, not the PAC. He then suggested that further studies were required and that "the health aspects should be kept in proper perspective and regulations on emission standards should be promoted and advanced for what they are: measures limiting nuisance and discomfort". Generally speaking the



mutagenic risk from diesel exhaust is far less than other sources, e.g. smoking.

### 1.1.2 Regulation and Control of Diesel Emissions

The current petrol and diesel regulations are covered by EEC directive 70/220/EEC amended in December 1987 by 88/76/EEC for petrol and 88/77/EEC for diesels. These regulations are not as stringent as in the US. Currently, smoke emission is controlled by an opacity test (EEC directive 72/306/EEC) which is only qualitative, although proposals are being considered to control DP emission in quantitative terms.

Engines are tested with standard test cycles designed to mimic driving conditions, e.g. the US Federal Test Procedure and European Extra Urban Driving Cycle (EUDC) (Fig 1.1). The Federal Test Procedure measures the mass emission of DP over the driving cycle with a dilution tunnel to filter the exhaust.

Diesel particulates are defined as any dispersed matter collected on a filter at a temperature below 52°C, excluding condensed water (Hare *et al*, 1976; Khatin *et al*, 1978) and this definition is recognised by the EPA and used with special reference to dilution tunnels which simulate exhaust gases entering the environment (as detailed in Chapter 2). Any hydrocarbons present with the diesel particulates and having

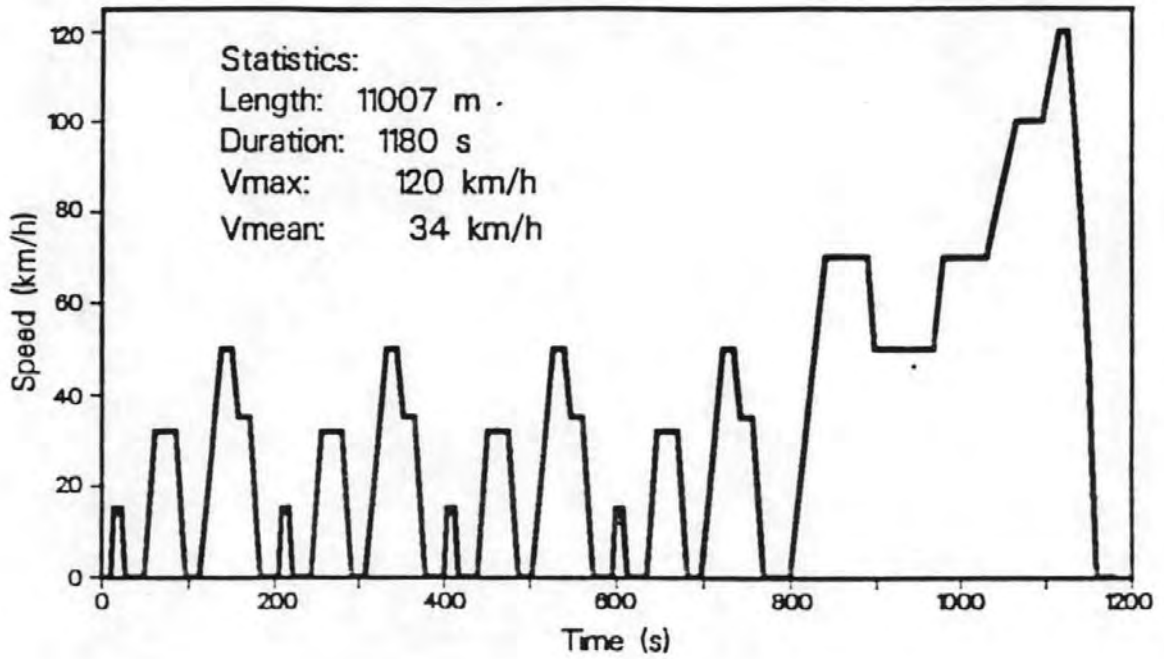


Fig. 1.1 The European Extra Urban Driving Cycle (E.U.D.C.)

Vmax: Maximum Vehicle Speed  
 Vmean: Mean Vehicle Speed

a dew point above 52°C will be condensed out. These condensed and adsorbed hydrocarbons may be extracted and identified. The SOF may amount to between 10-50% of the total unburnt hydrocarbons (UHC) (Cuthbertson et al, 1979) and constitute between 1 and 90% of the particulate material (Hare et al, 1976; Braddock and Gabelle, 1977; Frisch, 1979).

Strategies for the control of DP emissions require; improving engine design (combustion chamber, fuel injection), fuel improvements (reduction in aromatic content) and particulate traps (catalytic at low exhaust temperatures <400°C or heated to oxidise soot at >600°C).

## 1.2 DIESEL ENGINES AND COMBUSTION SYSTEMS

Diesel engines differ from spark ignition engines primarily because they use compression to ignite the air/fuel mixture and fuel volume controls engine power output. In typical naturally aspirated diesel engines, the volume of air drawn into the chamber is a function of speed, whilst the amount of fuel drawn in depends on speed and load. Thus the air/fuel ratio (AFR) for a diesel engine can vary over a wide range of conditions. Fuel supply is increased by injecting fuel over longer parts of the cycle and thus the fuel injection timing is critical to combustion efficiency and unburnt hydrocarbon emissions.

In direct injection (DI) engines, the fuel is mixed with air in the combustion chamber, whereas indirect injection (IDI) engines premix the air and fuel in a prechamber where combustion is initiated before entering the main combustion chamber. In a DI diesel engine, air is drawn in on the inlet stroke and compressed so that the temperature rises. When the piston almost reaches the minimum volume position (10-15° BTDC - Before Top Dead Centre) fuel is injected as a jet of fine droplets. The combustion sequence can then be divided into three stages: the delay period, when the injected fuel mixes with air to form locally over-lean mixtures, locally over-rich

mixtures and combustible mixtures. The fuel does not combust but undergoes chemical transformations involving pre-flame oxidation and thermal degradation or pyrolysis. The rapid combustion that follows in stage two, results in most of the mixed fuel simultaneously combusting causing a rapid increase in pressure. This stage is characterised by a low luminosity premixed flame which lasts 6° of the crankangle and burns with a peak temperature of over 2000°C (Haddad, 1984).

In an IDI system these first two stages occur in the restricted prechamber resulting in turbulent and incomplete combustion (due to lack of air). The unburnt/partially pyrolysed fuel then enters the cylinder at high velocity where the final stage - full combustion occurs. It lasts 40° of crankangle, produces a white carbon diffusion flame at 2500°C and completes combustion. Fig 1.2 shows the typical heat release diagram (Haddad, 1984).

Under 'hot' conditions, black smoke is produced by an engine, however white/blue smoke may be produced under 'cold' conditions such as starting, idling and low load. This white/blue smoke mainly consists of relatively low molecular mass hydrocarbons which originate from the unburnt or partially burnt fuel and lubricants.

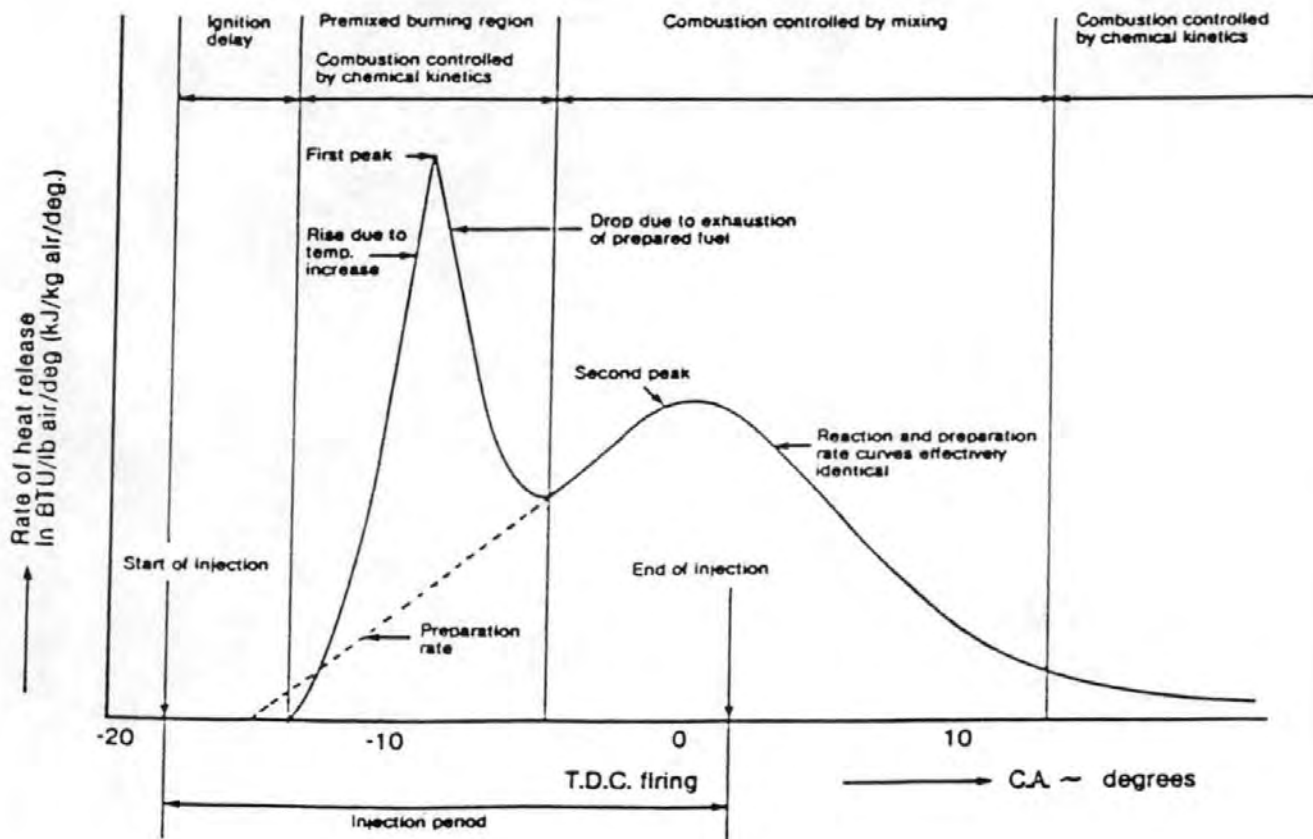


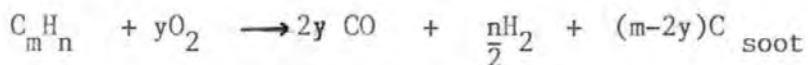
Fig. 1.2 A Typical Heat Release Diagram (Haddad, 1984)

### 1.2.1 COMBUSTION SYSTEMS

Simple combustion systems (e.g. burners) have been used to model the combustion of hydrocarbon fuel and the results applied to reciprocating engines (i.e. Diesel engines). Diesel engines operate on the diffusion (turbulent) principle utilising fuel sprays.

Combustion in premixed flames (where fuel vapour and oxidant can be mixed before combustion) can occur over a range of fuel concentrations between the lower and upper flammability limits. Hydrocarbon fuel 'lean' flames, i.e. below the stoichiometric fuel concentration (Equation 1.1), tend to be transparent and pale blue with OH<sup>-</sup> ions present. Towards the upper flammability limit, combustion tends to be inefficient (through lack of oxygen) and the flames become yellow and luminous because of the glowing particles of unburnt carbon.

From a thermodynamic viewpoint, the formation of soot should only occur when



(Haynes and Wagner 1981) (Equation 1.1)



and  $m$  becomes larger than  $2y$ , i.e. when the fuel-carbon to oxygen ratio (C/O) exceeds unity. Experimentally, the limit of soot formation is normally equated with the onset of luminosity, and occurs not at C/O equal to 1, but usually in the vicinity of the critical C/O ratio found in other flames. Even well mixed combustion systems are observed to emit soot when the C/O ratio in the fuel-oxidiser exceeds 0.5.

The most common flame type is the diffusion flame, where the fuel and oxidant must physically diffuse together at the flame surface before any chemical reactions can take place. Most research has been carried out using steady-flow combustors operating on the diffusion flame principal, forming a stable flame which can be easily adjusted to the conditions required. These flames form concentration fields with stable equilibria which is why they are preferred. In reciprocating engines with fuel injection into the cylinder, combustion occurs by mixing but the AFR is constantly changing and a stable equilibria cannot be reached. Even when the fuel/air mixture is formed outside the engine, the mixture does not burn homogeneously and this may give rise to the formation of intermediates in the flame zone. In steady flow combustors, the combustion rate is controlled by the turbulent transport of fuel and air at the boundary of the fuel spray. As Fig 1.3 shows, the flame can be



subdivided into three zones.

- 1) Central Core (Zone 1).
- 2) Middle (Zone 2).
- 3) Outer Area (Zone 3).

These zones may be defined by the local equivalence ratio  $\phi$ .

$$\phi = \frac{(\text{FUEL/OXIDISER})_{\text{actual}}}{(\text{FUEL/OXIDISER})_{\text{stoichiometric}}}$$

(Equation 1.2)

In Zone 1, a high local equivalence ratio exists due to the co-existence of droplets and fuel vapour (fuel 'rich') which cause the formation of soot. In Zone 2, only droplets exist and soot production stops, and in Zone 3 where the mixture is 'lean', the soot is combusted along with any remaining fuel. Whether soot survives to the exhaust system is a function of the relationship between its formation and oxidation.

In diffusion flames it is the local rather than overall stoichiometry which is important for soot formation and local equivalence ratio is therefore determined by the mixing characteristics in the cylinder of the engine.

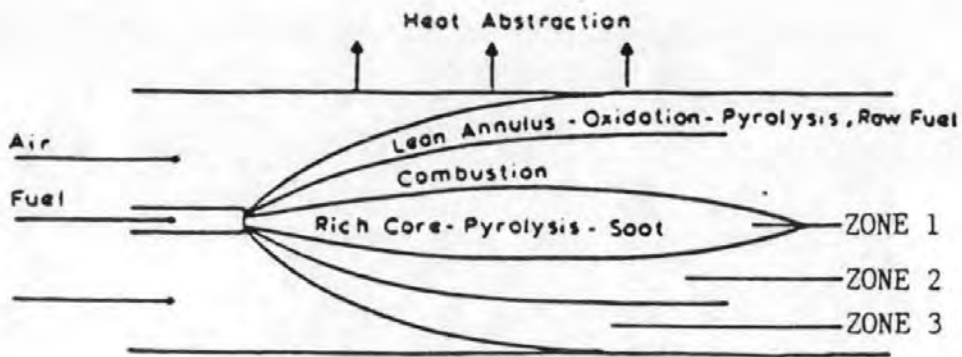


Fig. 1.3 Turbulent Diffusion Flame: Source of Soot and Its Oxidation (Longwell, 1982)

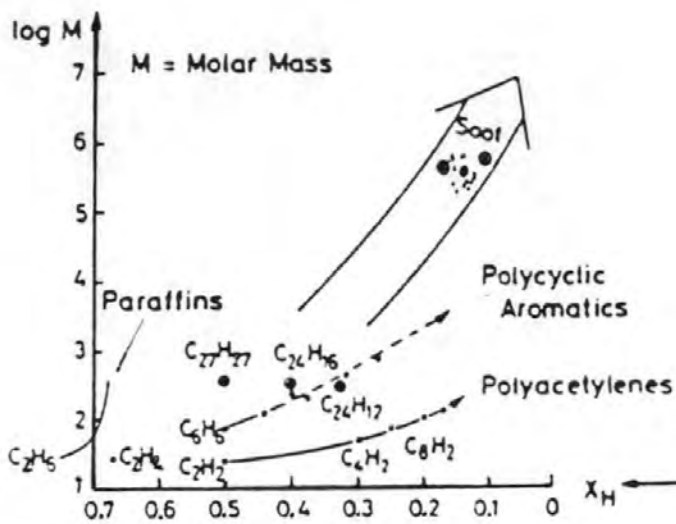


Fig. 1.4 Pathways to Soot Formation (Homann, 1978)

### 1.2.2 SOOT FORMATION

The mechanisms of soot formation (particularly pyrolysis and nucleation) have not yet been fully defined owing to the extreme complexity and difficulty of studying the dynamic systems involved. Researchers have reviewed the situation (Bittner and Howard, 1980; Calcote, 1981; Haynes and Wagner, 1981; Smith, 1981, and most recently Glassman, 1988), trying to formulate the reaction pathways from a variety of research data. This brief review merely presents a selected summary and the most recent review (Glassman, 1988).

In its simplest form soot formation consists of 5 overlapping stages as shown in Fig 1.5.

1) Pyrolysis (and oxidative pyrolysis) is the process which forms unsaturated hydrocarbon species with molecular masses lower than the parent compound and may occur with or without the presence of oxygen. Generally exothermic and therefore temperature dependent, it occurs by a free radical mechanism, enhanced by the addition of oxygen (O, O<sub>2</sub> or OH), which form further radicals due to branching reactions. Pyrolysis studies have been carried out on single hydrocarbon fuels such as benzene and acetylene in an attempt to model combustion.

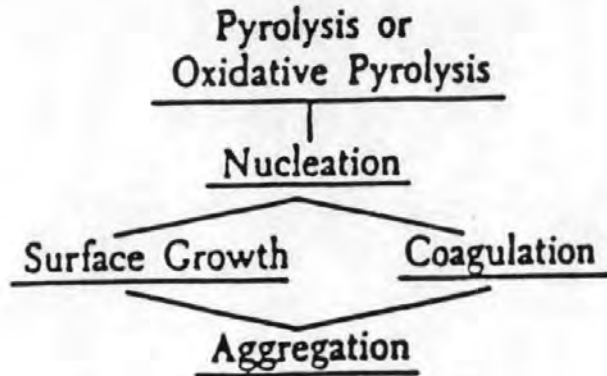


Fig. 1.5 The Mechanism of Soot Particle Formation in Combustion Systems (Smith, 1981)

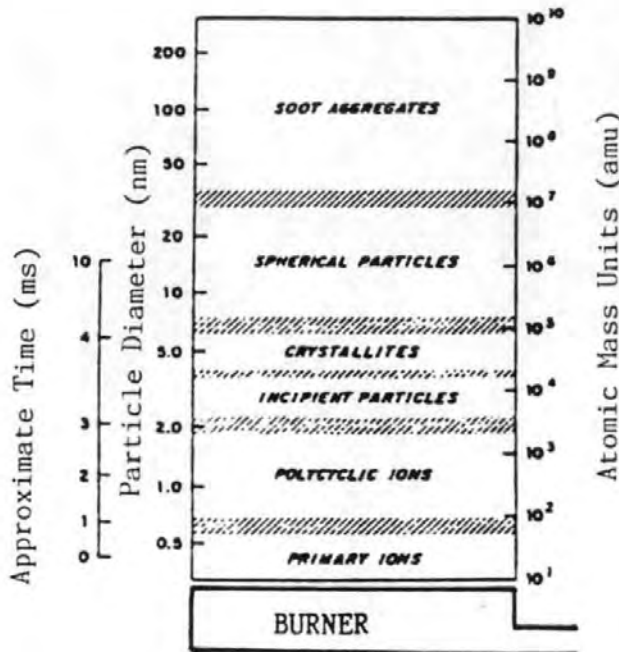


Fig. 1.6 Growth from Primary Molecular Species to Soot Aggregates (Calcote, 1981)

These simple fuels have been used to represent the common pathways for aromatic and aliphatic fuel combustion.

2) Nucleation is the process whereby the molecular system is transformed into a particle system by a series of reactions probably using acetylene as a "building block" molecule and the aromatic ring structure as the backbone

3) and 4) Growth occurs by surface "condensation" of hydrocarbons and/or coagulation which is the result of collision between similar sized particles.

5) Aggregation is when individual particles form chainlike structures.

Concurrent with these formation processes are destructive processes which occur in regions where oxidizing species are present (Calcote, 1981).

The overall process in a burner system, from primary molecular species to soot, is shown by Calcote (1981) in Fig 1.6.

Calcote summarises the problem by asking the following question: "How does the process proceed from molecular size to

particles with diameters three orders of magnitude greater, or equivalent molecular weights ten orders of magnitude greater, than the starting material in the order of milliseconds?".

Glassman (1988), in the most recent review, stated that the ionic mechanism and other mechanisms are fundamentally dependent on neutral radicals and presents a convincing theory to explain soot formation.

For aliphatic fuels, he summarises the formation mechanism by the process of cyclisation of the aliphatic molecule which creates the aromatic structures (by addition of alkyl groups) and becomes the particle nuclei. The particles then dehydrogenate at the high temperatures, physically and chemically absorbing gaseous hydrocarbon species, thus increasing soot mass and particle size. The growing particles agglomerate, and the adsorbed species undergo chemical reformation, which results in the carbonaceous DP structure.

Glassman concludes by saying, "the extent to which a given fuel system will produce soot depends strongly on the type of combustion system (flame structure) controlling the process and temperature of that system". In premixed flames the competition between pyrolysis and oxidative attack is temperature dependent,



with increasing temperature enhancing the rate of oxidation and therefore reducing soot formation. In premixed fuel 'rich' flames, soot formation is independent of fuel structure and soot is formed by pyrolysis to acetylene. In diffusion flames, since there is no oxidative attack on the fuel, regardless of the fuel, the higher flame temperature, the greater the propensity to form soot. Incipient particle formation begins at about 1100°C and depends on the degree of H atom concentration. Thus the DP formation depends highly on fuel structure.

Glassman adds "fuel pyrolysis chemistry (mechanism and rate) plays the dominant role in determining the sooting propensity by following a general chemical route through the C<sub>4</sub> molecules, butadienyl radical and acetylene, to the formation of the first aromatic rings. This mechanism has high and low temperature branches. The evidence shows that the H atom concentration, vinyl radicals and acetylene play a significant role in the rate processes leading to particle formation. The initial ring formation rate determines the mass evolution of soot because the growth of the PAH's soot inception, soot particle growth, etc, remain unchanged for a given fuel and represent processes that are controlled by the formation of the first few rings. More specifically, the rate of formation of the first rings is the rate controlling step to

soot formation".

This underlines the importance of fuel type to diesel combustion where in laminar diffusion flames the following sooting tendencies for fuel type exists:

Aromatics > Alkynes > Alkenes > Alkanes

The mechanisms of soot formation are complex and much work is still to be done before the processes are totally understood.

### 1.3 DIESEL EXHAUST EMISSIONS

The emissions from diesel engine have been reviewed in Section 1.1.1. Diesel particulate and unburnt hydrocarbons are of particular concern since they may offer a health risk and are perceived as an undesirable smokey input into the environment.

#### 1.3.1 UNBURNT HYDROCARBON EMISSIONS

Hydrocarbon emissions are composed of unburnt hydrocarbons (UHC) and partially combusted hydrocarbons. These in turn may both condense or adsorb onto soot particles, to form a soluble organic fraction (SOF) in an EPA dilution tunnel at 52°C. Griest and Caton (1983) have produced an excellent review of hydrocarbon extraction methods from DP. Primarily, four methods exist; solvent extraction, thermal extraction, extraction onto solid phases and digestion methods. Only solvent and thermal methods shall be discussed in this report, of which soxhlet extraction, ultrasonic extraction and vacuum sublimation (or thermal degassing) were employed. Comparison of extraction efficiencies between methods, rates ultrasonication above soxhlet extraction for efficiency and speed of extraction and equal to vacuum sublimation which is more time consuming. However, as will become evident in this work, thermal degassing

offers distinct advantages other the other methods and perhaps a hitherto unrealised higher hydrocarbon extraction efficiency.

The analysis of the hydrocarbon fractions has been widely reviewed as detailed by Trier (1988) in a parallel study. Usually the procedure has required separation according to polarity, followed by chromatographic separation of the complex hydrocarbon species, followed by a detection technique (e.g. electron capture, nitrogen selective thermonic detection, infra red spectroscopy, flame ionisation detection, mass spectrometry, ultra-violet spectroscopy) for individual compounds.

Considerable research has been applied to defining the sources of exhaust hydrocarbons so as to understand combustion. Andrews et al (1983) state that "SOF of particulate material in cooled diesel exhaust is principally partially pyrolysed fuel and constitutes 70-75% of the total UHC emissions". Trier et al (1987) however state that the Ricardo IDI engine of this study, produced 30-60% SOF from lubricating oil. It may be difficult to quantify the source of SOF but it is clear that fuel and lube oil both pass unburnt or partially pyrolysed through diesel engines to provide hydrocarbons (e.g. PAH's) in the exhaust.

UHC emissions originate from three primary sources; the lean mixture on a diffusion flame front, the nozzle sac emptying after injection, and the fuel rich mixture quenched during cylinder volume expansion (Greeves and Wang, 1981).

UHC emissions are also affected by ignition delay and by the temperature level in the main cylinder (Ikegami et al, 1983). Yu et al (1980) also detail further possible sources of UHC as being; local over-mixing, local under-mixing, bulk quenching, cyclic misfire, cyclic variation and the degree of interaction with the chamber walls. Their work shows that the formation of UHC is mainly controlled by transient fuel-air mixing and bulk quenching processes. UHC emissions depend on load and speed but not AFR (Lilly, 1984). The fraction of fuel appearing as UHC in the exhaust is greatest at light loads and retarded conditions, when the fuel is injected late in the combustion sequence. Fuel characteristics, such as aromaticity have also been shown to influence soot formation (Tosaka et al, 1989) and to directly affect ignition delay and exhaust emissions (Andrews et al, 1983; Mills et al, 1984).

Most diesel fuels contain a significant aromatic fraction and a small part of this includes PAC's. A selection of



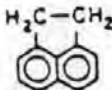
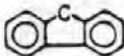
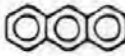

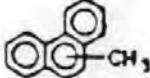





Molecular Mass	Name	Formula	Structure
128	Naphthalene	$C_{10} H_8$	
142	Methylnaphthalene	$C_{11} H_{10}$	
154	Acenaphthene	$C_{12} H_{10}$	
166	Fluorene	$C_{13} H_{10}$	
178	Anthracene	$C_{14} H_{10}$	
178	Phenanthrene	$C_{14} H_{10}$	
192	Methylphenanthrene	$C_{15} H_{12}$	
202	Fluoranthene	$C_{16} H_{10}$	
202	Pyrene	$C_{16} H_{10}$	
252	Benzo(e)pyrene	$C_{20} H_{12}$	
252	Benzo(a)pyrene	$C_{20} H_{12}$	
276	Benzo(ghi)perylene	$C_{22} H_{12}$	

Fig. 1.7 A Selection of Polycyclic Aromatic Hydrocarbons (PAH's) Identified in SOF Fractions from Diesel Particulate (Calcote, 1981)



PAH compounds are shown in Fig 1.7. The mass emission rate of PAC's from diesel exhausts are several orders of magnitude less than the input rate of fuel. This has led to the suggestion that PAC's are destroyed and not formed in diesel combustion processes (Williams, 1985). This group have also shown that when unburnt fuel is the main source of PAC in SOF then the PAC in the SOF varies directly with the levels of UHC. Wall and Hoekman (1984) however found no such correlation. This may not be contradictory since the former work assessed the fuel/PAC ratio with UHC/PAC ratio and the latter study considered absolute levels.

PAC's can be formed as a result of fuel combustion and are believed to be precursors in the formation of particles (Smith, 1981). They are clearly related and difficult to distinguish from UHC PAC's in the exhaust. Both fuel and oil have been proposed as sources of emitted PAC's. Lube oil acts as a sink for PAC's, with up to 85% of PAH in the cylinder scavenged by crankcase oil (Peake and Parker, 1980). Used engine oils have significant mutagenicity compared to unused oil (Warne and Halder, 1986) thereby indicating that this is derived from cylinder PAC's. Lube oil has been shown to correlate well with particulate emissions (Hilden and Mayer, 1984). Radio tracer work showed that an average lube oil consumption may be

0.25% of the fuel burnt but can rise to 25% at high speeds and low load (Mayer et al, 1980). The majority of lube oil forms SOF which has been estimated as 19-88% (Cartellieri and Tritthart, 1984), 32-95% (Hilden and Mayer, 1984), and 38-62% (Trier et al, 1987).

The formation of soot and PAC's are closely linked, albeit poorly understood. PAC's are known to be precursors of soot formation in both aliphatic and aromatic fuels (Prado and Lahaye, 1983).

### 1.3.2 DIESEL PARTICULATE EMISSIONS

The formation of DP depends on fuel type and engine stoichiometry, specifically temperature and equivalence ratio. DP (i.e. smoke) production is favoured in a high temperature fuel rich, diffusion flame environment, and is dependent on speed and load. Van Dell et al (1987) showed that in aromatic flames, particle size and specific surface area was related to equivalence ratio. Soots produced from the pyrolysis of o-dichlorobenzene had a particle size distribution which shifted from being bimodal at low equivalence ratios (<1.4) to being monodispersed (above >1.4), due to agglomeration, and increased in specific surface area (SSA) from <90m<sup>2</sup>/g to >300m<sup>2</sup>/g.

Ross (1981) studied EPA soots and determined a BET SSA of  $112.2\text{m}^2/\text{g}$ , and showed that preadsorbed layers (of UHC) altered the adsorption properties of DP.

Primary soot particles appear similar despite differing source combustion systems and their formation is often accompanied by the formation of a variety of high molecular mass hydrocarbons, which may become adsorbed or condensed onto the soot itself. The formation of diesel soot begins with a fuel molecule, typically of 12 to 22 carbon atoms and having a hydrogen/carbon ratio of about 2. This is transformed by pyrolysis and oxidation reactions into soot particles which contain upto  $10^6$  carbon atoms with mean particle diameters of 10-50nm and a hydrogen/oxygen ratio of 0.1. The carbon atoms are packed into hexagonal face-centered arrays commonly referred to as platelets (Abrahamson, 1977). The mean layer spacing is 0.355nm, slightly larger than graphite, and the density is between 1600 and 2000kg/m<sup>3</sup>. The platelets are believed to form crystallite layers (2-5 platelets per crystallite) with approximately 10 crystallites forming a spherical soot particle. This structure (similar to pyrolytic graphite) is thought to be responsible for its resistance to oxidation. Fig 1.8 shows the development of the structural system which correlates with the studies of Akhter et al (1984) who suggest a structure for

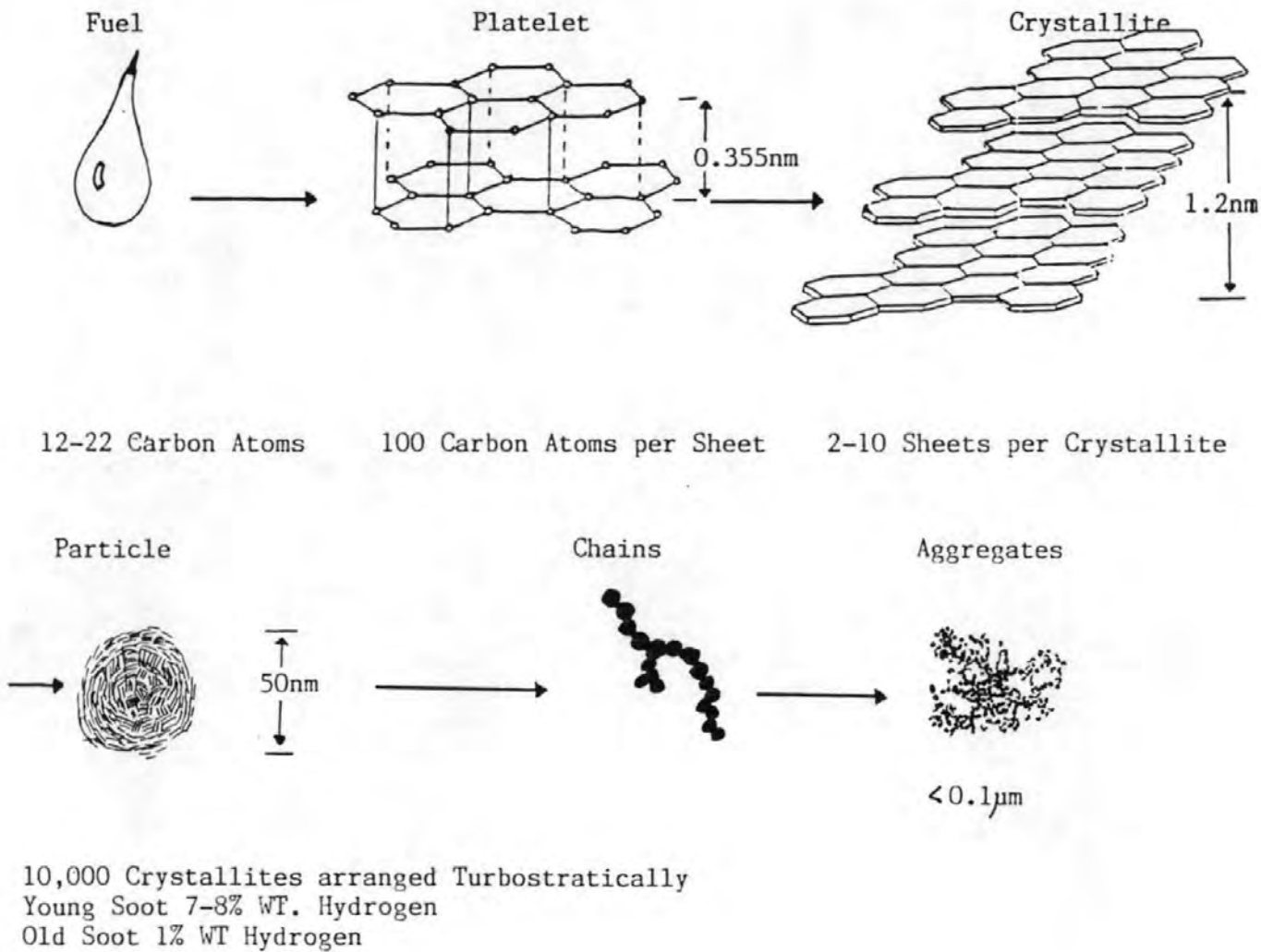


Fig. 1.8 The Structural System of Soot - Showing its Development from Fuel to Soot Aggregate (Smith, 1981)

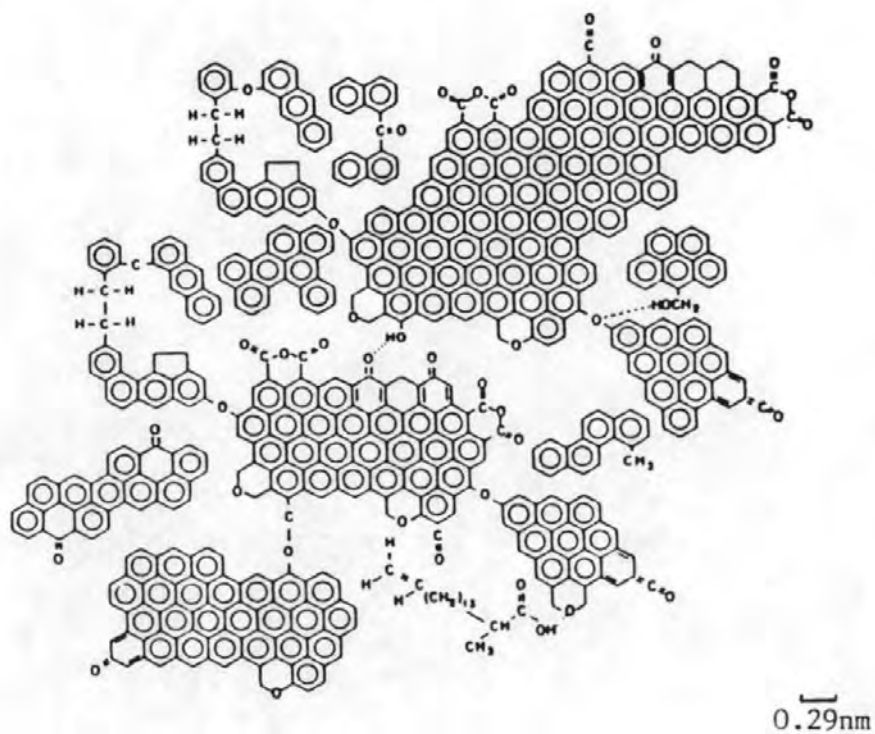


Fig. 1.9 Representation of Hexane Soot, with Occluded Substances, as Formed in Flames (Akhter et al, 1984)

hexane soot with occluded substances (Fig 1.9). Early work with X-ray diffraction indicated that the carbon platelet layers were merely randomly arranged, however recent high-resolution phase-contrast electron microscopy of similar carbon blacks have shown the turbostratic structure of lattices are arranged regularly around particle centers where the structure is less well ordered. Many dislocation and other lattice defects have also been noted and suggested as being adsorption sites. Heat treatment improves the internal order of the particles and reduces the interplanar spacing making it similar to graphite. The rate of graphitization (loss of hydrogen allowing better ordering) depends on the temperature so that the age of a particle and its degree of order are closely linked (Haynes and Wagner, 1981). Fresh soot has a higher hydrogen content and has considerable numbers of radicals as indicated by the high electron spin resonance of hexane soot platelets (Akhter et al, 1984). Electron diffraction indicates the presence of single C-C bonds in soot. Lahaye & Prado (1981) have reviewed the morphology and internal structure of diesel soots and have summarised much of the above information, and they suggest that diesel soots are very similar to carbon blacks. The soot particles in the exhaust form aggregates (straight and branched) which in turn form flocculates. The amount of soot formed in a combustion system is usually very small compared to the total carbon in the fuel.

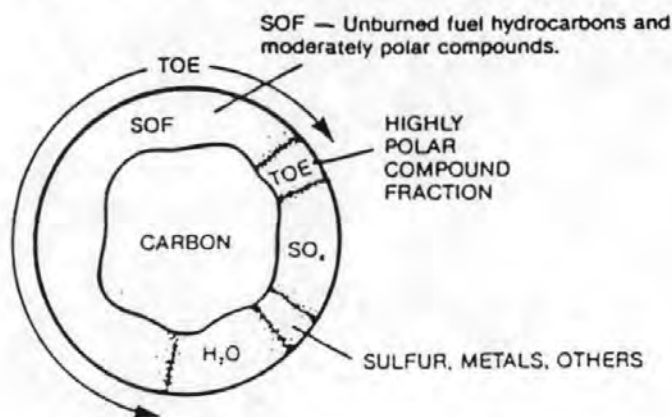


#### 1.4 THE PHYSICOCHEMICAL RELATIONSHIP BETWEEN SOOT AND PAH

Diesel particles are small agglomerates which show a strong adsorption affinity towards higher boiling point gaseous hydrocarbons emitted at the same time. The adsorbed species have been identified into distinct fractions according to extraction method and detailed by Perez et al (1984). Fig 1.10, describes some of these fractions and details a simplified model of a diesel particle. Of primary concern is the SOF and total organic extract (TOE), which are both removed by soxhlet extraction.

Amann's review (Amann et al, 1980) states that the SOF/Soot interaction process is primarily controlled by the two processes: condensation and adsorption. Condensation occurs when the vapour pressure of the gaseous hydrocarbons exceeds their saturated vapour pressure. The saturated vapour pressure varies with temperature and the boiling point of the hydrocarbon. Condensation is favoured in low dilution environments with low filter temperatures and high exhaust hydrocarbon concentrations. Plee and MacDonald (1980) found that condensation was most likely to be significant only if all of the hydrocarbons originated from the less volatile half of the lubricating oil, or if the unburned fuel had been transformed into higher boiling point hydrocarbons. Condensation fails to explain the existence of considerable SOF at standard engine

## DIESEL PARTICULATE COMPOSITION



### DEFINITIONS

TOTAL PARTICULATE MASS (TPM) — All material collected at  $52^{\circ} \pm 3^{\circ}\text{C}$  according to USEPA procedures.

SOLVENT EXTRACTABLE FRACTION (SEF) — Material removable by various organic and inorganic solvents.

COMBINED WATER — Water associated with sulfates and measured by drying TPM over drierite.

### SOLVENT EXTRACTABLE FRACTIONS

SOLUBLE ORGANIC FRACTION (SOF) — SEF removed by SOXHLET EXTRACTION with METHYLENE CHLORIDE.

TOTAL ORGANIC EXTRACT (TOE) — SEF removed by SOXHLET EXTRACTION with TOLUENE:ETHANOL.

WATER SOLUBLE SULFATES (SULFATES) — SEF removed by WATER and analyzed by ION CHROMATOGRAPHY.

### RESIDUAL CARBONACEOUS PARTICULATE (RCP)

$$\text{RCP} = \text{TPM} - \text{TOE} - \text{SULFATES} - \text{WATER}$$

Fig. 1.10 Diesel Particulate Composition. A Simple Model with Extractable Fractions. (Perez *et al*, 1984)

conditions, but may be more significant with higher concentrations of UHC in the exhaust.

Adsorption involves the adherence of hydrocarbon molecules to the surface of the soot particles by either chemical and/or physical (van der Waal's) forces. Clerc and Johnson (1980) and Plee and MacDonald (1980) all found that adsorption was the dominant mechanism controlling the collection of SOF by soot and fuel was the dominant source of hydrocarbons.

Various studies have been carried out using a modified Langmuir equation to examine the theoretical adsorption of PAH molecules on diesel particles (Kraft et al, 1982) and practical affects on carbons (Daisey et al, 1984; Ross et al, 1982). Kraft et al (1982) indicated that the portion of PAH adsorbed on the diesel particle is zero at 200°C rising to 98% at 52°C (Fig 1.11). They assumed that adsorption and desorption were in equilibrium and that the mole fraction Y of all PAH which were adsorbed on the particles could be calculated by the modified equation thereby relating the fraction of surface area occupied by the adsorbate to the partial pressure of the hydrocarbon gas and the temperature. The results are summarised in Fig 1.11 which shows the mole fraction Y varying with temperature.

Ross et al (1982) studied the isosteric heats of

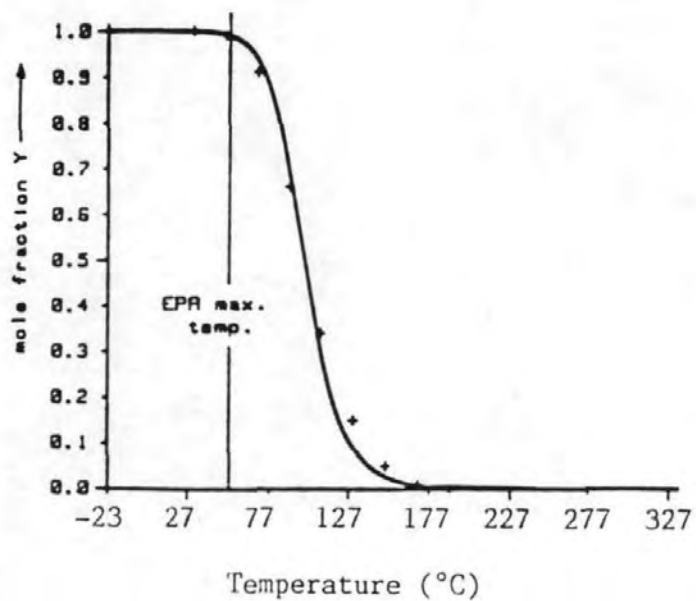


Fig. 1.11 Portion of PAH Adsorbed onto Diesel Particulate as a Function of Temperature in a Dilution Tunnel, for a Model by Kraft et al (1982)

adsorption of benzene on diesel particulate matter. He concluded that diesel soot contains high energy adsorption sites which become occupied by SOF. When a monolayer had formed, multilayer adsorption would occur requiring lower interaction energies. The molecules adsorbed onto the high energy sites would be tightly bound, but additional layers of adsorbed hydrocarbons might be more easily liberated.

It can be seen therefore that temperature influences adsorption. As these sites fill so multilayer adsorption occurs and these processes may be influenced by the adsorbate itself. However, these theoretical and simple experiments fail to examine actual exhaust particles produced from a variety of engine conditions.

## 1.5 OBJECTIVES OF THIS RESEARCH

- 1) To design and develop an experimental system capable of producing an artefact-free diesel particulate sample so that the interaction between DP and UHC may be examined in the exhaust at ambient temperatures.
- 2) To study the physical and chemical nature of the soot and UHC fractions of the DP.
- 3) To compare the emissions of UHC and soot from different types of engines (DI and IDI), when operated at different engine conditions.
- 4) To relate the research findings to the engine cylinder processes and environmental emissions, thereby producing results of significance for engine manufacturers and environmental scientists to aid in the formulation of control strategies.



## CHAPTER 2 DIESEL PARTICULATE FILTRATION

Filtration may be defined as the separation of solids from liquids and gases by passing a suspension through a permeable membrane medium which retains the particles (Svarovsky 1981). In this research diesel particles are suspended in a fast flowing high temperature exhaust gas stream of gaseous hydrocarbons and other gases. The objective of this research is to examine the physico-chemical relationship between the diesel particles (or particulate) (DP) and unburnt hydrocarbons (UHC) which may adsorb and/or condense onto the particles as exhaust gas temperature declines. It is therefore essential to maintain particulate integrity during filtration. In this study a significant amount of attention was given to the design and construction of an accurate sampling system and the selection of a suitable filter media.

Diesel combustion produces diesel soots which contain upto  $10^3$  carbon atoms with mean particle diameters between 5 and 100nm (Smith, 1981; Medalia and Rivin, 1982). These sub-micron sized particles may aggregate to form aciniform carbons having long chains of particles of an open fluffy structure. In addition, UHC from the partially pyrolysed fuel and lubricating oil are released. As exhaust temperature declines the highly porous carbonaceous DP may chemically adsorb (or condense) the UHC depending on individual hydrocarbon boiling

points. Concentrations of UHC and DP depend on engine condition (load, speed, timing etc) and engine stoichiometry which influences combustion temperature.

The research required the separation of DP from gaseous UHC to occur at a range of sample temperatures, pressures and locations down the exhaust system.

The filtration criteria were as follows:

- 1) To collect sufficient soot mass for physical and chemical analysis.
- 2) To collect a representative sample.
- 3) To prevent the formation of physical and chemical artefacts.

## 2.1 PARTICULATE ARTEFACTS AND FILTRATION SYSTEMS

Filter systems may be subject to physical and chemical artefact formation, that is the possibility of forming "false" particulate (matter formed, altered or destroyed by the filtration process) or chemically altering adsorbed UHC species. A recent report by the Diesel Exhaust Combustion Group of the Coordinating Research Council (CRC, 1980) reviewed published literature, particulate sampling data for dilution tunnel filters, and artefact formation. The group identified particulate filtration problems associated with engine produced mass emission variations, the sensitivity of measured particulate mass to dilution parameters, and random errors in the independent measurements which comprise a particulate measurement. They stated that no one filter could meet all sampling needs due to these problems and artefact formation. Furthermore, they identified several areas for further work, of which the need to investigate heat transfer reactions and particulate-hydrocarbon interactions between the exhaust valve and filter were of importance.

Chemical artefacts are changes to the organic species present in the exhaust via gas-phase chemical reactions, for example, enhanced nitro-PAH has been identified as a chemical artefact. Nitric acid is a trace constituent associated with the presence of nitrogen dioxide (Pitts et al, 1978) and may

cause the nitration of PAH in the exhaust. Filter methods (e.g. a dilution tunnel) usually have long sampling times when proportional splitting is employed. These long sampling times, of perhaps 45 minutes or more, may allow the nitrification reactions to occur on-filter. Schuetzle (1983) estimated that chemical conversion during dilution tunnel sampling accounted for 10-20% of the nitro-pyrene found in diesel exhausts. He also concluded that the problem of PAH loss and nitro-PAH formation during filtering on PTFE coated filters from a diluted exhaust containing less than 3 ppm NO<sub>2</sub>, could be minimised by using sampling times of <46 minutes and sampling temperatures of <43°C. Recent work by Williams (1985) emphasised that thermal decomposition and chemical reactions of PAH occur very rapidly above 200°C in the exhaust and that the life-times of some PAH species, could be very short. The influence of temperature and contact time between particles, filter and PAH during exhaust nitrification, does not appear to have been studied.

Sulphate and nitrate artefacts have been identified (CRC 1980). Sulphuric acid vapour has been shown to enhance the sulphate content of particulate, and this effect is directly related to the glass composition of the filter. Nitrate artefacts, both positive and negative changes to particulate mass, have been identified (Harker et al, 1977; Stevens, 1979). Nitrate variations were summarised by Shaw et al (1979) as

being from gaseous nitrates and nitrate loss due to on-filter reactions between the particulate and  $H_2SO_4$ .

Additional chemical artefacts might come from filter contamination during any solvent extraction and poor experimental technique.

Physical artefacts can be formed during filtration and particulate collection. One must ensure that during filtration, factors such as; dilution, back pressure, temperature, moisture content of filter, handling and sampling procedure do not unintentionally change the sample.

#### 2.1.1 DIESEL PARTICULATE SAMPLING SYSTEMS AND METHODS

A variety of sampling devices have been applied to diesel exhaust measurement and have been reviewed extensively (Lee and Schuetzle, 1983; Mills, 1983; Schuetzle, 1983; Stenburg et al, 1983). The Anderson Impactor (Vuk et al, 1976) has been used for diesel soot collection but failed to filter 80-90% of the smallest particles. Chan et al (1981) used an electrostatic precipitator to trap particles, but reactive ozone formed during corona discharge may transform the organic species adsorbed on the particles. The industrial techniques of cyclone and settling-tank separation suffer the problems of dilution, artificial condensation and cooling of the gas stream. Resin traps (e.g. Amberlite XAD-2 used by

Brörstrom-Lunden and Lindskog, 1985) have also been used for hydrocarbons after the filter, but may be subject to n-PAH artefact formation (as reviewed by Pellizzari et al, 1975). The dilution tunnel and solvent scrubbing techniques have been most commonly employed.

### 2.1.2 THE DILUTION TUNNEL

The majority of sampling systems follow the US Environmental Protection Agency (EPA) dilution tunnel layout (Schuetzle 1983) (Fig 2.1). It is designed to simulate the dilution of vehicle exhaust during the first couple of minutes in ambient air, after release from vehicles on the road. The process of dilution allows condensation of the majority of UHC onto the particles at 52°C, the rest passing through the filter. The dilution tunnel operates on the principle of diluting the whole exhaust, typically with a 12:1 flow of cold air, thereby reducing the gas temperature to 52°C. For regulatory purposes, soot mass measurements are taken by splitting the gas flow and filtering a small proportion of gas. Extraction of the UHC is typically by the soxhlet extraction technique (24 hours) using dichloromethane (DCM). Perez et al (1984) detailed the extractable fractions from dilution tunnel samples (Fig 1.10).

The dilution tunnel has many disadvantages; it has a long



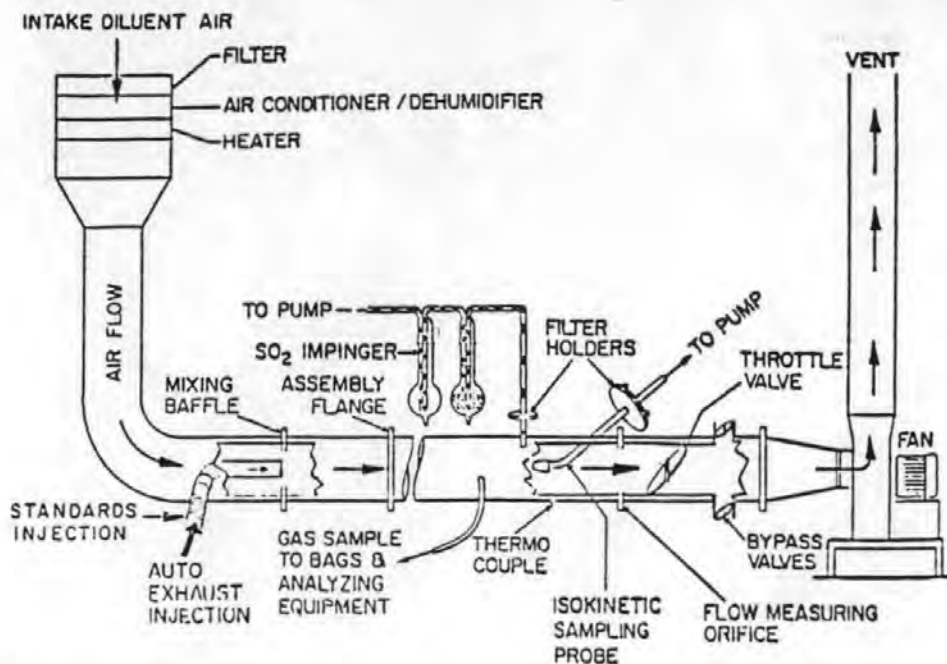


Fig. 2.1 The Typical Layout of a Dilution Tunnel (Schuetzle, 1983)

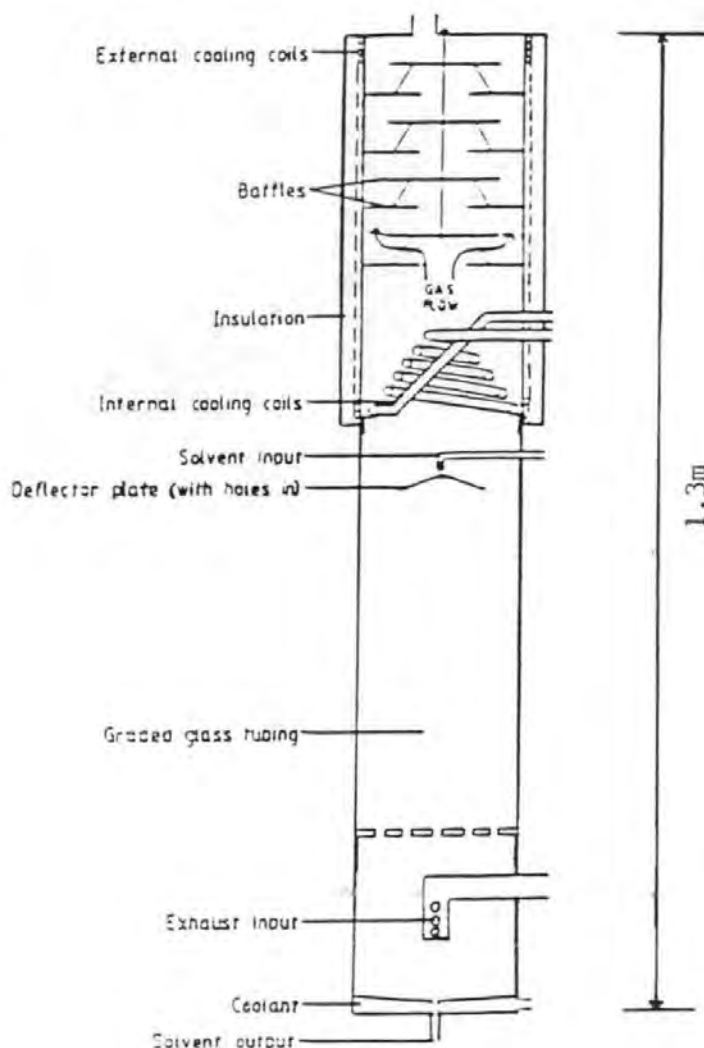


Fig. 2.2 The Stainless Steel Exhaust Scrubbing Tower (TESSA)

(Petch et al., 1987)

sampling time which enhances artefact formation, it is difficult to adapt to temperature studies, it is expensive to construct and operate, different tunnels have different dilution ratios and thus give variable results, and the soxhlet method fails to extract all of the available hydrocarbons. The dilution tunnel is largely a regulatory collection system for diesel particles.

This study required a filtration system that could rapidly collect sufficient DP mass to investigate the solid/gas reactions occurring at temperature as the DP travelled down the exhaust.

### 2.1.3 SOLVENT SCRUBBING SYSTEMS

Solvent scrubbing systems have been developed to collect UHC either in gaseous or DP-adsorbed form. Grimmer et al (1973) developed a vertical condenser system preceded by a large particulates filter. This was improved by Kraft et al (1981) facilitating better sampling and Stenburg et al (1983) who used a cryogradient technique for sampling part of the raw exhaust. A more effective method was detailed recently by Petch et al (1987) who employed the Total Exhaust Solvent Scrubbing Apparatus (TESSA) which stripped gaseous UHC into solvent. This method for hydrocarbons, developed at Plymouth (Fig 2.2), suffered from glass fragment and rust contamination

of DP mass caused by the exhaust gas abrading the internal graded glass tubing, thus making it unsuitable for DP mass emission studies. Furthermore, this research has suggested that TESSA is appropriate for the extraction of gaseous UHC and surface adsorbed species, but fails to extract tightly-bound microporous UHC. These methods do not study the interaction of UHC on DP because they extract adsorbed hydrocarbons from the particles before particle analysis.

#### 2.1.4 HOT WHOLE EXHAUST FILTRATION

The alternative methods failed to meet the filtration criteria, because they did not collect a representative sample of sufficient mass and sample integrity, in an environment that allowed investigation of the physico-chemical relationship between the DP and UHC compounds at ambient temperatures. To do this, the technique of hot whole exhaust filtration was developed to produce an artefact-free soot sample, filtered at exhaust gas temperatures to study both the particle microstructure and chemical composition in the exhaust, a system which overcame the deficiencies of the dilution tunnel and TESSA.

## 2.2 FILTER MEDIA

Collection of diesel particles is influenced by engine condition and the characteristics of the filter media. Since it is the former which is under analytical investigation it was prudent to find out how the filter might affect measurements of engine performance. Quantitative filtration (by mass) has been shown to be influenced by such characteristics as media construction, moisture retention, adsorption of organic (dibutyl phthalate) vapour and fibre blow-off during particle collection (CRC 1980).

Particle collection efficiency is influenced by filter porosity and particle size. Two filtration mechanisms occur, often co-existing; caking (Fig 2.3) and depth filtration (Fig 2.4). Caking occurs with a surface filter, when particles of the same size or larger than, the pore openings, wedge into these openings and create smaller passages which remove even smaller particles from the gas stream. With a depth filter, the particles are smaller than the filter medium openings and may proceed through relatively long and tortuous pores before being trapped internally (Svarovsky 1981). In this research the Pallflex medium (Fig 2.5) showed some surface filter action to the sub-micron sized particles and gave high collection efficiencies. However some particles were still buried within its matrix. Unfortunately these buried particles may contribute

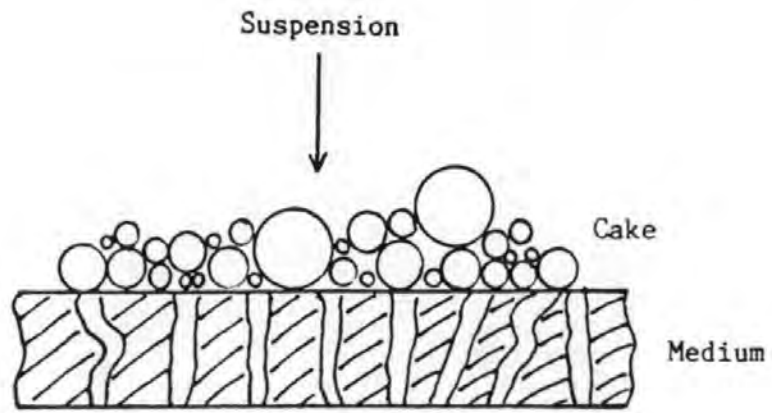


Fig 2.3 Mechanism of Cake Filtration

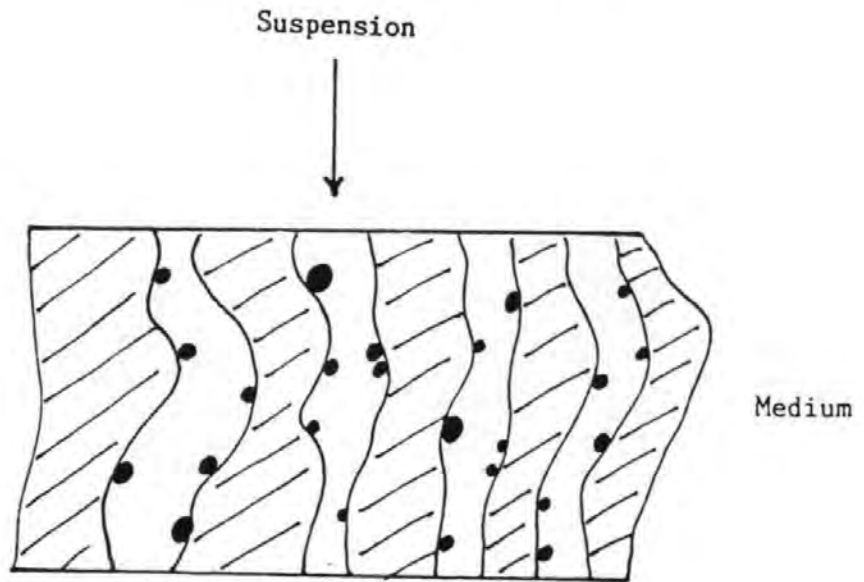


Fig 2.4 Mechanism of Depth Filtration

(Svarosky 1981)

significantly to soot mass and surface area measurements. Filtration for hydrocarbons employed the Box Cassette Filter and Whatman QM-A filter (Fig 2.6) which showed depth filtration characteristics.

Diesel engines produce particles in the sub-micron range, often associated with high levels of moisture and organic vapour. For these reasons, mass measurements and efficiencies must be carefully examined. The results of the CRC survey, indicated that no one filter was ideal for all potential filtration requirements, and that the selection of a filter media depended upon it's application. Different media showed different sensitivities to selected test variables. The factors of particulate collection efficiency, pressure drop, moisture sensitivity, blow-off, commercial availability, and handling ability were all important considerations in the choice of filter.

Filter composition proved an influential constraint on selection. Filters with synthetic polymers show high organic vapour pickup, whereas glass fibre and PTFE filters do not, but the glass fibre media, do have a high moisture retention potential (CRC 1980). The report selected four of the most promising media, of which the Pallflex T-60 was included. The Pallflex EMFAB TX-40 medium used in this research is identical to the T-60 filter varying only in density and higher sub-micron particle collection efficiency, which caused higher

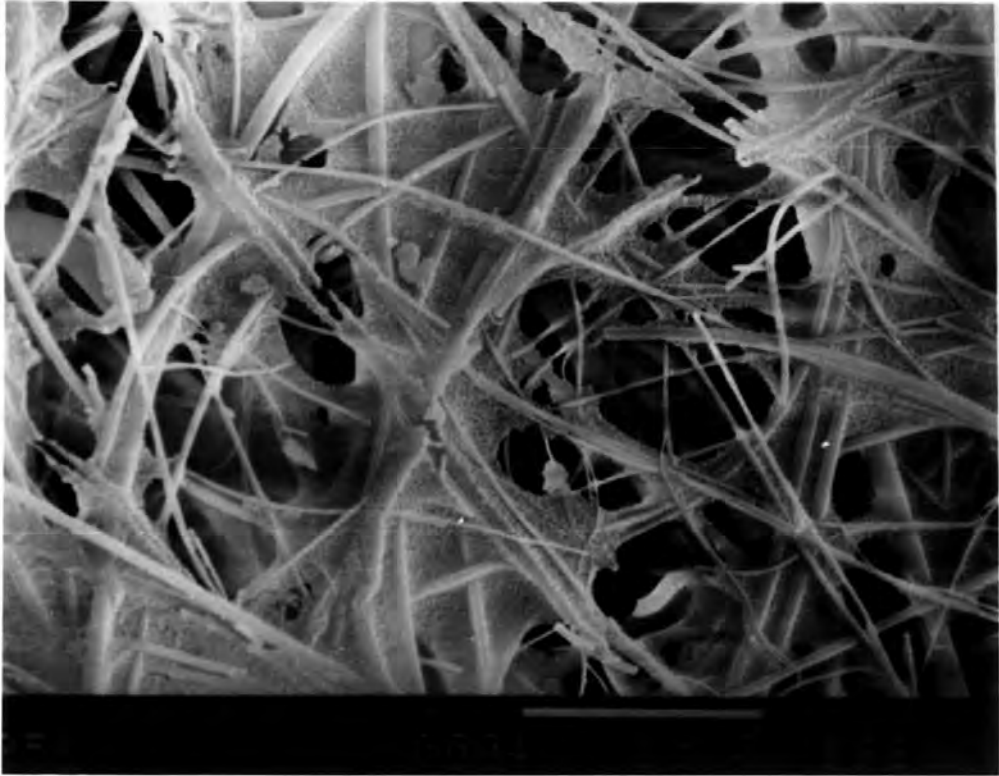


Fig. 2.5 TX-40 Pallflex Filter. Electron Micrograph Showing Borosilicate Glass Fibre with Teflon Webbing.  
(1 bar = 10 $\mu$ m)

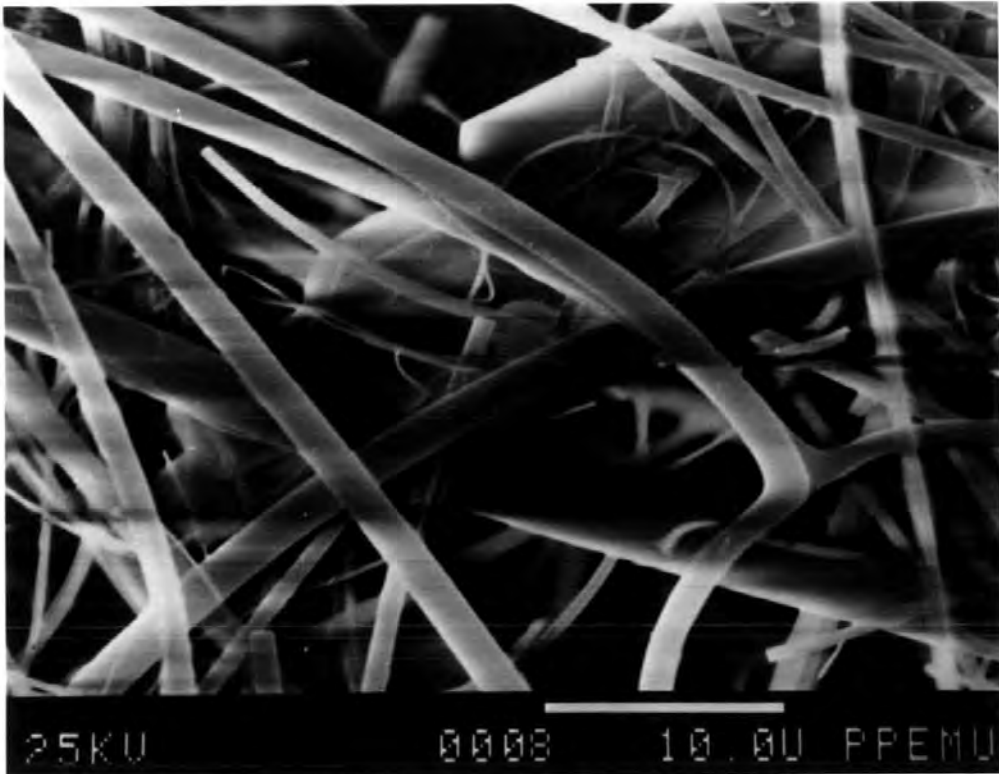


Fig. 2.6 QM-A Whatman Filter. Electron Micrograph Showing Pure Quartz Filter.

(1 bar = 10 $\mu$ m)

pressure drops for nearly dispersed DOP (dioctyl phthalate) particles (Kittelson et al, 1984). Kittelson and co-workers showed that the pressure drop was a function of loading, not filter media type. The fluorocarbon-based filters are currently required for particulate collection in EPA emission certification of light-duty diesel engines and unlike glass fibre filters do not catalyse the oxidation of soot (Lin and Friedlander, 1988). The choice of filter media was shown by Lindskog et al (1987) not to catalyse the chemical nitrification of PAH although it might alter the chemical species in other ways. Lee et al (1980) demonstrated that glass-fibre filters enhance the oxidation of benzo(a)pyrene.

#### 2.2.1 RATIONALE FOR FILTER SELECTION

Selection of a suitable filter media depends on the purpose of the sample. In this study the media needed a low reactivity to prevent artefact formation, to have a sufficient collection efficiency for sub-micron sized particles, and yet not to be prone to excessive pressure drops which may break the filter or alter loading rate.

Choice of filter changed with filter system development. Initially, Whatman QMA (Fig 2.6), a high purity quartz filter was used for reasons of availability, resistance to chemical degradation, low nitrate and sulphate artefact formation



potential, and would collect particles of the size  $>0.6\mu\text{m}$  with a retention level of 99%. This medium however was moisture sensitive (measured thermo-gravimetrically as being 0.6% w/w), was physically weak and proved inconsistent in sampling, often suffering considerable blow-off and break-up effects when exposed to high gas velocities. It operated by the depth filtration mechanism with considerable DP burial.

The EPA selected the Pallflex EMFAB TX-40 type of medium (Fig 2.5) for light-duty diesel vehicle certification. It has a filter efficiency of 99.8% for particles of  $>0.035\mu\text{m}$  size range, which was found to be the size of incipient diesel particles. It was thermally stable to  $440^{\circ}\text{C}$  (measured thermo-gravimetrically at s.t.p), more durable than the QMA medium having a stronger weave pattern. The addition of fluorocarbons (PTFE) formed a web between fibres, so reducing pore size. This media resisted organic and moisture-gas reactions, having a low moisture content (experimentally measured at 0.2% w/w). A summary of filter properties is listed in Table 2.1.

	WHATMAN QM-A	PALLFLEX TX-40
Base Weight	85g/m <sup>2</sup>	55.6g/m <sup>2</sup> ±20%
Thickness	0.45mm	0.125mm-0.24mm
Bulk Density	180kg/m <sup>3</sup>	280kg/m <sup>3</sup> -360kg/m <sup>3</sup>
X-ray Density	2250kg/m <sup>3</sup>	2080kg/m <sup>3</sup>
Composition	Ultra-pure Quartz (Si O <sub>2</sub> )/5% Borosilicate Glass Fibre	Pure Borosilicate Glass Fibre bonded with Teflon Fluorocarbon (TFE)
Temperature Resistance	500°C at s.t.p.	440°C at s.t.p.
Particle Retention	99.9% of 0.6µm particles at 5cm/sec face velocity	99.9% of 0.035µm particles at 5cm/sec face velocity
Special Properties	Low Nitrate and Sulphate Artefact Formation due to Purity	Resists Moisture/Gas reactions due to Teflon
Moisture Content (determined experimentally)	0.6% w/w	0.2% w/w
Specific Surface Area (SSA)	----	2.47m <sup>2</sup> /g ±5%

Table 2.1 Technical Data on the Filters used in this Research.  
(Whatman and Pallfex Inc, 1988)

### 2.2.2 FILTER HANDLING PROCEDURE

For chemical analysis, QMA filters were pre-extracted by solvent elution in a TLC tank (with DCM) and then equilibrated at a relative humidity of 60%, to a constant weight, in a light sealed box. The Pallflex TX-40 media, being more chemically resistant were not pre-extracted and only equilibrated. All filters were weighed before exposure to the exhaust, and after exposure were re-equilibrated and re-weighed to obtain a DP mass loading.

Mass data was taken using the TX-40 medium because it was less sensitive to moisture and was used to collect soot over longer sampling times. Chemical analysis was initially performed on the QMA filters, but later using the Improved Cassette Filter System, TX-40 media were employed for the thermal degassing (TD) chemical extraction method.

Details of the experiments carried out with each media type are presented in Chapter 3. Recently obtained data (Kittelson et al, 1984) suggested that membrane filters (e.g. Zefluor) might be more advantageous for future work. Membrane filters have well defined pore structures and particle collection is therefore mostly by the surface filtration mechanism, which should be easy to remove by mechanical means thereby avoiding lengthy solvent extraction methods.

## 2.3 ENGINE FACILITIES

### 2.3.1 RESEARCH ENGINE RICARDO E6/T

This research employed the use of a Ricardo E.6/T single cylinder, four-stroke, poppet valve, reciprocating internal diesel combustion engine with a compression ratio of 22:1, cylinder bore of 72mm and a piston stroke of 105mm (Fig 2.7) (see Trier, 1988 for full details). The engine had a Comet Mk.V swirl chamber head, which is connected to the compression cylinder by a narrow passage and thus is defined as indirect injection (IDI). The standard fuel used was BP gas oil (a class A2-Derv, BS-2861970) with the following physical characteristics; density  $840\text{kg/m}^3$ , sulphur content 0.5%, boiling point range  $200\text{-}360^\circ\text{C}$  and a viscosity of 35sec (on Redfern Scale). The lubrication oil was Shell Rimula X (15/40) with a density of  $887\text{kg/m}^3$  (at  $15^\circ\text{C}$ ), aromatic content of 25-30%, close-flash point of  $208^\circ\text{C}$  and a sulphated ash content of 1.3%. The engine was set on a fixed bed with a hydraulic dynamometer for steady state engine operation.

Before each sampling session the engine was preconditioned to its maximum operating condition to preheat the combustion chamber (3000rpm speed, 24.7Nm load,  $80^\circ\text{C}$  circulating water, 60 minutes) and then stabilised to the required engine state. Single cylinder engines are notorious for their variable

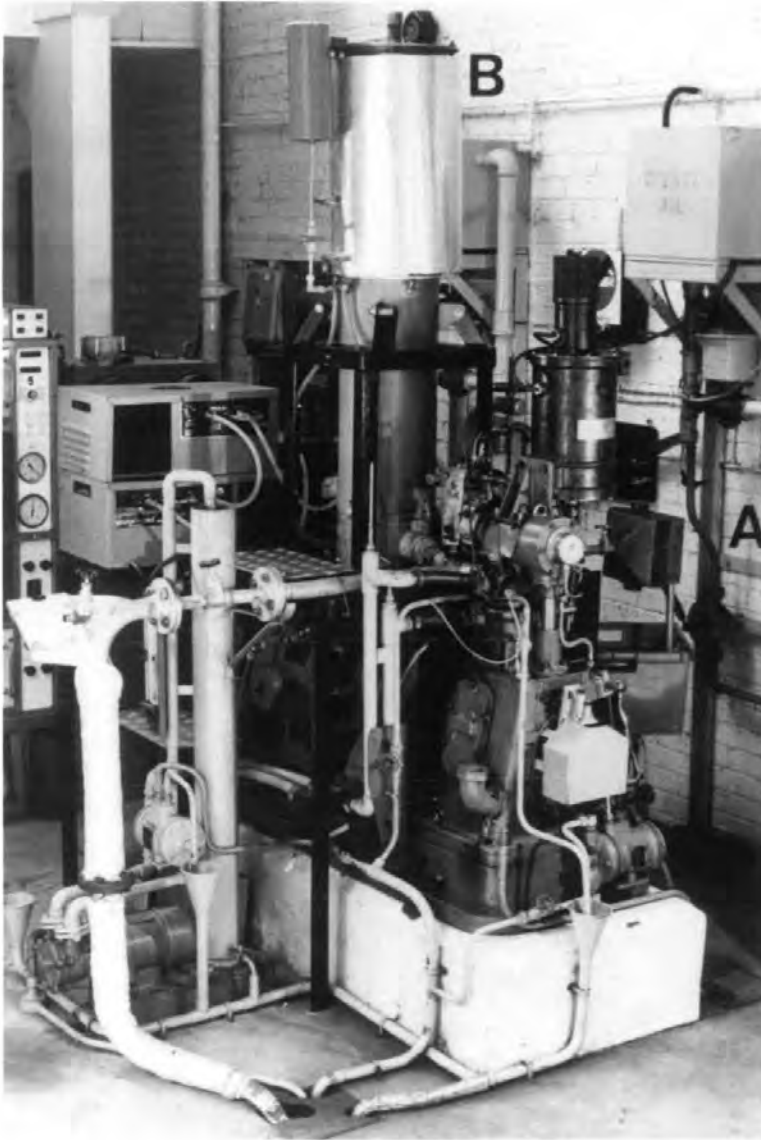


Fig. 2.7 The Ricardo E6/T Diesel Research Engine with BCF Unit 'A' and TESSA 'B' in situ.

performance and are difficult to stabilise, particularly at low loads. The Ricardo E6/T engine was used for development of the filter system, culminating in numerous experimental series using the Improved Cassette Filter (ICF).

### 2.3.2 RESEARCH ENGINE FORD

A Ford, four cylinder (2.5l) in-line OHV, four-stroke reciprocating engine with a cylinder bore of 93mm, piston stroke of 90mm, compression ratio of 19:1 and direct injection (DI), was also employed for samples. It used the standard fuel and lubrication oil and was coupled to a Froud hydraulic dynamometer.

This engine (at the time of thesis submission) had just been commissioned, and therefore only preliminary comparisons with the Ricardo E6/T engine are reported. Samples were collected with the ICF using the same sampling procedures outlined for the Ricardo engine. The ICF was connected to the exhaust system by an approximate 75% split, to collect DP samples for analysis. Further details may be found in later chapters and under Experiment 4A.

### 2.3.3 ANCILLARY EQUIPMENT

Additional devices were available to monitor engine performance and exhaust emissions;

- 1) Inductive needle lift transducer (Cussons)
- 2) Degree marker system for engine timing (Cussons)
- 3) Piezo pressure transducer in-cylinder (Cussons)

The data generated by the instruments were captured by a Transient Recorder (Datalab) which obtained single 'snap' shots of the engine cycle at any desired engine condition. A Gould Oscilloscope and Apple IIe micro computer were available for data recording and presentation.

Exhaust gas analysis was performed with a Lamdascan (Cussons), which gave a continuous and direct measurement of mass air/fuel ratio, equivalence ratio ( $\lambda$ ), and residual oxygen, together with a Long Line Emissions Trolley loaned by Perkins Technology Business, which gave continuous and direct measurements of CO, NO<sub>x</sub>, and HC in the exhaust. These emissions trolleys were fitted to the exhaust system by heated sample lines (at 180°C to 190°C) and protected by a heated sample filter (which removed particles but not gaseous hydrocarbons). The HC levels were measured by a heated flame ionisation detector (HFID), the NO<sub>x</sub> levels by a chemiluminescence system and the CO levels by non-dispersive infra-red, the theory of which was reported by Wheeler (1984). The emissions data was used to select the sampling conditions.

#### 2.3.4 RICARDO EMISSION MAPS

A variety of engine parameters were measured over the full range of engine conditions to provide a standard set of operating conditions from which to carry out further research. The results presented in Table 2.2 show the parameters measured for the Ricardo engine. No emissions data base had been obtained for the Ford engine at the time of thesis submission. The exhaust emissions (HC, CO, NO<sub>x</sub> and Bosch Smoke N<sup>o</sup>) were plotted on contour maps (Figs 2.8-2.11), by Perkins Technology Business. These emission maps were used to set the sampling conditions so that reproducible samples were obtained.



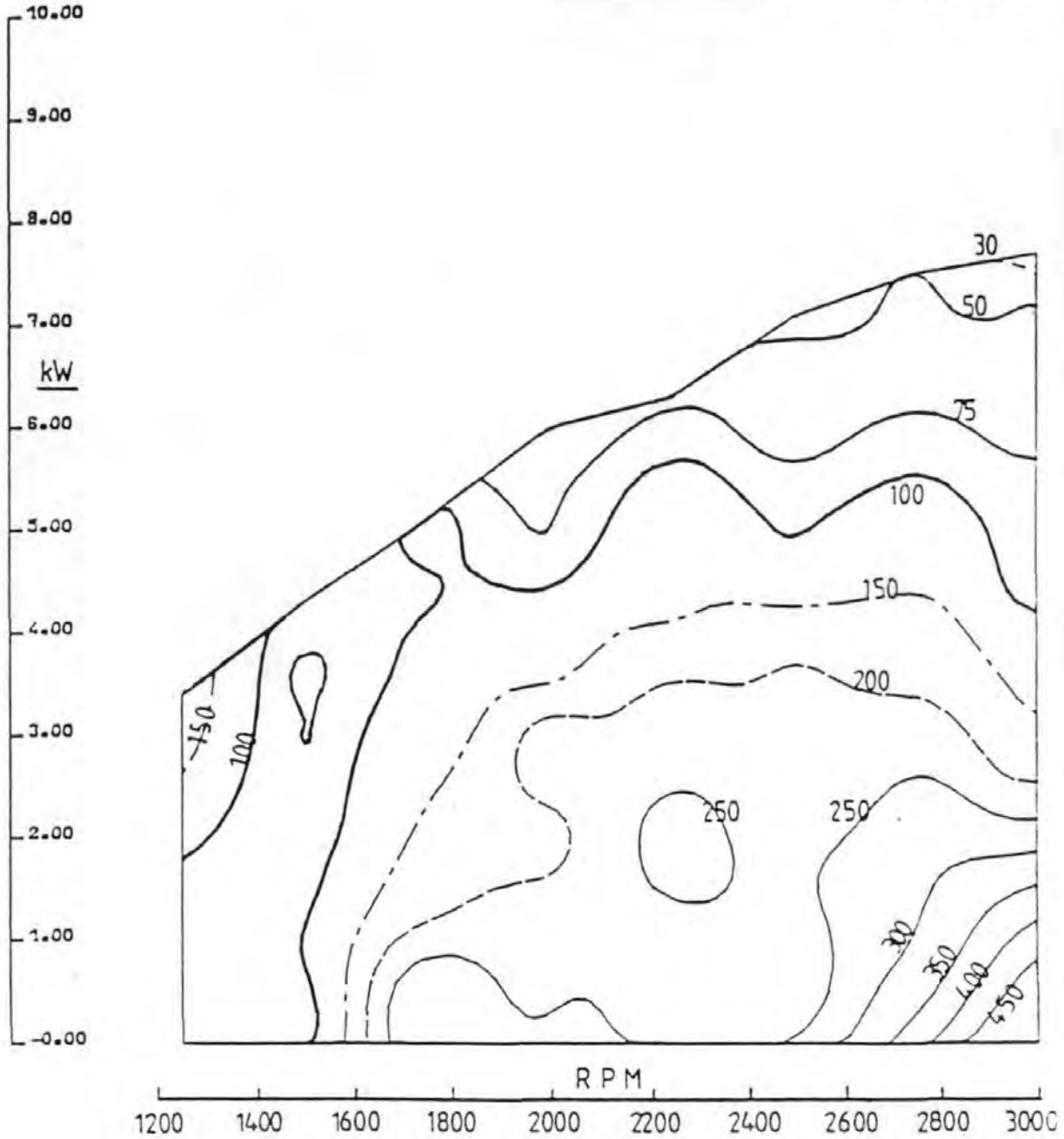
SPEED rpm	LOAD Nm	HC ppm	NO ppm	CO ppm	AFR	LAMBDA	OXYGEN %	FUEL cm <sup>3</sup> /min	INJECTION TIMING		BOSCH N°
									Start deg BTDC:	Finish deg ATDC:	
3000	1.6	490	129	330	48.4	3.3	14.3	19.4	4.0	37.0	0.7
3000	9.1	165	329	220	32.5	2.2	11.3	27.8	4.0	38.0	1.1
3000	13.7	95	431	210	26.6	1.8	9.2	34.1	4.0	40.0	1.5
3000	18.3	75	503	220	22.4	1.6	7.3	41.1	3.0	42.0	5.6*
3000	22.9	50	586	420	18.3	1.2	4.0	50.0	3.0	43.0	3.2
3000	24.7	25	718	800	16.4	1.1	2.1	55.6	3.0	43.0	4.6
2750	1.6	330	120	235	53.2	3.7	14.9	16.3	5.0	32.0	0.6
2750	9.1	250	347	160	35.2	2.4	12.3	23.6	7.0	34.0	0.8
2750	13.7	170	515	60	29.3	2.0	10.2	28.8	6.0	35.0	1.0
2750	18.3	110	550	150	24.0	1.6	7.9	35.7	5.5	36.0	1.7
2750	22.9	60	718	220	19.3	1.3	4.8	43.5	5.0	38.0	2.9
2750	25.6	50	688	900	17.1	1.2	2.8	49.2	5.0	39.0	3.6
2500	1.6	230	120	250	60.0	4.0	15.6	13.4	8.0	28.0	0.3
2500	9.2	220	347	160	36.5	2.5	12.9	20.3	8.0	30.0	0.5
2500	13.7	205	461	230	31.3	2.1	10.8	23.3	8.0	30.0	0.8
2500	18.3	105	539	270	25.0	1.8	8.7	31.2	8.0	31.0	1.6
2500	22.9	60	580	200	21.0	1.4	6.1	37.0	7.0	33.0	2.3
2500	26.5	45	652	875	17.3	1.2	3.2	44.1	7.0	34.0	4.1
2250	1.6	235	138	210	62.0	4.3	15.7	11.5	8.0	23.0	0.2
2250	9.1	260	371	195	38.0	2.6	12.6	18.3	9.0	25.0	0.7
2250	13.7	220	461	230	31.7	2.2	10.9	22.6	9.0	26.0	1.0
2250	18.3	140	527	265	26.2	1.8	9.0	27.3	9.0	27.0	1.1
2250	22.9	115	556	210	21.6	1.5	6.5	32.6	8.0	29.0	1.9
2250	28.8	70	634	250	18.9	1.3	4.6	37.5	7.0	30.0	3.3
2000	1.5	250	144	170	64.0	4.3	15.9	9.9	9.0	18.0	0.1
2000	9.3	190	455	140	38.7	2.7	12.9	16.0	10.0	19.0	0.7
2000	14.2	225	503	220	32.0	2.2	11.1	19.0	10.0	20.0	0.8
2000	18.7	125	574	210	26.5	1.8	9.1	23.8	10.0	22.0	0.8
2000	23.6	80	574	240	23.2	1.6	7.4	27.8	10.0	24.0	1.5
2000	29.5	50	562	380	18.0	1.2	3.6	36.1	10.0	25.0	2.7
1750	1.6	310	203	170	65.0	4.5	16.1	8.7	11.0	12.0	0.1
1750	9.1	165	514	110	38.5	2.7	12.7	14.2	12.0	16.0	0.2
1750	14.6	145	532	120	32.6	2.2	11.3	16.8	13.0	16.0	0.3
1750	18.3	110	568	135	27.4	1.9	9.4	20.4	13.0	17.0	1.5
1750	22.9	100	503	195	23.5	1.6	7.8	23.8	13.0	19.0	1.7
1750	27.9	105	503	375	19.8	1.4	5.4	28.8	14.0	21.0	3.1
1500	1.3	90	273	105	60.3	4.7	16.3	7.1	15.0	12.0	0.1
1500	9.1	95	473	95	43.3	3.0	13.7	11.0	17.0	10.0	0.1
1500	13.7	75	485	100	35.7	2.5	12.2	13.5	17.0	12.0	0.6
1500	18.3	75	449	179	30.0	2.1	10.3	16.4	16.0	14.0	1.7
1500	22.9	70	407	225	25.6	1.8	8.7	19.4	15.0	16.0	2.7
1500	27.4	95	323	460	20.4	1.4	5.9	24.6	15.0	20.0	4.5
1250	1.4	90	263	110	71.7	4.8	16.5	5.6	19.0	7.0	0.1
1250	26.5	180	437	205	22.4	1.5	6.9	20.0	18.0	16.0	4.5
1000	26.5	120	443	190	21.3	1.5	6.4	16.1	19.0	12.0	0.1

POWER may be calculated in kw:  $\text{Power (kw)} = \frac{\text{Load (Nm)} \cdot \text{Speed (rpm)}}{9549}$

Table 2.2 Ricardo Emission Data for Emission Maps

KEY TO PROFILE VALUES

-----	30.0000
=====	50.0000
=====	75.0000
=====	100.0000
- - - - -	150.0000
-----	200.0000
=====	250.0000
=====	300.0000
=====	350.0000
=====	400.0000
=====	450.0000

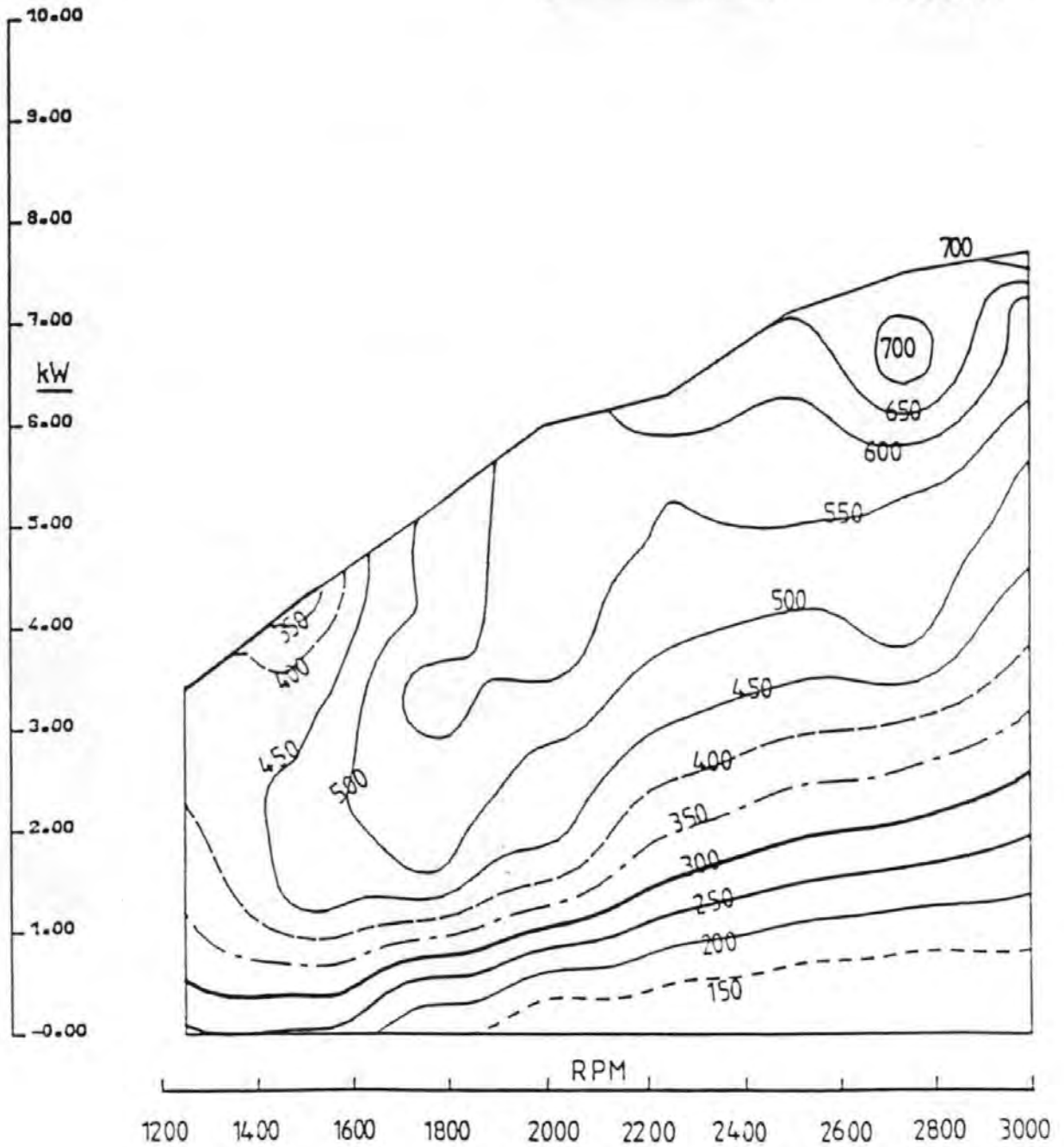


ISO-HC EMISSIONS VPM. RICARDO E6 ENGINE.

Fig. 2.8 Ricardo Hydrocarbon Emission Map

KEY TO PROFILE VALUES

-----	150.000
=====	200.000
=====	250.000
=====	300.000
-----	350.000
-----	400.000
=====	450.000
=====	500.000
=====	550.000
=====	600.000
=====	650.000
=====	700.000

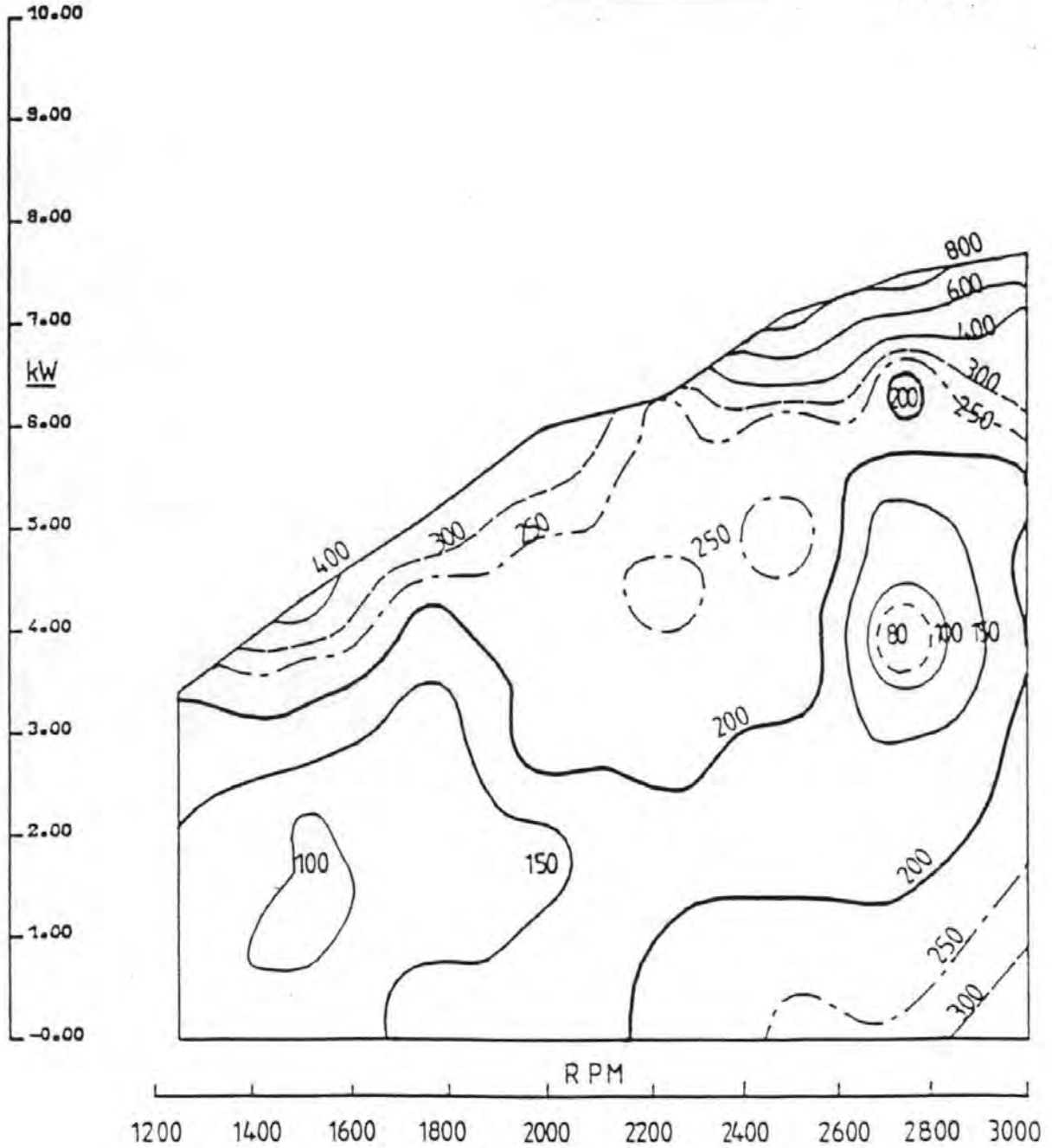


ISO-NOx EMISSIONS UPM RICARDO E6 ENGINE.

Fig. 2.9 Ricardo Oxides of Nitrogen Emissions Map

KEY TO PROFILE VALUES

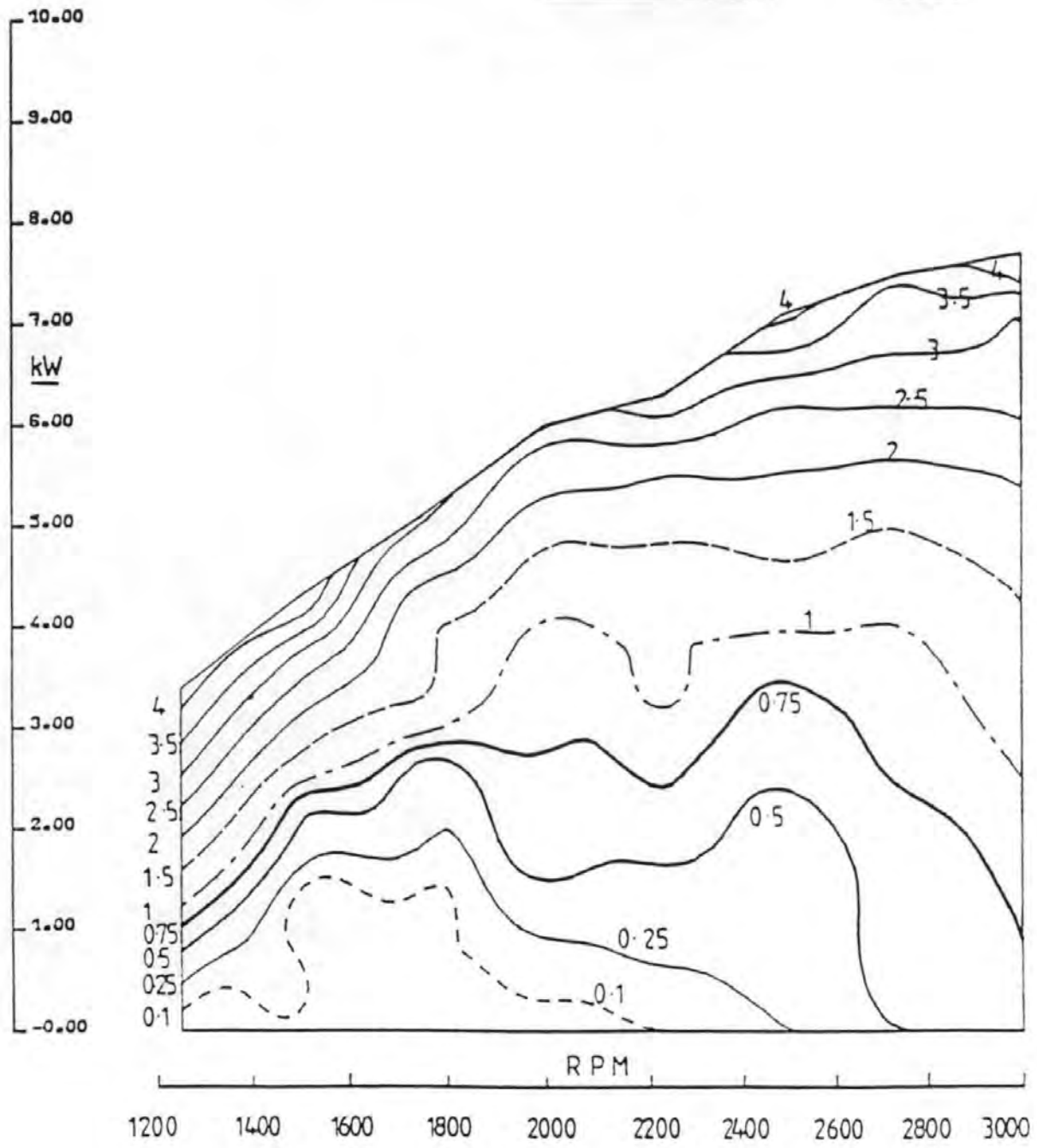
-----	80.000
=====	100.000
=====	150.000
=====	200.000
-----	250.000
-----	300.000
=====	400.000
=====	600.000
=====	800.000



ISO-CO EMISSIONS VPM RICARDO E6 ENGINE.

Fig. 2.10 Ricardo Carbon Monoxide Emission Map

-----	0.100
-----	0.250
-----	0.500
-----	0.750
-----	1.000
-----	1.500
-----	2.000
-----	2.500
-----	3.000
-----	3.500
-----	4.000



ISO-BOSCH SMOKE RICARDO E6. PLYMOUTH POLYTECHNIC

Fig. 2.11 Ricardo Bosch Smoke N° Emission Map

## 2.4 FILTER SYSTEM DESIGN

The filtration programme dictated that the filter design should collect sufficient soot for thermogravimetric and chemical analysis at all engine conditions and that the sample should be free of physical and chemical artefacts. The system had to give reliable results, measure all relevant parameters, be easy to use for rapid sampling and the sample should be taken from a variety of sampling positions. These objectives were achieved over a 3 year period after extensive prototype development. Some of the filter designs were inherited from a previous worker. All designs were employed with the Ricardo E6/T engine. The Ford engine exhaust was only filtered with the Improved Cassette Filter.

### 2.4.1 MINI CASSETTE FILTER

This small brass filter was constructed to provide samples for electron microscope studies. The exhaust sample was collected via a sample probe using vacuum suction onto a small QMA filter. This method could not collect sufficient sample mass for thermo-gravimetric analysis. The Mini Cassette Filter is shown in Fig 2.12.

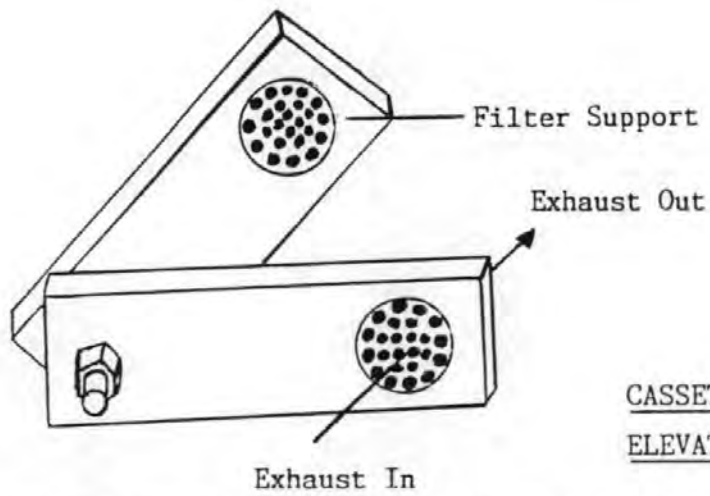
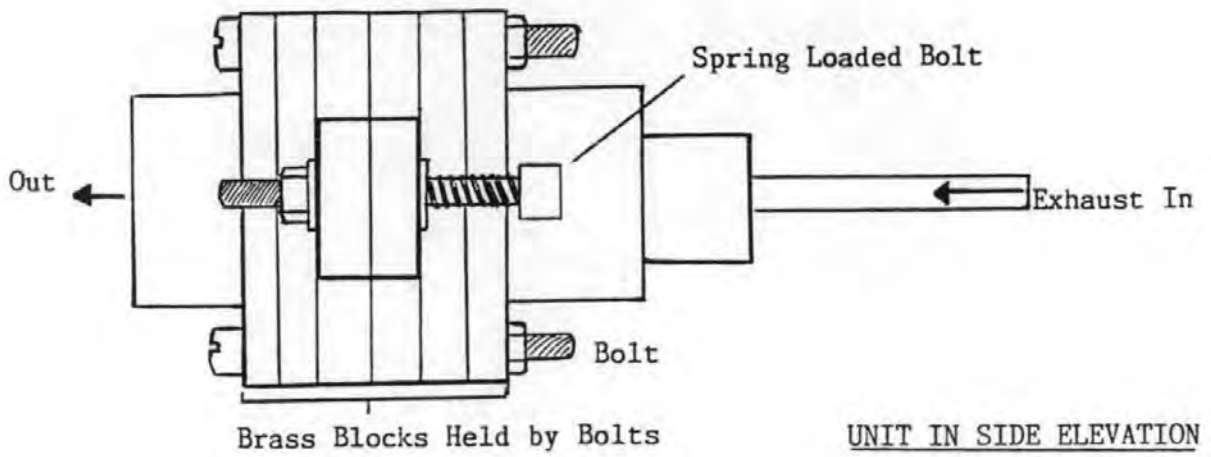


Fig. 2.12 The Mini Cassette Filter with Cassette in View (To Scale)

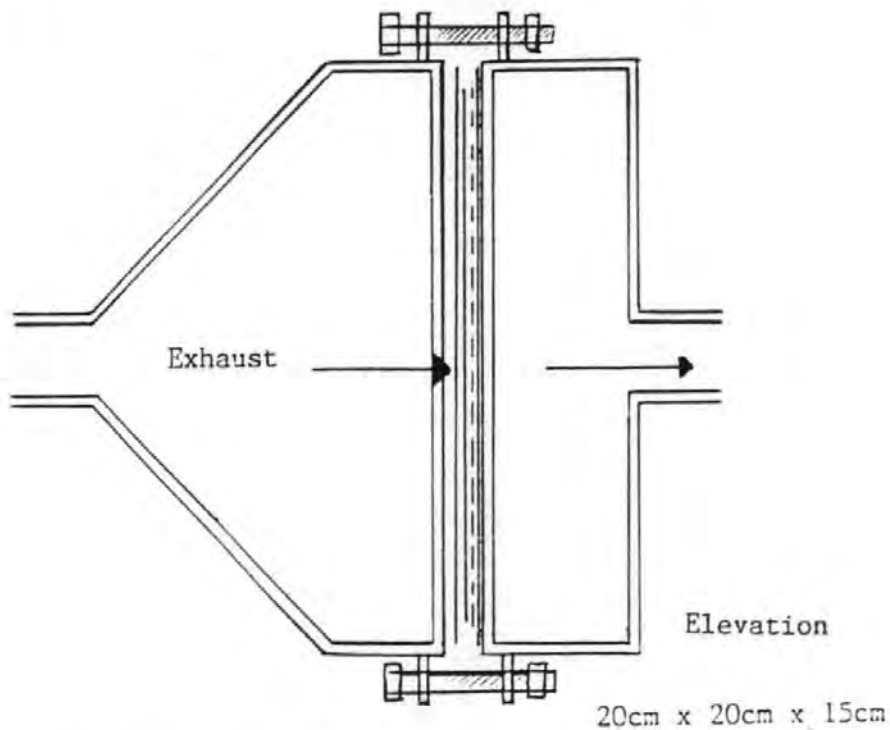


Fig. 2.13 The Box Filter Design.

#### 2.4.2 BOX FILTER SYSTEM

A series of box filter designs were considered and constructed. The final design is shown in Fig 2.13. In-house design and construction was considered the most feasible method for development because of budget constraints and the need for a flexible design approach. Early designs suffered from poor operation and a tendency for the filter to break during sampling. Investigation into filter disintegration concluded that the pulsating nature of the exhaust, from the single cylinder engine, caused fibulations of the filter surface leading to breakage. Gas velocity was also important and although not measured, the narrow exhaust pipe (2cm diameter) of the early work, increased gas flow magnifying the fibulation and disintegration problem at high speeds and gas velocities. This problem was partially overcome by applying a 600W vacuum pump (gas flow 32 l/min) behind the filter to reduce filter vibration. The vacuum pump was protected from the hot exhaust gases by a heat exchanger. The vacuum had no measurable effect on engine performance unlike the filter system alone, which over prolonged sampling times, reduced engine performance depending on exhaust gas flow rate. In these cases, a drop of 100rpm speed was used as an arbitrary cut-off point for sampling to obtain a sample at a given engine condition. Back pressure was evaluated and it was found that the high load engine conditions caused a pressure across the filter of between 35-47mm Hg



depending on filter location. These data are shown in Table 2.3 along with exhaust gas temperature, and shows that gas velocity and soot loading were critical to filter break-up. It was noted (reported in Chapter 4.1) that drop-out increased down the exhaust thereby reducing the loading on the filters. Further problems were encountered when trying to obtain a supportive backing plate for the filter. It was found that the backing plate required a minimum hole (1mm diameter) density of 16 hole per  $\text{cm}^2$ .

The final design consisted of a filter box, cooling element and vacuum, with two sample positions separated by 2m of narrow bore steel exhaust (Fig 2.14). It was used extensively for the early experimental studies. It was the first design to allow regular sampling using both filter media. However each filter had to be individually loaded, sealed and run, thus consuming considerable research time.

#### 2.4.3 BOX CASSETTE FILTER

The Box Cassette Filter (BCF) (Fig 2.15) was modified from the box filter design and increased the rapidity of filtration by the addition of a sliding filter holder. It incorporated all the system features of previous designs and could filter repeatedly without fault. Exhaust exposure area was  $12\text{cm}^2$ . Experiments were carried out in association with temperature and

ENGINE CONDITION				Maximum Pressure Difference Across Filter (mm Hg)	Time for 100rpm Speed Drop (sec)
Speed (rpm)	Load (Nm)	Distance (m)	Temperature (°C)		
1500	13.7	0.3m	130°C	30mm Hg	41sec
		2.3m	100°C	28mm Hg	60sec
	27.4	0.3m	335°C	47mm Hg	30sec
		2.3m	150°C	42mm Hg	60sec
1750	14.2	0.3m	190°C	26mm Hg	58sec
		2.3m	145°C	24mm Hg	76sec
	27.9	0.3m	340°C	35mm Hg	31sec
		2.3m	260°C	31mm Hg	80sec

Table 2.3 Pressure Drop Across Filter and Time taken for Engine to lose 100rpm. Samples taken with BCF.

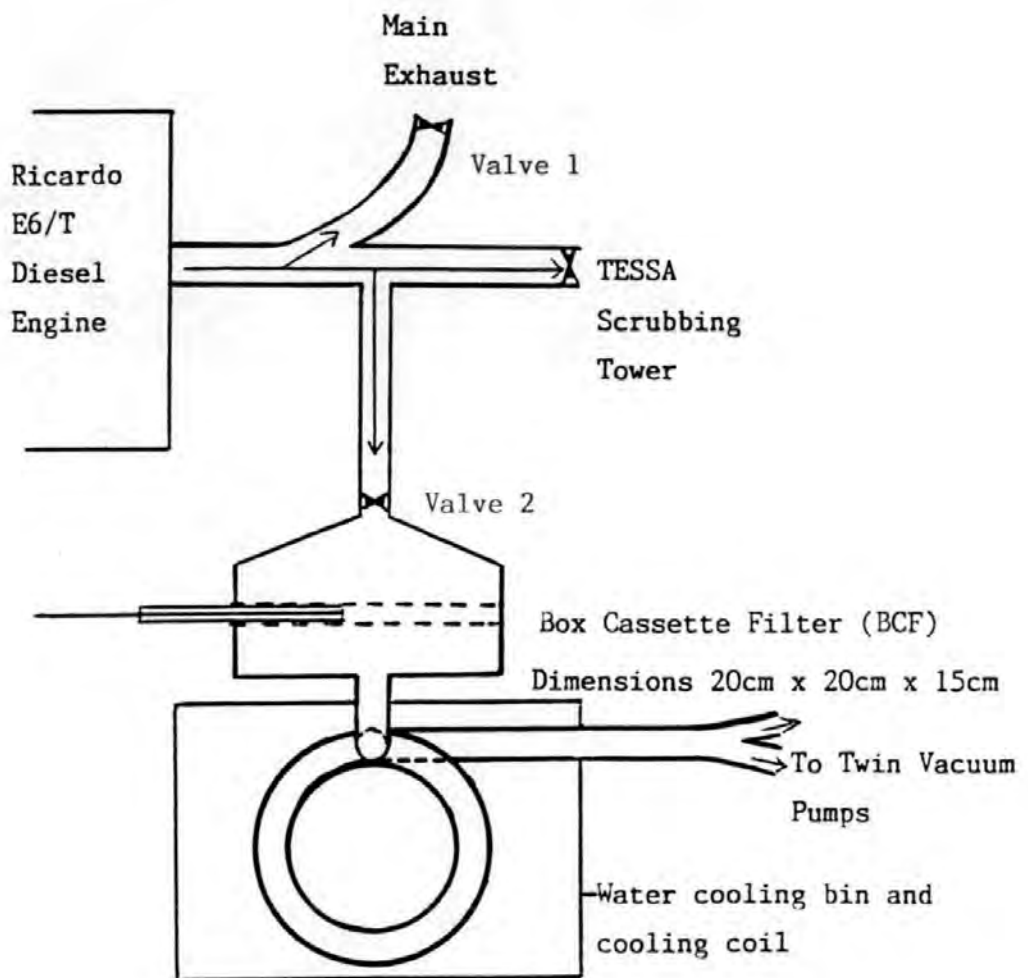


Fig. 2.14 The Box Cassette Filter System

filter pressure monitoring. Valuable data and samples were collected and used for microstructural analysis and UHC characterisation.

During TX-40 filtration, it was found that only over-fuelled high load samples provided sufficient surface cake for mechanical brushing of DP from the filter. At other engine conditions especially low loads, the soot became inaccessible, being buried within the filter matrix. Microstructural characterisation required a DP mass of >20mg for normal operation. To obtain this quantity of buried DP, an ultrasonication method was developed (UDCM method).

A further problem with this system was soot caught behind valve 2 (Fig 2.14) when it was shut, and when opened the DP was swept onto the filter, giving higher masses. To minimise this, filter insertion was carried out between brief times of valve closure (<30 seconds). The combined problems of the narrow exhaust pipe and small filter area, caused back pressure effects which reduced engine performance as with the previous design. Furthermore, accurate filter-exposure timing during soot collection was awkward, requiring synchronisation of the twin exhaust valves (Fig 2.14) by the operators. This could lead to timing errors over short sampling periods. Therefore after this initial study a new working filter system was commissioned.



Fig. 2.15 The Box Cassette Filter (BCF) with Sliding Filter Holder

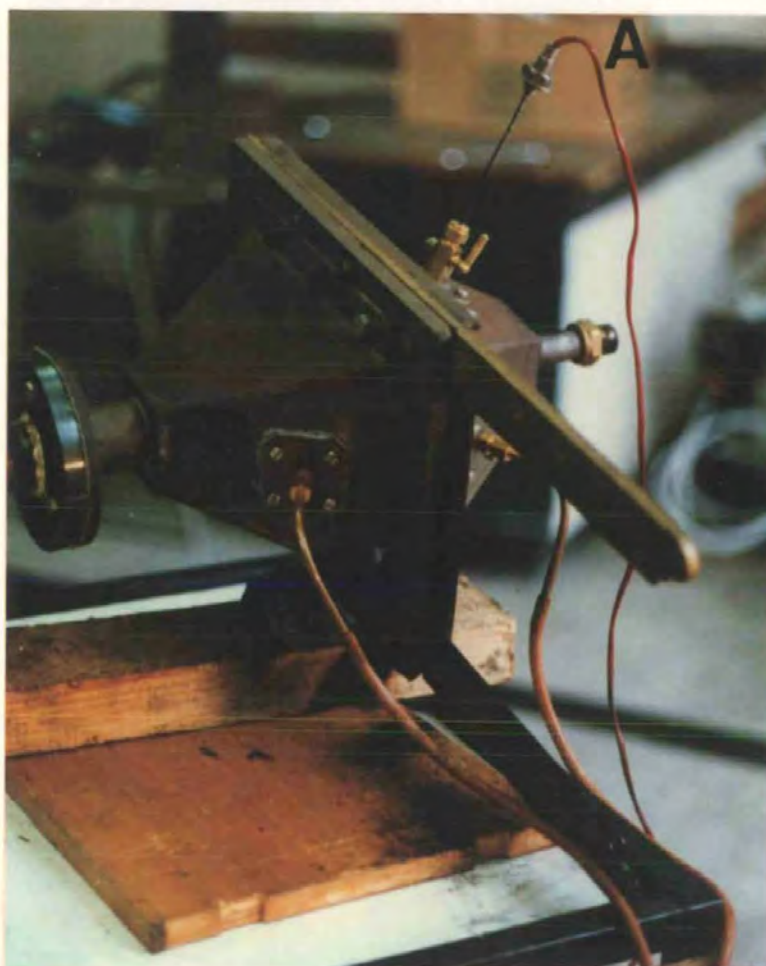


Fig. 2.16 The Improved Cassette Filter (ICF) with Thermocouple 'A' and Pressure Manometer Fittings 'B'

#### 2.4.4 IMPROVED CASSETTE FILTER SYSTEM

The Improved Cassette Filter (ICF) System (Fig 2.16) was constructed to facilitate the collection of sufficient soot for brushed extraction, especially at low load engine conditions. Unfortunately despite enlarging the system to allow longer sampling (5 minutes), the soot could still not be physically removed from the filter at low load. The diesel particles were buried and further lengthy exposure would only enhance the possibility of artefact formation. On-filter degassing and surface area determination were therefore developed to analyse the soot.

The ICF system had a compressed air operated piston valve (Fig 2.17) for rapid operation and accurate exposure timing. The filter system was positioned left of the engine, constructed of stainless steel and with a wider bore (4.5cm diameter), did not constrict gas flow. The filter area was increased to 20cm x 25cm, a standard filter size. Flanged 1m pipes could be joined together to extend the length of the exhaust, upto 4.3m. The wider exhaust and larger exposure area minimised engine back-pressures. The Pallflex filter medium had a low heat capacity and therefore did not require pre-heating. Exhaust gas temperatures were measured with a thermocouple probe connected to an electronic thermometer (Comark). Pressure was measured across the filter with a mercury manometer. The full



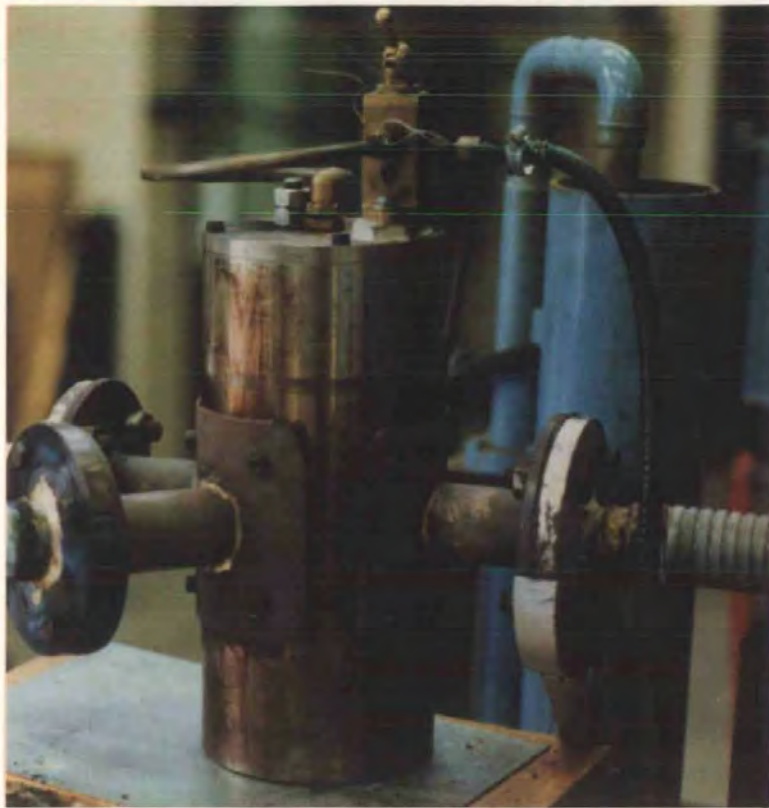


Fig. 2.17 The Compressed Air Operated Piston Exhaust Valve

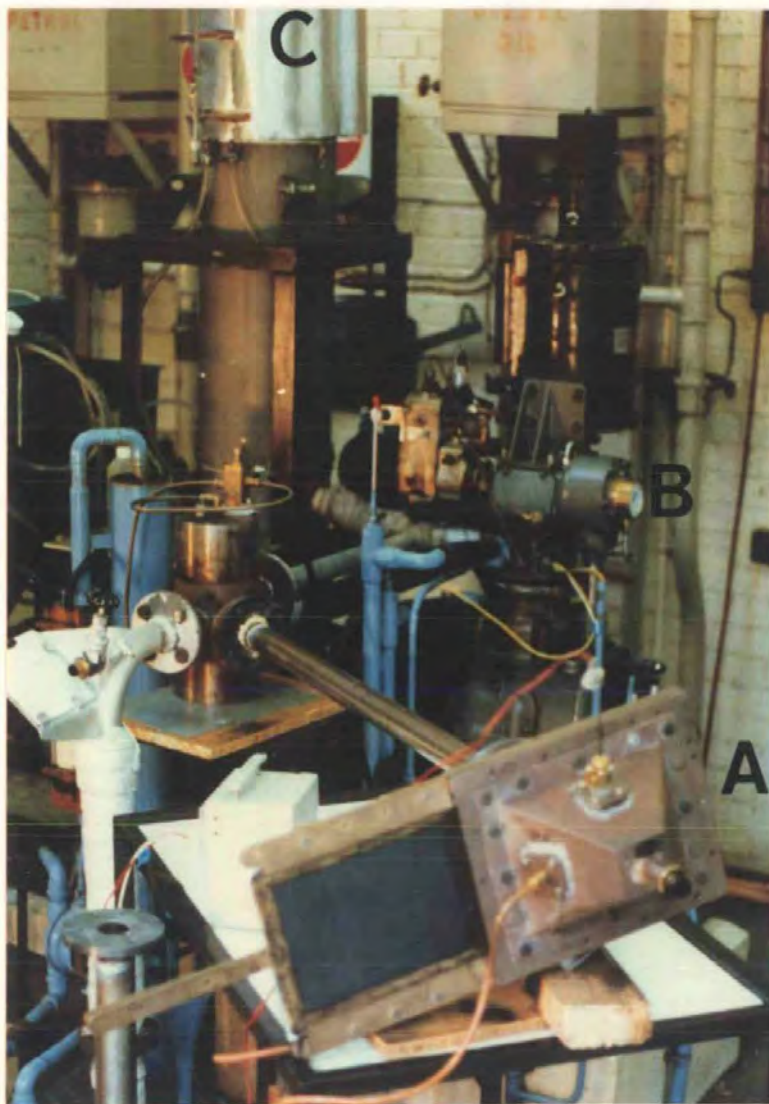


Fig. 2.18 The Improved Cassette Filter (ICF) System 'A' with Engine 'B' and TESSA 'C'

working system is demonstrated in Fig 2.18.

Table 2.4 details the combined temperature and pressure measurements obtained with the ICF. Fig 2.19 shows how the pressure changed with sampling. The system showed less pressure drop across the filter compared to the BCF during all sample conditions. The temperatures and pressures reflected the emission conditions, showing that exhaust temperature increased with increasing speed and load, and that pressure differences were highest when full load was operated. The 1.3m sample position showed an increasing pressure across the filter which indicated that trapping and filter pore blocking was continuously occurring. At other positions, the pressure stabilised indicating that the process had equilibrated. Both temperature and pressure decreased along the exhaust as temperature declined and particles 'dropped out' onto the exhaust pipe wall. When DP loading was high the DP adsorbed heat and lowered the exhaust temperature behind the filter. This feature caused a 20% decline in temperature, but did not occur at low load when the holder acted as a heat sink. It was found that if the holder was exposed to the gas stream alone, then the post-filter temperature would increase by about 20%, because the brass holder re-radiated energy to the gas. It was decided that despite the temperature change during filtration itself, the measured exhaust gas temperature without filter, would be defined as the actual exhaust temperature to

ENGINE CONDITION			Exhaust Temperature (°C)	Maximum Pressure Difference Across Filter (mm Hg)	Exhaust Gas Velocity (l/min)
Speed (rpm)	Load (Nm)	Distance (m)			
1500	13.7	1.3m	165°C	16mm Hg	3751/min
		3.3m	240°C	9mm Hg	
		4.3m	80°C	10mm Hg	
	27.4	1.3m	240°C	29mm Hg	
		3.3m	170°C	22mm Hg	
		4.3m	120°C	18mm Hg	
1750	14.2	1.3m	181°C	12mm Hg	4381/min
		3.3m	120°C	8mm Hg	
		4.3m	97°C	No Sample	
	27.9	1.3m	245°C	31mm Hg	
		3.3m	172°C	21mm Hg	
		4.3m	109°C	18mm Hg	
2000	14.6	1.3m	183°C	12mm Hg	5001/min
		3.3m	140°C	13mm Hg	
		4.3m	119°C	No Sample	
	29.5	1.3m	248°C	27mm Hg	
		3.3m	215°C	13mm Hg	
		4.3m	130°C	36mm Hg	

Table 2.4 Maximum Pressure Across ICF Filter and Exhaust Gas Temperature, noted during Series 1C.



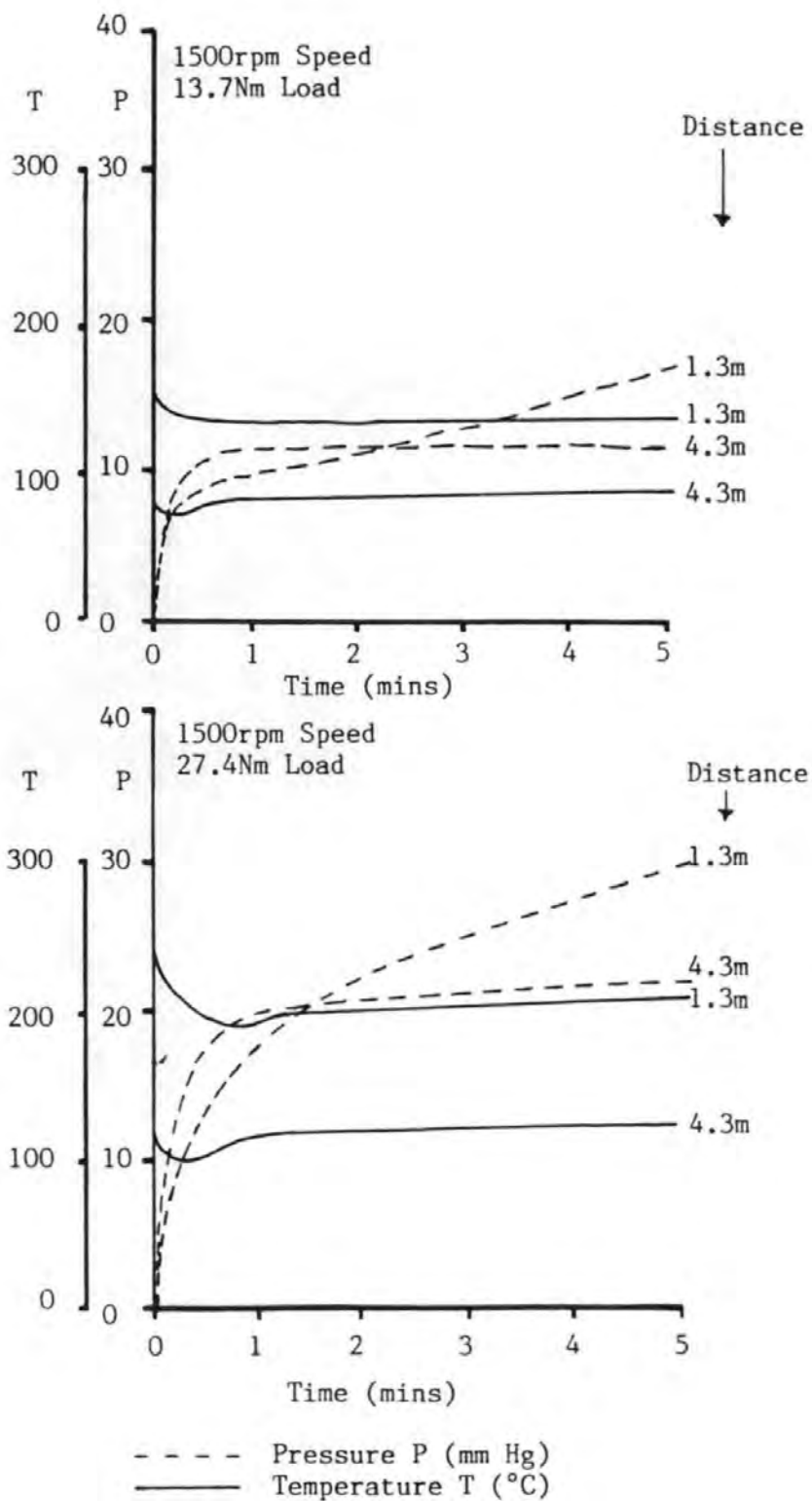


Fig. 2.19 Graph of Pressure and Temperature During ICF Operation at 1.3m and 4.3m from Exhaust Port.

standardise the data.

This system was employed to characterise diesel particulate from a full experimental series (Series 1C) with evolved gas analysis of the thermally degassed FES.

## 2.5 PROCEDURES AND VALIDATION OF SYSTEM

The research initially focussed on the construction of a filter system tailored to the Ricardo E6/T single cylinder diesel engine and its exhaust output. Considerable development time was spent over-coming the problems of collecting a hot whole exhaust sample. Later a series of experiments collected data for UHC and soot analysis using the Box Cassette Filter. Both of these experimental programmes showed further problems in the system and lead to the development of the Improved Cassette Filter System.

### 2.5.1 PRECONDITIONING

Before any quantitative measurements could be made, the new ICF exhaust system was pre-conditioned, that is coated with soot to form an equilibrium state between deposition and removal from the pipe walls. Contact with Perkins Technology Business (personal communication, 1987) revealed that a dilution tunnel required approximately 10 runs for this apparent equilibrium state to be achieved. Evidence from several experimental runs showed that particle 'drop-out' onto the exhaust pipe wall, still occurred even after over 50 hours of operation due to the pulsating flow and high exhaust gas flow. Thus no equilibration could be achieved.

## 2.5.2 SAMPLE COLLECTION

The soot samples were collected using the pre-weighed Pallflex TX-40 filter loaded into the Improved Cassette Filter holder. The exhaust system was pre-heated and pre-equilibrated for 15 minutes, following engine warm up for 60 minutes at 3000rpm, 27.4Nm, 80°C circulating water temperature.

The ICF holder was inserted into the ICF unit whilst the valve switched exhaust flow to the exhaust extraction system. The flow was immediately redirected onto the filter for the sample time (usually 5 minutes). Simultaneously temperature and pressure measurements were recorded. The coefficient of variation for filter sample mass was  $\pm 20\%$  for BCF and  $\pm 4\%$  for the ICF, which showed the improvement in reproducibility of the newer system.

After filtration, the exhaust was redirected to the extraction system, the filter was removed to be placed in a humidity box (RH 60%), re-weighed after 24 hours and then stored in tinfoil envelopes, at 4°C, in darkness until analysis.

### 2.5.3 CONCLUSIONS ON SAMPLE INTEGRITY IN THIS STUDY

It was difficult to assess the potential for physical and chemical artefact formation except to minimize the exposure time required by the sampling method. Chemical artefact formation might be assessed along the lines of Schuetzle (1983) who spiked the filter with PAH compounds and then measured the transformed nitro-PAH's. This was carried out at 52°C in a dilution tunnel when the PAH compounds selected would be unlikely to be removed by evaporation. Lindskog (1983) however suggested that spiking experiments were inappropriate for studying nitrification because any spiked solution adsorbed on particulates would remain unexposed to exhaust gas and thereby confuse quantification. Suffice it to say, the short sampling times considerably reduced the artefact formation potential and the work was specifically directed towards investigating the physico-chemical effect of UHC adsorption on the soot structure rather than specific PAH reactions. It was concluded that the Improved Cassette Filter System minimised the formation of physical and chemical artefacts.

### CHAPTER 3 THE CHARACTERISATION OF DIESEL PARTICULATE AND ADSORBED UNBURNT HYDROCARBONS

The characterisation of diesel particulate (DP) required that a range of analytical techniques be applied to the soots along the lines of Medalia and Rivin (1982) for carbons. Physical characterisation employed a gas adsorption microbalance technique (BET method) to measure specific surface area (SSA) and porosity, and electron microscopy (EM) to measure incipient particle size. Chemical characterisation of the adsorbed unburnt hydrocarbons (UHC) required extraction by the soxhlet technique and the exhaust scrubbing system (TESSA), followed by analysis using gas chromatography (GC). An evolved gas analysis (EGA) system was developed to allow a solvent-free extraction involving thermal degassing (TD).

The following chapter outlines the experiments undertaken, methods employed and developments required during this research. Particular attention has been paid to the BET SSA method and development of the EGA technique since these have been employed in a novel way. The EM and GC methods followed routine practice.

Extensive experiments were carried out on the Ricardo IDI diesel engine to characterise DP. Table 3.1 summarises these experiments by series and method. Detailed methodology may be

EXPT SERIES	SYSTEM DETAILS			ANALYTICAL TECHNIQUES			
	ENGINE CONDITION	FILTER TYPE	HOLDER TYPE	EXTRAC METHOD	EM	BET	GC
SERIES 1A	A	TX-40	BCF	UDCM	✓	✓	
SERIES 1B	A	QM-A	BCF	SOX			✓
SERIES 1C	B	TX-40	ICF	TD	✓	✓	✓
SERIES 2A	A			TESSA			✓
ADDITIONAL EXPERIMENTS							
EXPT 3A	1500rpm 27.4Nm 1.3m	TX-40	ICF	SOX UDCM TD		✓	✓
EXPT 4A	FORD and RICARDO (see text)	TX-40	ICF	TD	✓	✓	✓
EXPT 5A	1500rpm 13.7Nm & 27.4Nm	TX-40	ICF	TD		✓	✓

ENGINE  
CONDITION

- A 1500rpm, 13.7 and 27.4Nm  
1750rpm, 14.2 and 27.9Nm  
Samples at 0.3 and 2.3m Distance
- B 1500rpm, 13.7 and 27.4Nm  
1750rpm, 14.2 and 27.9Nm  
2000rpm, 14.6 and 29.4Nm  
Samples at 1.3, 3.3 and 4.3m Distance.

Table 3.1 Summary of Experiments and Techniques Undertaken in this Research Project.

found in the appropriate sections. Experimental series were carried out simultaneously with filter system development and advances in experimental technique.

The Box Cassette Filter (BCF) was employed to obtain background data. Series 1A collected soots for microstructural characterisation using ultrasonic extraction with dichloromethane (UDCM method). Series 1B examined the filter extractable sample (FES) using soxhlet extraction and GC identification of the hydrocarbons. The development of the Improved Cassette Filter (ICF) system and TD technique (Series 1C) allowed characterisation without solvent extraction, and facilitated quantifiable measurement of the interaction between DP and UHC, down the exhaust.

Series 2A utilised the TESSA system (Petch et al, 1988) to obtain a tower extractable sample (TES) of exhaust UHC before DP adsorption had occurred. These total exhaust samples were compared with the Series 1B FES samples. Additional experiments investigated how extraction method affected FES and DP microstructure (Experiment 3A) and compared the Ford DI engine to the Ricardo IDI engine at similar operating conditions (Experiment 4A). Experiment 5A, studied how the microstructure of DP changed after thermal degassing at successively higher temperatures (120, 190, 290 and 340°C) and collected the degassed hydrocarbon fractions. This was carried out for high



and low load engine exhaust soots, and facilitated a better understanding of DP composition.

### 3.1 MICROSTRUCTURAL CHARACTERISATION OF DIESEL PARTICULATE USING A NITROGEN ADSORPTION VACUUM MICROBALANCE TECHNIQUE

The specific surface area (SSA) and pore character of a particulate sample can be determined by the application of a N<sub>2</sub> adsorption technique developed by Brunauer et al (1938) and called the BET technique for SSA, and the Cranston and Inkley (1957) method for pore structure. This method has been previously employed at Plymouth (Carter, 1983; Glegg, 1987 and Titley, 1988) for particles from a range of sources.

Surface area determination of a solid is regarded as specific to method (preparation, analytical technique and theoretical treatment (Van den Hul and Lykema, 1968)). Therefore the diesel particles were prepared in a consistent way to ensure that the SSA data was intercomparable even though the SSA values were not absolute.

#### 3.1.1 SERIES 1A EXTRACTION OF DIESEL PARTICLES FOR MICROSTRUCTURAL ANALYSIS

The Pallflex TX-40 filters functioned as a partial surface filter, and some of the soot became buried within the filter matrix, particularly at low engine loads when particulate emission was low. Therefore it was found necessary to extract the DP by ultrasonic extraction (with DCM) to obtain sufficient

DP mass for the techniques of microstructural analysis.

Ten repetitive samples, taken at a variety of engine conditions and filter positions with the BCF, were individually extracted using a frequency sweep ultrasonic bath (150ml, DCM) for 5 minutes. It was recognised that some hydrocarbons would be extracted by this method. Each sample was filtered through a single pre-weighed Millipore 0.45 $\mu$ m filter in a vacuum assisted Millipore filter apparatus. Particulate extraction efficiency (from the TX-40 media) was 50-60%.

After drying in air, the DP could be scraped off the Millipore filters to give an extracted particulate mass loading. The filtered diesel soot was analysed for its physical characteristics (specific surface area (SSA), pore size distribution, physical shape and size). The objective of these experiments was to provide fundamental size and SSA data, and to compare different engine conditions.

The combined FES was reduced in volume by reduced pressure rotary evaporation (30°C), transferred to a pre-weighed vial and reduced to dryness by N<sub>2</sub> blow-down to obtain an FES extracted mass, which was used to give an approximate figure for the relative quantities of adsorbed FES.

### 3.1.2 THE VACUUM MICROBALANCE

The apparatus used to determine SSA and pore character was a CI Electronics Mk 2B gravimetric vacuum microbalance constructed in 1974 and used for carbons by Carter (1983). Adsorption of  $N_2$  at  $-196^\circ C$  was measured gravimetrically with microgram to milligram sensitivity. The increase in particulate weight was noted and plotted against the change in relative pressure of the sample compared to atmosphere ( $P/P_0$ ). The microbalance had a maximum weighing capacity of 1g and accuracy of  $0.5\mu g$ .

The balance head consisted of a photo-electronic bridge circuit, maintained in a glass vacuum flask designed to work at pressures down to  $10^{-6}$  mm Hg. The balance operated with a shutter system which opened or closed with weight change and thereby induced a change in the relative illumination of the balance photocells proportional to the weight change. This gives the microbalance a rapid response time ( $<100ms$ ), and it was sensitive to internal changes in weight but not external vibrations. The electrical output was fed to a compatible analogue control unit with various counterweight ranges. This was coupled by an electronic damping bridge to a chart recorder for simultaneous data recording.

The balance was coupled to a two stage rotary pump (Edwards, 0.01mm Hg maximum vacuum), a mercury manometer, a gas reservoir

and a 'White Spot' N<sub>2</sub> (99.9% purity) cylinder. Fig 3.1 shows the complete vacuum microbalance system. This apparatus has been further adapted for the thermal degassing experiments.

### 3.1.3 THEORY OF MICROSTRUCTURAL ANALYSIS AND CALCULATION OF SPECIFIC SURFACE AREA

A solid will adsorb gas at a definite pressure. The amount of gas adsorbed depends on pressure, temperature, nature of gas, character of the solid surface and the adsorption process (i.e. chemisorption and/or physisorption). Gas adsorption isotherms can be determined by a plot of N<sub>2</sub> uptake against pressure, for specific temperatures and gas types, and will yield information about a solid surface (Gregg and Sing, 1982). This allows characterisation of different solid surfaces based on five different types of adsorption isotherm (Fig 3.2) as initially identified by Brunauer et al (1938) and often referred to as the BET classification. These isotherms can be interpreted to obtain a specific surface area value and pore character due to liquid N<sub>2</sub> condensation using available theory, such as the BET model:

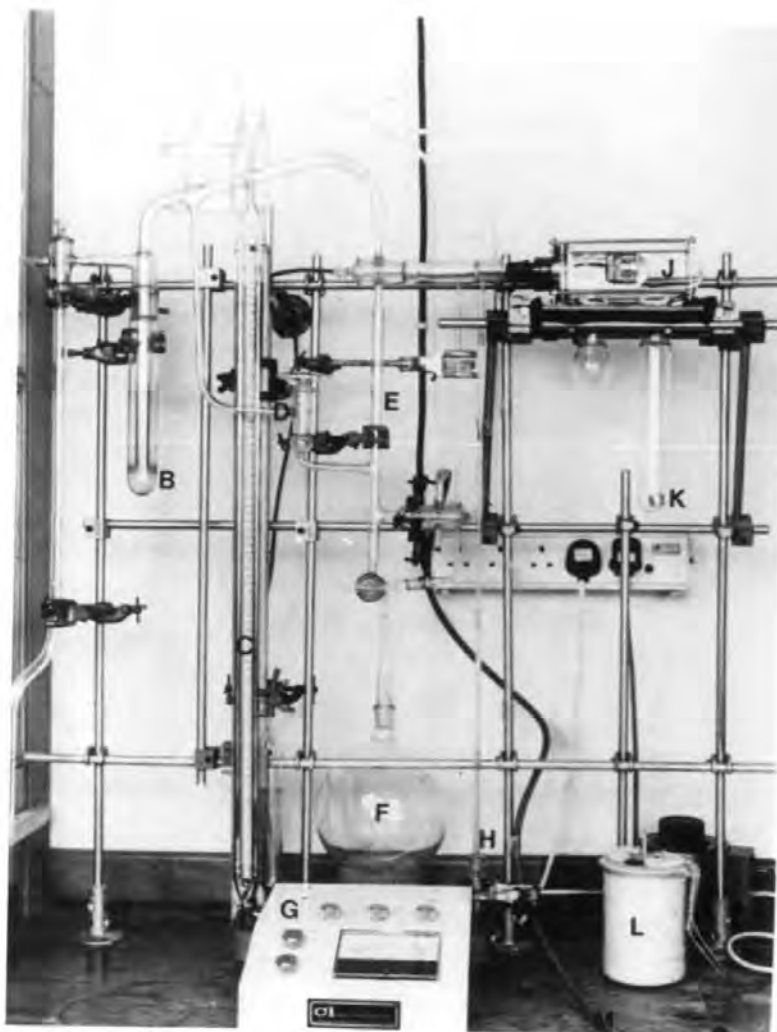


Fig. 3.1 The BET Apparatus - A Vacuum Microbalance

- Key:
- B Cold Trap
  - C Mercury Manometer
  - D System for Flushing out Reservoir and Doser
  - E Nitrogen Doser
  - F Nitrogen Reservoir
  - G Control Unit
  - H Reservoir Manometer
  - J Balance Head
  - K Sample Bucket in Sample Envelope (Tube)
  - L Heating Bucket for Thermal Degassing

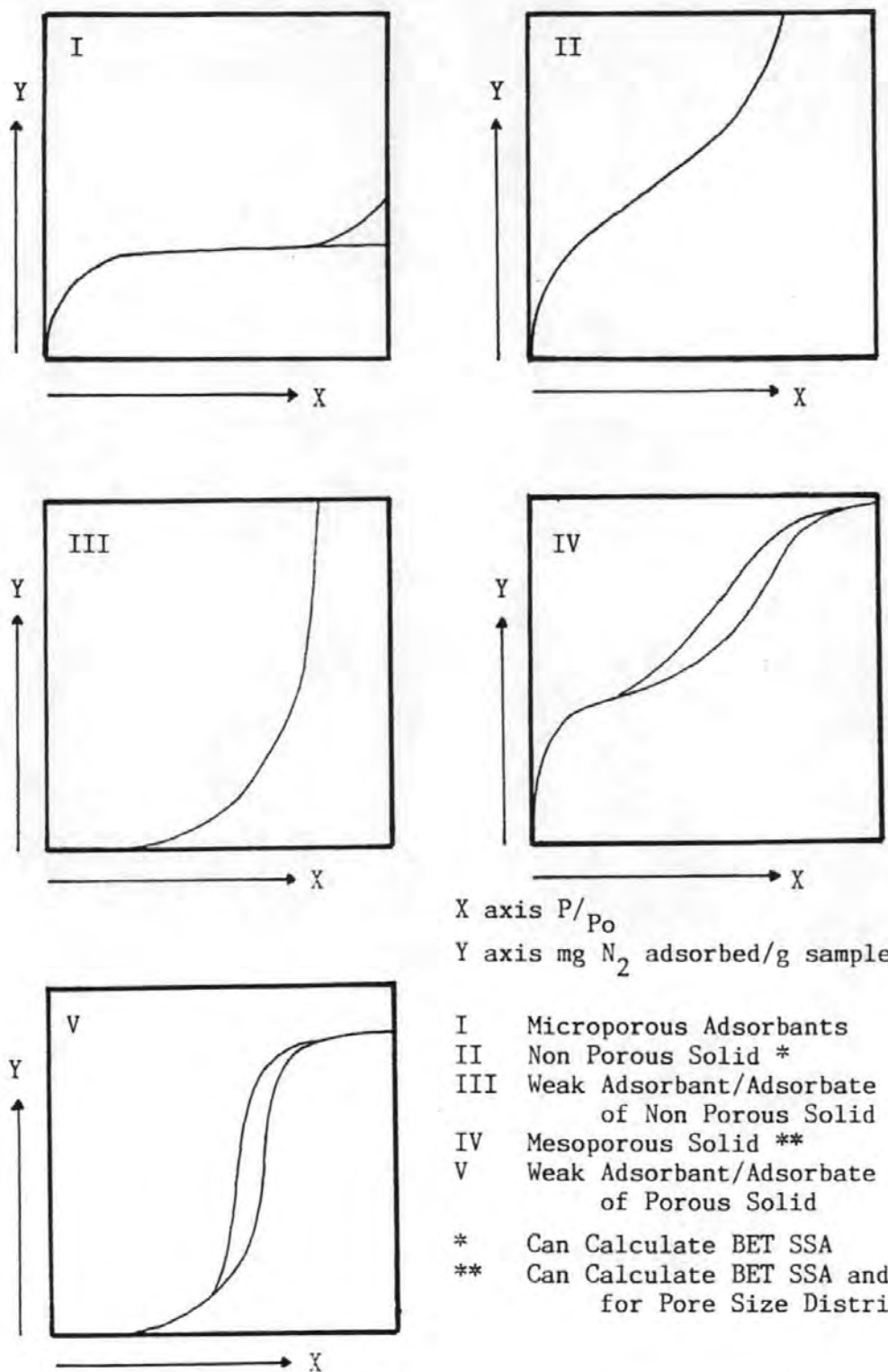


Fig 3.2 Adsorption/Desorption Isotherms Type I to V Characterised to Different Solid Surfaces. (Gregg and Sing, 1982)

$$\frac{p}{x(p_0 - p)} = \frac{1}{x_m C} + \frac{C-1}{x_m C} \cdot \frac{p}{p_0} \quad \text{Equation 3.1}$$

where  $x$  = mass of adsorbate/unit mass of sample  
 $p$  = pressure of adsorbate gas (mm Hg)  
 $p_0$  = saturation pressure of adsorbate gas (mm Hg)  
 $C$  = energy constant, dependent on the nature of the adsorbate/adsorbent system.  
 $x_m$  = monolayer capacity (mg adsorbate/g sample)

The method employed is an extension of the work of Langmuir who regarded the surface of a solid as an array of adsorption sites of equal energy, each site being capable of adsorbing one molecule (e.g. nitrogen). The BET theory improves this concept by including a multi-layer component. The coverage of the total surface by the adsorbate (referred to as the monolayer capacity) is proportional to the surface area of the solid surface and the BET equation can be employed to obtain an SSA measurement. Despite simplifying assumptions (Adamson, 1976; Mikhail and Robeñs, 1983) the BET technique is widely employed using nitrogen gas as the adsorbate, and for Type II isotherms it is remarkably successful (Gregg and Sing, 1967).

If the data are plotted as  $p/x(p_0 - p)$  against  $p/p_0$ , the graph will have a slope of:

$$\frac{C-1}{x_m C} \quad \text{and an intercept of} \quad \frac{1}{x_m C}.$$

It can be shown that:

$$\frac{1}{x_m} = \frac{C-1}{x_m C} + \frac{1}{x_m C} \quad \text{Equation 3.2}$$

therefore the monolayer capacity can be calculated.



The SSA ( $\text{m}^2/\text{g}$ ) is related to  $x_m$  by the equation:

$$\text{SSA} = \frac{x_m \cdot N_A \cdot A_m}{M_r} \quad \text{Equation 3.3}$$

where  $M_r$  = relative molecular mass (g)  
 $N_A$  = Avogadro's constant ( $\text{mol}^{-1}$ )  
 $A_m$  = Area occupied by one adsorbate molecule ( $\text{nm}^2$ )

The  $A_m$  value for nitrogen gas is  $0.162\text{nm}^2$  (Adamson, 1976). This value is close to that calculated from the liquid density of nitrogen at its boiling point at the sample temperature ( $-196^\circ\text{C}$ ). Substituting  $M_r$ ,  $N_A$  and  $A_m$  into equation 3.3 gives equation 3.4 which can be used to calculate the BET surface area. Fig 3.3 shows a typical diesel soot BET plot determined from isotherm data.

$$\text{SSA} = 3.485 \cdot x_m \quad \text{Equation 3.4}$$

Pore character may be evaluated from the hysteresis loop produced from the full adsorption/desorption isotherm. Porous materials internally adsorb the gas which is then not released as easily during desorption thereby producing a weight difference at any partial pressure.

The position at which the hysteresis loop opens and closes is indicative of pore size range (Gregg and Sing 1982) and has led to the IUPAC classification of pore sizes:

Micropores	diameter $<2\text{nm}$
Mesopores	diameter $2-50\text{nm}$
Macropores	diameter $>50\text{nm}$

Pore shape may be estimated by examining the isotherm

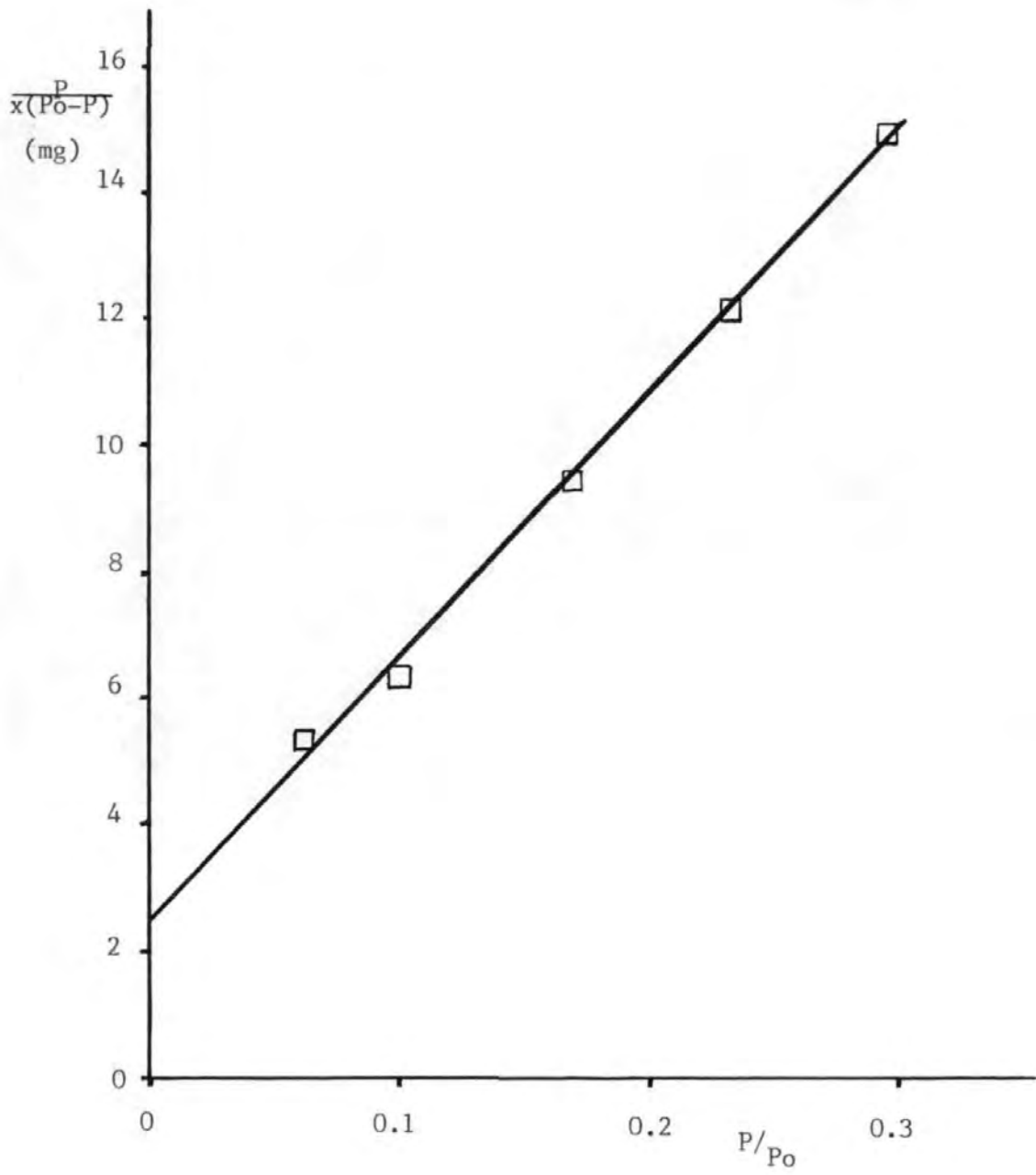


Fig. 3.3 A BET Plot of a Diesel Particulate Extracted by Brushing Soot from a Filter. The Plot was Derived from Isotherm Data Shown in Fig. 3.4. The Plot was Obtained by Visual Best-fit

Sample: Speed 1500rpm  
 Load 27.4Nm  
 BCF at 2m Distance

hysteresis (Fig 3.4), since the particular shape of the adsorption branch can be related to the specific pore shapes (Robens, 1980, Gregg and Sing 1982).

Using hysteresis loop data combined with the Kelvin equation:

$$\ln (p/p_0) = -((2Vj/rRT)) \quad \text{Equation 3.5}$$

where V = molar volume of adsorbing gas (m<sup>3</sup>/mol)  
j = surface tension of the condensed gas (J/m<sup>2</sup>)  
r = pore radius (nm)  
R = universal gas constant (JK<sup>-1</sup> mol<sup>-1</sup>)  
T = temperature (K)

Taking V as 34.68cm<sup>3</sup>/mol; and j as 8.72x10<sup>-7</sup>J/cm<sup>2</sup>, allows pore diameter to be calculated and an example is shown in Fig 3.4.

Barrer et al (1956) and De Boer (1958) characterised the pore shapes to fit the hysteresis loops shown in Fig 3.5. Many samples in this research showed open loop hysteresis where nitrogen was irreversibly trapped either physically by narrow pores of the same diameter as the nitrogen molecule and/or chemisorbed to the adsorbent surface.

The density of adsorbents is used to calculate the Archimedes buoyancy weight effect that occurs as the sample tries to 'float' - thereby changing its weight in any atmosphere. Diesel soot extracted from filters by the

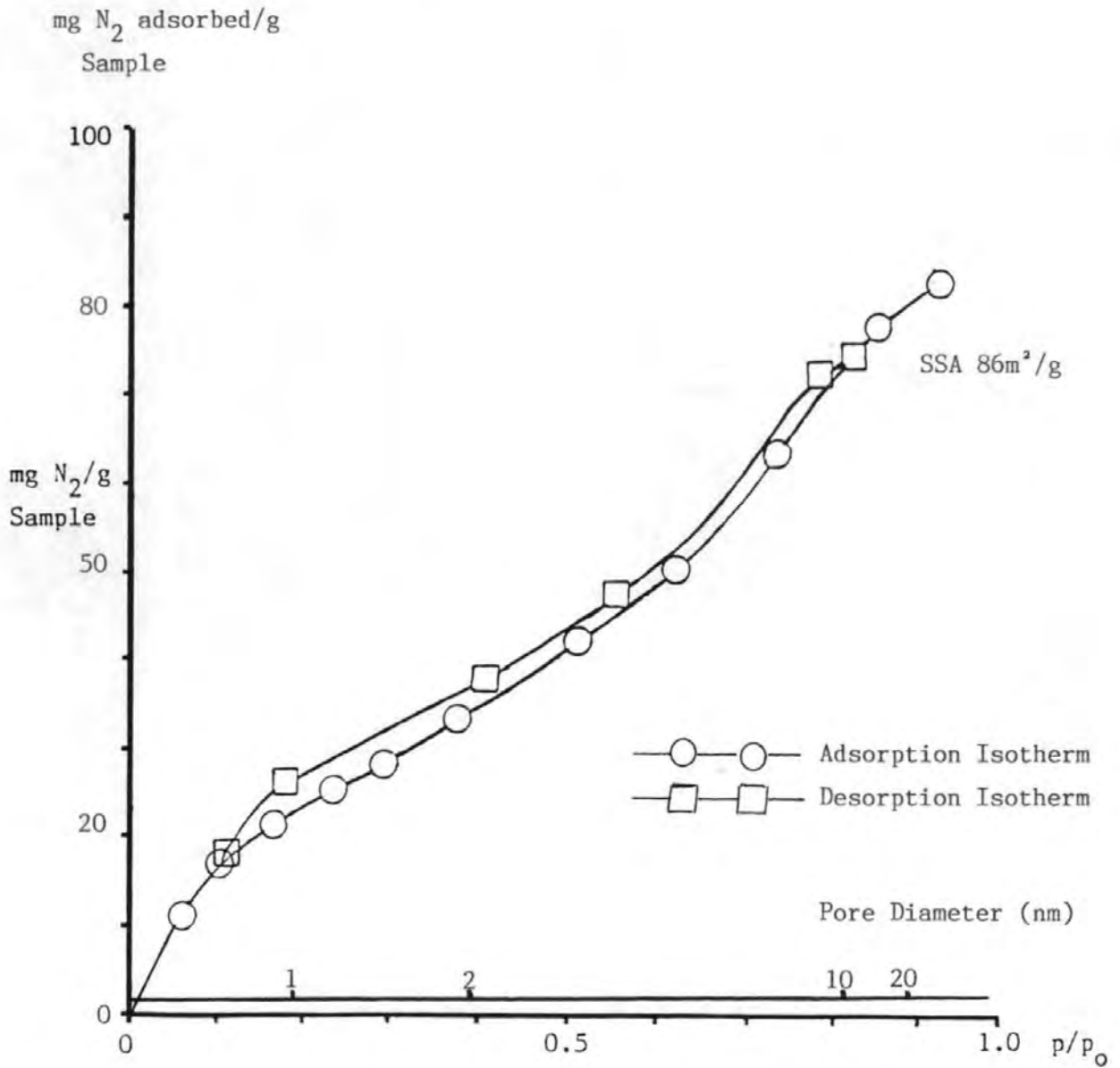
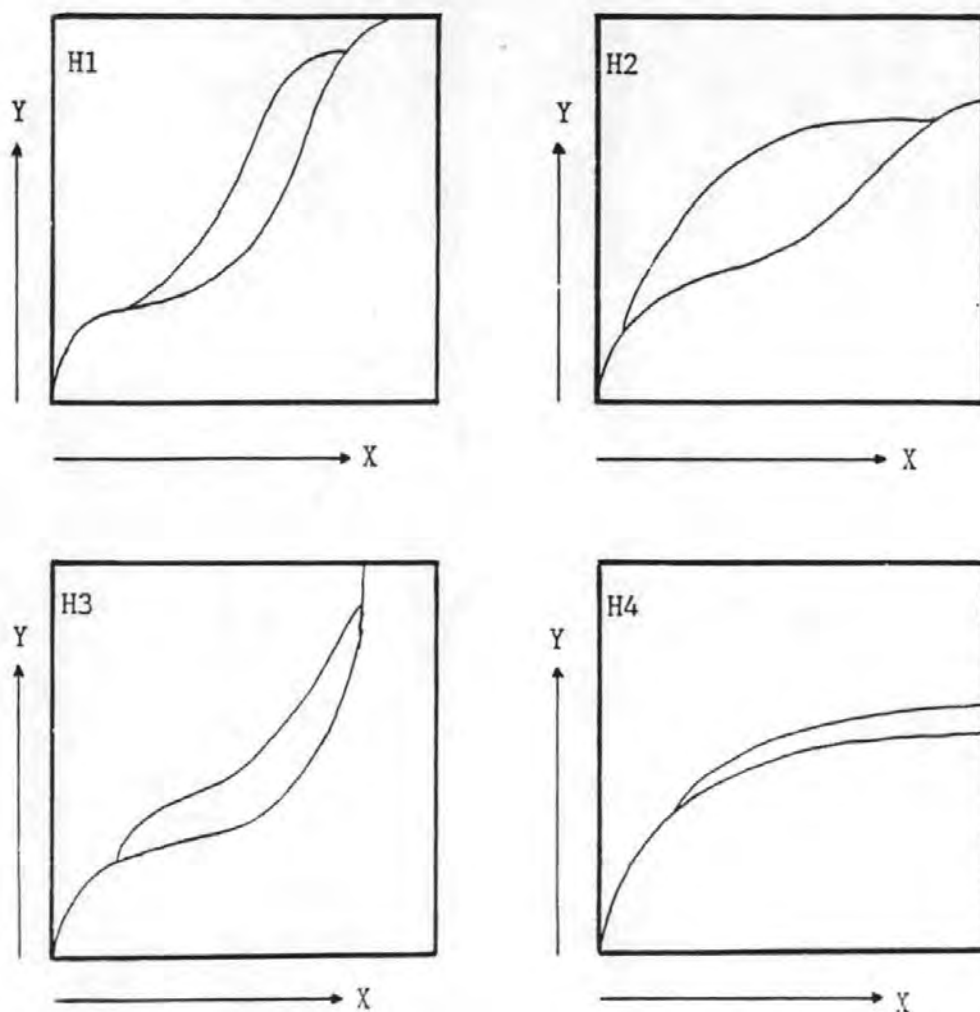


Fig. 3.4 Adsorption/Desorption Isotherm Showing Hysteresis Loop for a Brushed Diesel Particulate. Pore Diameter is Shown to Illustrate the Size of Pores Blocked by Volatiles.

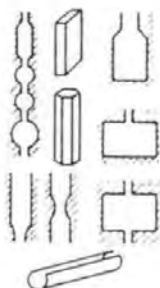
Sample: Speed 1500rpm  
Load 27.4Nm  
BCF at 2m Distance.



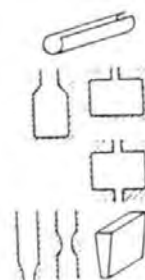
X axis  $P/P_0$

Y axis mg  $N_2$  adsorbed/g sample

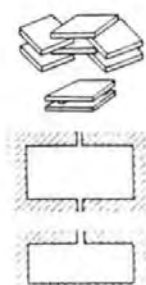
H1  
Agglomerates  
Ink-bottle  
Pores



H2  
Corpuscular  
Systems



H3  
Slit-shaped  
Pores and  
Platelets



H4  
Slit-shaped  
Pores and  
Platelets from  
Type I Isotherms

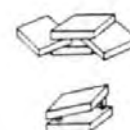


Fig. 3.5 IUPAC Classification of Hysteresis Loops for the Characterisation of Pore Systems. (Gregg and Sing, 1982)

ultrasonication method is assumed to have a sample density of 2000kg/m<sup>3</sup>, similar to graphite. Pure graphite has a density of 2265kg/m<sup>3</sup>, but in coals and cokes the structure is not so perfectly crystalline and is taken to be 1900 or 2000kg/m<sup>3</sup>.

On-filter analysis requires that the relative masses and densities of soot and filter be used to calculate the final SSA. The TX-40 media has a mean bulk density of 300kg/m<sup>3</sup> (measured experimentally). However, bulk density is not appropriate for this work because the porous filter has internal surface area. Therefore the X-ray density was determined as being 2080kg/m<sup>3</sup> from density data of borosilicate glass and PTFE assuming a 80/20 mix. This was determined by thermal degradation of a PTFE filter in a muffle furnace (at 500°C in air). The filter media was found to possess its own SSA measured at 2.47m<sup>2</sup>/g ±5% and showed small amounts of porosity in all ranges.

The on-filter correction equation (Equation 3.6) allows for the relative masses of filter and DP and their respective SSA.

$$\text{SSA of Soot} = \frac{S_1 - (S_2 \times R_2)}{R_1} \quad \text{Equation 3.6}$$

Where S<sub>1</sub> the total SSA from Equation 3.4 (m<sup>2</sup>/g)  
 S<sub>2</sub> the SSA from filter (2.47m<sup>2</sup>/g)  
 R<sub>1</sub> ratio of the particulate dry mass divided by total sample mass (Particles and Filter)  
 R<sub>2</sub> ratio of the filter dry mass divided by dry sample mass

The correction enables estimation of the SSA's on filters

and it gave from a number of replicate samples (n=4) a coefficient of variation of  $\pm 5\%$ . However this method assumes that the carbon deposited on the filter, does not firmly coat the surface of the filter and that all of the surface of the filter is accessible to nitrogen molecules.

But in some of the experiments, the surface area of the filter with the carbons deposit was less than the surface area of the filter alone and gave a negative SSA. Thus at least some of the surface of the filter is coated with carbon sufficiently firmly to be inaccessible to nitrogen molecules of only 0.4nm diameter. The carbon acted as a micro-pore blocking agent for the filter, but did not contribute enough of its own SSA to overcome the effect of its blocking. Thus a significant proportion of the filter surface ceased to contribute to the total surface area recorded. Assessment of the maximum SSA (assuming no filter contribution) revealed that for high load engine conditions the soot cake had indeed blocked filter pores because maximum values were similar to corrected results. However, for low load samples the correlation was poor and values very different, because the filter was still making a significant contribution to total SSA.

The maximum SSA's did not show the typical trend of declining SSA with UHC adsorption down the exhaust, presumably because the aggregation lead to enhanced drop-out in low exhaust gas flows in the exhaust. Thus the total SSA increased, as the

particle size distribution shifted to smaller particles within the exhaust.

For this report, values that were calculated as negative will be reported as being less than three times the filter SSA ( $2.47\text{m}^2/\text{g}$ ) i.e.  $7.5\text{m}^2/\text{g}$ , to express the idea that the SSA were not detectable for some samples.

#### 3.1.4 VALIDATION OF EXPERIMENTAL METHOD

The BET technique has been previously employed and validated by Titley (1988). A silica standard from the National Physical Laboratory (Ref M11-03) was used with a reported SSA of  $151\text{m}^2/\text{g} \pm 0.2\%$ . Control experiments reproduced this SSA.

The accuracy of the TX-40 media correction calculation was tested by varying the standard silica mass on a known filter mass. The SSA from a number of replicate samples was determined to be  $131\text{m}^2/\text{g} \pm 5\%$ , indicating that the method gives good intercomparison but lower SSA values than expected. The cause of this was probably the density value for the filter and not the calculation.



### 3.1.5 DISCUSSION OF EXPERIMENTAL ERRORS

Erroneous operation was minimised by experience and standard samples. Mikhail and Robens (1983) reviewed microbalance theory and application, and the most significant problems are listed here:

1) Buoyancy errors proportional to the increase in pressure as liquid N<sub>2</sub> in the dewar boils off. This was minimised by keeping the dewar full.

2) Electrostatic fields present between glass and sample whilst under normal pressure. This was reduced by application of an anti-static vacuum grease, fine glass hang-downs and anti-static sprays.

3) Incomplete degassing which left pores blocked with water molecules and added additional weight. Experience and sample knowledge minimised this error. The addition of the coupled chart recorder facilitated the evaluation of the point when the sample was fully outgassed.

Microbalances must also be securely mounted against vibration and shielded (if light sensitive) against solar radiation, and ideally the room should be thermostatically controlled to within  $\pm 0.5^{\circ}\text{C}$ .

Archimedes buoyancy must be calculated for each item of

different density within the BET apparatus at its temperature. The BET apparatus has been designed to be symmetrical, ensuring that the buoyancy of those parts remaining at room temperature was kept small. Each item (and samples) across the symmetrical beam was corrected for density and temperature (-196°C) to give the total system buoyancy which was applied to the recorded N<sub>2</sub> adsorption weight readings. The densities of items were as follows:

Aluminium Bucket/Foil	2700	kg/m <sup>3</sup>
Glass hangdown	2250	kg/m <sup>3</sup>
Particulate (as graphite)	2000	kg/m <sup>3</sup>
Hydrocarbons	800	kg/m <sup>3</sup>
TX-40 (80/20 mix)	2080	kg/m <sup>3</sup>

Errors in this correction stem from poor measurement of individual item weight, e.g. hydrocarbons. The contribution that the HC's made to the DP mass was significant (in some cases >80% of DP mass) and required that the FES mass be known. A mean density value of 800g/cm<sup>3</sup> for HC was used to reflect the range of individual HC densities of oil and fuel. The filter's density was calculated from an assumed 20:80 mix of PTFE and Borosilicate glass fibre. The ratio may be inaccurate but the value was applied to all samples, and the filter mass between samples tended to be very similar, thereby minimising the potential for error.

### 3.1.6 EXPERIMENTAL PROCEDURE

Diesel particulates extracted by ultrasonication (typically 10-50mg) were weighed into an aluminium adsorbent bucket. Particulates for on-filter determination of SSA were also weighed (with mass of soot calculated from initial filter loading). They were then quartered and one quarter wrapped in an aluminium foil envelope, suspended on the pyrex hang-down and counterbalanced. The sample (collected by either method) was then sealed and evacuated by the pump to a pressure of 0.01mm Hg (measured experimentally by Edwards Pirani 10 gauge). This removed adsorbed moisture and those volatiles with molecular masses less than n-dodecane, which were trapped in a liquid N<sub>2</sub> cold trap. The true 'dry' sample weight (i.e. less weight lost on degassing) was noted, the balance zeroed and sample test tube immersed in a dewar of liquid N<sub>2</sub> such that the sample was at least 15cm below the coolant surface thereby keeping the sample temperature at -196° (Glasson and Lindstead Smith, 1973).

The loss of hydrocarbon volatiles was assumed to be minimal at this stage. Calculation using a vapour pressure equation:

$$k = \frac{(0.2185 \cdot A)}{((\log_{10} P) - B)} \quad \text{Equation 3.7}$$

where P = Pressure (mm Hg)  
k = Temperature (K)  
A = Molar heat of Vapourisation (J mol<sup>-1</sup>)  
B = Specific hydrocarbon Constant

(C.R.C. Data book, 1972)

at different temperatures and pressures established that hydrocarbons upto n-dodecane would be removed but not naphthalene at room temperature. Since naphthalene is the most volatile hydrocarbon normally collected by the TESSA system (Trier, 1988) this was sufficient. A table of boiling points at pressure and temperature is shown in Table 3.2 for thermally degassed hydrocarbons and the calculated graph detailed in Fig 3.6.

For the BET SSA determination (upto a relative pressure p/p<sub>0</sub> of 0.3) nitrogen gas (40mm Hg) was dosed into the sample and allowed to equilibrate (10-30 mins as indicated by a stable weight recording). The sample weight and nitrogen pressure were then recorded. Upto 6 readings were taken to obtain sufficiently accurate data for the BET surface area calculation. Further additions (70-100mm Hg of N<sub>2</sub>) were then made (with stabilisation periods) until the maximum relative pressure was

Relative Molecular Mass	Compound Name	Boiling Point at Pressure:		
		760mm Hg	1mm Hg	0.05mm Hg
128	Naphthalene	218°C	47°C	4°C
142	Decane	174°C	16°C	-23°C
212	Pentadecane	270°C	89°C	43°C
178	Phenanthrene	340°C	117°C	63°C
352	Pentacosane	390°C	194°C	139°C
408	Nonocosane	422°C	234°C	179°C
18	Water	100°C	-11°C	-23°C

Table 3.2 Boiling Points of Representative Hydrocarbons and  
Water at Various Pressures used in these Studies.  
CRC 1972

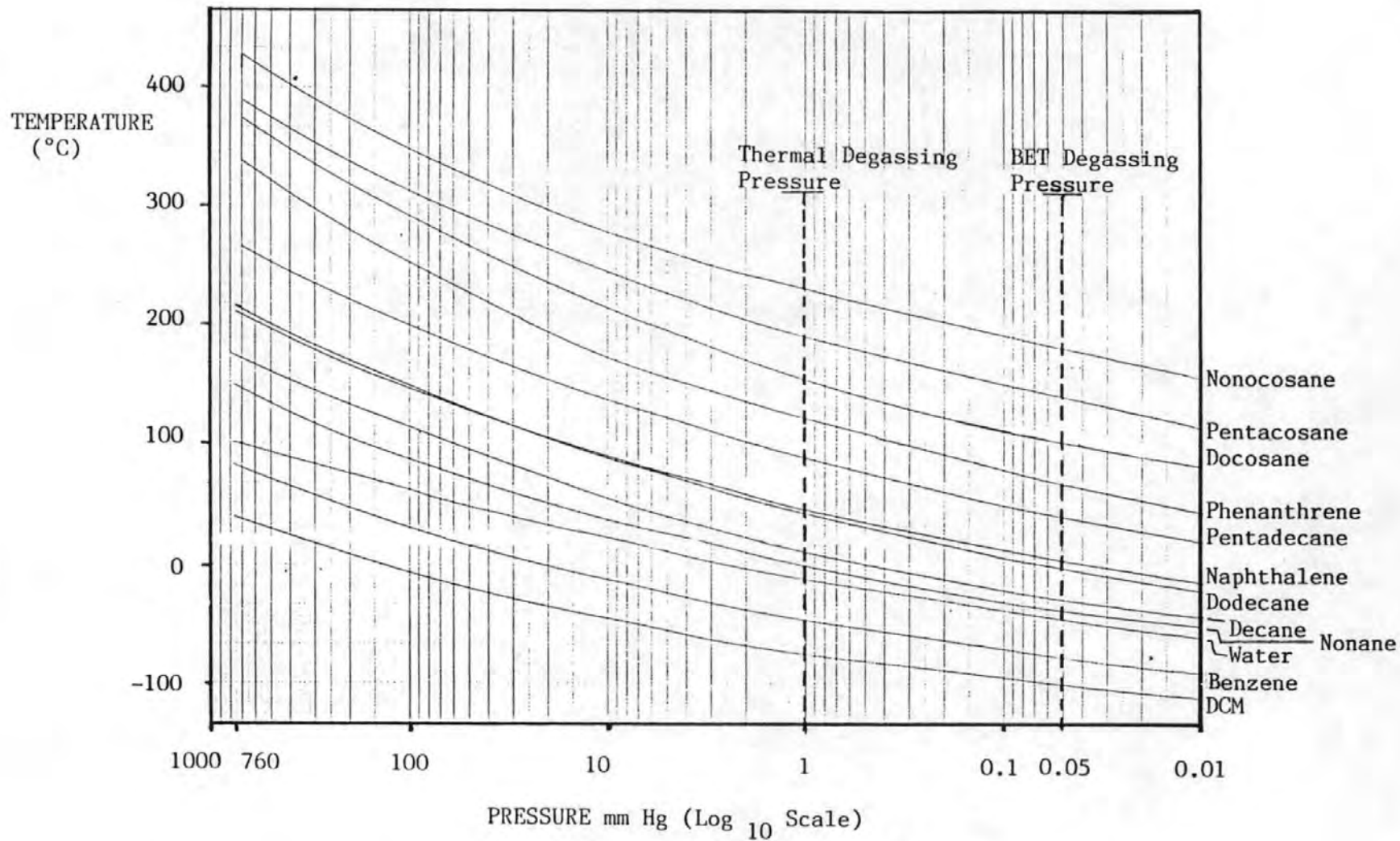


Fig. 3.6 Graph of Selected Hydrocarbons and Water. A Plot of the Variation in Boiling Point with Pressure.  
CRC 1972

reached (about 0.95 relative pressure) and an adsorption isotherm could be plotted.

The desorption isotherm was then determined by reducing the N<sub>2</sub> pressure in the opposite manner to the adsorption stage. A graph (Fig 3.7) was plotted of the weight change against time over the full adsorption/desorption cycle. In Fig 3.7 (A), was the initial weight loss due to room temperature degassing; (B), was the adsorption stage ( $<0.3 P/P_0$ ) from which the BET calculation was derived; and C, was the top of the isotherm when desorption of N<sub>2</sub> was initiated. With equilibration steps, this would normally take 2-3 hours. A hysteresis loop could then be plotted (as weight against relative pressure).

During Series 1A, DP were thermally degassed using a heating pot (Fig 3.1, item L) raised around the sample envelope. The degassing was carried out at 350°C at 0.05mm Hg pressure. This allowed assessment of the thermally degassed DP and a measure of the actual SSA, but FES could not be collected, and so the EGA system (Section 3.4) was developed.

Sample  
Weight (mg)

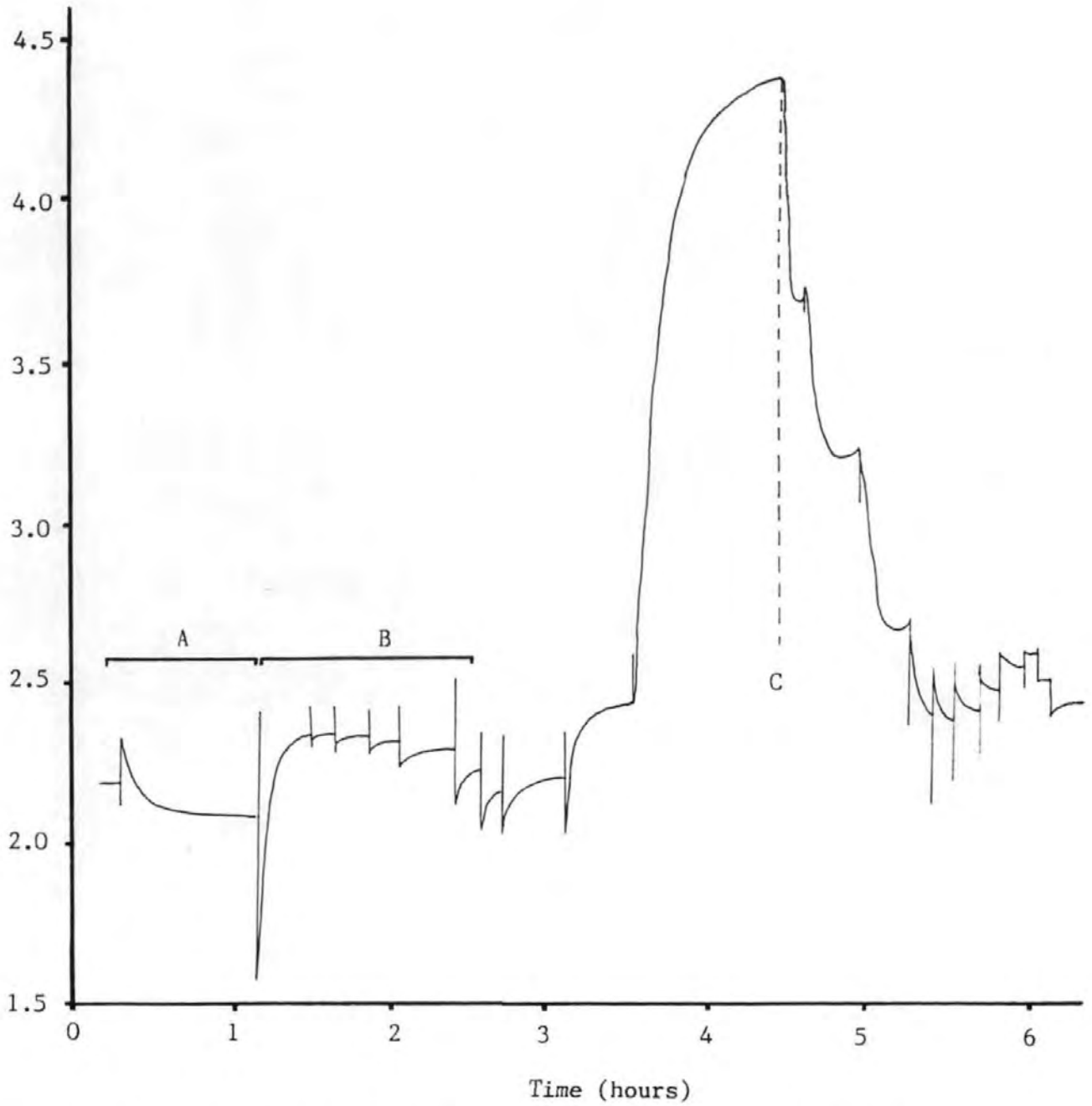


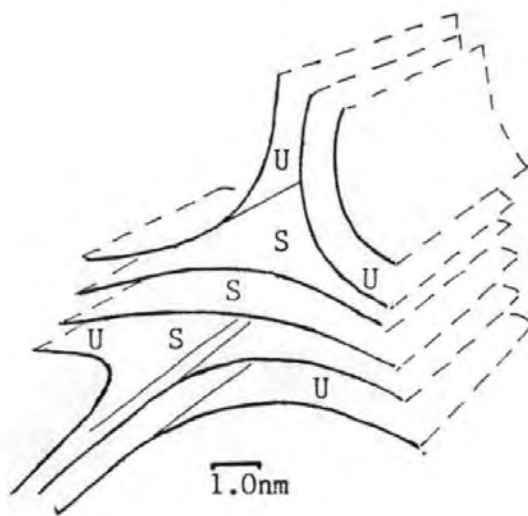
Fig 3.7 Graph of Weight Change Against Time for a Particulate Sample During a Full Isotherm Series.



### 3.1.7 ADSORPTION IN MICROPOROUS CARBONS

Microporous carbons are industrially important because of their adsorbative and physical properties (e.g. carbon blacks, activated carbons and carbon molecular sieves). Studies of microporous carbons are wide ranging, often combustion related (e.g. coal (Carter, 1983; Adams, 1988) and fly ashes (Low and Batley, 1988)). Casquero-Ruiz et al (1988) investigated n-nonane preadsorption, and Boehn et al (1982) studied chlorine chemisorption and pore blocking.

McEnaney (1988) reviewed the subject and detailed a model of the fine structure of microporous carbons (McEnaney and Masters, 1983) (Fig 3.8). The microstructure of general carbons consists of a tangled network of defective carbon layer planes with the micropores being the spaces between layer planes. Adsorption by these carbons is very complex. First, gases are strongly adsorbed at low pressures in micropores because there is strong enhancement of the adsorption potential due to overlap of the force fields of opposite pore walls. This has been calculated as being enhanced by a factor of 2 compared to the free surface. Second, constrictions in the microporous network cause activated diffusion effects at low adsorption temperatures when the adsorptive has insufficient kinetic energy to penetrate fully the micropore space. Third, microporous carbons can exhibit molecular sieve action. Carbons also exhibit molecular-shape



U possible ultra-micropores  
 S possible super-micropores

Mean Inter-layer Spacing of DP quoted by Smith (1981)  
 as being 0.355nm.

Fig 3.8 A Model of the Fine Structure of a Microporous Carbon  
showing Micropores as Spaces between Carbon Layer Planes.  
Taken from McEnaney and Masters, 1983.

selectivity by preferential adsorption of flat molecules, as expected in slit-shaped pores (McEnaney, 1988). An essential feature of the planar microstructure are cross-linked aliphatic bridging groups.

The BET equation is subject to limitations when applied to microporous carbons and can give unrealistically high SSA for activated carbons, due to the enhanced adsorption potential which induces an adsorption process described as primary or micropore filling. This applies to the BET equation if all the isotherm data is used. Glasson (personal communication, 1989) explains that if the BET equation was only applied to data  $<0.3 P/P_0$ , then this problem is greatly reduced. In any case the DP samples had SSA far less than activated carbons which may be as high as  $1500\text{m}^2/\text{g}$ .

### 3.2 ELECTRON MICROSCOPIC EXAMINATION OF DIESEL SOOTS

Scanning and transmission electron microscopy (SEM and TEM) were employed to examine the size and shape of the incipient soot particles. The theory and practical applications of electron microscopy are described elsewhere (Agar et al, 1971; Goldstein et al, 1981). The instruments used were a Joel model T-20, a Joel SEM-35 and a Philips 300 TEM.

DP are aciniform carbons (AC), composed of small spherical incipient particles varying from 5 to 100nm in diameter, which may fuse thereby forming long agglomerate chains (Fujiwara and Fukazawa, 1980; Medalia and Rivin, 1982). The degree of fusion is generally such that the individual particles can still be discerned in electron micrographs, but their individual size may be difficult to measure. This research found that the SEM technique coated the particles with a gold layer which improved particle clarity. TEM studies, showed the fused particles had indefinable boundaries. This research attempted to assess the size and shape of particles produced from the engines at Plymouth and studied the relationship between DP, UHC and particle growth down the exhaust.

For SEM samples, small sections of soot laden filter were mounted on aluminium stubs and coated with gold (12nm thickness) in a Polaron SEM E5100 sputtering unit which ensured electrical

conductivity during scanning (Fig 3.9). For TEM samples (Fig 3.10), vacuum carbon coated grids with Formval supporting film, were exposed to the exhaust gas and DP collected as the gas exited the ICF.

Series 1A (analysed using the T-20 instrument) supplied samples for SEM studies and by exposing the filter in reverse profile it was possible to reduce filter surface collection efficiency, thereby reducing cake formation and allowing individual particles to be clearly seen. Series 1C and Experiment 4A also supplied caked samples which were analysed under the high resolution JSM-35 instrument with technician support.

Towards the end of the SEM studies and research period, it was realised that the gold sputtering unit was adding material to the small particles and increasing their diameter. TEM was employed on some fresh samples to assess this effect. It was discovered that the actual mean particle sizes were around 30-40nm, not the 100-180nm reported by SEM data. This was attributed to the gold coating individual and adjacent particles and increasing the apparent size by 160%. This did not appear to affect the particle size trends noted in the exhaust only the actual size values. These particle sizes correlated with literature values for a similar IDI engine which reported that mean particle diameter increases down an exhaust from 25nm (at

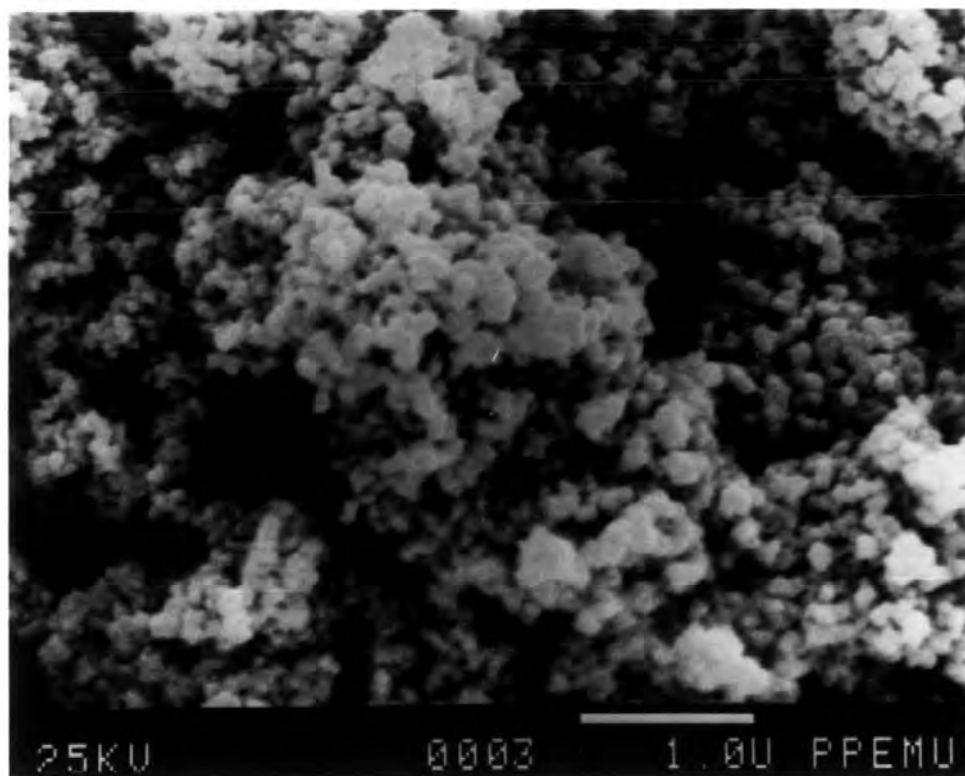


Fig. 3.9 Scanning Electron Micrograph of Caked Diesel Particulate  
(1 bar = 1 $\mu$ m)

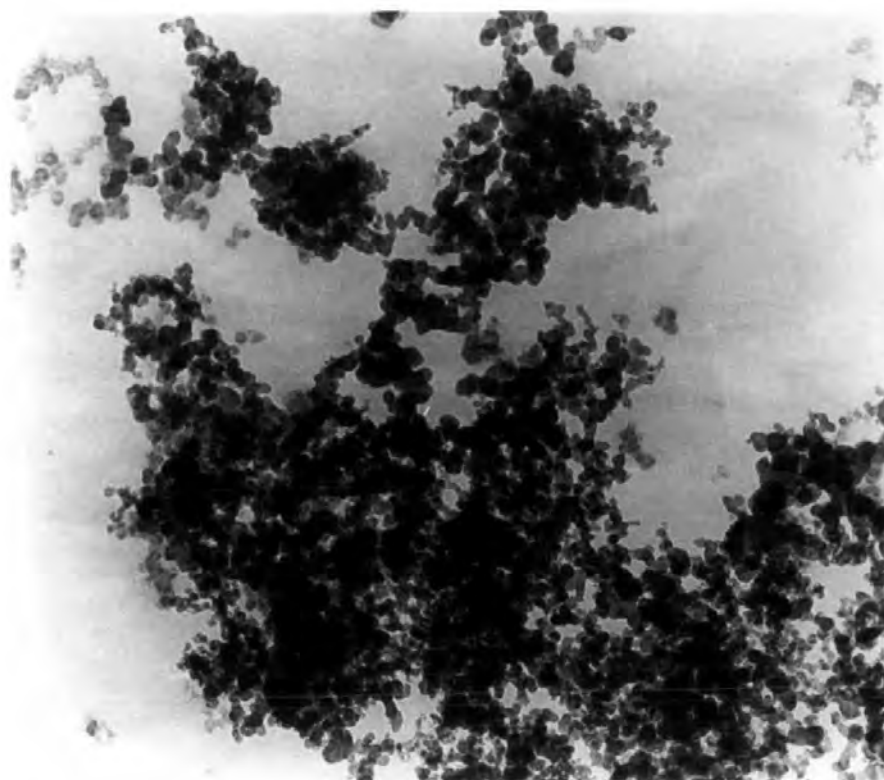


Fig. 3.10 Transmission Electron Micrograph of Diesel Particulate  
(1 bar = 120nm)

0.064m from engine) to 35nm (at 5.164m from the engine) due to temperature declining below a threshold temperature of 150°C (Fujiwara and Fukazawa, 1980)

A Bosch Smoke quartz filter was also examined by SEM to evaluate its potential as an EM sampling device.

### 3.2.1 GEOMETRIC SURFACE AREAS OF DIESEL SOOTS

The geometric surface area of a spherical particle can be calculated from the mean particle diameter and density of graphitic carbon. Thus a surface area in m<sup>2</sup>/g of DP can be compared to the BET SSA values to give a measure of internal and external surface area.

The simplified equation:

$$\text{Geometric Surface Area} = \frac{6}{dl} \quad \text{Equation 3.7}$$

where:

d is the density (g/m<sup>3</sup>)

l is the diameter of the particle (m)

It has been derived from the surface area of a sphere (4πr<sup>2</sup>) divided by the volume ( $\frac{4}{3}\pi r^3$ ) multiplied by density.

For DP with mean particle diameters of 40nm the external specific surface area is 75m<sup>2</sup>/g. This suggests that if

total SSA is  $220\text{m}^2/\text{g}$ , then the internal microporous area contributes 66% of total surface area.

Correction for the SEM coating was determined, assuming that the gold was evenly distributed across the soots. The mean particle diameter determined by SEM was about 100nm of which 25nm could be ascribed to the gold coating on the particle surface. If the particle diameter is corrected for this coating, giving a diameter of 75nm, then the geometric surface area is  $40\text{m}^2/\text{g}$ . This is not dissimilar to values obtained for TEM analysed soots.



### 3.3 CHEMICAL ANALYSIS OF UNBURNT HYDROCARBONS

Unburnt hydrocarbons (UHC) samples were prepared for analysis by gas chromatography (GC). The samples were quantitatively compared to each other, and to standards, fuel and oil. Intersample comparisons were carried out in a quantitative manner by processing each sample with identical volumes of solvent (in extraction and analysis). DCM was selected as the extracting solvent because of its high solubility for substances over a wide polarity range (Obuchi et al, 1984).

The extraction and identification of UHC from diesel exhausts has been reviewed (Chapter 1). The soxhlet technique is most frequently employed and used for EPA dilution tunnel studies for filters at 52°C to obtain a soluble organic fraction (SOF). The method, it is claimed, extracts 99.9% of available DCM soluble UHC (Bjorseth, 1984). Filter extractable samples (FES) are those UHC samples obtained from a filter at any temperature in a non-diluted exhaust. The TESSA UHC samples are called the tower extractable sample (TES).

### 3.3.1 FES EXTRACTION FROM FILTERS

Initially, the soxhlet method was selected to extract the Series 1B QMA filters. The physical nature of the media limited exposure to 7 seconds. The objective was to validate the BCF filter and collect samples from a variety of sample positions and engine conditions.

The pre-weighed filters were exposed to the exhaust stream at known temperatures. The filters were reweighed and re-equilibrated (24hrs) to obtain a diesel particulate (DP) mass. An FES sample was obtained by soxhlet extraction (150ml DCM, 24hrs) in a light protected glass apparatus and the sample was prepared as detailed in Section 3.3.3. All handling was by forceps to avoid contamination.

### 3.3.2 SERIES 2A THE TOTAL EXHAUST SOLVENT SCRUBBING APPARATUS (TESSA)

The Total Exhaust Solvent Scrubbing Apparatus (TESSA) and method, developed by Petch et al (1987), was employed to extract all the gaseous UHC and strip the particulate of adsorbed HC's.

TESSA consisted of a modular cylinder solvent scrubbing system with a graded glass filling, baffles and internal cooling

coil. Solvent (DCM/methanol 50/50 v/v) passed down the system over the glass which provided a 'wet' enhanced surface area for reactions and stripped rising exhaust gas of its UHC component. Solvent, UHC and suspended particulate passed out of the bottom of TESSA and was collected into distilled water. The TESSA system was shown in Fig 2.2.

After sampling (for 360 seconds), the solvent mixture was filtered under reduced pressure using Whatman filters (GF/F 5cm). The two solvent phases were separated by liquid/liquid partition in a separating funnel (2 litres). The DCM fraction (lower layer) was removed and the remaining aqueous methanol fraction was washed with further DCM volumes (150cm<sup>3</sup>) to ensure complete transfer. The DCM fractions were combined and reduced in volume by rotary evaporation as described in Section 3.3.3 Further elucidation of methods and validation may be sought in the thesis by Trier (1988).

Electron microscopic investigation of the TESSA particulate material showed it to be composed of glass fragments and a small quantity of iron, presumably from pipework. Further investigation by X-ray analysis proved inconclusive due to the mixed composition of the sample.

### 3.3.3 UHC SAMPLE PREPARATION

After collection (by any technique) the UHC samples were reduced in volume by reduced pressure rotary evaporation at 30°C. Care was taken to ensure the slow removal of solvent during this concentration step to avoid sample loss. A 2ml aliquot was retained and quantitatively transferred to a preweighed vial (1.75ml). Gentle N<sub>2</sub> blow-down reduced the sample to a constant weight from which the % extractable sample was calculated. All UHC samples were stored in vials, in a dry condition at -8°C, protected against the light. Whole filters were stored in foil at 4°C (also protected against the light) to avoid water expansion if frozen.

Filters spiked with fuel and oil were extracted by this technique and collection efficiency measured at 96% ±2%.

#### 3.3.4 OPEN-COLUMN CHROMATOGRAPHY

Open-column chromatography with silica gel columns was used to fractionate the TESSA TES samples (Series 2A) into their component groups; aliphatic, aromatic and polar. Sequential elution by suitable solvents according to polarity separated the fractions. Sample fractionation of complex mixtures by this technique is now standard (Robbins and McElroy, 1982). The soxhlet extracted silica gel (DCM, 24hours, oven dried, 120°C) was stored at 50°C, which ensured a constant moisture content of 5-8% water (w/w) to avoid poor reproducibility (Later et al 1985).

The columns were prepared by pouring a mixture of silica (3g) and hexane (2ml) (stirred to remove air bubbles) into an empty pipette (10ml volume), previously plugged with solvent extracted cotton wool. The column was tapped with a small piece of rubber tubing to vibrate and tightly pack the column. The column was never allowed to become dry.

The method was as follows: Hexane (1ml) was added to the TES sample vial and ultrasonicated (5mins) which re-dissolved the sample. This solution was applied rapidly to the top of the column, rinsing the vial twice (0.5ml). The column was eluted sequentially with Hexane (10ml), DCM (15ml) and methanol (15ml) to remove the aliphatic, aromatic and polar compounds

respectively. Recovered fractions were quantitatively determined after N<sub>2</sub> blow down in preweighed sample vials. Some very polar material may remain on the column and may constitute an error. This method was taken from Trier (1988).

Fractionation of Series 1B samples was attempted but the application of micro-column fractionation to FES masses often <0.2mg proved impossible.

### 3.3.5 GAS CHROMATOGRAPHIC ANALYSIS OF SAMPLES

High Resolution Gas Chromatography (HRGC) was used to identify hydrocarbon species. Sample preparation was identical for the UHC samples and fractionated samples, both being diluted for injection using DCM.

Samples were analysed with a Carlo Erba HRGC 5360 equipped with cold on-column injection and a flame ionisation detector (FID). The FID response was integrated using a Shimadzu CR3-A integrator. Standard HRGC conditions are listed in Table 3.3.

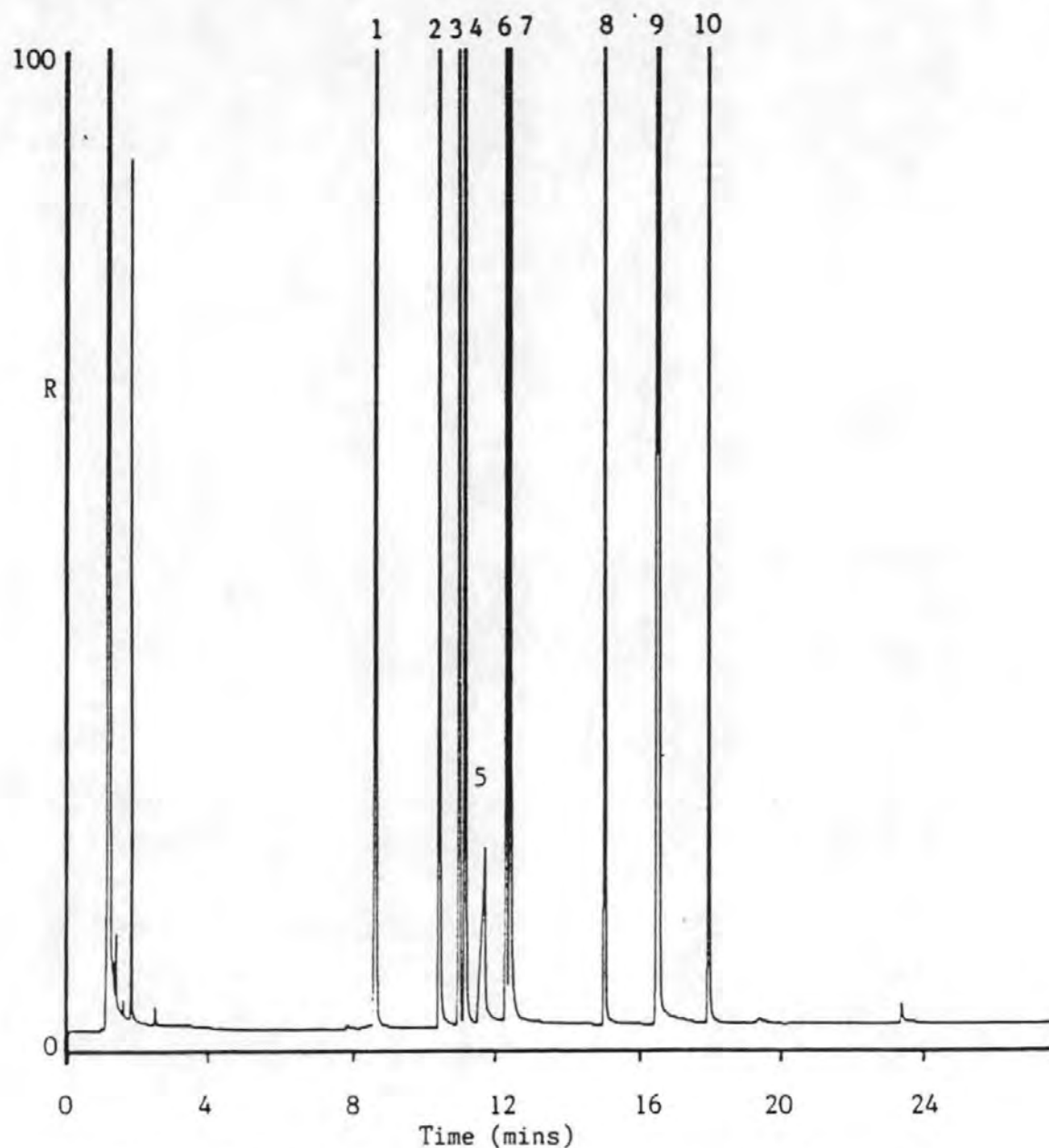
Daily checking of instrument gas flows and injection of a GROB mix standard (Fig 3.11) (Grob, 1985) ensured that consistent column conditions were maintained.

Sample injection was standardised using a 5.0ml syringe for

DETAILS

Column Type	SE-54 Fused Silica Capillary
Length	25m
I.D.	0.25mm
Film Thickness	0.025mm
Injector Type	Cold On-Column
Injector Volume	0.5mm <sup>3</sup>
Injection Volume	0.1µl and 0.5µl
Solvent	Dichloromethane (DCM)
Detector Type	Flame Ionisation (FID)
Detector Temperature	320°C
Detector Sensitivity	approx. 5ng per component
Gas Pressures	H <sub>2</sub> 70kPa Air 100kPa N <sub>2</sub> 100kPa
GC Oven Temperature Program	50°C for 5 mins, Ramp 10°C/min, Final Temp 300°C for 20 mins.
Chart Speed	5mm/min

Table 3.3 High Resolution Gas Chromatographic Conditions



Peak N°	Retention Time (mins)	Identification Name	Concentration (mg/ml)
1	8.6	Decane	0.031
2	10.4	Octanol	0.037
3	10.9	Undecane	0.029
4	11.1	2,6, Dimethylphenol	0.042
5	11.7	2, ethyl Hexanoic acid	0.036
6	12.3	2,6, Dimethylaniline	0.035
7	12.4	Nonanol	0.047
8	15.0	Methyl Decanoate	0.044
9	16.5	Methyl Undecanoate	0.043
10	17.9	Methyl Dodecanoate	0.044

Fig. 3.11 Chromatogram of GROB Standard, Plotted as Time Against 'R' Response with a Table of Identification.



semi-quantitative research, and a 0.5ml syringe for quantitative samples. Trier (1988) showed that the coefficient of intersample injection between the two syringes using the same injection technique was 8.5% compared to 2.3% for the smaller syringe.

### 3.3.6 STANDARDS AND IDENTIFICATION

A standard mixture of three compounds were used to identify specific compounds within the sample fractions. The three standards used were from the Lee retention index; naphthalene, phenanthrene and chrysene and are shown with the concentrated solvent system blank (Fig 3.12). Using co-injection, the sample compounds could be identified (Lee et al, 1979).

Oil and fuel samples were prepared (Fig 3.13) to compare against samples. The lubricating oil had a retention window between 24 and 36 minutes which accounted for 95% of the total high molecular mass hydrocarbons (Trier, 1988). It consisted of a prominent hump, an unknown complex mixture (UCM) thought to be polar, branched and aromatic compounds. In addition several peaks crested the hump, and were identified as the Hopane series of highly cyclic aromatics which have been used as exhaust marker compounds (Trier et al, 1987). The fuel was found to have a retention window between 8 and 24 minutes and had a normalised distribution of n-alkanes (around n-C<sub>16</sub>) with identifiable isoprenoids (Pr - Pristane and Ph - Phytane) co-eluting with n-C<sub>17</sub> and n-C<sub>18</sub>.

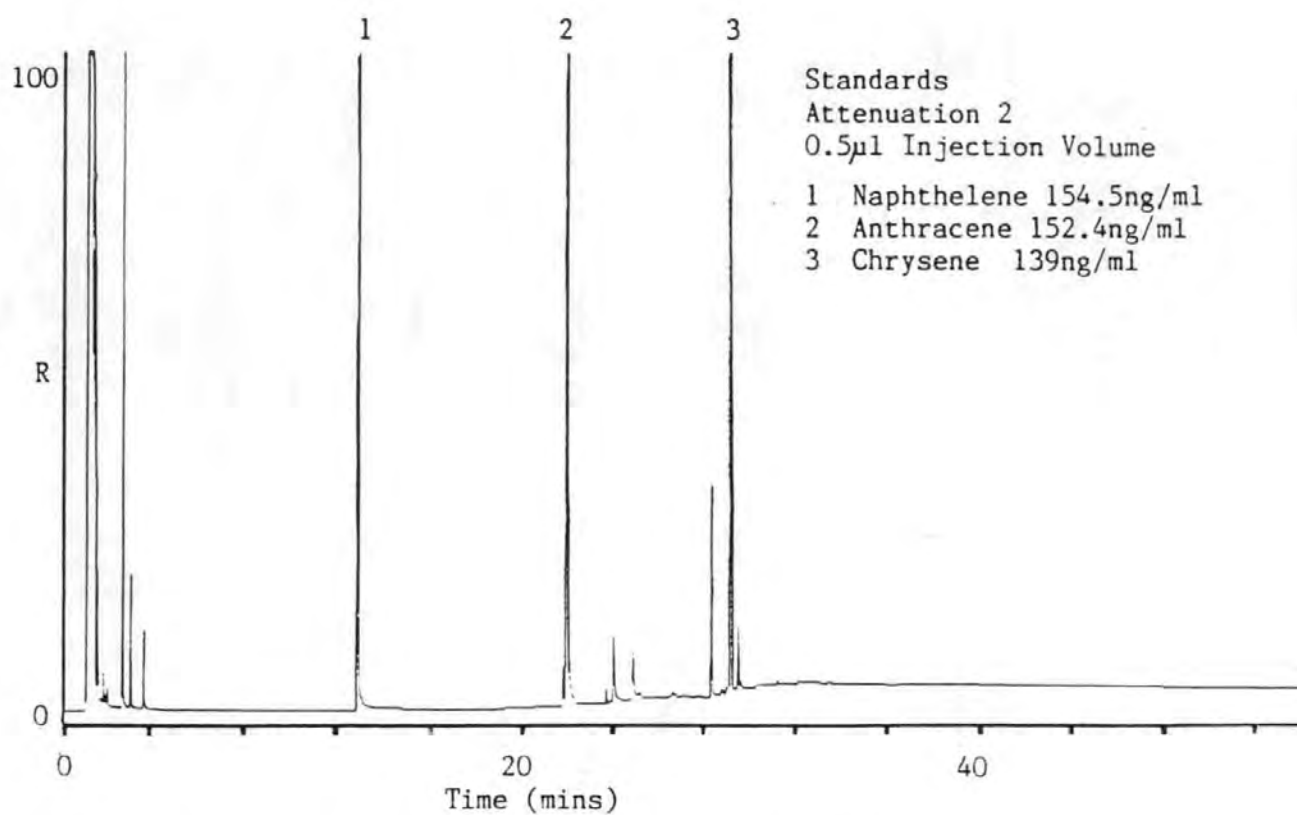
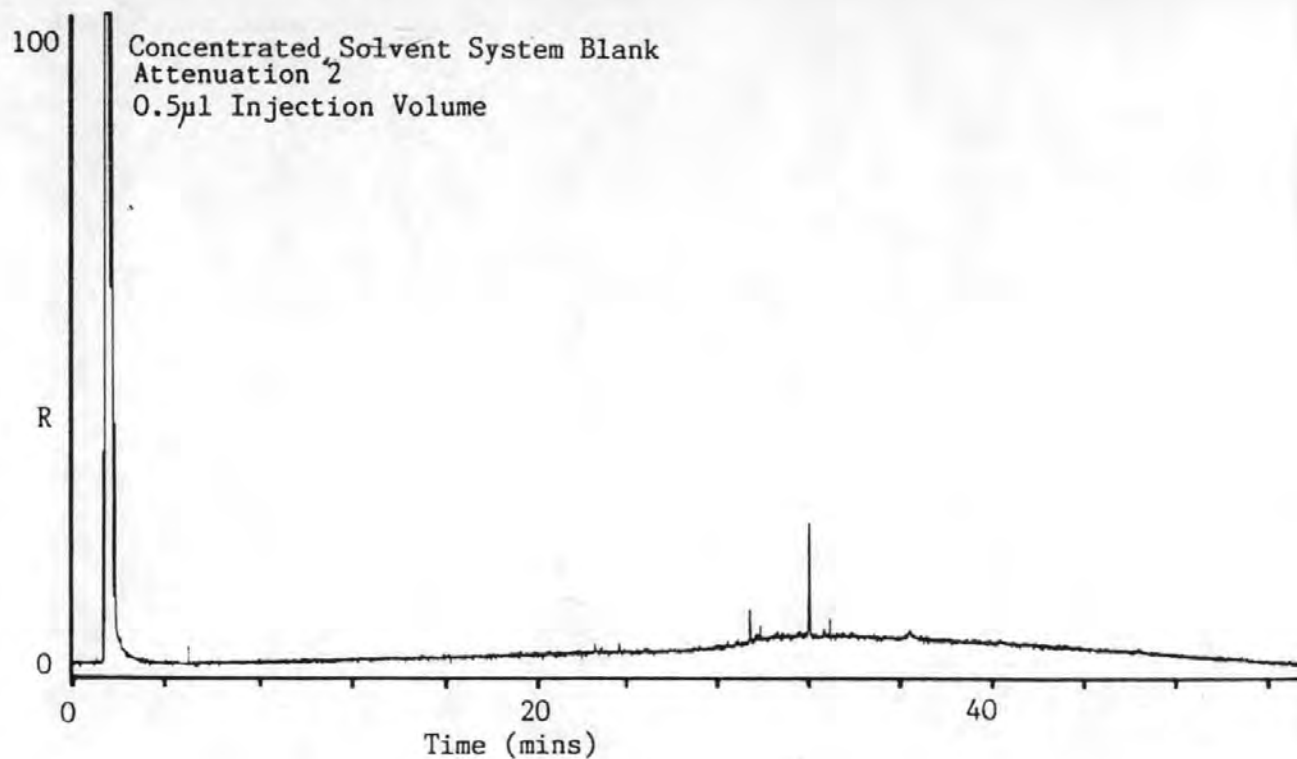


Fig. 3.12 Chromatograms of the Concentrated System Blank and PAH Standards used in the Lee Retention Index. (Lee *et al.*, 1979)

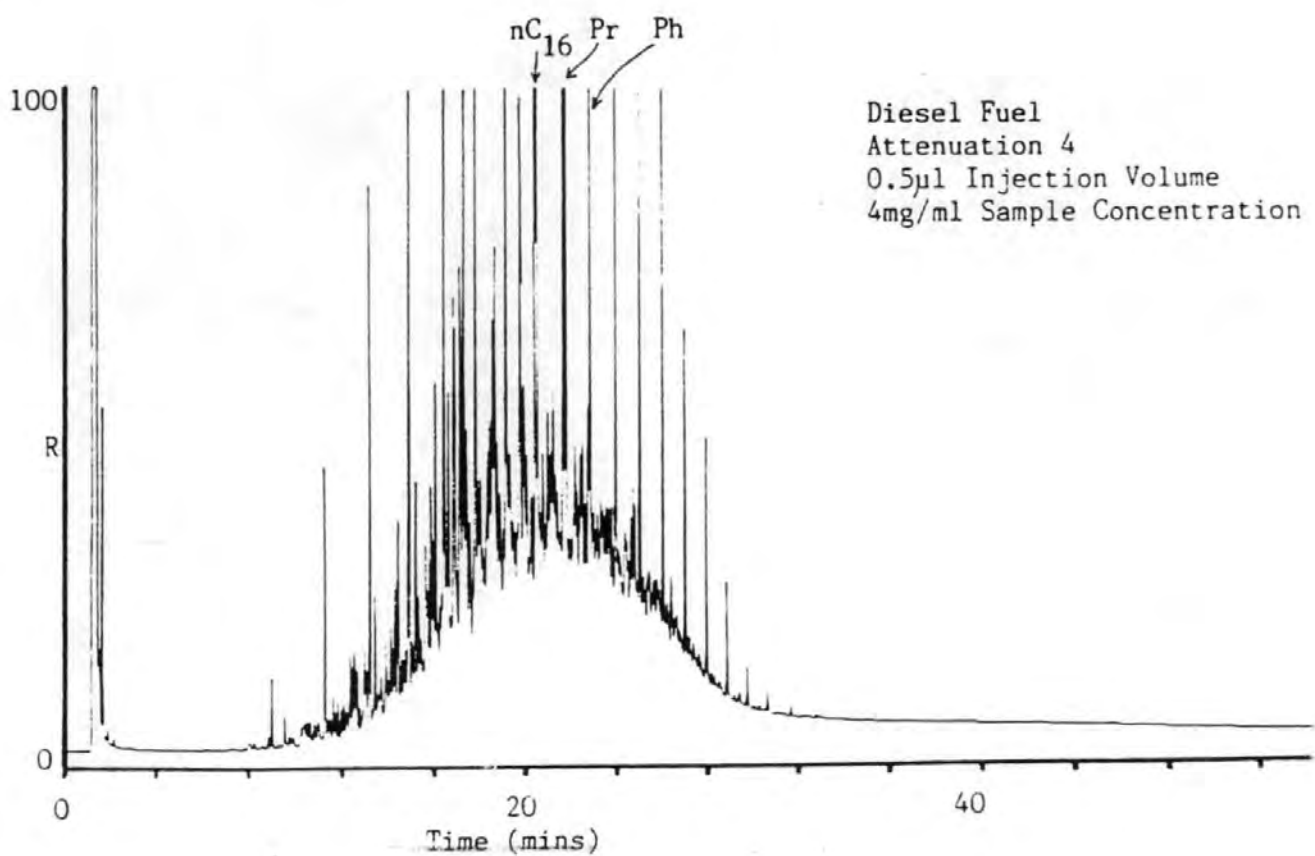
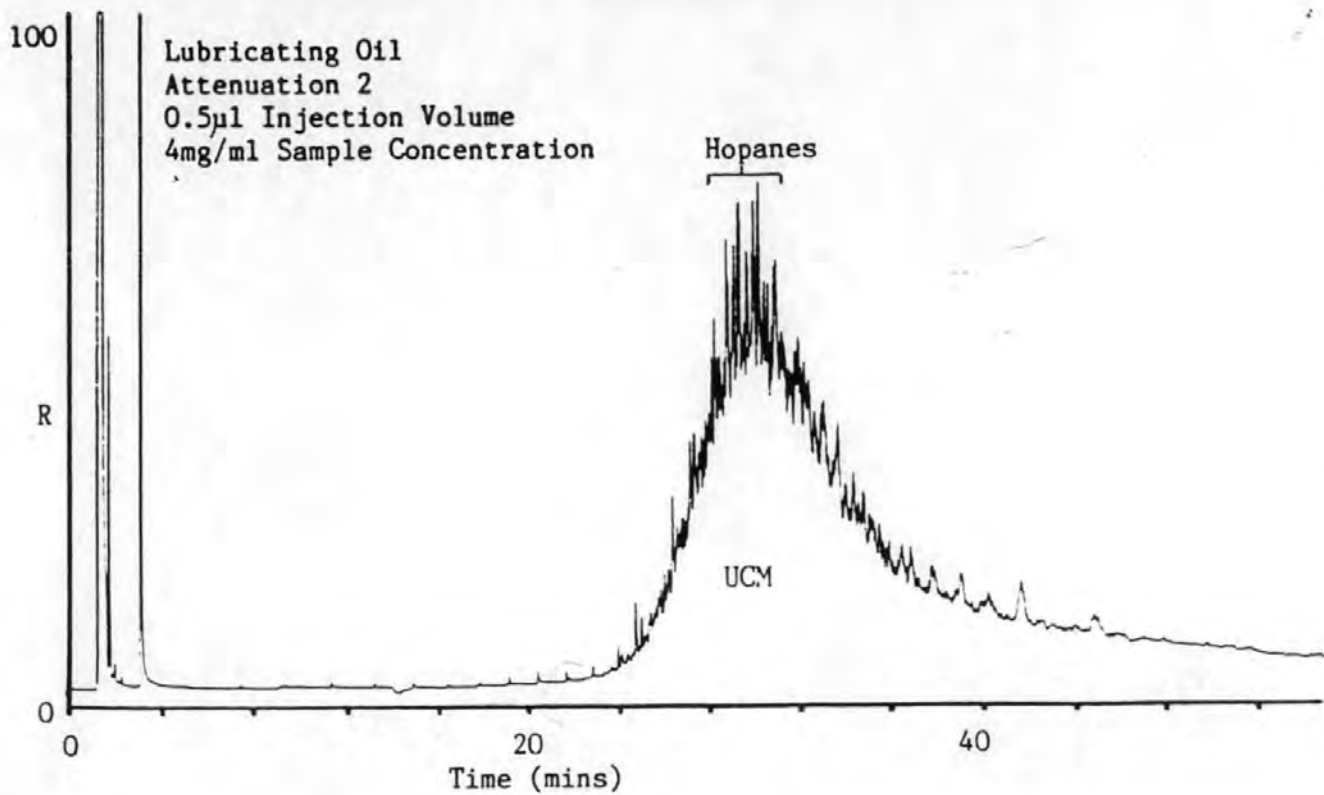


Fig. 3.13 Chromatograms of Lubricating Oil and Diesel Fuel.

### 3.3.7 DISCUSSION OF SOURCES OF CONTAMINATION

Sample integrity was maintained by a number of precautions employed to reduce contamination. All solvents employed in this work were previously redistilled in a glass apparatus (Walker 1979) to ensure a contamination free solvent, as evaluated by GC and a purity greater than 99.99%. Crude solvents and once used DCM was soaked in suitable drying agents to remove any traces of water (Vogel 1956). It was essential to maintain cleanliness because of the concentration steps during sample preparation.

All glassware, prior to use was soaked (24 hrs) in a 5% solution of Decon 90. This was followed by rinsing in cold tap water (10 times) and a single wash with distilled water. If rapid drying was required then the glass was further rinsed with distilled acetone (to remove water) and dried at 50°C in an oven. Prior to use, glassware was further rinsed with DCM.

Silica gel, cotton wool, anhydrous sodium sulphate and anti-bumping granules were pre-extracted overnight in a soxhlet apparatus with DCM, in order to remove contaminants. Schwartz (1978) recommends this approach for glass wool.

During this study, it was found that the foil lined screw-caps of the sample vials caused contamination. The source was determined to be the cork inlay, which was confirmed by a

article by Denney et al (1978). Further problems may come from phthalate contamination enhanced during concentration steps. These compounds are ubiquitous (Levine et al, 1982) and have been identified (Trier, 1988) and may be difficult to exclude, although they were not noted in this study.

### 3.4 EVOLVED GAS ANALYSIS

Evolved gas analysis (EGA) is the technique of determining the nature and amount of volatile product or products formed during thermal analysis (Wendlandt, 1986). Thermogravimetric (TG) balance systems have been coupled to detection instruments and extensive reviews of the combined systems are available (Wendlandt, 1986). For example, a TG-GC instrument was developed by Chiu (1968) which allowed the collection and analysis of evolved products. Zitomer (1968) coupled a DuPont model 950 thermobalance to a Bendix mass spectrometer to produce a TG-MS which gave fast analysis and minimised secondary sample reactions during transfer. Additionally, Gallagher (1978) developed an EGA-MS system and Onodera (1977) has used Pyrolysis-GC for total decomposition work. Cuthbertson *et al.*, (1979) used an HFID to detect lubricating oil and fuel UHC (Fig 3.14) from the thermogravimetric analysis of DP, but did not collect the volatiles. Stenburg and Alsberg (1981) (Fig 3.15) developed a vacuum sublimation system for the extraction of PAH's from carbonaceous materials but failed to consider surface effects or examine microstructure.

With these established techniques in mind, a non-destructive EGA system, capable of separating the UHC from DP, was developed. The volatiles were trapped and analysed by GC, and microstructural changes were examined.

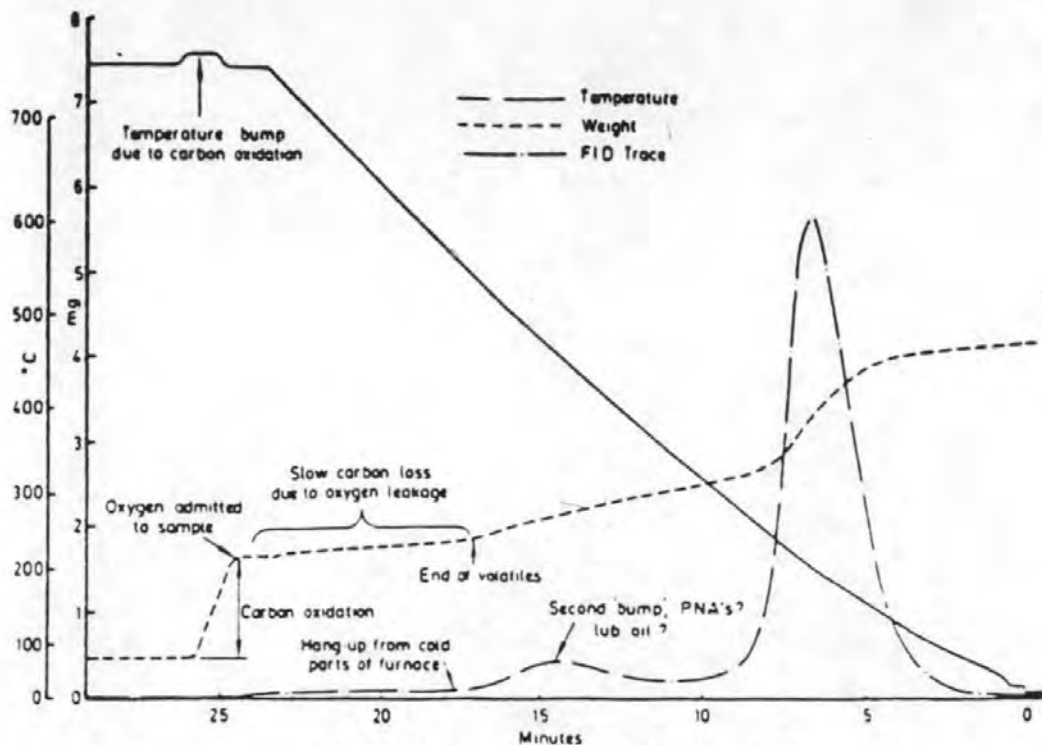


Fig. 6 - TGA interfaced with an HFID - weight loss and HC curves for a soot sample

Fig. 3.14 TGA and HFID Results of an Analysed Diesel Particulate (from Cuthbertson *et al*, 1979)

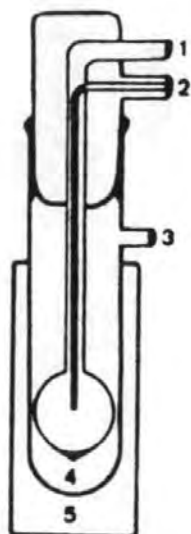


Fig. 3.15 All Glass Sublimation Apparatus: 1) Water Outlet, 2) Water Inlet, 3) Connection to Vacuum Pump, 4) Vacuum Chamber, 5) Oven. (from Stenberg and Alsberg, 1981)



EGA avoids fibre and soot contamination and has short extraction times (typically less than 3 hours compared to 24hours for soxhlet extraction). Furthermore, the possibility of artificial solvent-induced agglomeration and solvent extraction of UHC is avoided. Stenburg and Alsberg (1981) pointed out that some degradation may occur of very labile species, especially diketones, cyclopenteno[c,d]pyrene and anhydrides if prolonged extraction or high temperatures are employed. The system (time and temperature) can be tailored towards the study of specific molecular mass compounds thus minimising such degradation. EGA offers the advantage of efficient extraction of high molecular mass hydrocarbons and reassessment of DP microstructure without solvent influences. This study intended to reproduce the tentative work of Ross et al (1982), who showed that temperature degassing of a non-extracted DP sample, increased its SSA, equivalent to the DCM extractable fraction.

The system was developed to thermally degass (TD) the volatile compounds adsorbed on the diesel particulate (DP). The specifications for the design were as follows;

- 1) To thermally degass the volatile hydrocarbons (fuel and oil derived) from the DP, without structural and/or chemical modification of either component.

- 2) To collect efficiently the desorbed volatiles.
- 3) To obtain a contamination free sample which can be analysed by gas chromatography.

#### 3.4.1 THERMAL DEGASSING EXPERIMENTS FOR THE CHEMICAL AND MICROSTRUCTURAL CHARACTERISATION OF DP

After the completion of Series 1A (which included thermal degassing of UDCM soots) and Series 1B it was necessary to develop an extraction method which enabled particulate to be analysed for BET SSA determination without solvent pre-extraction, as occurred with the UDCM method. A thermal degassing (TD) method was developed, which also enabled evolved gas analysis to be performed. The method was similar in principal to the technique outlined by Stenborg and Alsberg (1981), when vacuum sublimation of carbon blacks was compared to soxhlet extraction methods. They stated that "vacuum sublimation is a solvent free procedure which possesses the advantage of easy handling and high yields in short extraction times" and that for "PAH's the method is a good substitute for the conventional soxhlet technique". They used a environment of 300°C and 0.1mm Hg which extracted the volatiles as efficiently as a range of solvents, of which DCM was the most effective during solvent extraction.

The thermal degassing method developed at Plymouth, used

similar degassing operating conditions to exploit the favourable hydrocarbon vapour pressures at 0.1mm Hg pressure which avoided high temperature DP degradation (e.g. microstructural swelling).

Series 1C compared DP from different engine conditions collected on TX-40 filters using the ICF system. Pre-equilibrated, pre-weighed filters were used and mass loadings obtained for a wide range of engine conditions, sample positions and exposure times. Exhaust temperature and filtration pressure changes were monitored. Each filter was reweighed after exposure and stored at 4°C, protected against the light until analysis (usually less than a week). On-filter SSA and on-filter TD were performed to characterise the particulate.

#### 3.4.2 THE EGA SYSTEM

The EGA system developed over 8 months, improving collection efficiency and sample integrity. The final design employed much of the previously described BET microbalance apparatus and was a pyrex glass construction. The CI Instruments balance head and control unit were used with the vacuum system, and a larger sample hangdown envelope. A cylindrical furnace was constructed and positioned around the sample, and temperature monitored by thermocouples. A cold trap collected desorbing volatiles before analysis.

### 3.4.3 EXPERIMENTAL DESIGN AND DEVELOPMENT

Choice of sample environment was important in the experimental design. Since this was a thermal technique with the possibility of DP and volatile oxidation, air was excluded from the sample apparatus. Nitrogen ( $N_2$ ) carrier gas (White Spot, 99% purity) and vacuum (1mm Hg) were tested, both being readily available and used in the BET apparatus.

Nitrogen was advantageous for safety reasons and would allow the volatiles to be released at room pressure. However, with a gravimetric technique, a carrier gas causes problems; sample vibration (enhanced by convection currents at high temperature), weight changes caused by flow pressure and direction of gas sweep, complex bouyancy corrections for temperature and the large volume of gas required, posed to many problems to be surmounted. Some developmental experiments were carried out with  $N_2$ .

A vacuum atmosphere (1mm Hg) was chosen, having the advantages of minimising bouyancy and oxidation, allowing lower degassing temperatures and higher efficiencies for high molecular mass hydrocarbons, thereby not subjecting the DP to high temperatures that might cause thermal swelling, and did not cause any sample vibration. Routine precautions against

implosion were taken and safety glasses worn at all times. The vacuum system allowed the use of a cold trap at liquid N<sub>2</sub> temperatures facilitating the trapping of all volatiles.

Various designs of EGA system and trap were tested. Naphthalene crystals (Melting Point 80°C) were sublimed in place of a sample to indicate where desorbed hydrocarbons might collect in colder regions of the system. In each design the recrystallised naphthalene, was dissolved in solvent (DCM) and dried to give a crystal weight and % efficiency.

Initial prototypes consisted of a vertical envelope around the sample with a side-arm connected via gas taps to a vertical cold trap and operated with a N<sub>2</sub> atmosphere (Fig 3.16). Heating tape (>200°C) enhanced volatile transfer. Naphthalene recrystallisation indicated that the poor trapping (approx 25%) was due to poor flushing by N<sub>2</sub> and condensation in cold regions above the furnace.

The design was modified to accept carrier gas input from beneath the sample but this caused recrystallisation in the balance head because the heating tape acted as a thermal barrier to trapping. Split gas flows (50/50 and 25/75 mixes) from above and below the sample, increased the efficiency to 33% and 50% respectively, after the tape was removed.

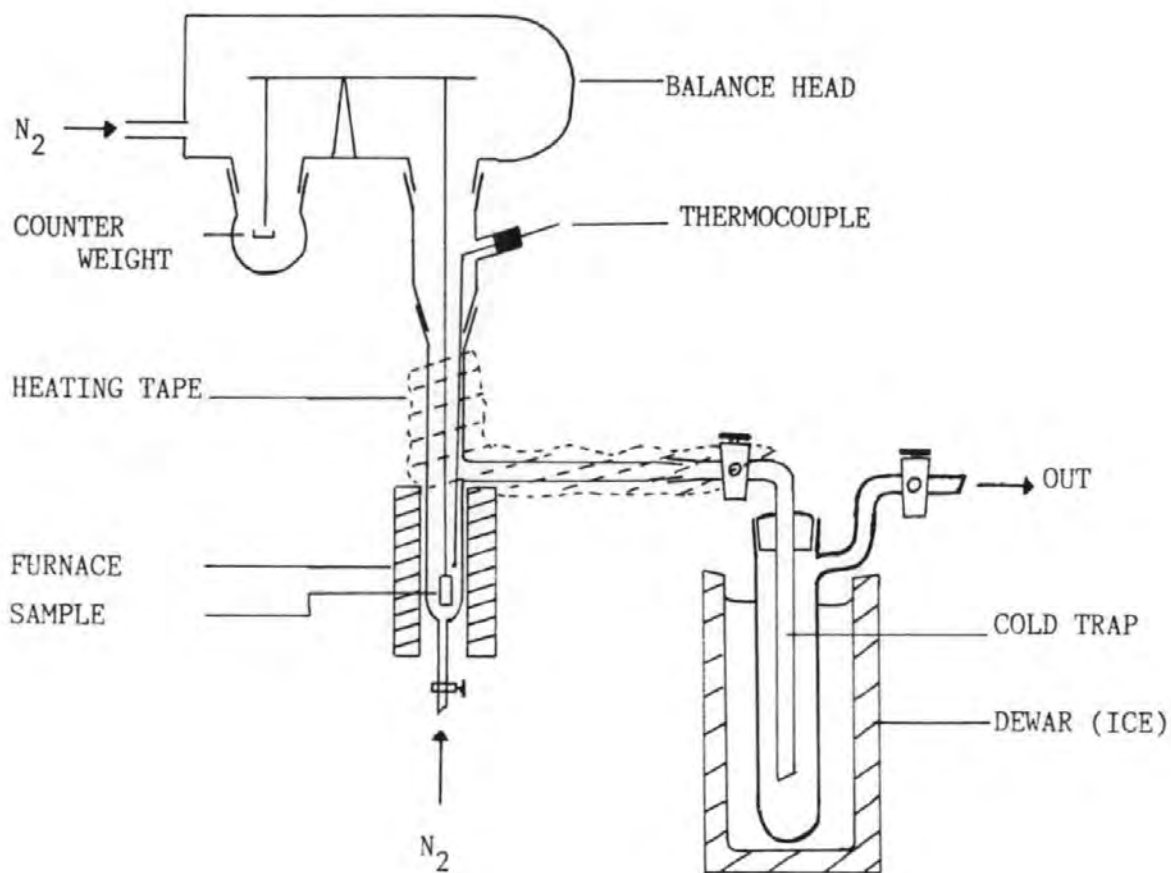


Fig. 3.16 Prototype EGA Apparatus Design for Nitrogen Gas

These efficiencies were viewed as unacceptable because often very small quantities (<0.5mg) of volatiles were often released. The apparatus was modified to accept a coil cold trap, positioned beneath the sample, which minimised the transfer distance (<4cm). The furnace was reconstructed with new electric winding to produce a temperature gradient favouring downwards volatile movement. The glass hangdown envelope was enlarged and sealed after the positioning of a sample thermocouple (Pt/Rh 13%). The thermocouple was calibrated using an ice-water cold junction at 0°C. Simultaneous temperature and weight readings were recorded against time by a chart recorder set on appropriate voltage scales. The samples, previously analysed by the BET technique, were balanced and brought on scale (typically 0-10mg). The pyrex glass envelope was assembled around the sample and the furnace lifted around the envelope and coil trap connected. The apparatus was sealed against air leakage using teflon seals (Fivac ribbed sleeves, with a quoted leak rate of  $10^{-4}$  mmHg l/sec). The apparatus is illustrated in Fig 3.17.

This system gave a naphthalene collection efficiency of over 95% by mass. Doped diesel fuel on ultrasonicated DP had a similar collection efficiency.

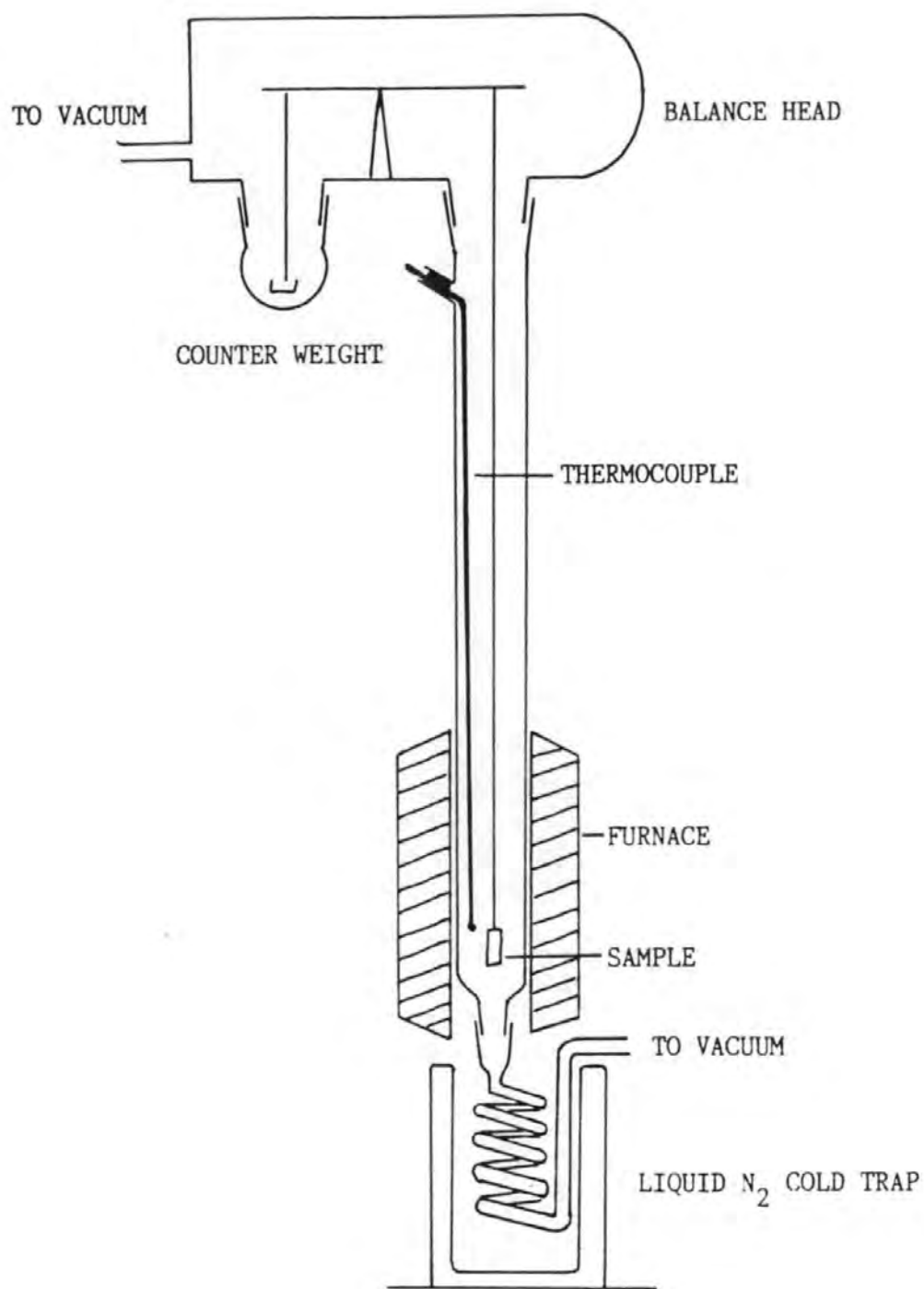


Fig. 3.17 The Thermal Degassing Apparatus for EGA



#### 3.4.4 OPERATIONAL PROCEDURE

The sample was first outgassed to remove water which took from 1 to 30 minutes depending on adsorbed moisture content. Table 3.3 showed how the vapour pressures of hydrocarbons and water change with pressure and temperature. The degassing was operated at 1mm Hg pressure and the moisture drawn to the pump.

After the sample weight had stabilised, the balance was zeroed and the liquid N<sub>2</sub> poured into the cold trap dewar. The furnace was switched on and temperature raised to 300°C at approximately 5°C/min heating rate where it was held for 30 minutes. The temperature and pressure was sufficient to remove all UHC without PTFE seal degradation nor any adverse effects on balance operation. Occasionally the dewar was topped up. After this period the furnace was switched off, sample cooled, cold trap lowered and nitrogen gas (400mm Hg) allowed into the envelope to apply a inert partial pressure, and stop any leaking air bringing in moisture.

The FES was removed from the trap by washing with DCM (20ml), rotary evaporated to reduce solvent volume (30°C, low vacuum) and quantitatively transferred to a clean preweighed vial (1.75ml). The FES weight was obtained by careful N<sub>2</sub> blow down to a constant weight. All samples were stored 'dry' in darkness at -4°C.

To show that the UHC was adsorbed to the DP and to test the system, a DP sample was degassed and the TG weight loss curve compared to the desorption TG weight curve of fuel doped on a filter. The result is shown in Fig 3.18 and proved that the doped fuel is weakly adsorbed compared to the DP UHC. The degassed doped fuel sample was analysed by GC and compared to normal fuel. Fig 3.19 illustrates the slight loss of low molecular mass n-alkane that occurs during room temperature out-gassing but also shows the excellent collection efficiency (>95%) and validated the system. Pristane (Pr) and Phytane (Ph) aid identification of the n-alkane peaks, coeluting with n-C<sub>17</sub> and n-C<sub>18</sub>.

#### 3.4.5 ADDITIONAL EXPERIMENTS

The TD method was used for the routine characterisation of the DP from a wide range of engine conditions (Series 1C). Additional experiments were also performed to investigate specific aspects of the research.

Experiment 3A, followed the work of Stenburg and Alsberg (1981), by comparing different extraction methods with thermal degassing. One sample (1500rpm, 27.4Nm, 3.3m) was sub-divided and each quarter extracted by either soxhlet, ultrasonic or thermal degassing. This was after initial microstructural

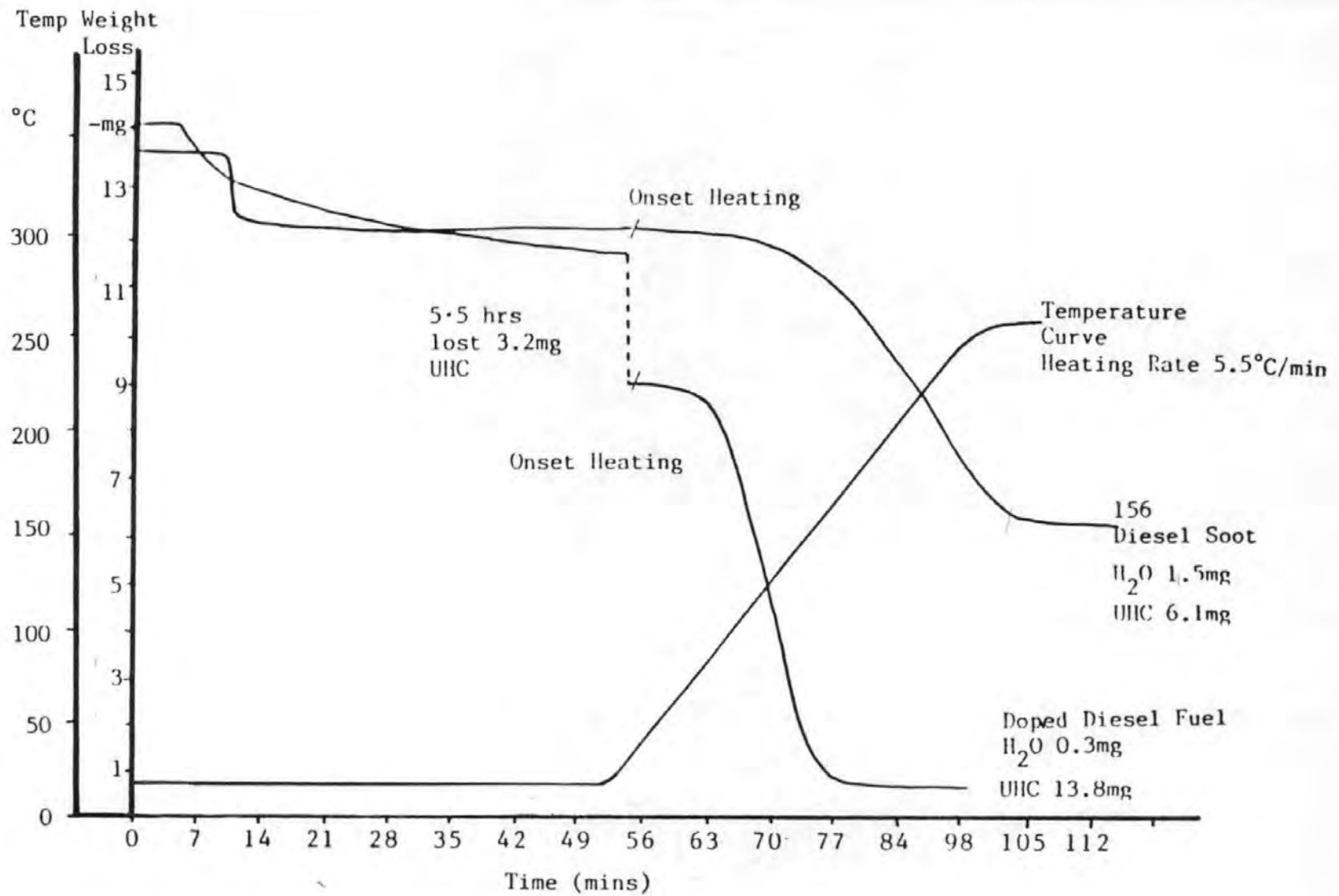


Fig. 3.18 Thermal Desorption Curves of Diesel Particulate and a Doped Diesel Fuel (On-Filter).

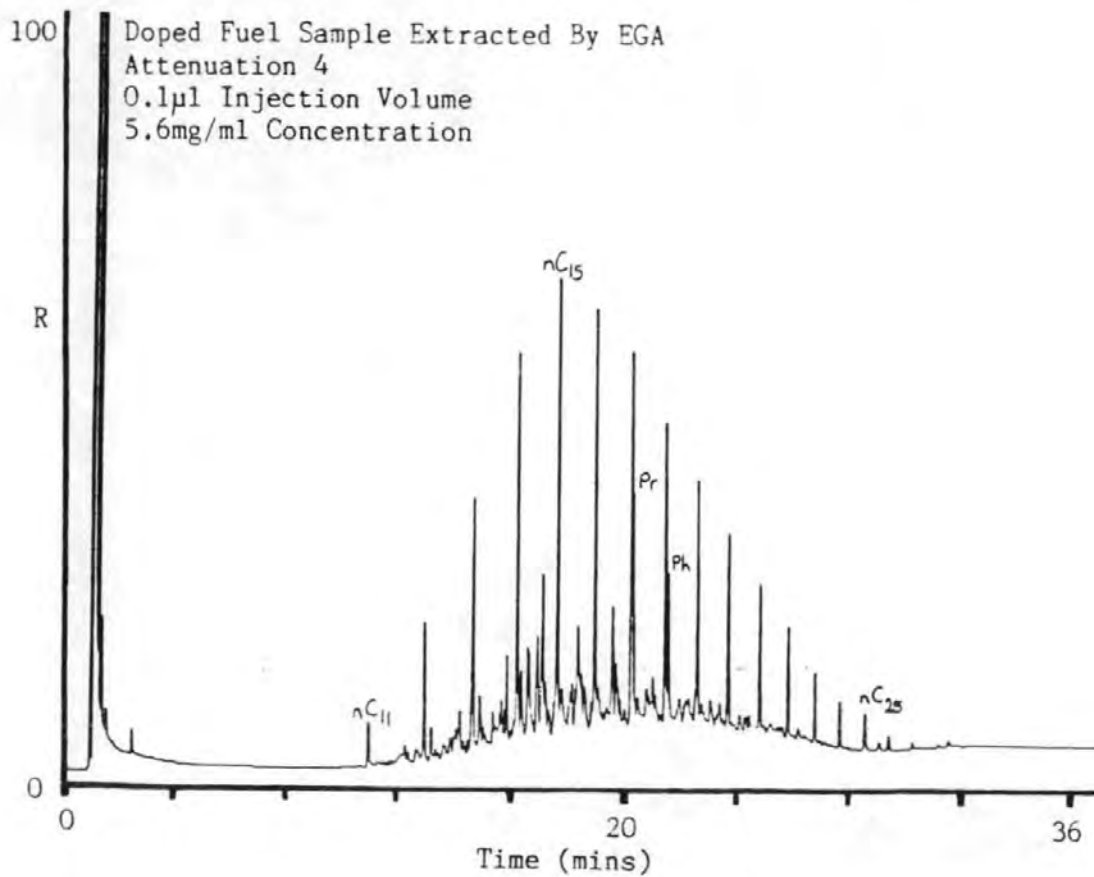
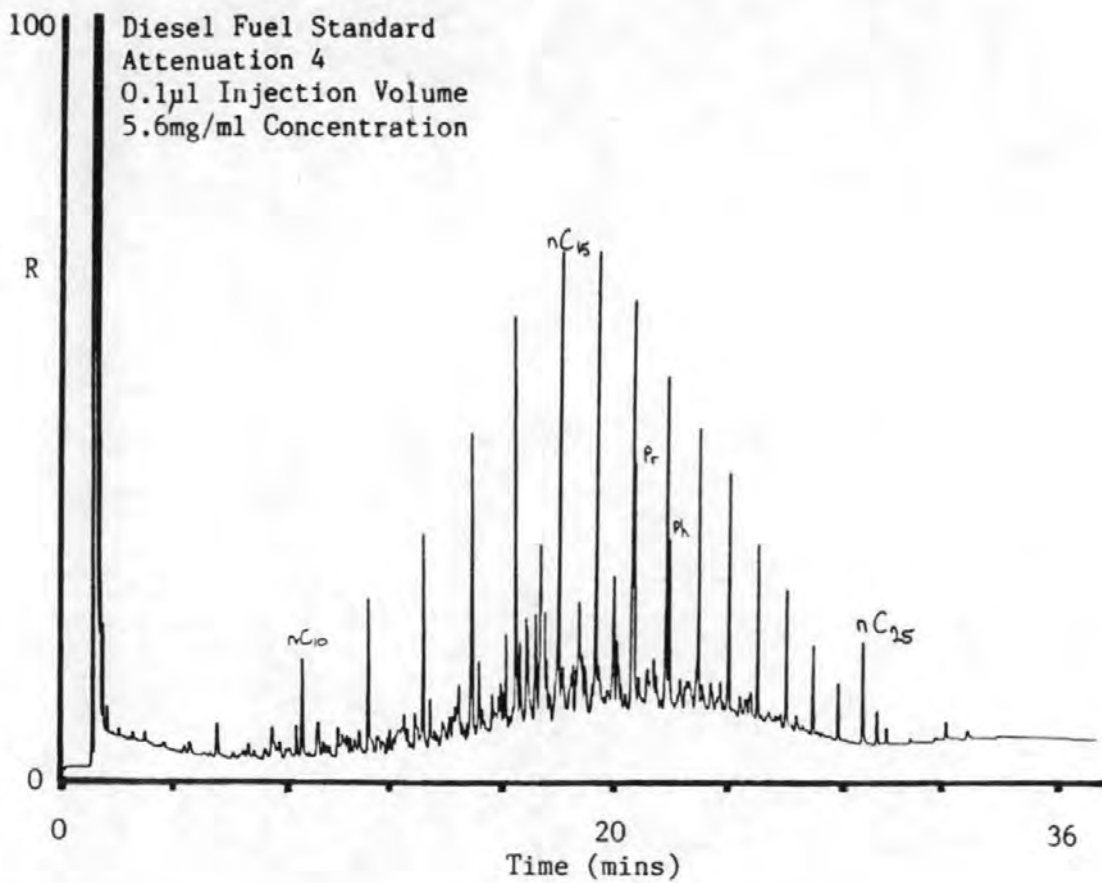


Fig. 3.19 Chromatograms of Diesel Fuel and the Thermally Degassed Filter-Doped Diesel Fuel Sample.

analysis to obtain a SSA value. Each FES fraction was analysed by GC and microstructural characterisation was repeated after extraction, to show the relative effectiveness of each method for extracting FES.

Experiment 4A, compared the character of DP gained from the exhausts of the DI Ford research engine with the IDI Ricardo engine. Some results from this study have been presented (Seebold et al, 1989). The engines were operated at similar relative conditions (1500rpm speed, full and half load). The standard methodology was followed although the filter was only exposed to 3/4 of the full exhaust of this larger engine (2.5l) swept volume.

Experiment 5A, studied how DP microstructure changed with successive thermal degassing. Two DP laden filters (1500rpm speed, 13.7Nm and 27.4Nm loads) were degassed at 120, 190, 290 and 340°C. Before and between each degassing the microstructure was examined. This highly time consuming series confirmed the sources of adsorbed FES in DP.

## CHAPTER 4 RESULTS AND DISCUSSION OF EXPERIMENTS UNDERTAKEN

The results are summarised in the relevant sections to reflect the complex nature of the relationship between DP and UHC in the exhaust. Salient inter-relationships are concluded in Chapter 5. The Ricardo IDI engine was almost exclusively used, so reference is always applied to this engine unless otherwise stated. During this section, the engine load conditions of 13.7 and 14.2Nm, and 27.4 and 27.9Nm will be referred to as 'low' and 'high' load respectively to show the significant differences in emissions between them, at any one speed.

---

DP and UHC emissions data from this study support the emission map database (Chapter 2.3). Fig 4.1 and Table 4.1 summarise the emission data of the engine conditions employed during these studies. The typical emission trends of an IDI engine were evident: that with increasing load, DP production rises and HC emissions decline.

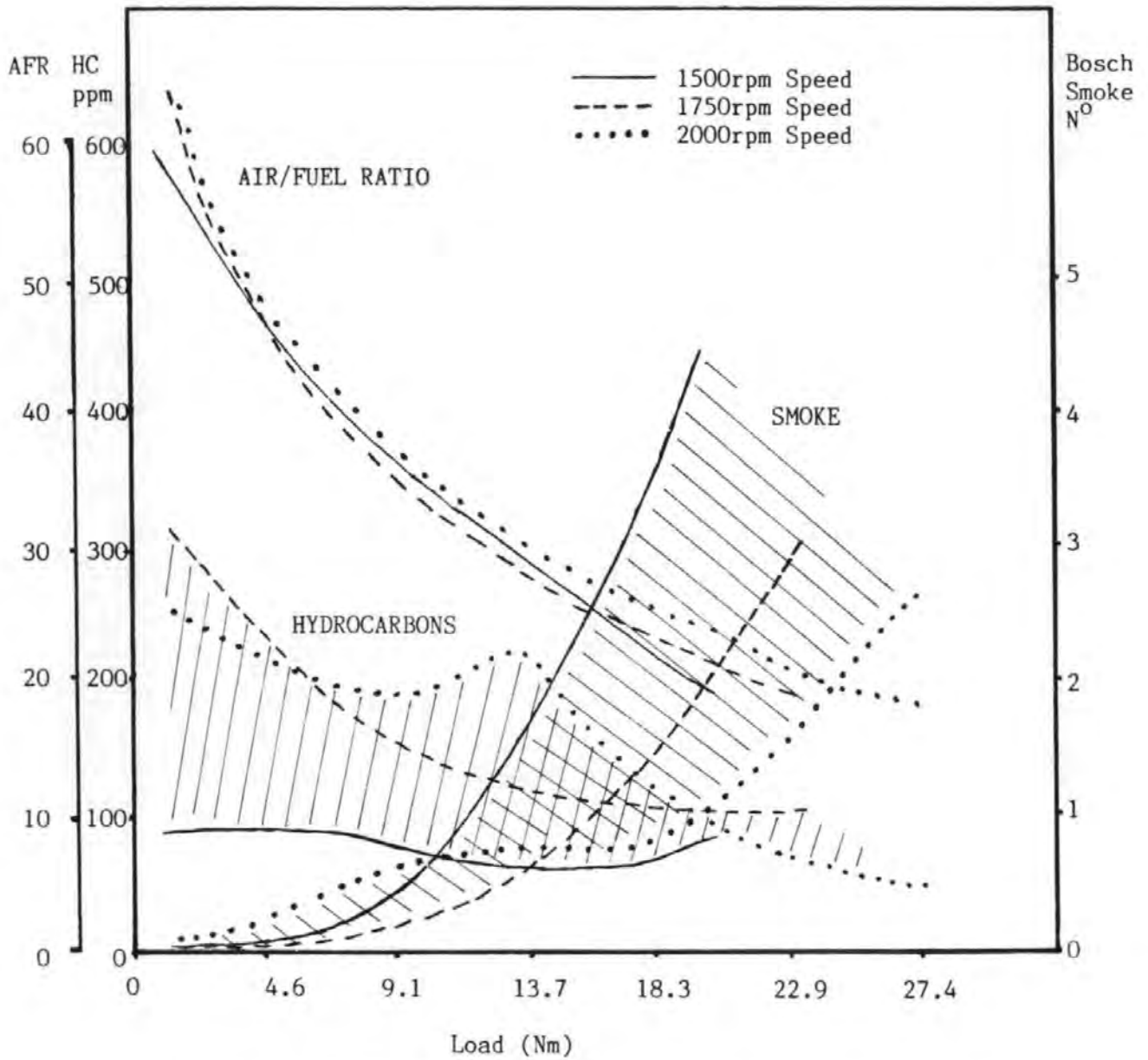


Fig 4.1 Emissions Graph of the Relationship Between Hydrocarbons, Smoke and Air/Fuel Ratio as a Function of Engine Condition. The Data Only Applies to the Ricardo IDI Diesel Engine.

ENGINE CONDITION			EMISSION DATABASE								
Speed (rpm)	Load (Nm)	Fuel Rate (ml/sec)	AFR	Lamda	Bosch N <sup>o</sup>	O <sub>2</sub> %	HC ppm	NO ppm	CO ppm	Injection Deg	Timing BTDC ATDC
1500	13.7	0.227	35.7	2.5	0.6	12.2	75	485	100	-17°	+12°
	27.4	0.403	20.4	1.4	4.5	5.9	95	323	460	-15°	+20°
1750	14.2	0.279	32.6	2.2	0.3	11.3	145	532	120	-13°	+16°
	27.9	0.48	19.8	1.4	3.1	5.4	105	503	375	-14°	+21°
2000	14.6	0.327	32	2.2	0.8	11.1	225	503	220	-10°	+20°
	29.5	0.602	18	1.2	2.7	3.6	50	562	380	-10°	+25°

Table 4.1 Emission Map Database for the Ricardo IDI Diesel Engine Over the Engine Conditions Used During these Studies.

ENGINE CONDITION			MASS DATA				
Speed (rpm)	Load (Nm)	Distance (m)	DP Emission Rate (mg/sec)	Co. V. %	UDCM FES Rate (mg/sec)	% FES of DP	N <sup>o</sup> of Samples
1500	13.7	0.3m	0.38	18.4	0.042	11.1	5
		2.3m	0.28	18.4	0.06	26.1	9
	27.4	0.3m	1.33	17.0	0.023	1.7	5
		2.3m	1.05	18.4	0.031	3.0	4
1750	14.2	0.3m	0.2	27.4	0.025	12.5	10
		2.3m	0.19	12.8	0.065	34.2	9
	27.9	0.3m	0.88	10.7	0.021	2.4	10
		2.3m	0.566	14.1	0.016	2.9	8

Table 4.2 Filter Emission Data from Series 1A (BCF) Showing DP Mass Emission Rate and % UDCM Extracted FES.

Co. V = Coefficient of Variation for Repetitive Samples (%).



#### 4.1 SERIES 1A DIESEL PARTICULATE MASS EMISSION AND CHARACTERISATION

Diesel Particulate from the Ricardo Engine produced the mass emission and FES composition data shown in Table 4.2 and Fig 4.2. The emission data reflected the Bosch Smoke N° and HC emission trends characteristic of this engine. As AFR and load increased, so smoke (DP) increased and HC (FES) decreased. Thus at low load (13.7Nm - 14.2Nm), low DP emissions were coupled with relatively high HC emissions which gave %FES values of 11.1% and 12.5%. At high load (27.4 - 27.9Nm), the DP emission were much higher, but FES were <3% of DP mass. The overall high HC emissions of this engine were probably due to the old injection system and which had an injector sac volume which contributed significantly to UHC emissions when cylinder temperatures were relatively low and combustion less efficient.

This study demonstrated that the process termed Temperature Dependent Chemical Scavenging (TDCS) (Glasson et al, 1988) was occurring down the exhaust pipe. As temperature declined, so % FES more than doubled, between the two sample positions at low load. At high load, the increase was less marked, because the low concentration of gaseous UHC and the relatively high exhaust temperatures (>150°C), meant that there was less TDCS prior to sampling.

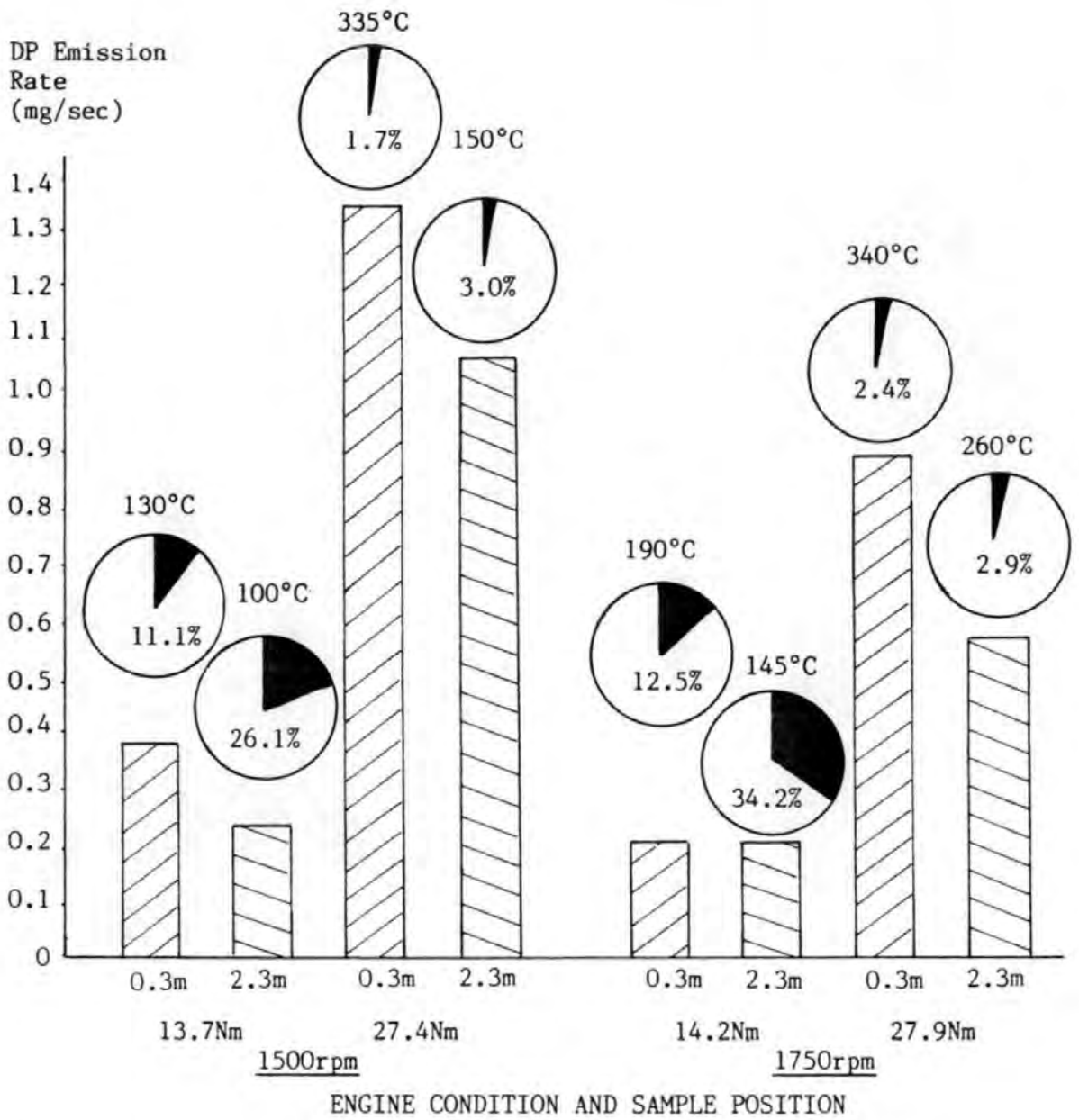


Fig 4.2 Histogram and Pie Graphs of DP Mass Emission and % UDCM Extractable FES with Temperature.

The reproducibility of collected DP mass between filter samples was good (coefficient of variation 10-27%) despite the back pressure effects on the engine, caused by the BCF.

Particle drop-out onto the exhaust wall, a result of declining gas velocity and increasing particle size (due to aggregation and UHC adsorption) (Abbass et al, 1989), was noted between the two sample positions (Section 2.5.1)

#### 4.1.1 MICROSTRUCTURAL ANALYSIS OF DIESEL PARTICULATE

DP microstructure was found to vary with extraction method, so each method will be considered independently. As described earlier, filter DP mass loading was critical to the selection of the extraction method. The UDCM method was developed to remove DP buried in the filter matrix, and this method was applied to all Series 1A samples. A heating pot (item 'L', Fig 3.1) positioned around the BET sample envelope allowed thermal degassing of UDCM soot to 350°C in vacuo (at 0.05mm Hg pressure). The later development of the thermal degassing apparatus (Fig 3.17) allowed the DP to be assessed on-filter (Series 1C), and the degassed volatiles were trapped for GC analysis. This section details the microstructural results of the UDCM extracted soot, both before and after thermal degassing.

Soot from an over-fuelled engine run, which therefore produced a copious emission of DP, was brushed from the filter surface and analysed (i.e. not pre-extracted in DCM). The brushed sample was referred to earlier (Fig 3.4). The sample (1500rpm, 27.4Nm, 2.3m) had an excellent open fluffy structure and was compared to the UDCM samples as detailed below:

1) The isotherm profile of the brushed soot (Fig 4.3) and the SSA data, showed it to be a cross between a Type II and Type IV isotherm with a surface area of  $86\text{m}^2/\text{g}$ . This indicated the combination of a non-porous and a meso-porous solid, i.e. a semi-porous solid. The hysteresis loop showed slit-shaped pore character typical of H3 loops and also H1 influence at the top of the isotherm (a tailing-off to the horizontal), derived from 'ink-bottle' pores formed between agglomerates. The isotherm showed closure in both the micro (ultramicropores  $<1\text{nm}$ ) and upper meso/macropore ( $>8\text{nm}$ ) ranges.

2) After TD, the SSA values were seen to increase to  $156\text{m}^2/\text{g}$  and the hysteresis loop opened in the previously closed pore ranges. The volatiles released (later confirmed by on-filter EGA), were hydrocarbons, which had been trapped in the pores as distinct pore-bound FES fractions. The mesopore range appeared largely unchanged, indicating that for this high load engine condition, hydrocarbons were not significantly trapped in this pore region.

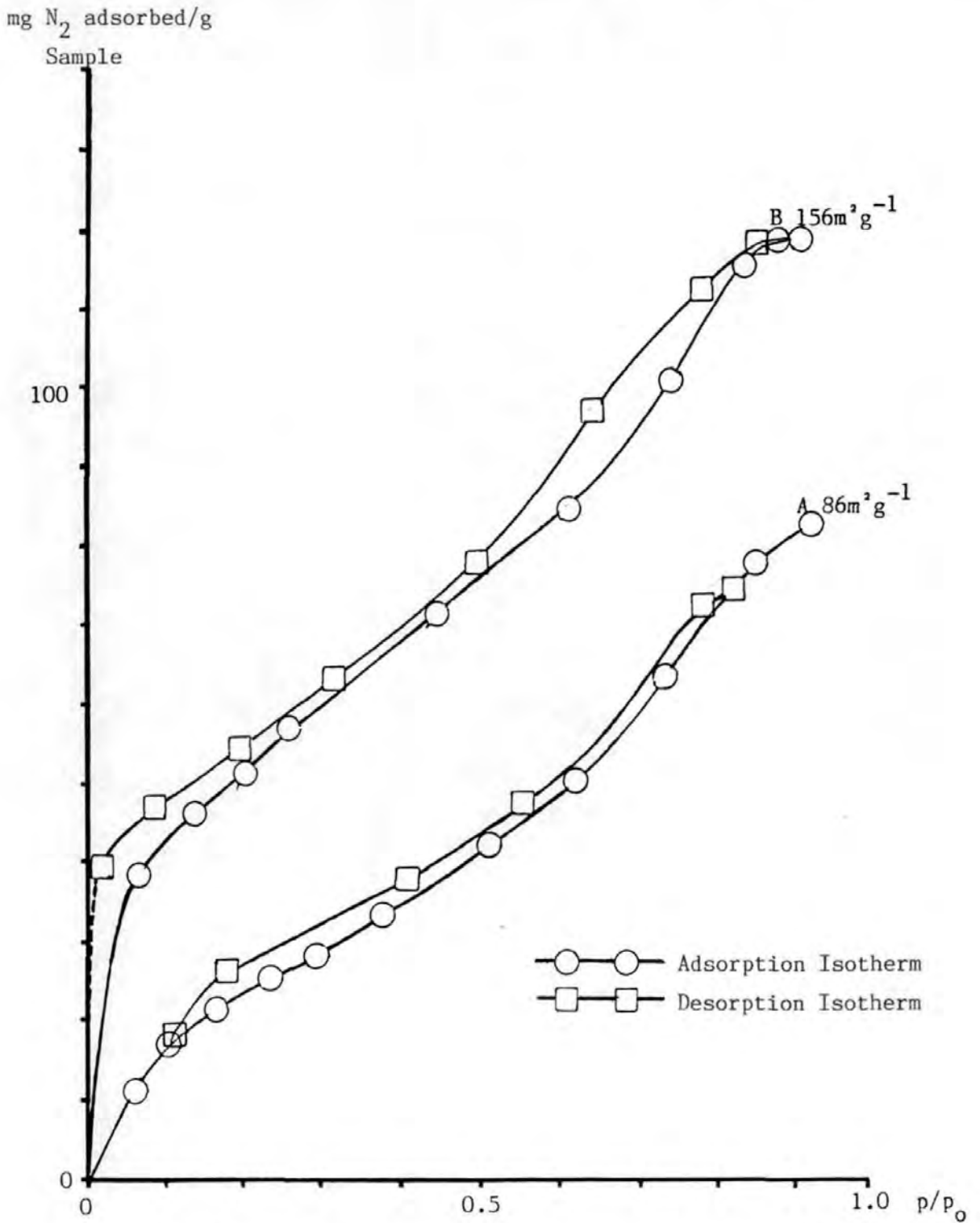


Fig. 4.3 Adsorption/Desorption Isotherms and Hysteresis Loops of a DP Brushed from a Filter exposed to the Exhaust of the Ricardo IDI Engine. The Figure shows the Sample Before 'A' and After 'B' Thermal Degassing.

Sample: Speed 1500rpm  
 Load 27.4Nm  
 BCF at 2m Distance

This sample was thought to be representative of DP microstructure, and it was selected to be compared to other soots. Later studies confirmed its structure, which was modified by the extraction and analysis method (i.e. UDCM extraction of FES and the filter's own hysteresis for on-filter microstructural determination of DP).

The ultrasonic extraction method (UDCM) was developed to remove DP buried from within the filter matrix and was employed to compare the soots produced from different engine conditions.

3) Table 4.3 shows the effect of temperature and UHC availability on the BET SSA data before and after thermal degassing. The surface areas at room temperature reflect the DP formation conditions. UHC concentration and amount of DP in the combustion chamber influence how much FES may be trapped in the micropores during crystallite formation and particle aggregation. This was controlled by load and cylinder combustion temperatures. At low load with high UHC emissions, the reduction in the surface area (internal and external) was most marked. Diesel soots under these conditions had low initial surface areas which increased by the order of 20-40% when degassed at elevated temperatures (350°C). However, for soots produced at high load, the effect was less marked, and initial SSA's were higher because more soot was available to adsorb the smaller quantities

ENGINE CONDITION		FILTER POSITION	
Speed (rpm)	Load (Nm)	0.3m A / B	2.3m A / B
1500	13.7	51.4 / 66.6 (+23%) 130°C	70.5 / 106.3 (+34%) 100°C
	27.4	103.5 / 113 (+8%) 335°C	70 / 85 (+18%) 150°C
1750	14.2	47.3 / 64 (+26%) 190°C	46.5 / 80.3 (+42%) 145°C
	27.9	80.6 / 84.7 (+5%) 340°C	99 / 110 (+10%) 260°C
EXTRA BRUSHED SAMPLE			
1500	27.4	-----	86 / 156 (+44%) 150°C

Table 4.3 Nitrogen Adsorption Specific Surface Areas (BET) of UDCM Extracted DP Determined after Room Temperature (20°C) 'A' Degassing, and after Thermal Degassing (350°C) 'B'. The 'Brushed' Sample is also Shown Together with All Sample Temperatures.

All SSA values Expressed as m<sup>2</sup>/g.

of hydrocarbons, thus reducing the amount of pore blocking. The higher %SSA gain between exhaust sampling positions was further evidence that TDCS was occurring down the exhaust.

4) The hysteresis profile of UDCM soots determined before and after thermal degassing are shown in Fig 4.4. The slit-shaped pore character was evident (horizontal loop), but no tailing-off of the adsorption isotherm to the horizontal at  $>0.9 P/P_0$ , which normally indicates agglomerate character. This suggests that the formation of the soot cake on the filter burial, compacted the DP, and reduced or destroyed the open fluffy agglomerate character typical in brushed soots. The pre-extractive nature of the UDCM method also resulted in only a small gain in SSA after degassing.

5) It was noted that for fresh brushed DP, the nitrogen adsorption was difficult to stabilise during BET operation, and this was taken as evidence of the highly active nature of the adsorption sites, as detailed by Ross et al (1982). Puri (1970), has suggested that adsorption is influenced by functional groups (eg C-OH, C=O) bound on the periphery of layer planes. The UDCM soots, did not show this feature, presumably because the solvent had already extracted these functional groups from the DP. The UDCM method had also pre-extracted microporous FES, leaving the pores open, which were further unblocked by thermal degassing. Comparison between the brushed



mg N<sub>2</sub> adsorbed/g  
Sample

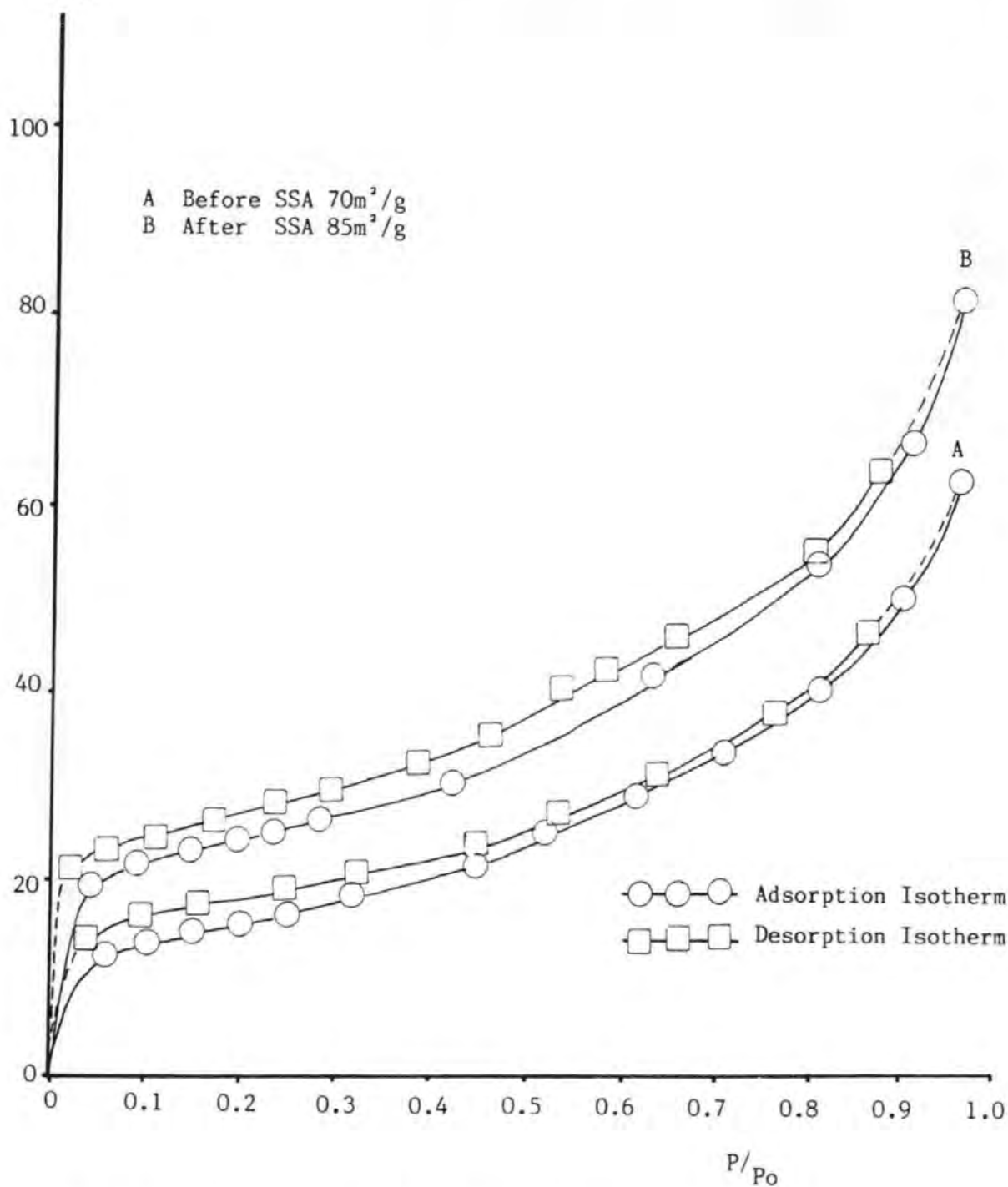


Fig 4.4 Adsorption/Desorption Isotherm Showing Hysteresis Loops for a UDCM Extracted Diesel Particulate Before and After Thermal Degassing.

Sample: Speed 1500rpm  
Load 27.4Nm  
Box Cassette Filter at 2.3m Distance

soot and its UDCM counterpart by %SSA gain, illustrated how the solvent method had pre-extracted FES (the gain was only 18% compared to 40% for the brushed soot).

#### 4.1.2 ELECTRON MICROSCOPIC EXAMINATION OF SERIES 1A DIESEL SOOT

Scanning electron microscopy (SEM) examined the size and shape of Series 1A soots. The gold coating improved the resolution of the particles but increased their sizes to those shown in Table 4.4. The appearance of DP depended on sampling method. Natural soot had an open fluffy aggregate structure, but filtered soot showed compaction or burial depending on the filter type, which has the additional effect of blocking filter pores. The main features were:

- 1) Assessment of the filters, showed that soot cake formation was most pronounced at high loads and speeds, as one would expect when DP production was high. This has already been intimated in the filter work. No visual differences in cake structure were noted between sampling positions.

- 2) DP cake, under high resolution SEM (x20,000) analysis (Fig 3.10), enabled particle diameter measurements to be obtained. As Table 4.4 showed, the data indicated that particle diameter increased with declining speed and increasing temperature for any load condition. The high loads produced the largest particles despite the higher temperatures (as has been reported by Glasson et al, 1988). Later work suggests the opposite (Series 1C), but the data may not be contradictory because; the exhaust diameter, dilution, gas velocities and

ENGINE CONDITIONS		FILTER POSITION AND TEMPERATURE			
Speed (rpm)	Load (Nm)	0.3m	°C	2.3m	°C
1500	13.7	102nm	130°C	103nm	100°C
	27.4	117nm	335°C	116nm	150°C
1750	14.2	91nm	190°C	98nm	145°C
	27.9	104nm	340°C	104nm	260°C

Particle Diameter  $\bar{x}$  from 20 observations

Table 4.4 Particle Sizes of Soots Taken at a Variety of Engine Conditions and Filter Positions with the BCF and Analysed by SEM.

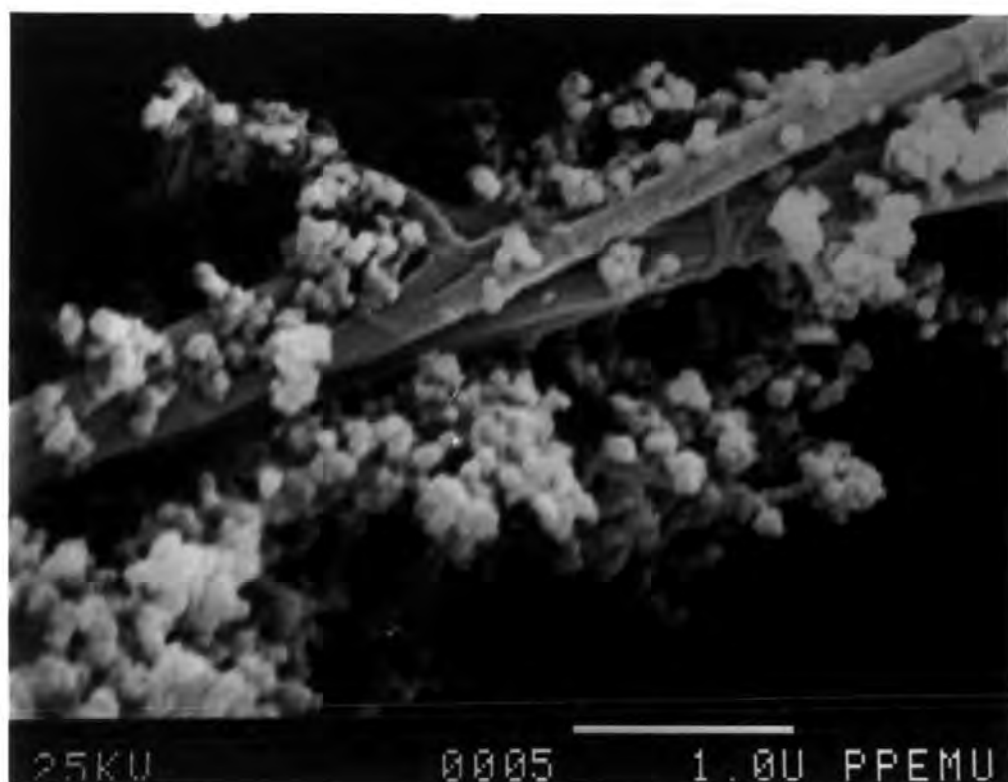


Fig. 4.5 Scanning Electron Micrograph of a Bosch Smoke Filter.  
(1 bar = 1 $\mu$ m)

temperatures in the BCF and ICF systems were slightly different. The Series 1A data may have shown the influence of higher temperatures (and higher gas velocities), whereas in Series 1C, the exhaust conditions favoured lower temperature UHC adsorption, which was more prominent at low load when UHC emissions were greatest. An alternative explanation may be BCF exhaust valve operation. During periods of valve closure, DP that collects behind the valve may agglomerate and adsorb UHC and become larger in size, particularly at high load. When this valve was operated, the enlarged DP were swept onto the filter. The piston valve minimised this problem. TDCS was not obvious in these samples presumably because the high temperatures and high gas velocities prevented UHC adsorption.

Fig 4.5 shows a Bosch Smoke filter with a fibre covered with aggregated particles. This electron micrograph shows the character of diesel soot when cake compaction is not allowed to occur.

#### 4.2 SERIES 1B FES FROM BCF

The FES extracted from the QMA filters were prepared to be directly intercomparable by mass for gas chromatographic analysis (Fig 4.6 and 4.7). The relationship between FES and load was evident, with the low load engine conditions having the highest emissions of UHC and therefore FES. At the elevated sample temperatures (>100°C), the filters were dominated by a hump, an unknown complex mixture (UCM) of branched, polar and aromatic hydrocarbons, which corresponded with the retention window (24-36 minutes) of lubricating oil. The following features were recorded:

- 1) The samples obtained from the BCF, were noted for their high temperatures, stress on the engine operation and short sampling times. Thus the samples had low FES masses (often <0.2mg).

- 2) The similarity between chromatograms indicated that load (and not speed), was responsible for influencing FES composition. At the elevated exhaust temperatures, lubricating oil dominated the chromatograms, with only a small n-alkane homologous series being shown in the fuel retention window (18-24 minutes).

- 3) The low load samples showed higher loadings of FES

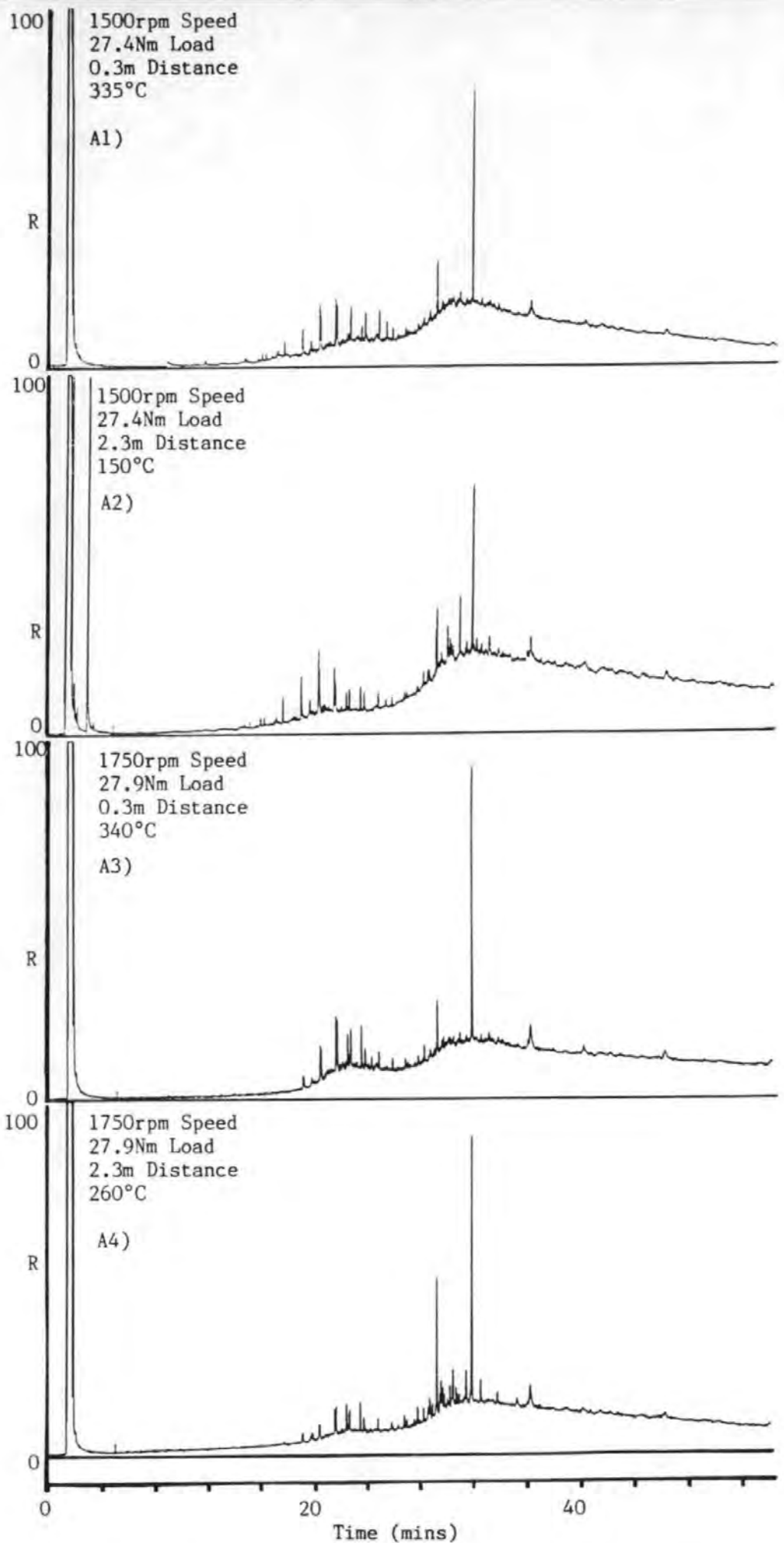


Fig. 4.6 Chromatograms of FES from Series 1B, Extracted by Soxhlet Extraction. Each sample was exposed to the Exhaust for 7 Seconds.

'R' is Response, Injection Volume was 0.5 $\mu$ l and Attenuation was 2.

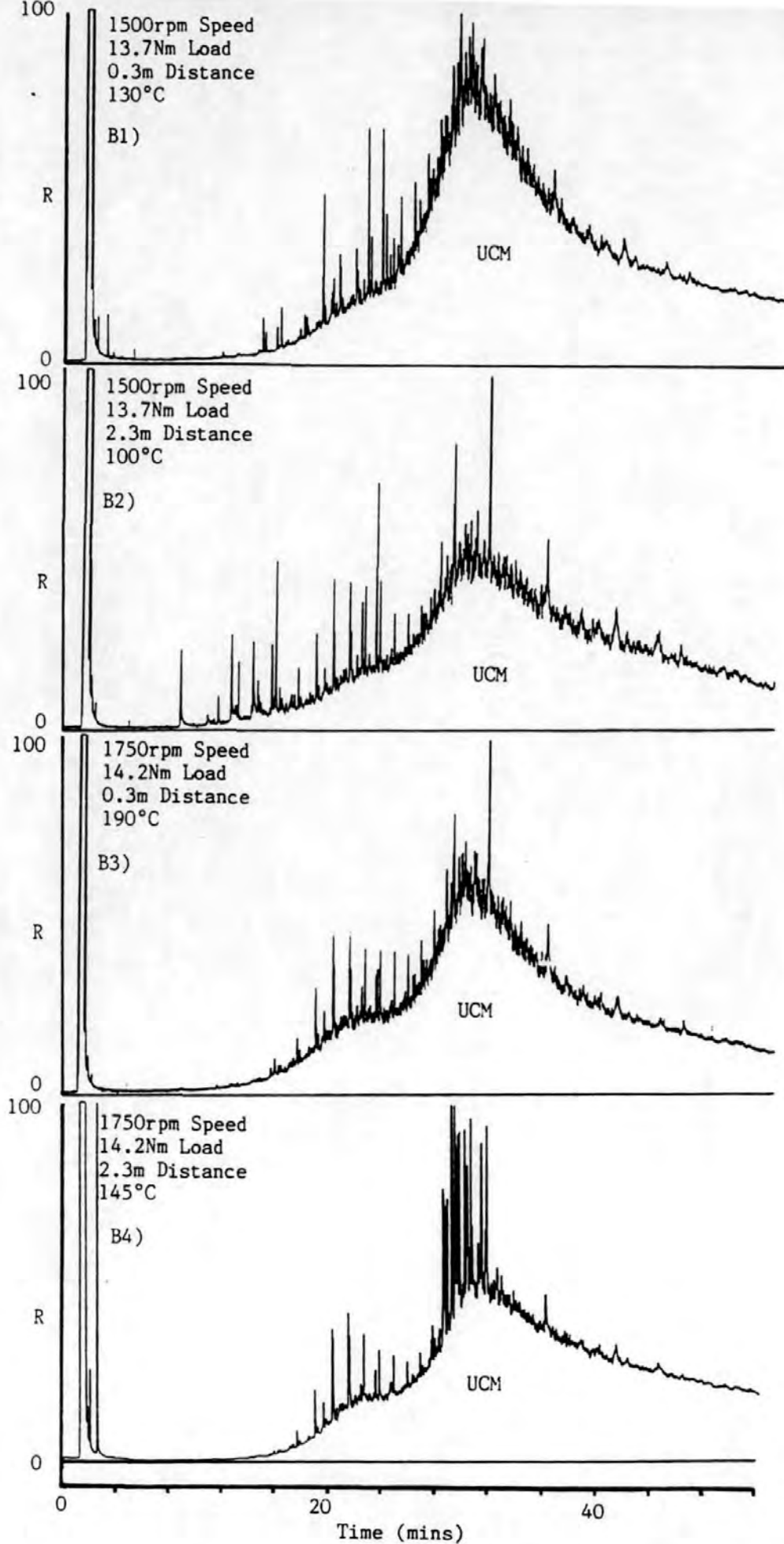


Fig. 4.7 Chromatograms of FES from Series 1B, Extracted by Soxhlet Extraction. Each Sample was exposed to the Exhaust for 7 Seconds, except 1500rpm, 13,7Nm, 2,3m which had 40 seconds.

'R' is Response, Injection Volume was 0.5 $\mu$ l and Attenuation was 2.



and the presence of more noticeable straight chain n-alkanes series derived from fuel, as one would expect from this engine condition. There were more differences between samples, because the lower exhaust temperatures favour the lower molecular mass compounds, which is illustrated by Sample B2 (1500rpm, 13.7Nm, 2.3m), which was taken at a temperature of 100°C, and had a longer exposure time (40 seconds).

4) Because of the short sampling times, no significant mass differences were noted between samples of the same engine condition but different filter positions.

#### 4.2.1 SERIES 2A TOWER EXTRACTABLE SAMPLE

Using TESSA, gaseous exhaust UHC was collected over longer sampling times (360seconds). Petch et al (1988) stated that this method extracted all exhaust UHC, stripping DP of its adsorbed hydrocarbons. It provided a total exhaust sample which included very low molecular mass UHC, which would normally pass through a dilution tunnel filter in gaseous form.

Petch et al (1988) and Trier (1988) discovered with TESSA, that the TES aromatic content (including PAC's) increased with speed and load, due to the pyrosynthesis of aliphatic fuel into aromatic compounds. This was demonstrated with radio-labelled <sup>14</sup>C-octadecane and benz(a)pyrene. In the exhaust, the

aliphatics were found to be preferentially combusted compared to the more stable aromatic compounds. Trier (1988) studied the TESSA residu and used standard soxhlet extraction (150ml, DCM, 24hrs) to determine the unextracted FES. This was found to be <1% of the total TES from the whole exhaust.

Comparison between TESSA and a dilution tunnel was also carried out by Trier et al, (1988), and it was reported that the filter method collected an SOF dominated largely by lube oil compared to the TES which had a considerable range of low molecular mass hydrocarbons.

The FES and DP mass data is shown in Table 4.5. The TESSA DP data reflected the HC emission trend (Fig 4.1) but suffered glass debris contamination. The TES data showed excellent correlation to UHC emission map data. The chromatograms (Fig 4.8-4.10) illustrated the wide range of hydrocarbons present within the TES samples. The results are presented below:

- 1) The unfractionated TES chromatograms showed the dominance of fuel to the total UHC, when the whole exhaust was examined, compared to filter samples taken at elevated temperatures. The low load samples showed highest FES, and an n-alkane series corresponding to the fuel retention window, with only a small oil UCM after 28 minutes. The FID response of oil was less than for fuel (Trier, 1988) thereby further

ENGINE CONDITION		PARTICULATE MASS RATE (mg/sec)	TES MASS RATE (mg/sec)
Speed (rpm)	Load (Nm)		
1500	13.7	0.139	0.24
	27.4	1.08	0.127
1750	14.2	1.68	0.31
	27.9	1.75	0.09

Table 4.5 Particulate Mass and TES Mass Emission Rates from the Ricardo Engine and Collected by TESSA.

PEAK ID	COMPOUND NAME
A	Naphthalene
B	1 and 2 Methyl Naphthalene
C	2,6 and 2,7 Dimethyl Naphthalene
D	1,2 Dimethyl Naphthalene
E	Methylfluorene
F	Phenanthrene
Pr	Pristane
Ph	Phytane

Table 4.6 Tentative Identifications of Compounds in the TES Fractions. Peaks A-F in Aromatic Fraction, Pr and Ph in Aliphatic Fraction.

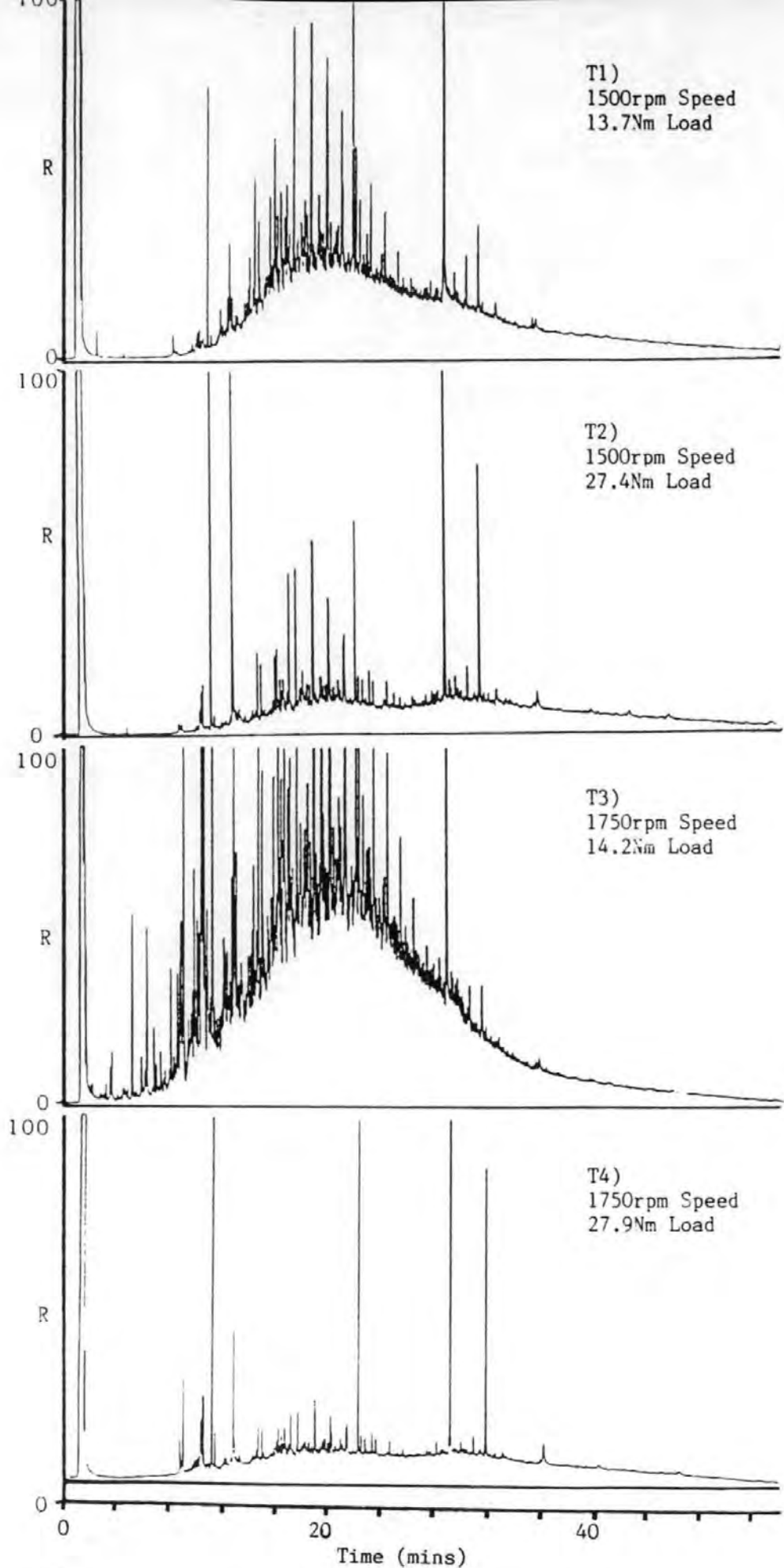


Fig. 4.8 Chromatograms of Unfractionated TES (TESSA).  
 'R' is Response, Injection Volume was 0.5 $\mu$ l and Attenuation was 4.

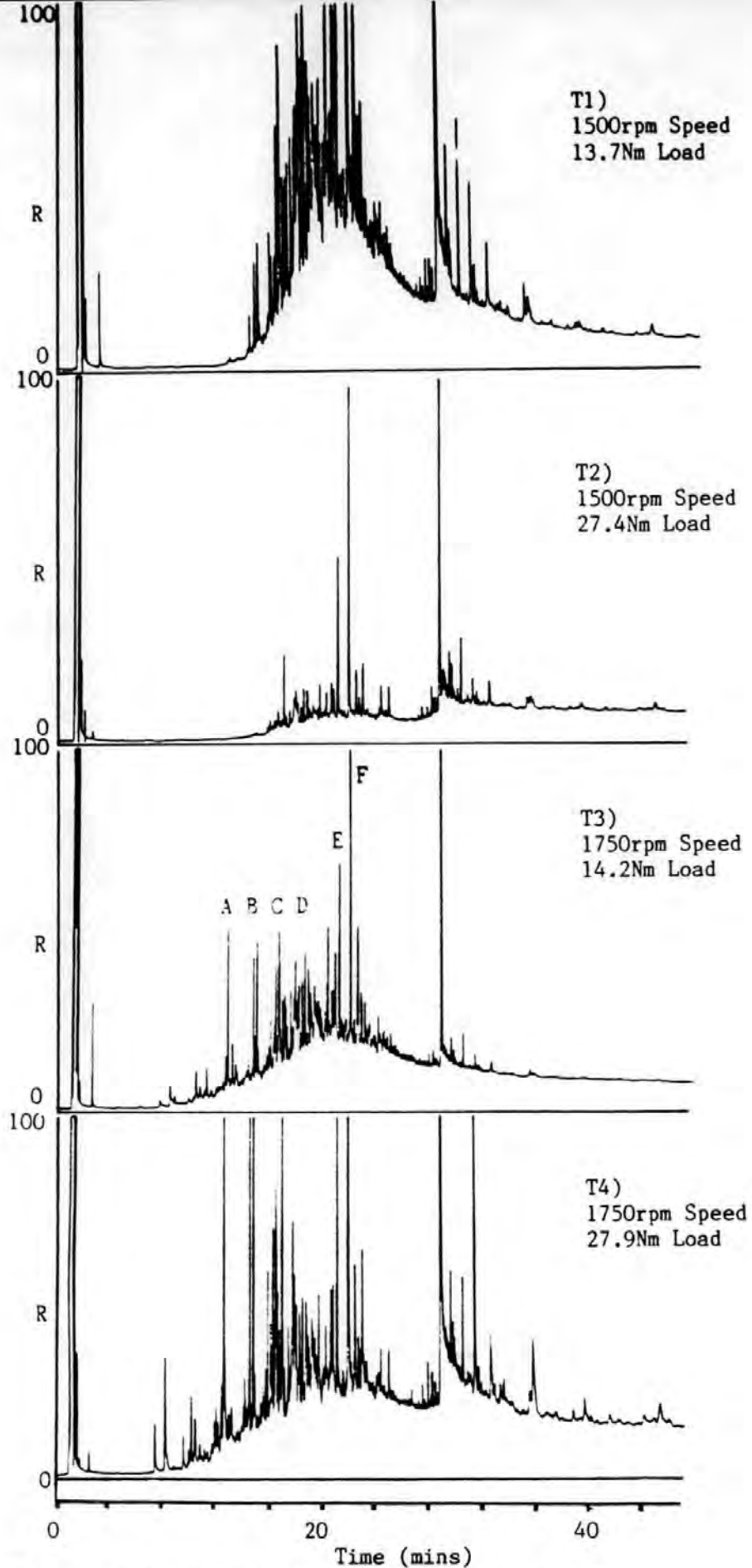


Fig. 4.9 Chromatograms of the Aromatic Fractions of TES.

'R' is Response, Injection Volume was 0.5 $\mu$ l and Attenuation was 2.

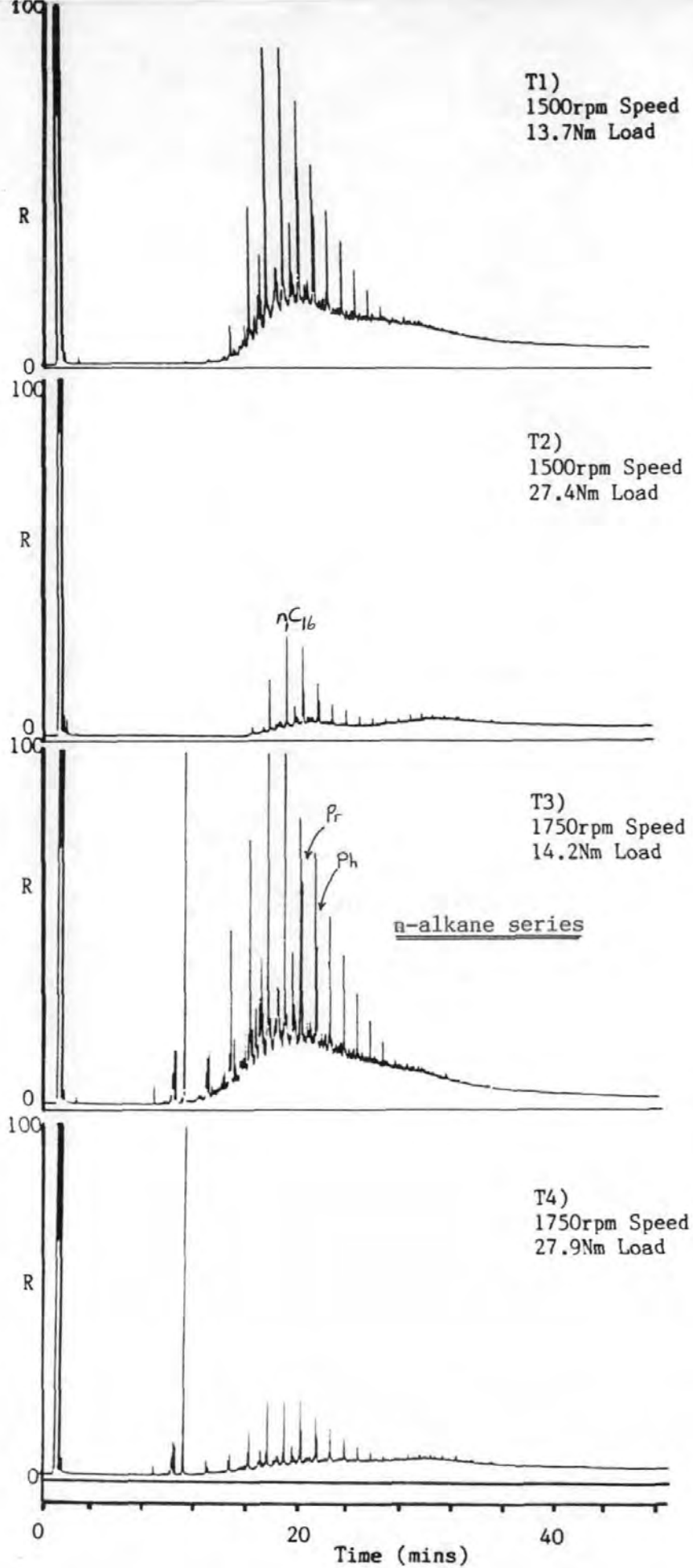


Fig. 4.10 Chromatograms of the Aliphatic Fractions of TES.  
'R' is Response, Injection Volume was 0.5 $\mu$ l and Attenuation was 4

reducing the apparent influence of oil in the overall chromatogram.

2) The TES aliphatic fraction was compared to the fuel aliphatic fraction (Fig 4.11) from Petch et al, (1987). The TES distribution showed strong similarity with the fuel, particularly the isoprenoids (i.e. pristane and phytane). The TES had a similar n-alkane normal distribution with the highest peaks corresponding to n-C<sub>16</sub> and n-C<sub>17</sub> (Table 4.6). There was a small aliphatic oil contribution after 28 minutes which can be seen in Fig 4.12. At low load, it appeared that unburnt fuel dominated the chromatogram but with higher speeds, when combustion of the low molecular mass fuel hydrocarbons was more efficient, lubricating oil began to dominate.

3) Comparison between the TES aromatic fractions and the aromatic fractions of fuel and oil (Fig 4.11 and 4.12), showed that the TES was dominated by the parent and alkyl naphthalenes and phenanthrenes, indicating that the aromatic TES came primarily from the fuel. This study has supported the work of Petch et al, (1987) and Trier (1988). Tentative identification of the aromatic compounds was made in Table 4.6.

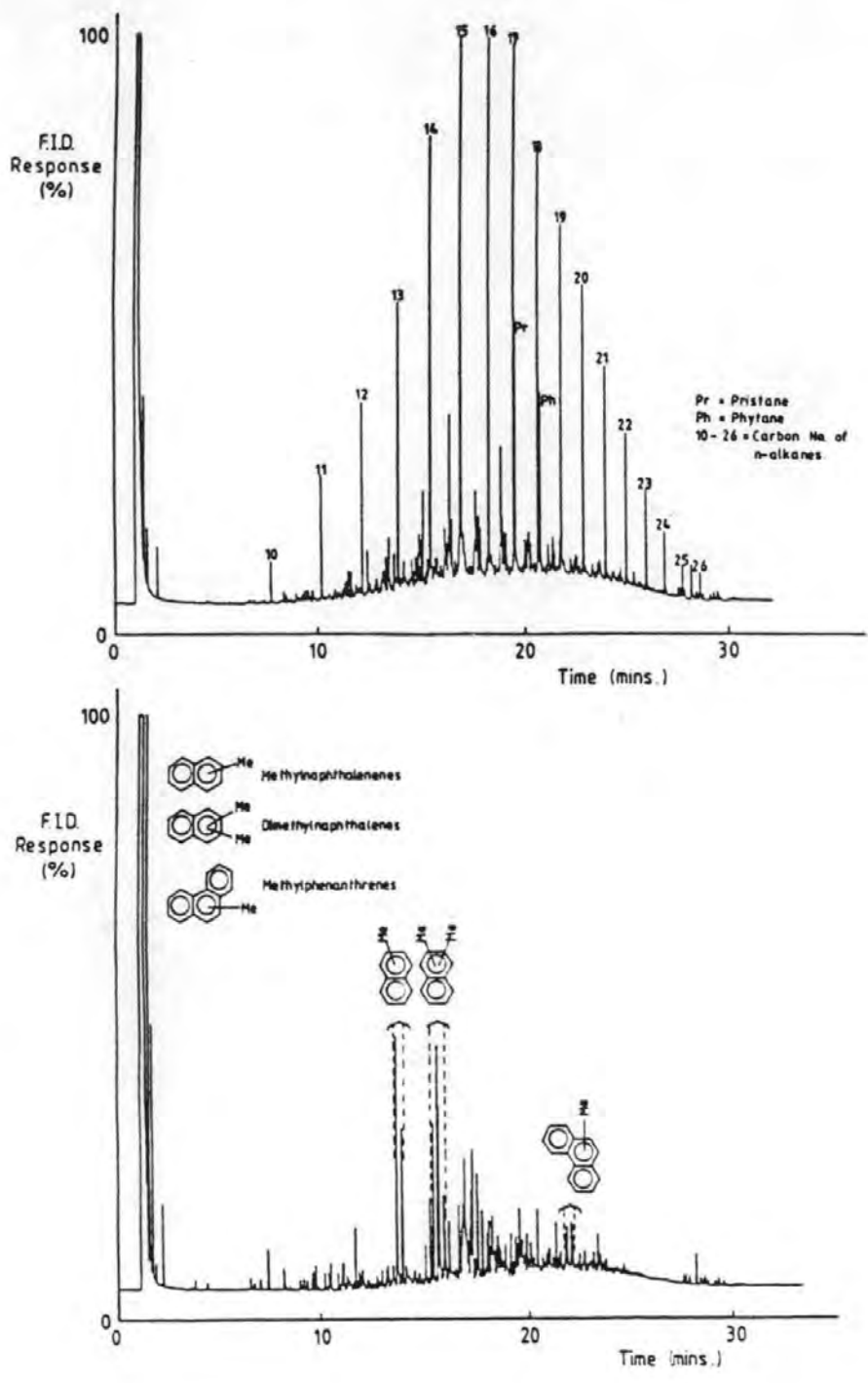


Fig. 4.11 Reference Chromatograms of Fuel Fractions (Aliphatic - top, Aromatic - Bottom). From Petch *et al*, 1987.



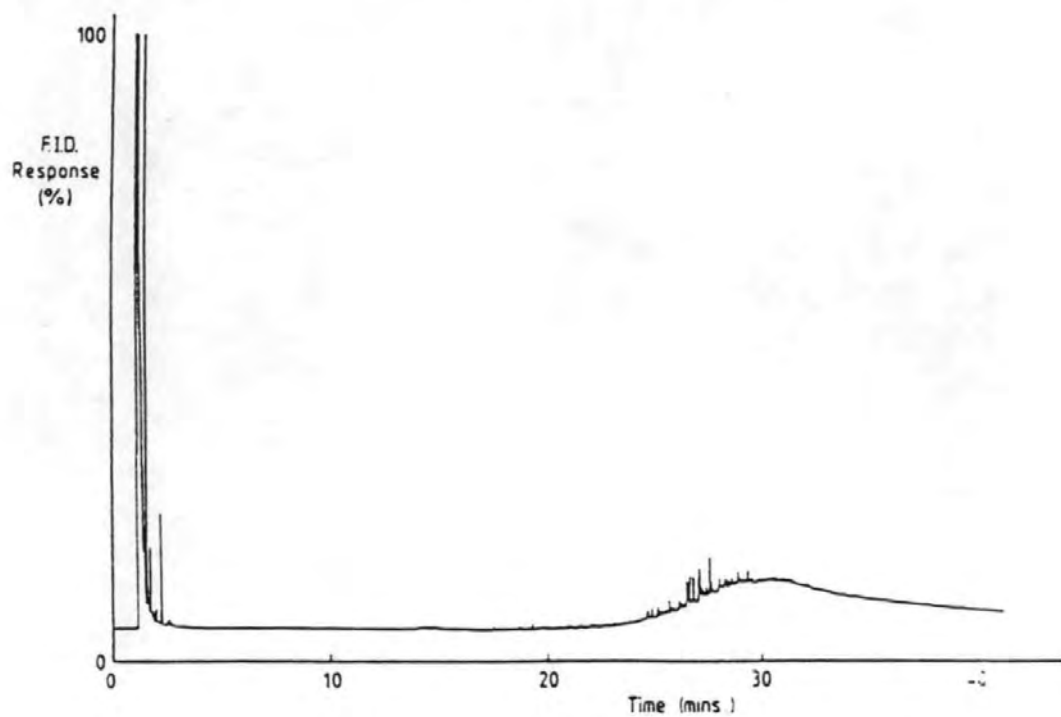
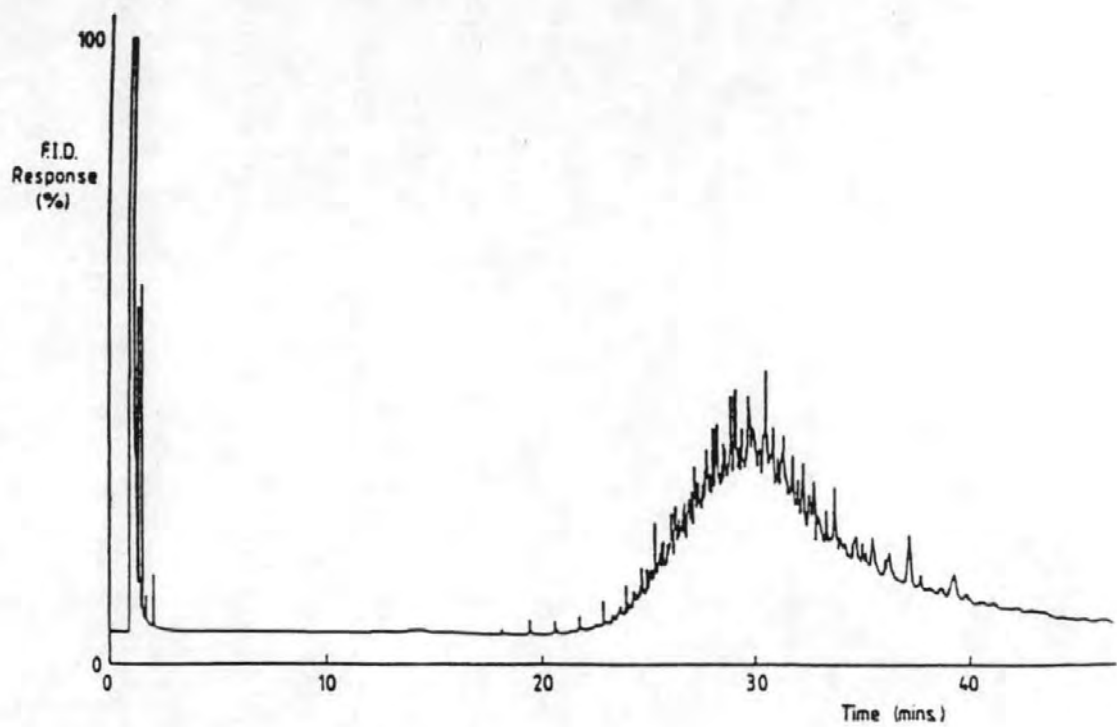


Fig. 4.12 Reference Chromatograms of Lubricating Oil Fractions (Aliphatic - top, Aromatic - bottom). From Petch *et al.*, 1987.

#### 4.3 SERIES 1C TOTAL CHARACTERISATION OF DP

The ICF was employed in conjunction with the thermal degassing method (TD), the BET technique and scanning electron microscopy to collect and characterise the DP and adsorbed UHC. DP samples were analysed on-filter. An extensive database of compositions, SSA values, particle sizes from Series 1C results was prepared (Fig 4.13, Table 4.7 and 4.8) which showed some features previously detailed by other authors (Fujiwara and Fukazawa, 1980; Abbass et al, 1989).

1) TDCS occurred in the exhaust, shown by the increasing % FES of DP mass with declining temperature. This feature was consistent with Series 1A, and showed the greatest % FES at low load (47% to 84%) when low exhaust temperatures (183°C to 80°C) were coupled to high UHC emissions (Fig 4.1). The high load samples had consistent % FES values (between 8% to 15%) over a wide range of temperatures (248°C to 133°C), which suggested that the UHC were not being scavenged due to low UHC availability and high temperatures. Indeed, this consistent FES value, indicated that a constant (regardless of speed) internally bound FES fraction existed which had been trapped during DP formation. Low load conditions were estimated to have about 50% internally bound FES.

2) Hydrocarbon adsorption induced incipient particle

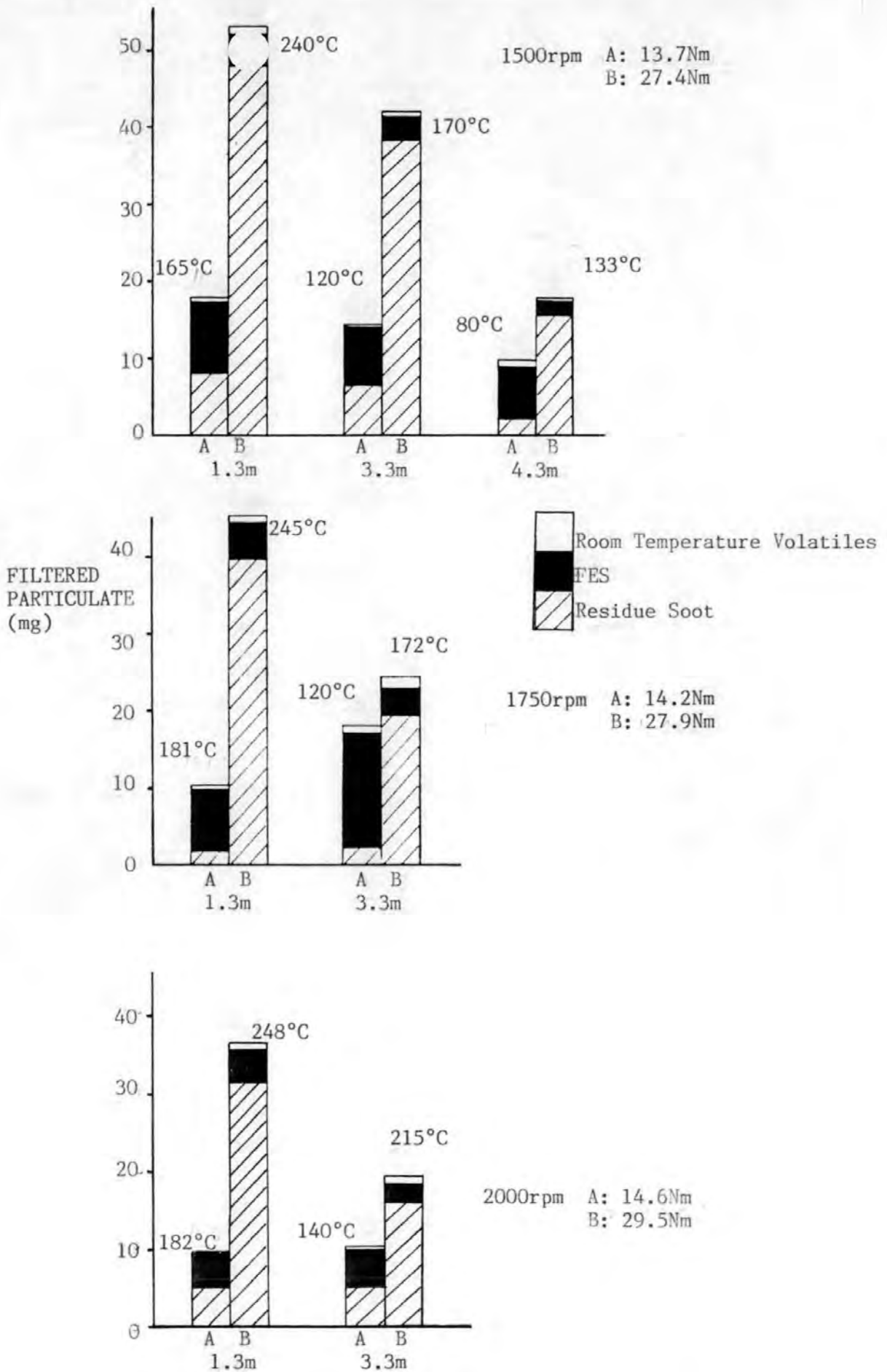


Fig. 4.13 Histograms of the Composition of DP Collected from Different Engine Conditions and Filter Positions. The Exhaust Gas Temperature is quoted and SSA data displayed in Table 4.7.

ENGINE CONDITION		FILTER POSITION					
SPEED (rpm)	LOAD (Nm)	SSA expressed in m <sup>2</sup> /g, Before 'A' and After 'B' TD					
		1.3m		3.3m		4.3m	
		A	B	A	B	A	B
1500	13.7	24 165°C	211	19 120°C	226	<7.5 80°C	153
	27.4	103 240°C	149	109 170°C	147	101 133°C	163
1750	14.2	<7.5 181°C	240	<7.5 120°C	231		
	27.9	101 245°C	147	139 172°C	235		
2000	14.6	24 183°C	155	<7.5 140°C	323		
	29.5	156 248°C	211	130 215°C	205		

Table 4.7 SSA Data from Series 1C shown with Exhaust Gas Temperature. Values which were calculated as negative are expressed as less than three times the Filter SSA (i.e. <7.5m<sup>2</sup>/g).

ENGINE CONDITION		SAMPLE POSITION								
Speed (rpm)	Load (Nm)	$\bar{x}$ Particle size, Standard Deviation and Exhaust Temp								
		1.3m			3.3m			4.3m		
		$\bar{x}$ (nm)	SD	Temp (°C)	$\bar{x}$ (nm)	SD	Temp (°C)	$\bar{x}$ (nm)	SD	Temp (°C)
1500	13.7	103	0.57	165	113	0.74	120	125	1.1	80
	27.4	84	0.51	240	108	0.87	170	117	0.73	133
1750	14.2	143	1.14	181	142	0.94	120	NO SAMPLES		
	27.9	121	0.89	245	122	0.74	172	NO SAMPLES		
2000	14.6	161	1.5	183	177	1.5	140	NO SAMPLES		
	29.5	155	1.34	248	164	1.91	215	NO SAMPLES		

Table 4.8 Particle Size Evaluation for Different Engine Conditions and Filter Positions Collected by the ICF System

$\bar{x}$  sizes obtained from 70 observations of particles from SEM micrographs of caked DP.

growth down the exhaust as temperature declined. There was no evidence of the sudden particle size shift at temperatures less than 150°C and subsequent collection of DP on pipe walls, reported by Fujiwara and Fukazawa (1980). Loss of soot to pipe walls was noted for most speeds, when the exhaust gas flow was relatively low (375 l/min), and DP emissions high (i.e. at high load). At other speeds, significant particulate mass increase was noted at low temperatures and low load (2000rpm, 14.6Nm) presumably due to hydrocarbon adsorption. Particle aggregation could not be demonstrated using the filter method due to impaction problems, and thus the wall drop-out feature could not be directly related to particle aggregation.

3) The SSA data (before and after TD) supported the theory that a consistent FES fraction was bound within the DP matrix (Table 4.7). The soots had similar SSA between engine loads regardless of the engine speed. At low load the initial SSA varied (from 7.5m<sup>2</sup>/g to 24m<sup>2</sup>/g) reflecting cylinder conditions, when significant quantities of fuel could be trapped within the soot matrix. TD released the volatile FES producing a soot with a high SSA. The high load soots, were formed at high temperature, with the fuel being almost totally converted into non hydrocarbon gases or carbonaceous soot. The low % FES content and relatively high initial SSA (101 to 156 m<sup>2</sup>/g) supports this theory. TD improved these SSA values (approx 25% to 41%), greatest for samples collected at lower exhaust

temperatures. These general trends correlated well with the % FES masses of Series 1A, although the UDCM method did pre-extract the soots before SSA determination.

4) Engine load appeared to control particle size via UHC adsorption processes (Table 4.8). Particle size increased with increasing speed and decreasing load which was contrary to previous results (Series 1A). This study did not examine how extraction method influenced particle size, which might show that low load DP were smaller than high load DP after thermal degassing had removed the adsorbed volatiles. At temperatures >150°C, the UHC was largely high molecular mass hydrocarbons derived from lubricating oil (as with Series 1B). At lower temperatures, lower molecular mass fuel UHC may be adsorbed, causing the previously reported particle size shift. Mayer *et al* (1980) showed that the oil contribution to DP was greatest at low load and high speeds and thus might contribute significantly to particle growth. The standard deviation of the SEM particle diameters increased with particle size, suggesting that the enhanced oil availability at these engine conditions increased the particle size distribution of the soots. Kamimoto and Yagita (1989) proposed that soots are formed in flamelets within the cylinder and this theory may be modified to explain the size distribution change. The process of flame impingement could scavenge oil from cylinder walls forming large incipient particles, whilst other particles formed by air quenching or

surviving within the fuel itself, are smaller, since they were formed away from the oiled wall surface and do not have a significant oil coating.

#### 4.3.1 MICROSTRUCTURAL CHARACTERISATION OF ON-FILTER DP

Typical isotherms of diesel soot analysed on-filter are shown in Fig 4.14 and 4.15. They show the 13.7Nm and 27.4Nm load conditions of the 1500rpm speed condition taken at 3.3m with the ICF, before and after thermal degassing.

The filter has its own porosity (Fig 4.16), and low SSA, which is included in the DP microstructural analysis. Consequently the DP profile became flattened by the filter's influence and because the micropores of the media remain partially unblocked during filtration (depending on loading), the DP micropores fail to show micropore closure during nitrogen adsorption. The carbon particles also appear to affect filter hysteresis and partially block the mesopores, thereby reducing the SSA. The interaction between DP and filter is highly complex and difficult to evaluate.

Both samples show closure of mesopores at around 0.8-0.9 partial pressure which equated to a pore diameter of 10nm, which existed between the particles with mean diameters of 40nm (from TEM work). When degassed, the volatiles were released and the

mg H<sub>2</sub> Adsorbed/g  
Sample

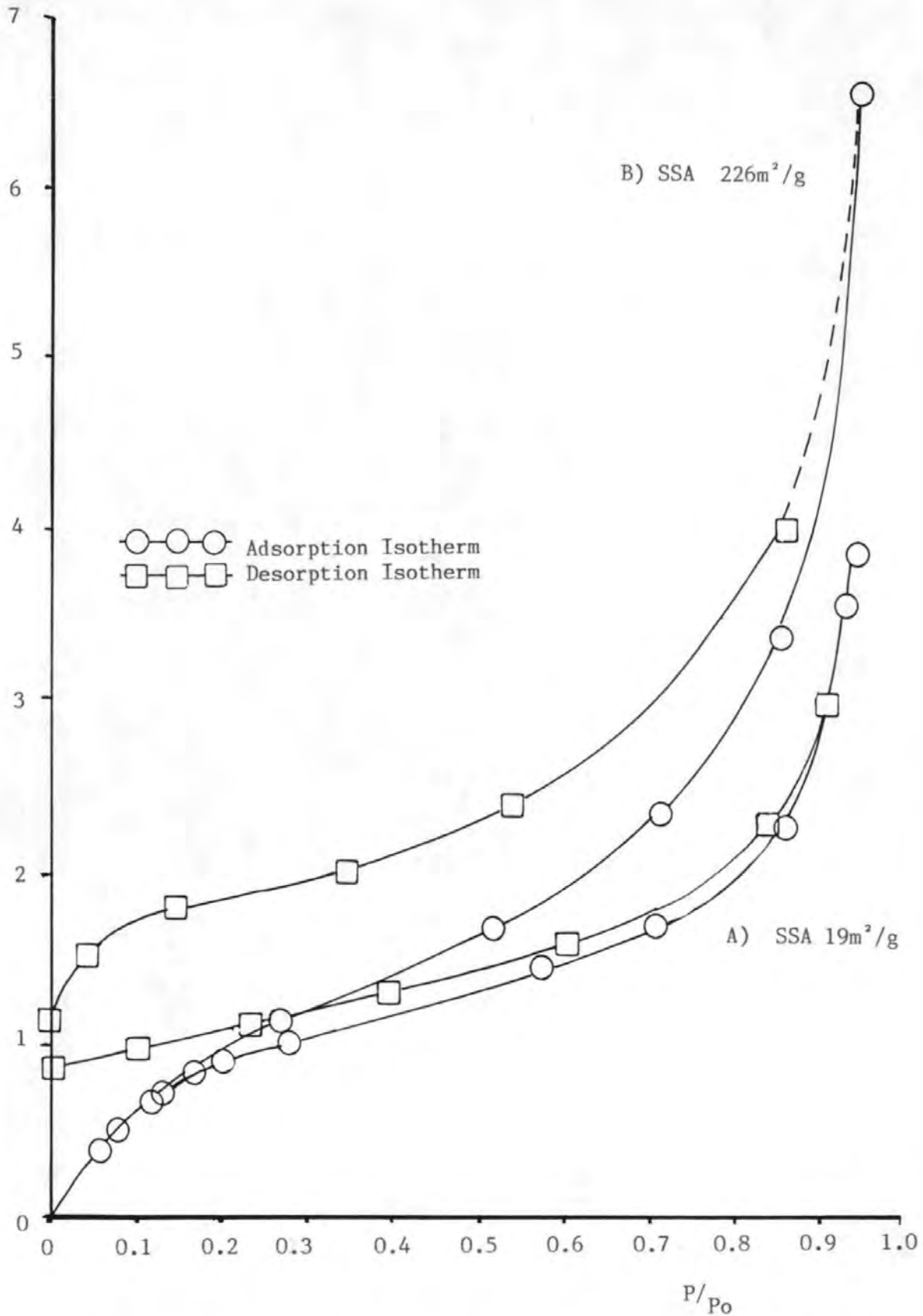


Fig. 4.14 Adsorption/Desorption Isotherm and Hysteresis Loops of a DP Sample, Before 'A' and After 'B' Thermal Degassing.

Sample: 1500rpm Speed  
13.7Nm Load  
ICF at 3.3m



mg N<sub>2</sub> Adsorbed/g  
Sample

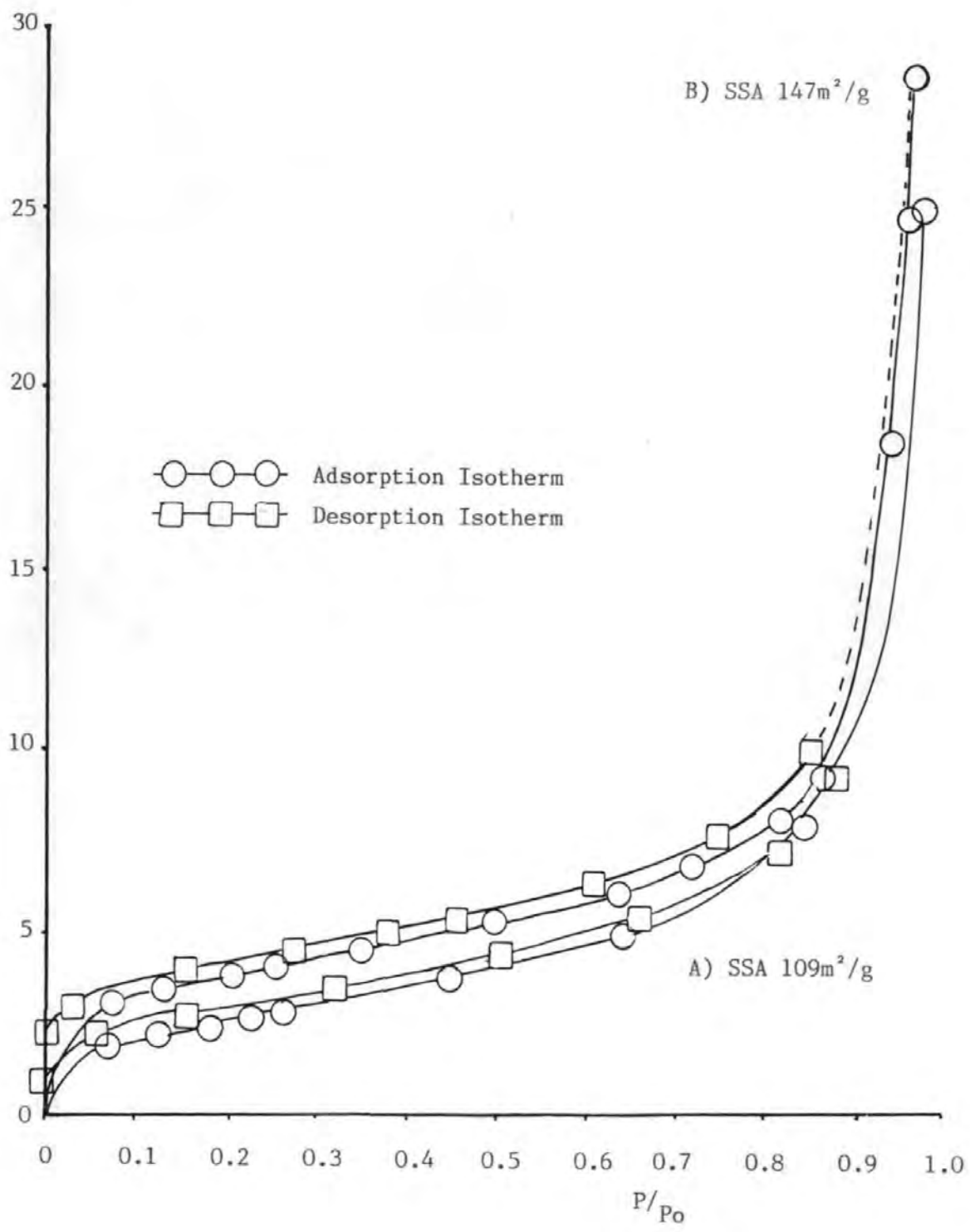


Fig. 4.15 Adsorption/Desorption Isotherms and Hysteresis Loops of a DP Sample, Before 'A' and After 'B' Thermal Degassing.

Sample: 1500rpm Speed  
27.4Nm Load  
ICF at 3.3m

mg N<sub>2</sub> Adsorbed/g  
Sample

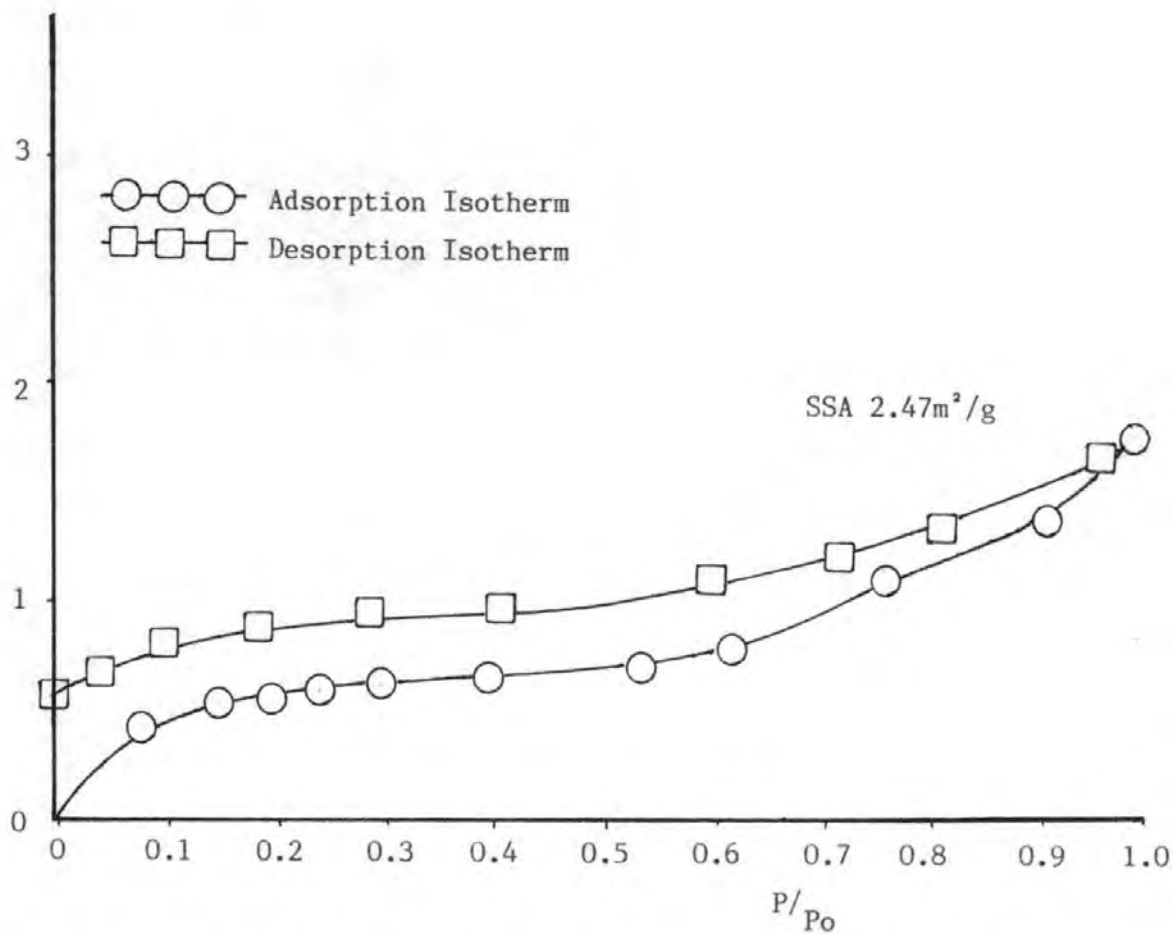


Fig. 4.16 Adsorption/Desorption Isotherm of the TX-40 Filter Media

mesopores unblocked producing significant gains, as detailed in Table 4.7. Both isotherms showed that the micropores had opened, by increasing their quantity of irreversibly adsorbed  $N_2$ .

The smaller quantity of DP from the half load sample, produced smaller changes of weight during analysis and proved to be more difficult to operate, with the buoyancy effect sometimes producing an apparent weight loss after nitrogen dosing. Due to plotted scale the structure appeared to open more than for other soots and the influence of the filter's hysteresis more significant.

#### 4.3.2 CHARACTERISATION OF TD FES FROM ON-FILTER DP

The following sections detail the results of the specific experiments undertaken. The EGA system was developed and facilitated the quantifiable thermal degassing of adsorbed FES. The labile volatile hydrocarbons were identified and the structural changes that occurred to the DP were determined.

The degassed and volatile fractions from the DP samples of Series 1C were characterised by GC. Fig 4.17-A (in Section 4.3.3) shows a typical chromatogram of the TD extracted FES. The most prominent features (as with the Series 1B samples) were

two broad humps, which corresponded to the retention windows of the oil and fuel derived hydrocarbons; lower molecular mass n-alkane series of fuel hydrocarbons and a high molecular mass UCM hump of oil compounds. Due to time constraints, fractionation of this FES was not carried out.

#### 4.3.3 EXPT 3A COMPARISON BETWEEN EXTRACTION METHODS ON THE MICROSTRUCTURE OF DP AND THE ADSORBED FES

Quartered sections of soot laden filter were extracted by different techniques. Thermal degassing (TD) (2hrs) was compared to the standard solvent extraction techniques of soxhlet (24hrs) and ultrasonication (0.5hrs) (dichloromethane (DCM), 150ml). Changes in microstructure, SSA and FES were noted. The results are shown in Fig 4.17-4.19 and SSA data in Table 4.9. The isotherm of each sample was determined but has not been included since they all appear similar to Fig 4.14.

The SSA data showed how the extraction method may influence SSA. For the solvent methods, DCM molecules penetrated the pores, extracting surface and mesoporous-bound hydrocarbons. However the DCM became permanently adsorbed and reduced the SSA by 17-24m<sup>2</sup>/g. The more energetic ultrasonication method enabled DCM molecules to penetrate more deeply and reduce the SSA to 74m<sup>2</sup>/g. The TD method released considerable volatiles and increased the SSA, although not as

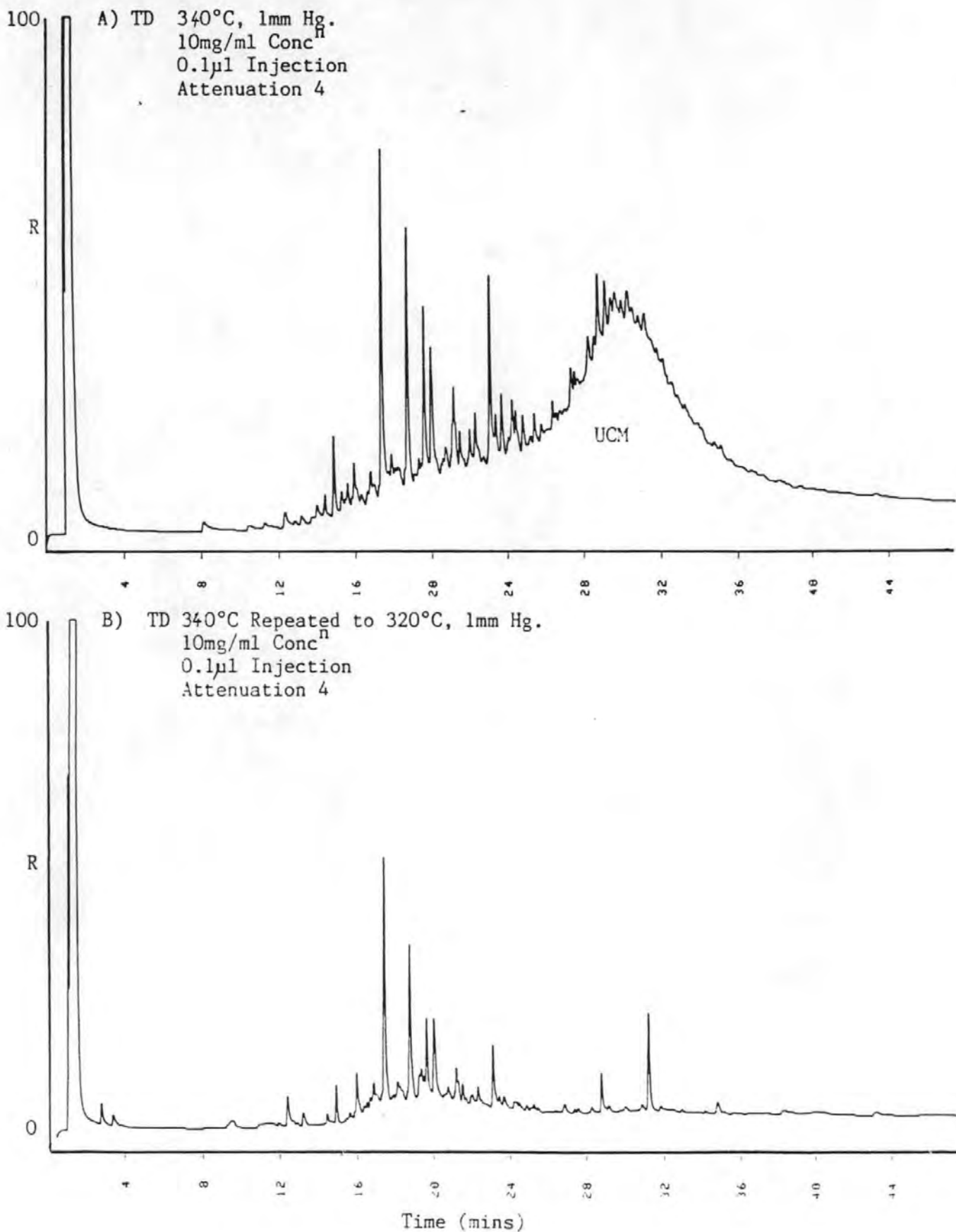


Fig. 4.17 Chromatograms of FES Extracted by TD from DP.  
 ('R' is Response Factor)

Sample: Speed 1500rpm  
 Load 27.4Nm  
 ICF at 3.3m

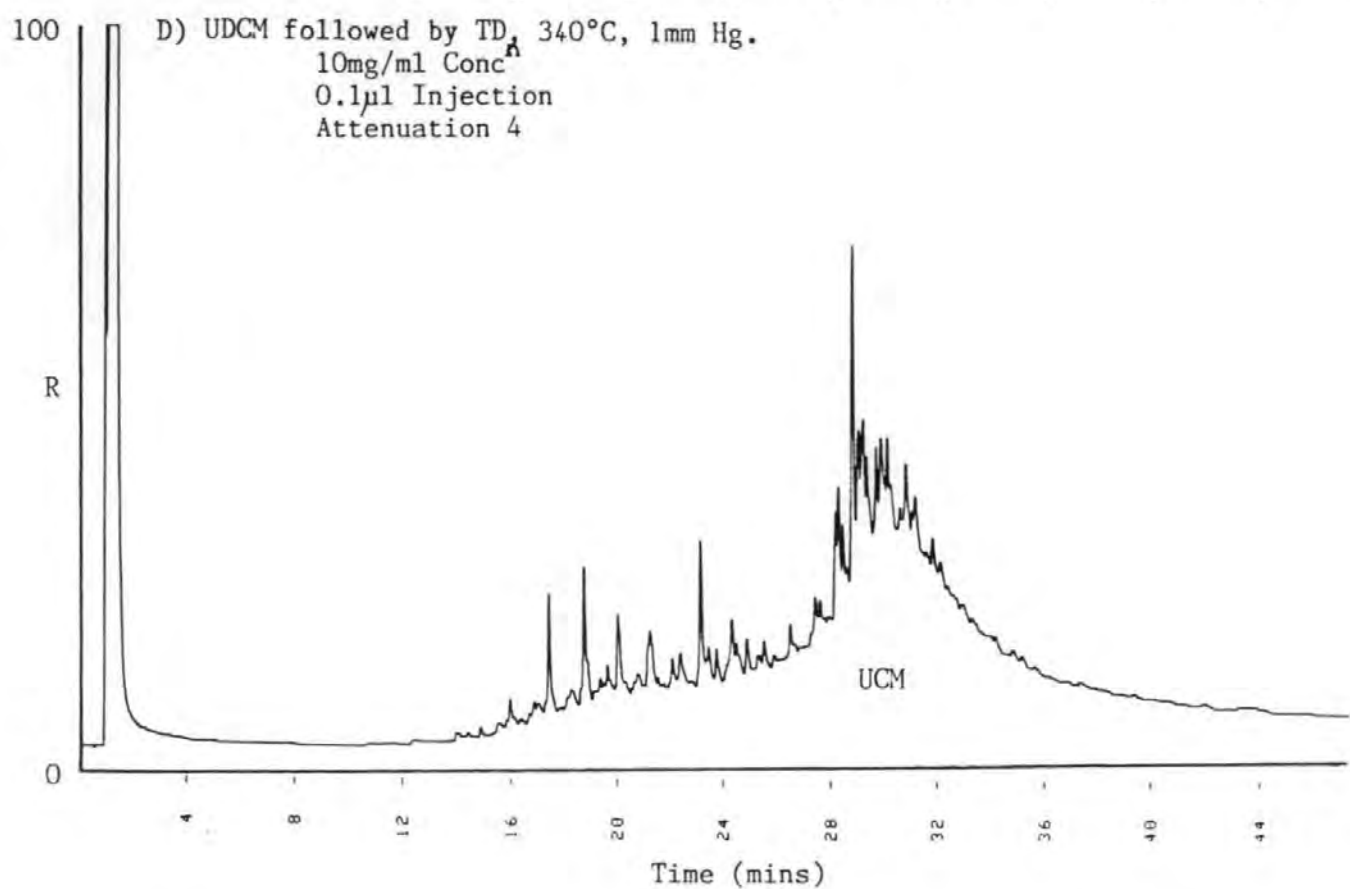
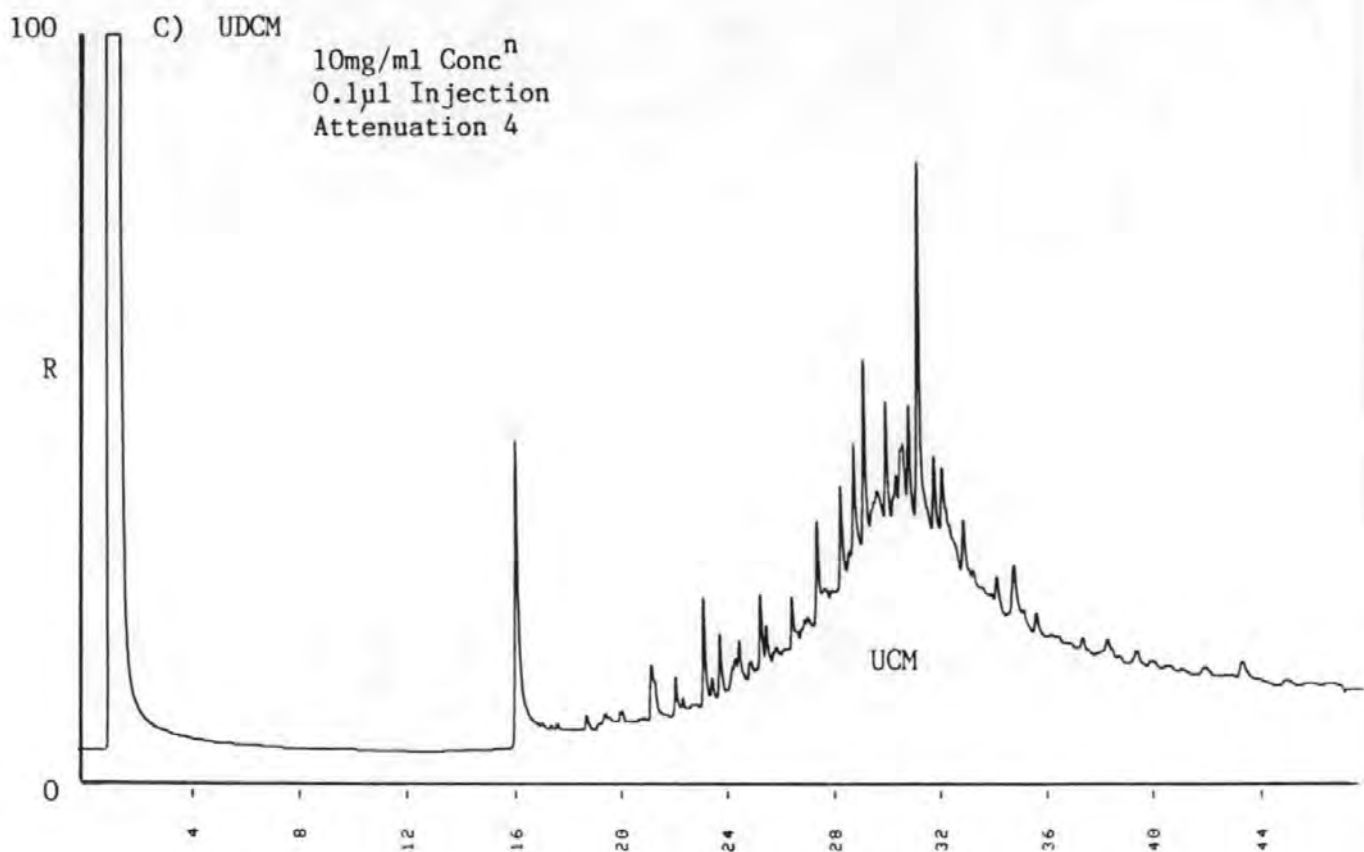


Fig. 4.18 Chromatograms of FES Extracted by Ultrasonication (UDCM) and TD from DP. ('R' is Response Factor)

Sample: Speed 1500rpm  
 Load 27.4Nm  
 ICF at 3.3m

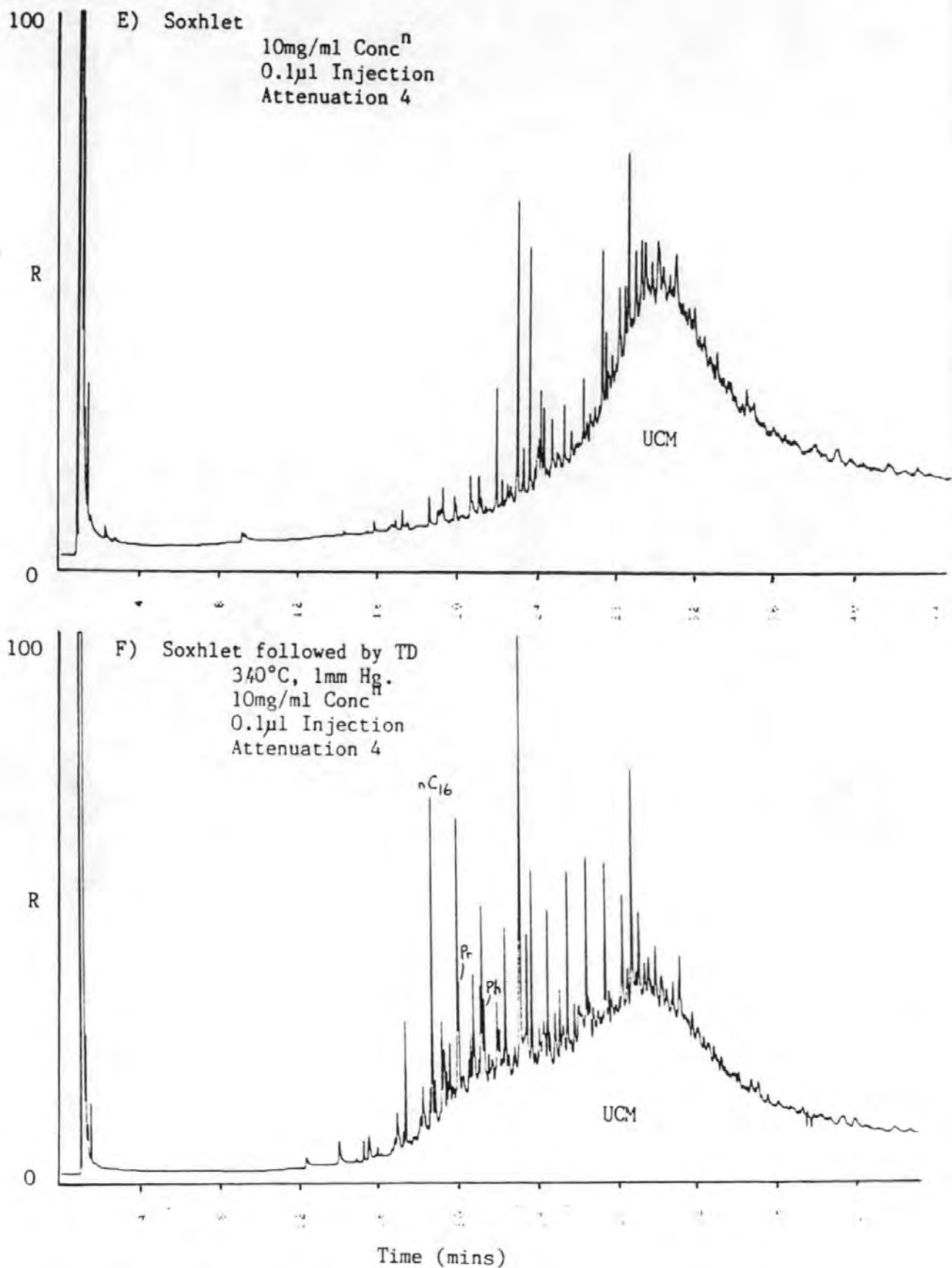


Fig. 4.19 Chromatograms of FES Extracted by Soxhlet and TD from DP ('R' is Response Factor)

Sample: Speed 1500rpm  
 Load 27.4Nm  
 ICF at 3.3m

EXTRACTION METHOD	INITIAL SSA	SSA AFTER 1st EXTRACTION	SSA AFTER FURTHER TD EXTRACTION
TD	98m <sup>2</sup> /g	102m <sup>2</sup> /g	91m <sup>2</sup> /g
UDCM	XXXXXX	74m <sup>2</sup> /g	136m <sup>2</sup> /g
SOX	XXXXXX	81m <sup>2</sup> /g	110m <sup>2</sup> /g

Table 4.9 Variation of SSA with Extraction Method.

ENGINE SPEED (rpm)	ENGINE CONDITION LOAD (Nm)	COMPOSITION: DATA FROM SAMPLE COLLECTED 3.3m FROM EXHAUST PORT	
1500	40.8	Filtered Particulate Mass	11.2mg
		Room Temperature Volatiles (Water)	7%
		Thermally Degassed Volatile (FES)	86%
		Carbonaceous Residue	7%
		Exhaust Gas Temperature	110°C
		SSA Before TD	<7.5m <sup>2</sup> /g
		SSA After TD	430m <sup>2</sup> /g
		Particle Size by SEM	119nm
1500	84.3	Filtered Particulate Mass	22mg
		Room Temperature Volatiles (Water)	1%
		Thermally Degassed Volatiles (FES)	61%
		Carbonaceous Residue	38%
		Exhaust Gas Temperature	130°C
		SSA Before TD	<7.5m <sup>2</sup> /g
		SSA After TD	110m <sup>2</sup> /g
		Particle Size by SEM	101nm

Table 4.10 Composition: Data of Soot Obtained from the Ford DI Engine with the ICF System at 3.3m



much as expected (i.e.  $150\text{m}^2/\text{g}$ ). The pre-extracted soots were then re-extracted by thermal degassing, and further volatiles were released. The chromatograms revealed the release of straight-chain n-alkane species tightly bound in the slit-shaped micropores. The release of highly adsorbed FES also results in a dramatic gain in SSA to the values reported in Table 4.9, as the DCM and FES is released.

The thermally degassed control sample gave poor results. The initial SSA after the first extraction was only slightly higher (it was expected to be around  $150\text{m}^2/\text{g}$ ) than the starting SSA, despite a definite release of volatiles. Further degassing released fuel molecules from the micropores but the SSA declined. This was determined to be due to reordering of the lattice microstructure after removal of all FES.

Examination of data for approximate molecular sizes, using molecular collision diameters ( $\sigma$ ) (Rigby *et al*, 1986) indicated that the carbon layer planes ( $<0.355\text{nm}$ ) themselves could not act as pores but where the planes opened into ultramicropores ( $0.355 - 1\text{nm}$ ) (Fig 3.8) (i.e. at crystallite junctions) then fuel molecules could reasonably be trapped during particle formation. DCM could potentially penetrate these ultramicropores ( $<1\text{nm}$  diameter) but would require sufficient energy to overcome the overlapping van der Waal's forces effect to extract the adsorbed hydrocarbons.

The FES chromatograms showed the effectiveness of each method with TD being the most efficient extracting both fuel and oil-derived hydrocarbon species from all pore ranges. The solvent methods were less efficient (<85% by mass for this sample) and the solvent was permanently adsorbed within the micropores, reducing SSA.

These results question the validity of the standard extraction methods, although it must be pointed out the the soxhlet method did extract 85% by mass of total extractable FES of this sample collected at 170°C.

#### 4.3.4 EXPERIMENT 4A COMPARISON OF THE DP FROM THE FORD DI ENGINE AND THE RICARDO IDI ENGINE

The recently commissioned Ford DI diesel engine, was operated to produce DP samples to compare with soots from the Ricardo IDI engine. The fundamental differences between the engines (e.g. number of cylinders, injection method etc) and the lack of emissions data meant that only qualitative comparison could be achieved. The engines were operated at 1500rpm, 'half' (13.7Nm and 40.8Nm) and 'full' (27.4Nm and 84.2Nm) loads, over a five minute sample period at a sample distance of 3.3m with the ICF. The DP samples were fully characterised.

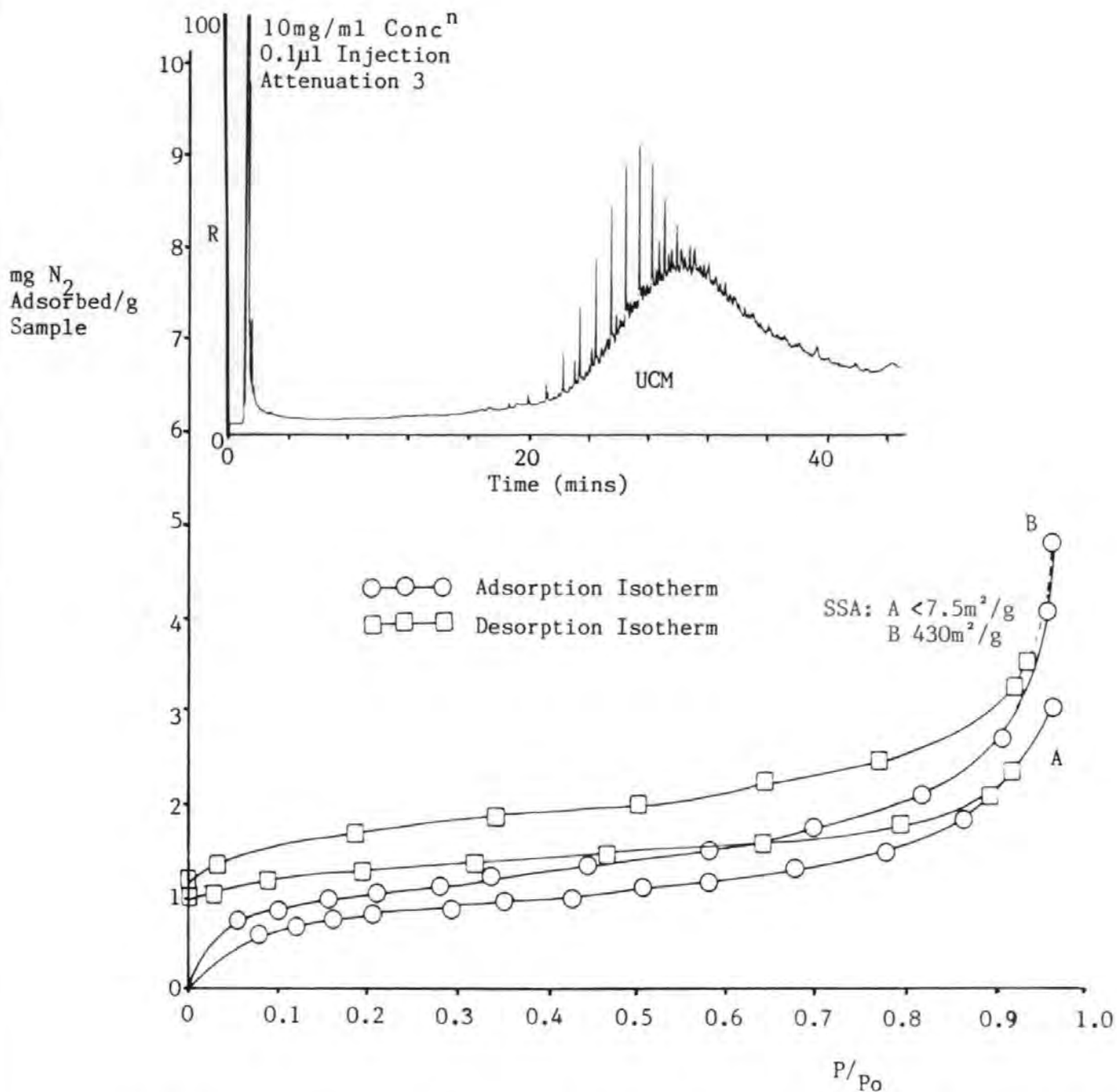


Fig. 4.20 Adsorption/Desorption Isotherms and Hysteresis Loops of a Ford DI Diesel Engine DP, Before 'A' and After 'B' Thermal Degassing. Also Shown is the Chromatogram of the Degassed FES Fraction Plotted as RResponse 'R' Against Time.

Sample: Speed 1500rpm  
 Load 40.8Nm  
 ICF at 3.3m

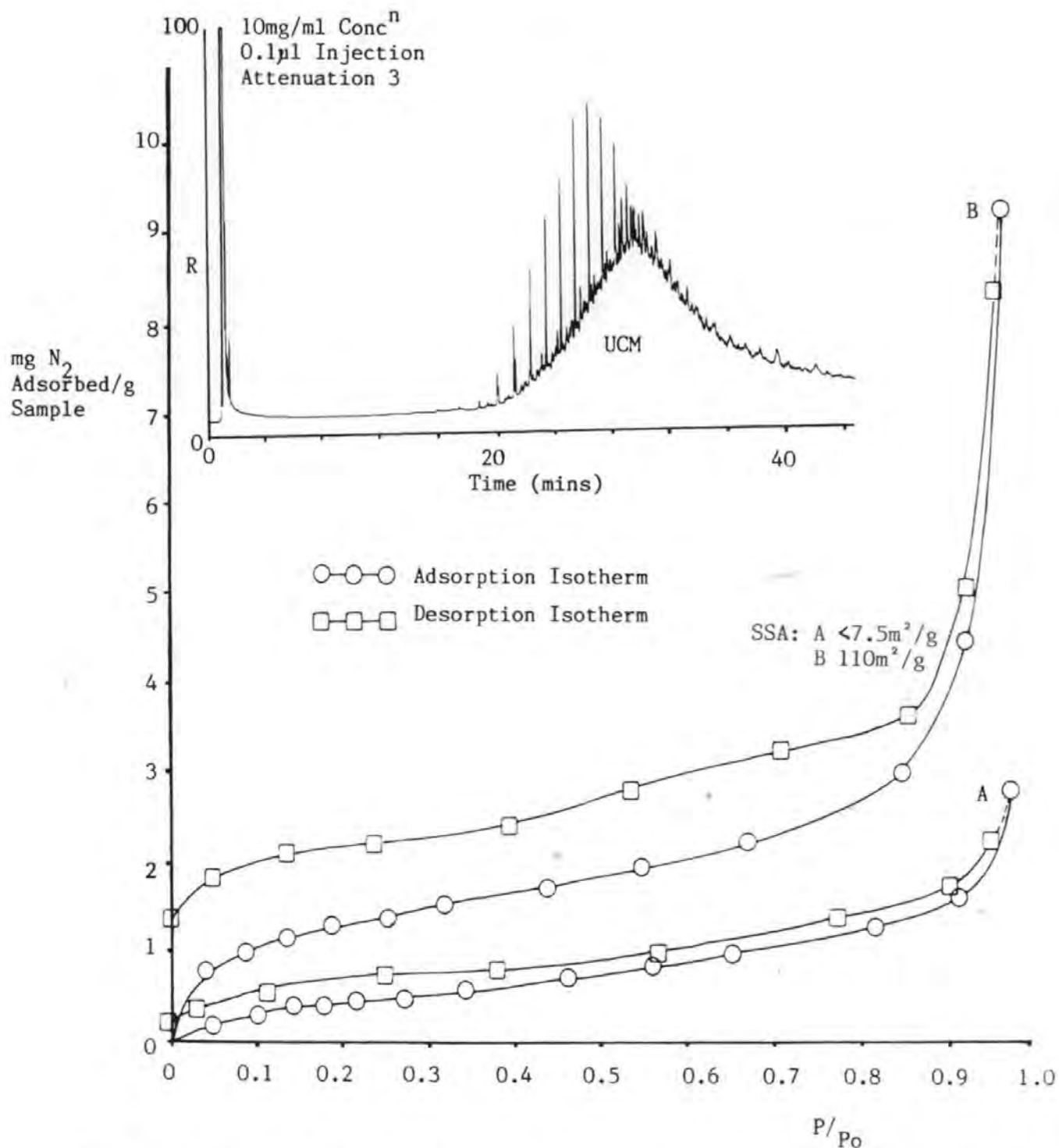


Fig. 4.21 Adsorption/Desorption Isotherms and Hysteresis Loops of a Ford DI Diesel Engine DP, Before 'A' and After 'B' Thermal Degassing. Also Shown is the Chromatogram of the Degassed FES Fraction Plotted as Response 'R' Against Time.

Sample: Speed 1500rpm  
 Load 84.2Nm  
 ICF at 3.3m

The microstructure and TD extracted FES chromatograms of the Ford engine soots are shown in Fig 4.20 and Fig 4.21, and may be compared with the SSA, FES and microstructural data to be shown in Section 4.3.5. The Ford DP had a similar microstructure and SSA values to the Ricardo soots and showed indication of closure in the upper-mesopore range. TD released (340° C, 1mm Hg) a clearly defined chromatogram with similarity between loads. The FES was composed of a regular oil derived UCM with a super-imposed n-alkane series derived from the fuel, which had experienced a distribution shift towards the higher molecular mass hydrocarbons as detailed by Trier (1988). Again, TD unblocked the pores with an increase in SSA. Table 4.10 displays the SSA data and compositional analysis for comparison with Table 4.7.

The % FES mass for the DI engine were higher than expected (Perkins - personal communication, 1989), and one possibility is that the fuel injector or engine timing was poorly adjusted. The modern DI engine has been designed to meet low particulate mass emissions legislation, so therefore the emitted hydrocarbons may be more significant because they would constitute a high % FES of DP mass and therefore the hydrocarbons would be less tightly bound and more bioavailable. The experiment showed that the filter system and analytical procedures were easily adapted to study other engines.

#### 4.3.5 EXPERIMENT 5A SEQUENTIAL EGA AND MICROSTRUCTURAL CHARACTERISATION OF DP

Two engine conditions (1500rpm, 13.7Nm and 27.4Nm) were selected to produce DP for a programme of thermal degassing over a range of temperatures. The samples were treated in the normal way, but extracted successively at increasing temperatures (120, 190, 290 and 340°C) with each volatile fraction collected for GC characterisation. After each degassing, a full adsorption/desorption isotherm was obtained to determine the change in microstructure after release of the volatiles.

The two microstructural and EGA thermal series are shown for both samples in Fig 4.22 - Fig 4.31 and the SSA data summarised in Table 4.11. They show how the successive thermal degassing released trapped volatiles firstly from the surface and mesopores of the DP and at high degassing temperatures from the micropores. The samples were taken from the exhaust at temperatures above 100°C and the volatiles released from the surface and mesopores were therefore largely high molecular mass hydrocarbons and predominantly oil derived, presumably adsorbed after incipient particle formation. Greatest gains in SSA occurred when the ultra-micropores opened with the release of fuel derived hydrocarbons. Differences in general isotherm appearance is due to the plotted scales.

1) Both samples initially had closed upper mesopores which when degassed at 120°C opened, releasing a range of weakly adsorbed hydrocarbons and increasing the SSA by 8-18m<sup>2</sup>/g. The upper mesopores correspond to the surface adsorption sites of the DP, and the removal of volatiles exposed external surface with a slight increase in SSA.

2) Degassing to 190°C, released further volatiles which was shown by the change in microstructure. At low load, when substantial quantities of FES existed on the small soot mass, the release of volatiles produced a significant increase of SSA to 43m<sup>2</sup>/g, and all pore ranges opened, with a release of oil. Thus FES existed in all pore ranges (including mesopores) and was released at relatively low temperatures at these pressures. The high load sample however, showed no change in microstructure or SSA and little FES release. This indicated that all surface and mesopore adsorbed FES (i.e. all weakly adsorbed volatiles) had already been removed by the first degassing and that high load soots do not have a significant surface coating of oil.

3) After thermal degassing to 290°C, both samples were seen to release significantly more FES, particularly oil derived hydrocarbons. The low load sample again opened in all pore ranges increasing its SSA to 54m<sup>2</sup>/g. More noticeable, was the high load sample which increased its SSA to 220m<sup>2</sup>/g due to the

release of an oil UCM and an n-alkane series derived from fuel, which had been highly adsorbed in the micropores. The low load sample was still releasing mesoporous FES, which prevented the release of microporous bound volatiles.

4) At 340°C, microstructural changes began to occur, due to the repetitive heating. These changes did not occur during single thermal degassing programmes. Such features have been previously noted (Section 1.3.2) and related to the reordering of the lattice structure. The low load sample increased its upper-mesopores, perhaps indicating that the agglomerate was disintegrating into individual more widely spaced particles. The SSA also rose to 519m<sup>2</sup>/g, a very high value which may question the accurate mass determination of DP on the filter at low loads. Mass correction incurs greatest error at low DP mass, thereby making the SSA multiplication factor in Equation 3.6 too large. The FES were n-alkanes, which intimated that the increase in micropore volume was due to a release of straight-chain fuel molecules, which had been trapped in the slit-shaped micropores. The full load sample lost SSA by a decline in micropore volume, indicating that the prolonged sample heating and loss of volatiles allowed contraction of the lattice structure, becoming more ordered and graphitic in nature.

In conclusion, it appears that thermal degassing



efficiently removed FES from DP. Initially at temperatures <290°C, weakly adsorbed surface hydrocarbons were extracted which produced a small gain in SSA, and released FES whose composition was largely oil-derived (this is related to exhaust sampling temperature) scavenged by adsorption processes in the exhaust. At higher temperatures micropores were unblocked, giving high SSA values and releasing oil and fuel derived hydrocarbons; the fuel hydrocarbons, dominated by linear n-alkane molecules, were released from the smallest pores (ultramicro pores 0.355 - 1nm) and only released after prolonged degassing. The oil hydrocarbons existed in larger micropores (super micropores 1-2nm). The low load DP with its high % FES, had FES adsorbed in all pore ranges, whereas the high load sample with low % FES had two distinct fractions; a surface FES (adsorbed during TDCS) and a microporous FES (trapped during soot formation).

ENGINE CONDITION AND DP SSA

SPEED	LOAD	LOAD
1500rpm	13.7Nm	27.4Nm
RT 0°C	<7.5m <sup>2</sup> /g	109m <sup>2</sup> /g
100°C	≈7.5m <sup>2</sup> /g	127m <sup>2</sup> /g
170°C	43m <sup>2</sup> /g	127m <sup>2</sup> /g
270°C	54m <sup>2</sup> /g	220m <sup>2</sup> /g
320°C	519m <sup>2</sup> /g	147m <sup>2</sup> /g

Table 4.11 Engine Condition and SSA for Two DP Samples  
Sequentially Degassed at Successively Higher Temperatures

mg N<sub>2</sub> Adsorbed/g  
Sample

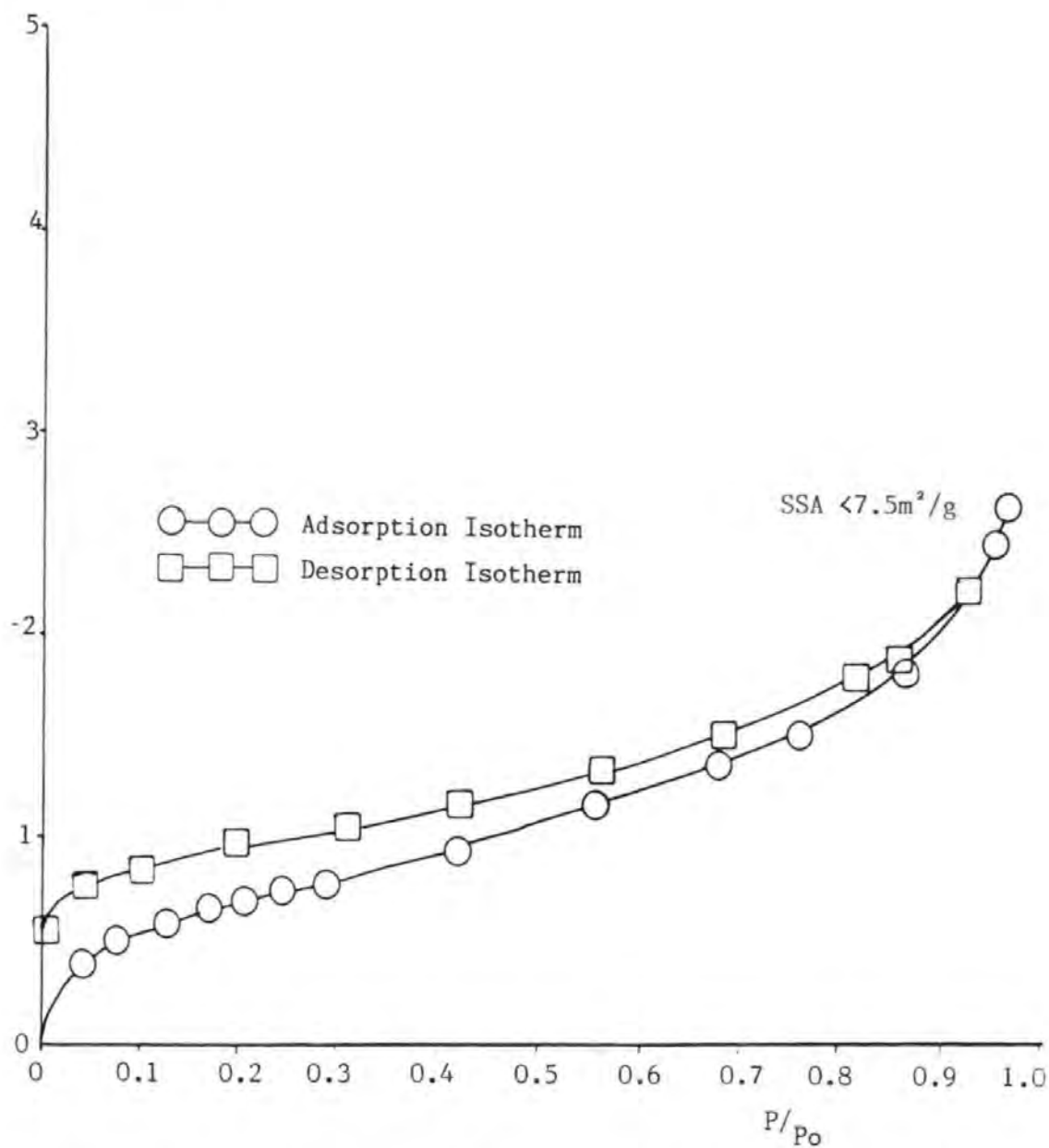


Fig. 4.22 Adsorption/Desorption Isotherm and Hysteresis Loop of a DP Sample Determined On-Filter.

Sample: Speed 1500rpm  
Load 13.7Nm  
ICF at 3.3m

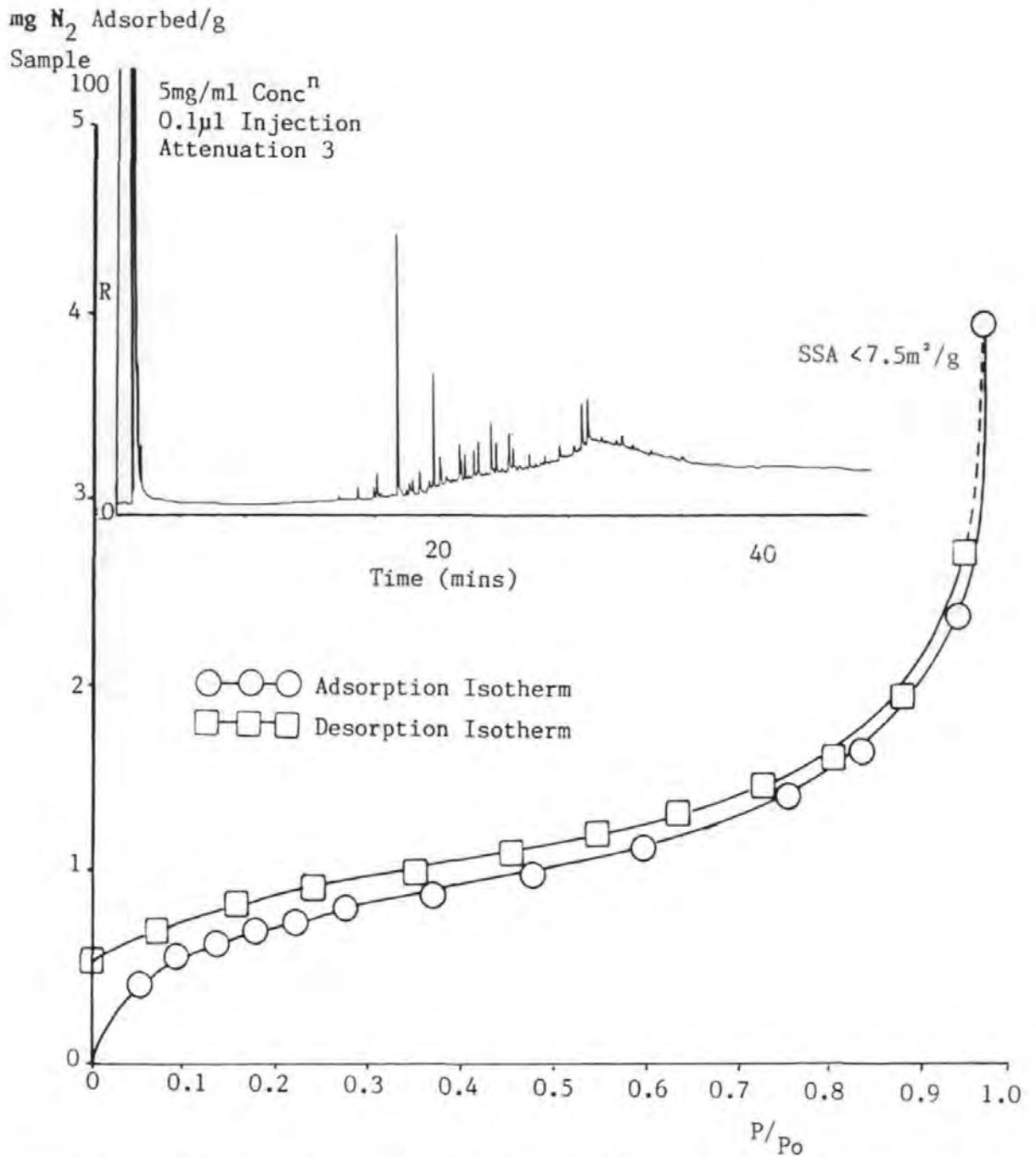


Fig. 4.23 Adsorption/Desorption Isotherm and Hysteresis Loop of a TD Extracted ( $120^{\circ}\text{C}$ , 1mm Hg) DP Determined On-Filter. Also Shown is the Chromatogram of the Degassed FES Fraction, Plotted as Response 'R' against Time.

Sample: Speed 1500rpm  
 Load 13.7Nm  
 ICF at 3.3m

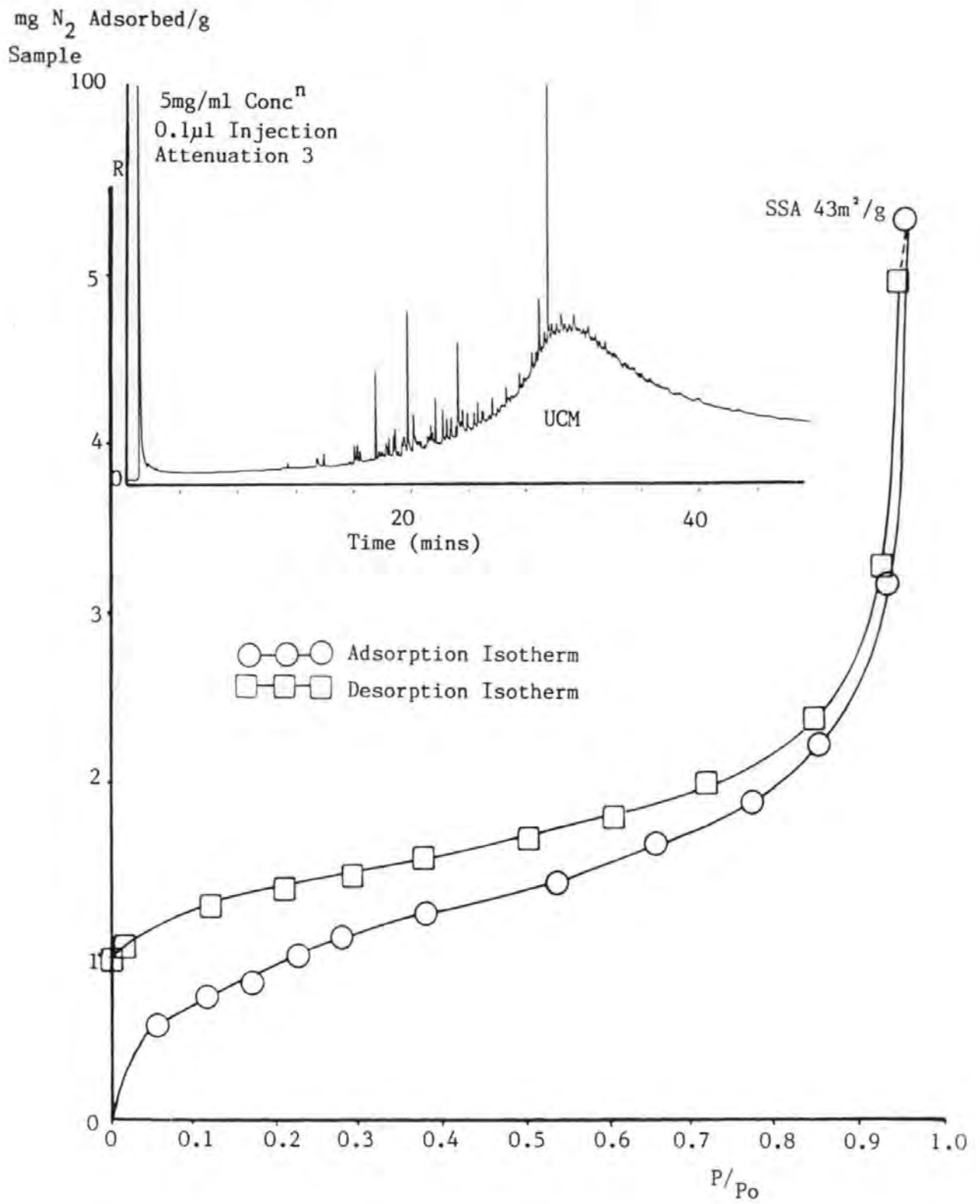


Fig. 4.24 Adsorption/Desorption Isotherm and Hysteresis Loop of a TD Extracted (190°C, 1mm Hg) DP Determined On-Filter. Also Shown is the Chromatogram of the Degassed FES Fraction, Plotted as Response 'R' against Time.

Sample: Speed 1500rpm  
Load 13.7Nm  
ICF at 3.3m

mg N<sub>2</sub> Adsorbed/g

Sample

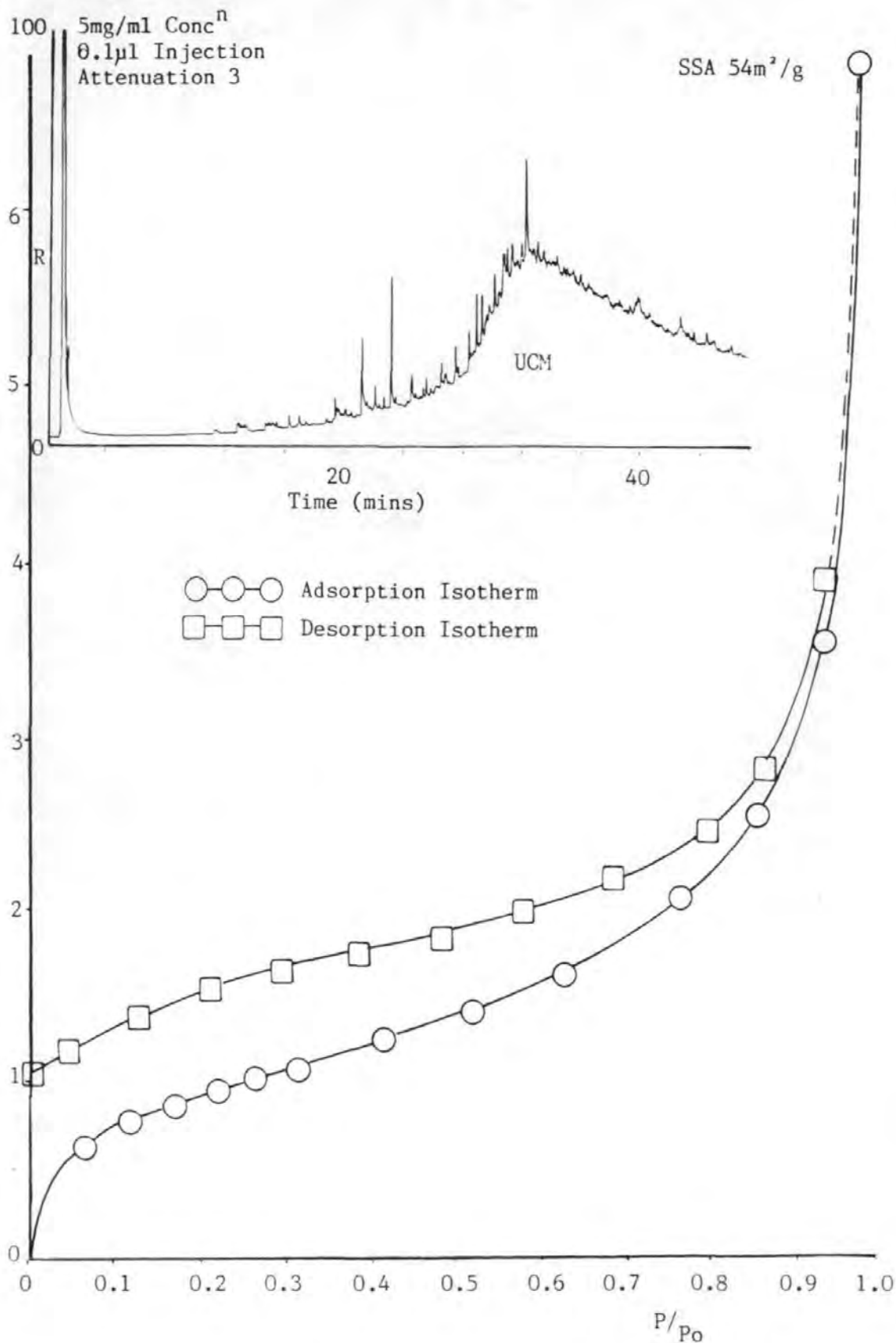


Fig. 4.25

Adsorption/Desorption Isotherm and Hysteresis Loop of a T $\Phi$  Extracted (290°C, 1mm Hg) DP Determined On-Filter. Also Shown is the Chromatogram of the Degassed FES Fraction, Plotted as Response 'R' against Time.

Sample: Speed 1500rpm  
Load 13.7Nm  
ICF at 3.3m

mg N<sub>2</sub> Adsorbed/g  
Sample

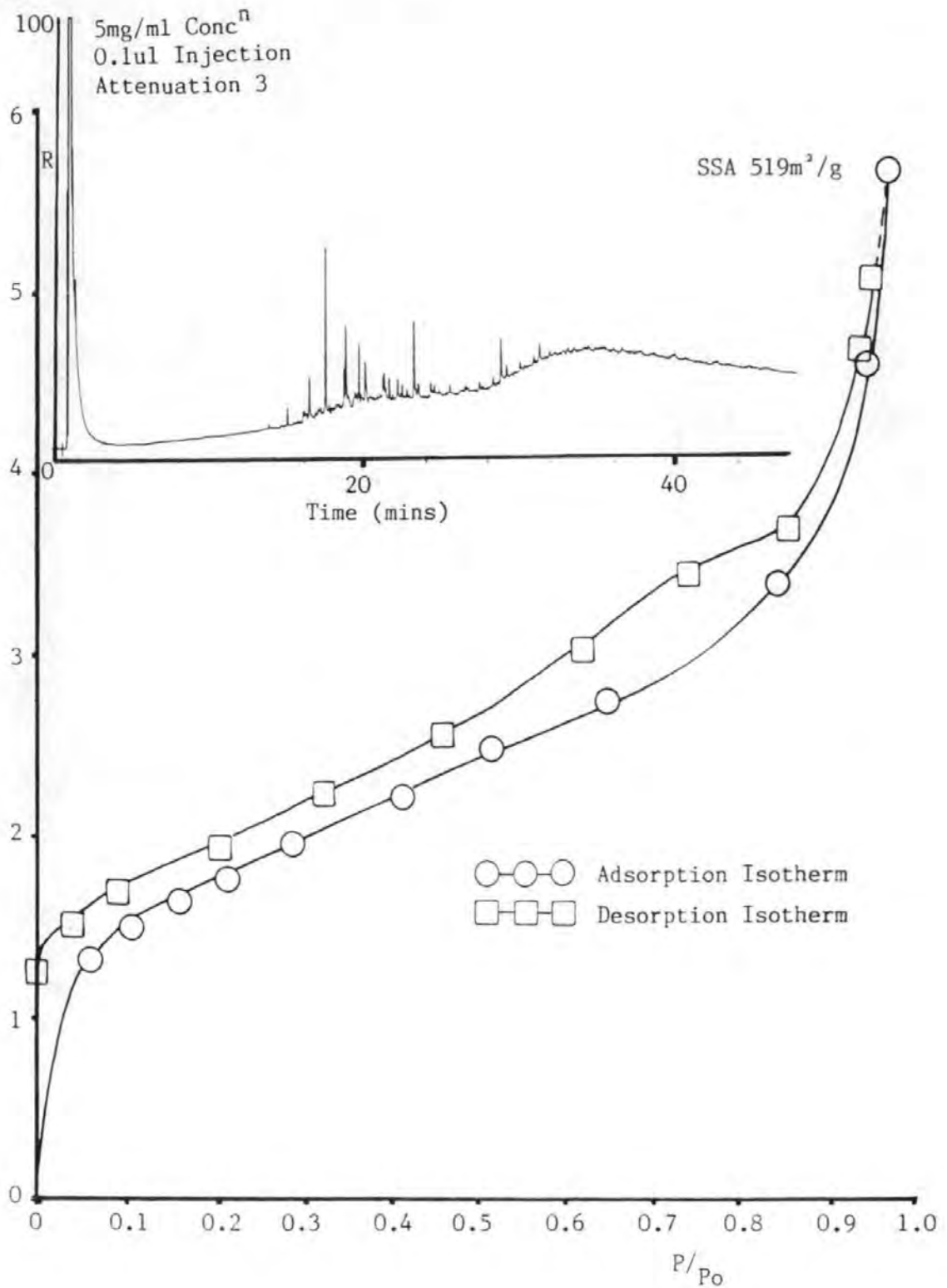


Fig. 4.26 Adsorption/Desorption Isotherm and Hysteresis Loop of a TD Extracted (340°C, 1mm Hg) DP Determined On-Filter. Also Shown is the Chromatogram of the Degassed FES Fraction, Plotted as Response 'R' Against Time.

Sample: Speed 1500rpm  
Load 13.7Nm  
ICF at 3.3m

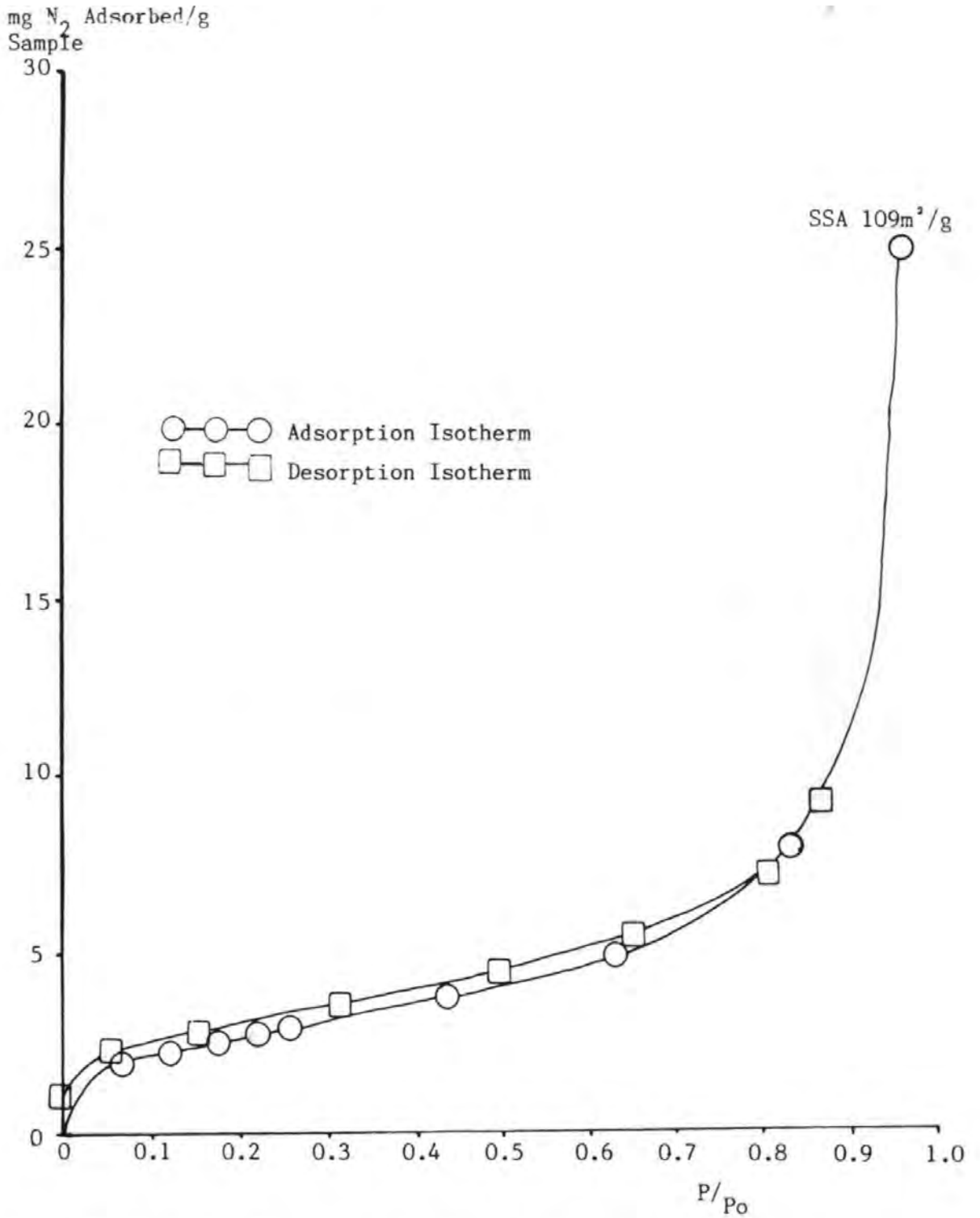


Fig. 4.27 Adsorption/Desorption Isotherm and Hysteresis Loop of a DP Sample Determined On-Filter.

Sample: Speed 1500 rpm  
Load 27.4Nm  
ICF at 3.3m



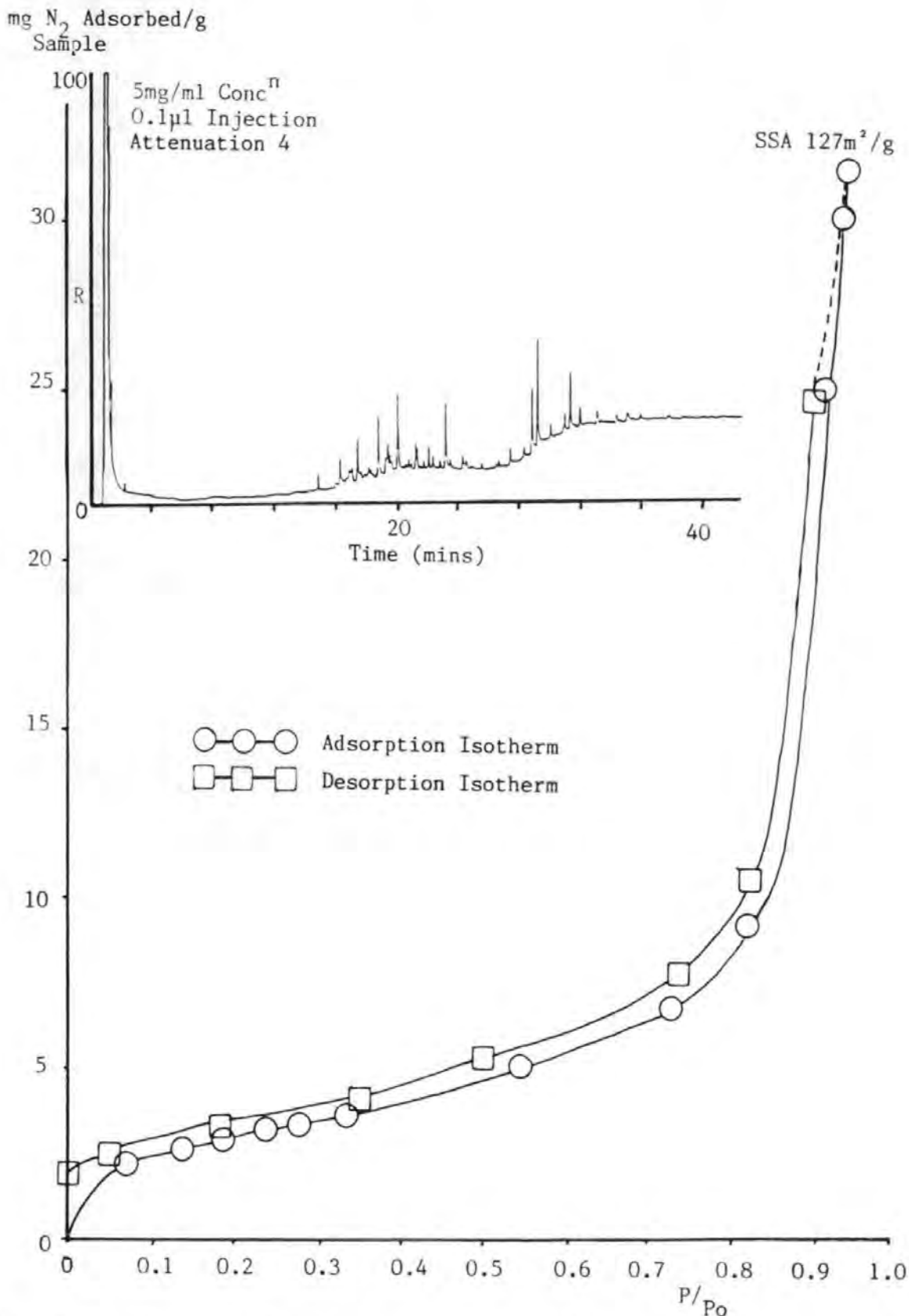


Fig. 4.28 Adsorption/Desorption Isotherm and Hysteresis Loop of a TD Extracted (120°C, 1mm Hg) DP Determined On-Filter. Also Shown is the Chromatogram of the Degassed FES Fraction.

Sample: Speed 1500rpm  
Load 27.4Nm  
ICF at 3.3m

mg N<sub>2</sub> Adsorbed/g  
Sample

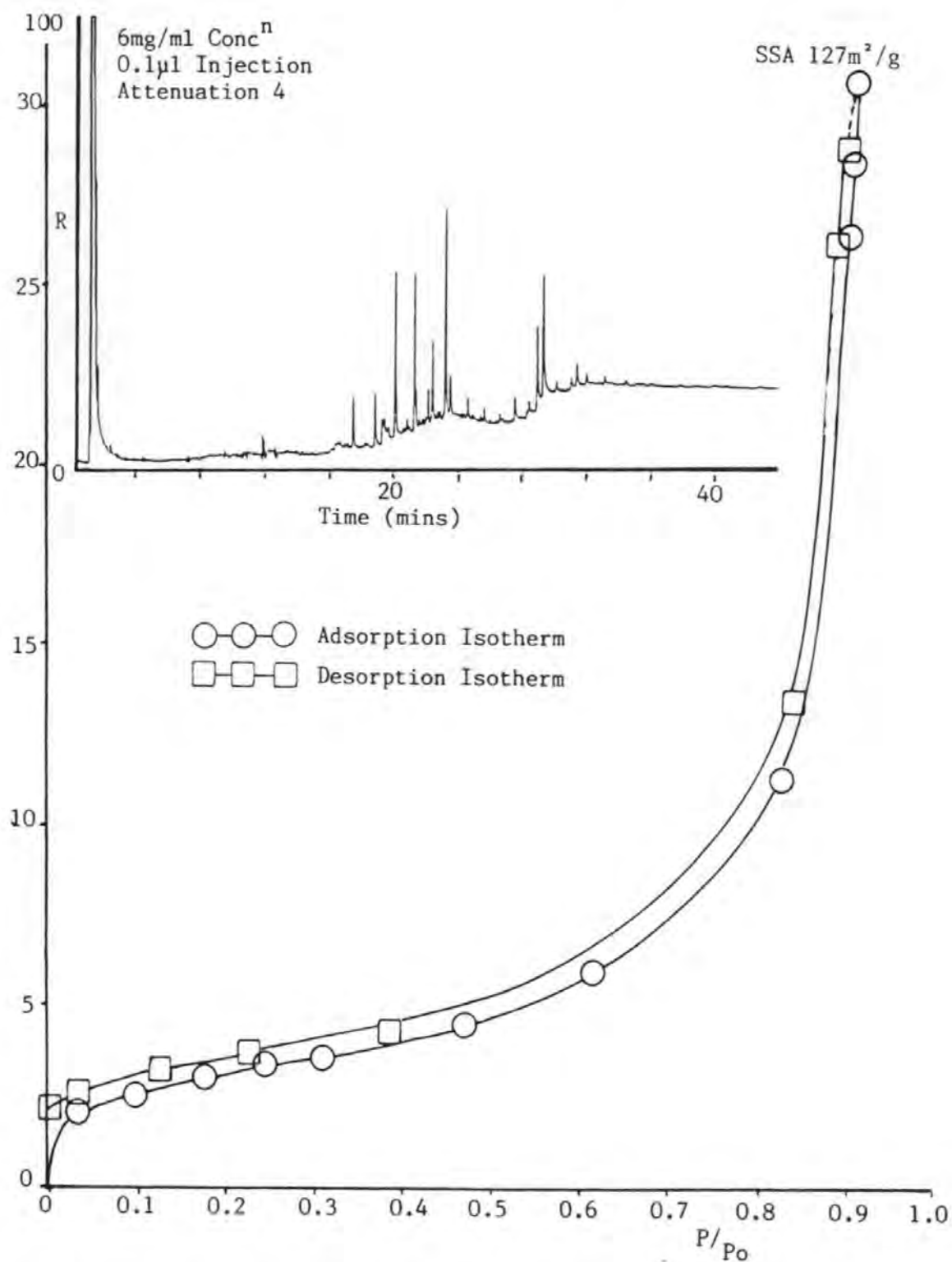


Fig. 4.29 Adsorption/Desorption Isotherm and Hysteresis Loop of a TD Extracted (190°C, 1mm Hg) DP Determined On-Filter. Also Shown is the Chromatogram of the Degassed FES Fraction, Plotted as Response 'R' against Time.

Sample: Speed 1500rpm  
Load 27.4Nm  
ICF at 3.3m

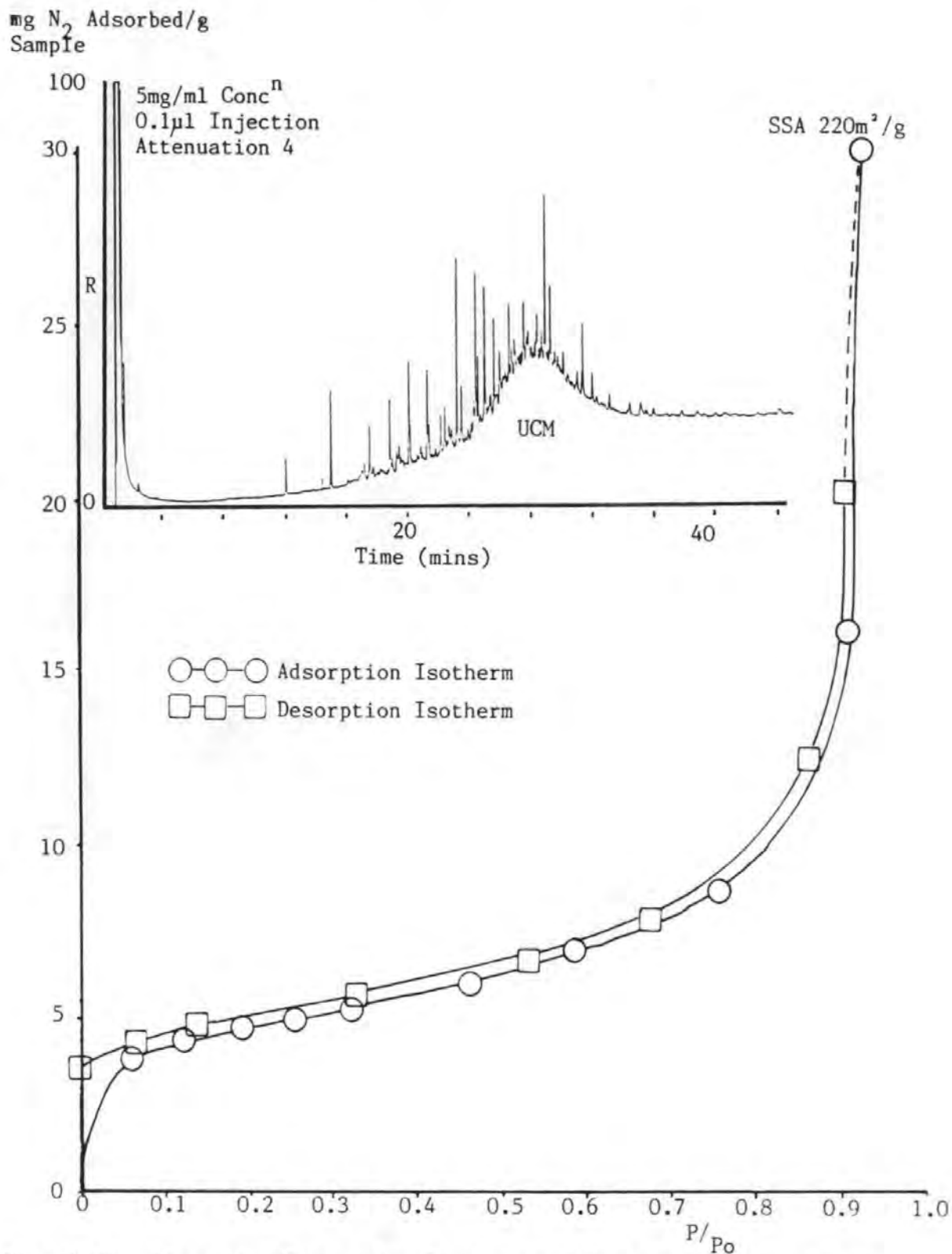


Fig. 4.30 Adsorption/Desorption Isotherm and Hysteresis Loop of a TD Extracted (290 °C, 1mm Hg) DP Determined On-Filter. Also Shown is the Chromatogram of the Degassed FES Fraction, Plotted as Response 'R' against Time.

Sample: Speed 1500rpm  
Load 27.4Nm  
ICF at 3.3m

mg N<sub>2</sub> Adsorbed/g  
Sample

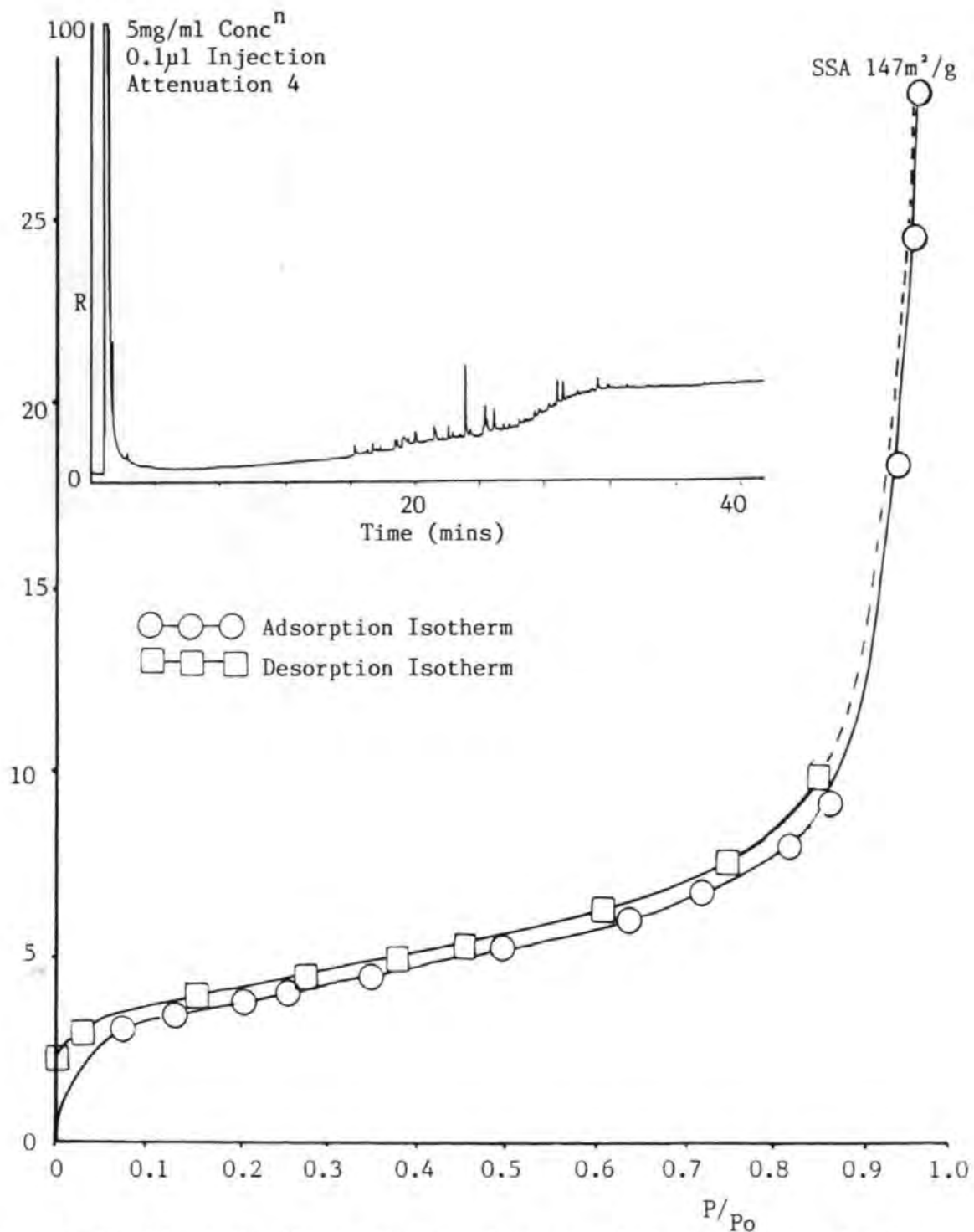


Fig. 4.31 Adsorption/Desorption Isotherm and Hysteresis Loop of a TD Extracted (340°C, 1mm Hg) DP Determined On-Filter. Also Shown is the Chromatogram of the Degassed FES Fraction, Plotted as Response 'R' against Time.

Sample: Speed 1500rpm  
Load 27.4Nm  
ICF at 3.3m

#### 4.4 SUMMARY OF RESULTS

The physical and chemical character of DP has been studied, together with the interaction between UHC and DP over a range of engine conditions. The experimental work was facilitated by the development of innovative methods of filtration, extraction and analysis. The significant results from the previous chapters are presented below, and the salient exhaust processes are synthesised in terms of a conceptual model.

##### 4.4.1 THE CHARACTER OF DIESEL PARTICULATE

The physical character of DP depended on fuel type and engine condition, specifically temperature and equivalence ratio. Soot production was favoured in a high temperature, fuel-rich diffusion flame environment and was greatest for the diesel engine at high speeds and loads. The carbonaceous diesel particles of 30-40nm mean particle diameter formed aggregates of upto  $0.1\mu\text{m}$  size during transport along the exhaust system and into the atmosphere. The microstructure of the DP consisted of platelets which were arranged turbostratically within the particle matrix. Structural analysis confirmed that slit-shaped micropores (Type II isotherms,  $<2\text{nm}$  pore diameter) were formed between these crystallite layers. Aggregated particles showed evidence of 'ink-bottle' mesopores (Type IV isotherm, 2-50nm pore diameter). The SSA of the soots varied (from  $<7.5\text{m}^2/\text{g}$  to

>220m<sup>2</sup>/g) depending on engine condition and the available quantity of adsorbable UHC in the cylinder and exhaust.

#### 4.4.2 IDENTIFICATION OF UNBURNT HYDROCARBONS IN THE EXHAUST

The TES samples indicated that the gaseous UHC's in the exhaust were primarily fuel-derived hydrocarbon species consisting of normally distributed n-alkanes and aromatic parent/alkyl naphthalenes and phenanthrenes. Oil derived species (as a UCM hump) were also observed, and they showed greater dominance in the TES when the engine was operated at higher loads because the oil consisted of higher molecular mass branched and aromatic hydrocarbons which were more resistant to pyrolysis.

#### 4.4.3 THE INTERACTION BETWEEN UNBURNT HYDROCARBONS AND DIESEL PARTICULATE IN DIESEL EXHAUSTS

The FES filtered samples, taken along the exhaust demonstrated that a number of processes were actively influencing the composition of the diesel particulate. The individual particles agglomerated to form larger soot flocculates. The UHC were taken up by the soots, possibly aiding the aggregation process. The coatings of carbonaceous material (primarily FES) reduced the SSA's of the soots by blocking the pores and reducing the amount of internal surface.

The inter-relationship between DP and UHC depended upon the in-cylinder formation conditions, exhaust temperature and relative quantities of the both adsorbent and adsorbate.

The results obtained in this thesis have been synthesised in terms of a conceptual model which interprets the soot-UHC processes along the exhaust system. Fig 4.32 summarises the formation and transport processes for diesel particles.

The diagram shows that:

- 1) At low load, the low DP mass formed, becomes saturated by the large quantity of in-cylinder UHC's which adsorb in the micropores (between the crystallites) giving the soots low SSA's ( $<20\text{m}^2/\text{g}$ ). Linear n-alkane fuel molecules fill the smallest pores (ultra-micropores, 0.355nm - 1.0nm pore diameter) having been trapped during the formation of the carbon lattice. Oil and fuel hydrocarbons may be scavenged later in the larger micropores (super-micropores, 1 - 2nm pore diameter), by bulk quenching and in-cylinder adsorption. The contribution that oil makes to DP FES at high exhaust temperatures, is significant (perhaps 40%), because as the oil exits the cylinder, it rapidly condenses onto the soots, whereas the lower molecular mass fuel molecules remain in gaseous state. High surface area soots (SSA's of  $>100\text{m}^2/\text{g}$ ) were formed at high temperatures and load when fuel was efficiently burned and less UHC was trapped within the large quantity of soot.

ENGINE COMBUSTION PROCESSES

EXHAUST PROCESSES

1500rpm Speed  
13.7Nm Load

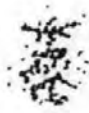
LOW LOAD

	1.3m	3.3m	4.3m
PART	17.5mg	14mg	9.7mg
SOOT	45%	45%	20%
FES	50%	53%	70%
H <sub>2</sub> O	4%	2%	10%
SSA	24-211m <sup>2</sup> /g (+89%)	19-226m <sup>2</sup> /g (+92%)	<7.5-153m <sup>2</sup> /g (>100%)
SIZE	103nm	113nm	125nm
TEMP	165°C	120°C	80°C

COMBUSTION (AFR) CONTROLS DP AND UHC EMISSION. IT INFLUENCES DP SSA BY MICROPORE FILLING. FUEL IN ULTRA-MICROPORES (1nm) OIL/FUEL IN SUPER-MICROPORES (1-2nm)

TDCS OCCURS DOWN THE EXHAUST INCREASING %FES, PARTICLE SIZE AND DECREASING (SLIGHTLY) SSA. IT OCCURS IN THE MESOPORES AND ON THE PARTICLE SURFACE.

Aggregation controlled by FES and Temperature. Threshold for aggregation reported to be less than 150°C.



V. Large Particles

1500rpm Speed  
27.4Nm Load

HIGH LOAD

PART	52.2mg	41.5mg	17.4mg
SOOT	90%	90%	88%
FES	8%	9%	10%
H <sub>2</sub> O	2%	1%	2%
SSA	103-149m <sup>2</sup> /g (+31%)	109-147m <sup>2</sup> /g (+26%)	101-163m <sup>2</sup> /g (+38%)
SIZE	84nm	108nm	117nm
TEMP	240°C	170°C	133°C

Fig.4.32 A Model of DP Formation and Exhaust Processes



The chemical changes in the DP are summarised in Fig 4.33, which shows, in conceptual form, the relative amounts of oil and fuel-derived FES. The diagram shows:

2) That oil forms a significant portion of the FES mass. The contribution that oil makes, appears consistent in the exhaust depending on engine condition (50% at low load and 5% at high load). Along the exhaust, a process termed Temperature Dependent Chemical Scavenging (TDCS) was observed. As the exhaust gas temperature declined, so adsorption of fuel derived UHC occurred onto the DP, increasing the particle size and enhancing the aggregation of the particle into soot chains. The FES may become a significant fraction (47-84%) of the DP mass, especially at low temperatures and low load. This adsorption of fuel UHC, reduced the SSA slightly, since the carbon surface only contributed about 33% to the total surface area of the soots.

The DP filtered from the Ricardo IDI engine, was compared to that filtered from the modern Ford DI engine. It was shown that the microstructures were similar which suggested that similar combustion processes were occurring in both engines. However, the modern engine had lower DP emissions which caused high relative % FES for all engine conditions, giving low SSA's. The filter system was easily transferable between exhaust

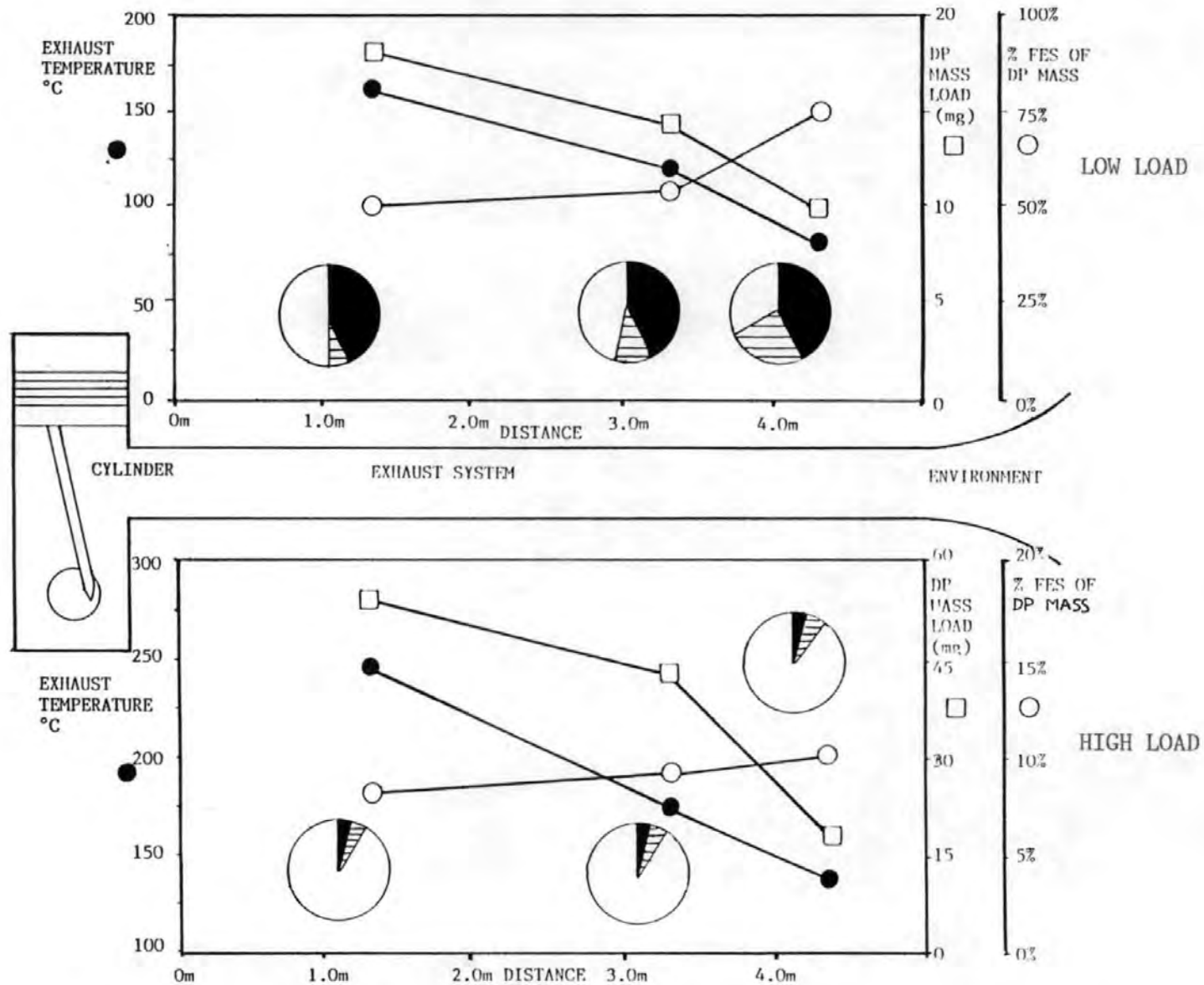


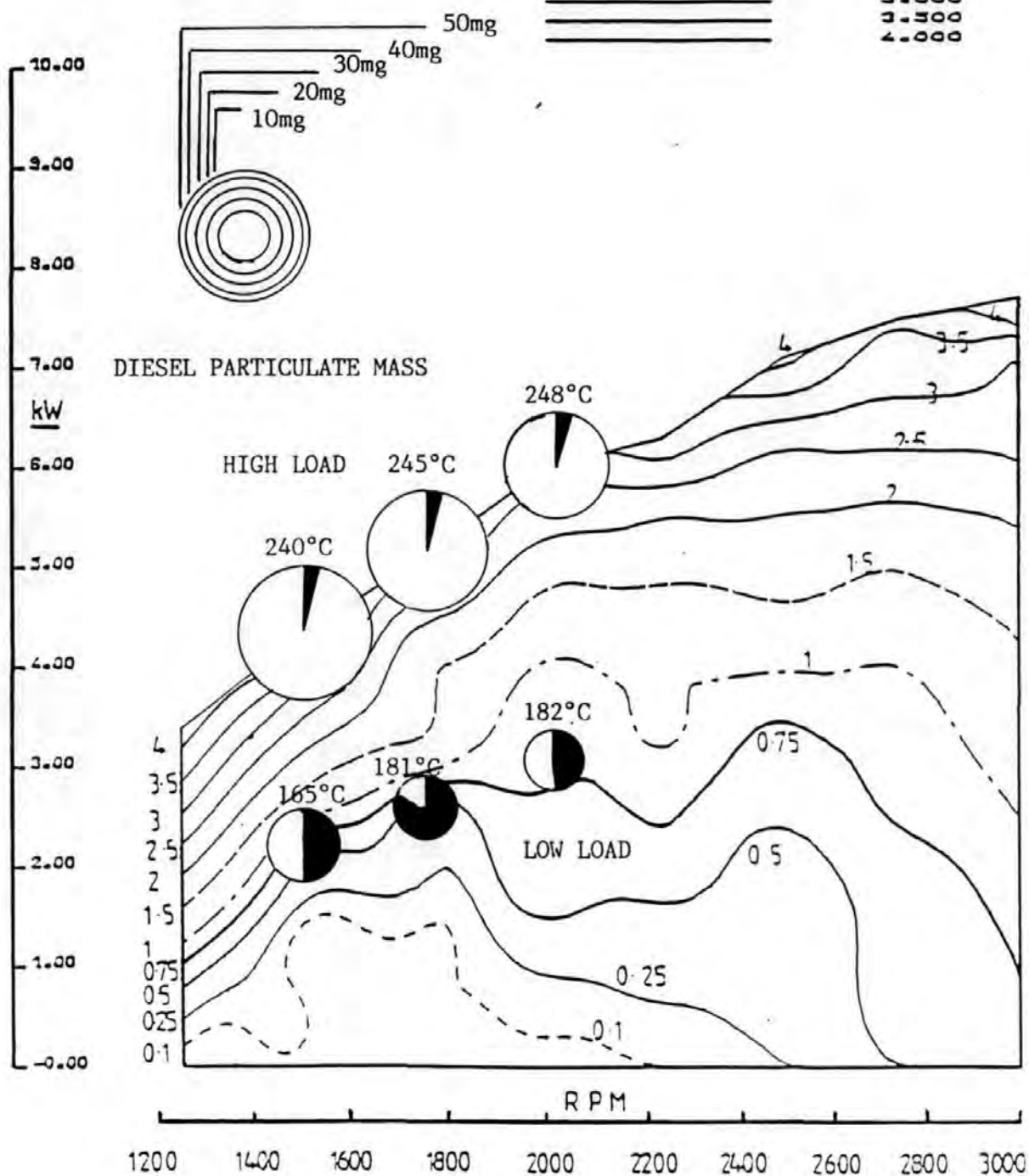
Fig. 4.33 Data Summary of Exhaust Model Showing the DP Subdivided into Estimated Fractions; ■ Oil Derived FES, ▨ Fuel Derived FES and □ Carbonaceous Residue. Also Shown is the Decline in Temperature and Changes DP Mass.

systems, showing the wide applicability of this cheap, reproducible sampling method.

As the sophistication of engines increases and the legislation on exhaust composition is tightened there is a need to improve the information contained in emission maps for engines. One of the possible ways of achieving this is shown in Fig 4.34 and 4.35. The former diagram shows the % FES and DP mass super-imposed on a conventional Bosch Smoke emission map for the Ricardo E6 engine. The data for the engine fitted with a 1.3m exhaust, shows that for Bosch Smoke values in the range 0.75 to 1.0, the DP mass is about 20mg and there is about 50% FES. On the other hand for Bosch Smoke values in the range 3.0 to 4.0, the DP mass is about 50mg, but there is only 10% FES. Figure 4.35 shows the data for the Ricardo engine fitted with the 3.3m exhaust. This shows similar results but the lower temperatures have increased the % FES on the soots.

KEY TO PROFILE VALUES

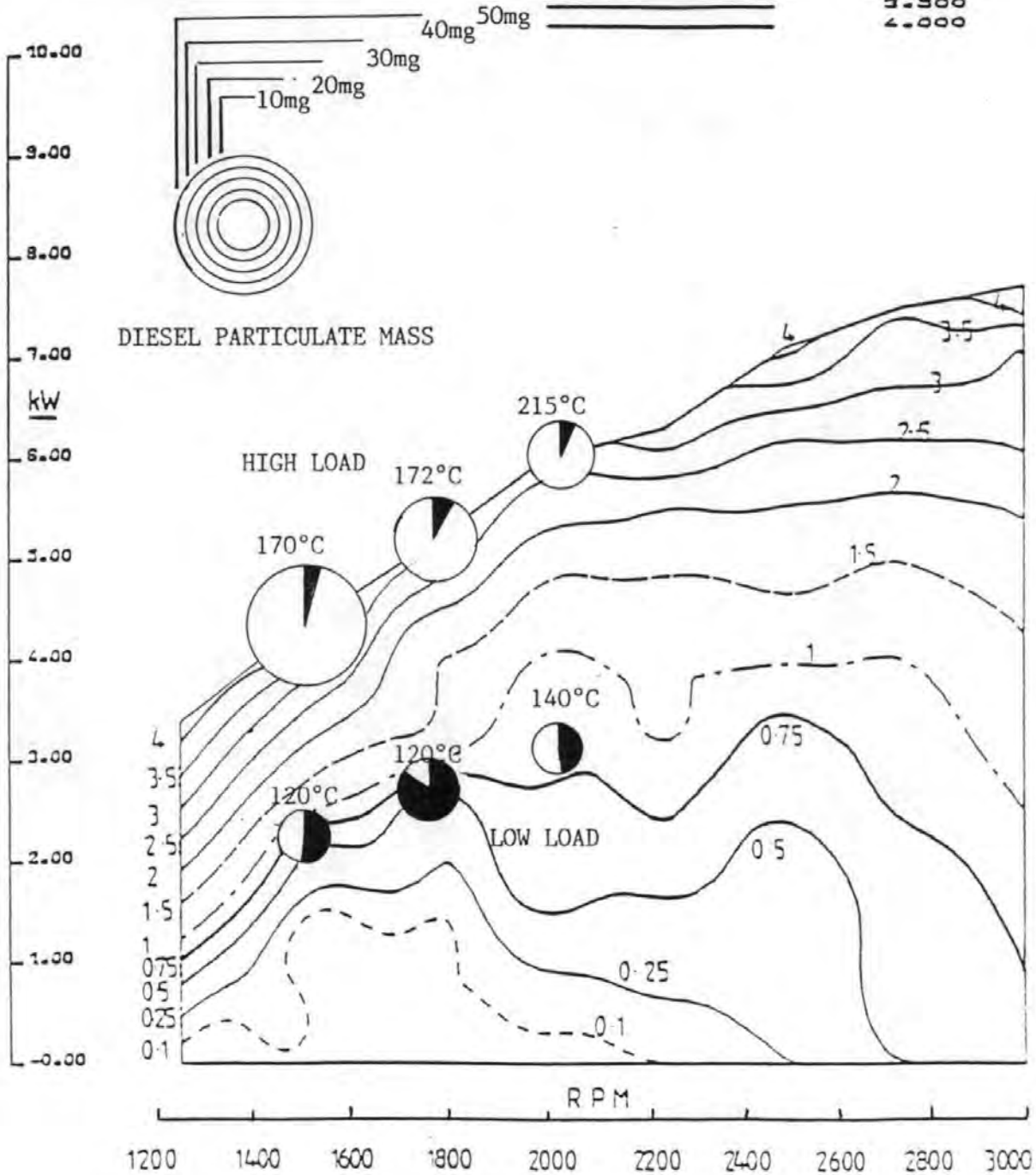
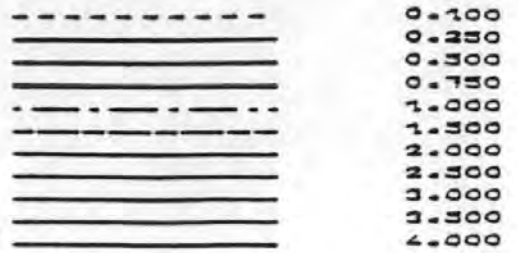
-----	0.100
=====	0.250
=====	0.500
=====	0.750
-----	1.000
-----	1.500
=====	2.000
=====	2.500
=====	3.000
=====	3.500
=====	4.000



ISO-BOSCH SMOKE RICARDO ES. PLYMOUTH POLYTECHNIC

Fig 4.34 Improved Emission Map showing Bosch Smoke Levels, %FES ■, DP Mass Emission and Sample Temperature. These Samples were gathered at 1.3m from the Engine.

KEY TO PROFILE VALUES



ISO-BOSCH SMOKE RICARDO ES. PLYMOUTH POLYTECHNIC

Fig 4.35 Improved Emission Map showing Bosch Smoke Levels, %FES ■, DP Mass Emission and Sample Temperature. These Samples were gathered at 3.3m from the Engine.

## CHAPTER 5 CONCLUSIONS, RECOMMENDATIONS AND FURTHER WORK

### 5.1 CONCLUSIONS

1) An innovative hot whole exhaust filtration system was developed to filter DP on selected filter media (Pallflex TX-40 and Whatman QMA). The technique was superior to other available methods of DP collection because; it provided sufficient sample mass for detailed gravimetric and chromatographic studies, it minimised artificial UHC condensation, it could sample at a range of temperatures (100-340°C), and allowed investigation of the interaction between UHC and DP at various locations along the exhaust of diesel engines. The method proved robust, portable, inexpensive and it gave reproducible results.

2) Microstructural analyses by electron microscopy (SEM and TEM) and by a gravimetric BET method were used to determine particle size and particle microstructure, respectively. An in vacuo gravimetric thermal degassing (TD) apparatus was constructed, which efficiently extracted the high molecular mass volatiles and trapped, for later analysis by gas chromatography. The thermal environment was tailored to suit the most favourable UHC volatile extraction conditions (20-440°C temperature, 760-0.1mm Hg pressure) thereby reducing the potential for hydrocarbon pyrolysis, DP oxidation and thermal changes to soot structure (e.g. swelling).

3) The thermal degassing (TD) apparatus was refined to allow on-filter evolved gas analysis (EGA) to be performed on the DP. Thus, labile FES volatiles adsorbed in the internal and external pore sites could be removed efficiently from the soot particles. The resultant changes in microstructure after desorption were noted and linked to specific hydrocarbon fractions and changes in SSA.

4) Characterisation of DP has shown them to be highly porous with two adsorbed FES fractions. Firstly, a highly adsorbed microporous FES fraction (trapped during in-cylinder formation) which predominantly influenced the soot SSA. Prolonged thermal degassing was shown to release the most tightly bound FES fractions giving high SSA's, but this eventually caused reordering of the lattice structure and loss of SSA. Secondly, a weakly adsorbed mesoporous and particle-surface FES fraction was observed which had been scavenged from the exhaust stream by Temperature Dependent Chemical Scavenging. Thus engine condition influenced SSA, but temperature and UHC emissions affected the scavenging efficiency of the DP.

5) The TD technique was shown to be superior to other available methods for the extraction of all pore-bound FES fractions. Soxhlet extraction failed to extract the microporous

FES which may amount to at least 15% of total adsorbed UHC depending on engine condition and sample temperature. The solvent methods were less effective because the solvent could not penetrate the micropores with sufficient energy to overcome the enhanced adsorption forces that tightly bound the hydrocarbon molecules. Furthermore the smaller solvent molecules tended to reduce the soot SSA's because they became permanently adsorbed in place of the UHC that had been extracted.

6) A conceptual model has been elucidated to summarise the interaction between UHC and DP in the exhaust. This successfully details the salient exhaust processes that influence the composition of soots formed from a diesel engine.

## 5.2 RECOMMENDATIONS

The physical and chemical character of diesel particulate and adsorbed hydrocarbons has been further elucidated by this research. Knowledge of the microstructure of diesel particulate is important for assessing the bioavailability of adsorbed PAH compounds. Clearly, highly adsorbed species, will not be easily extracted by body fluids, but may pose a chronic risk especially if the particle is broken up by body action.

This report suggests that hydrocarbon emissions must be reduced by better injection and combustion. This is important



since modern engines now produce lower levels of DP and therefore the UHC's will only be able to adsorb to the solid particle surface and in mesopores, therefore being more bioavailable.

An advantage of soot emissions, is that the DP readily adsorbs gaseous UHC, thus allowing both emission products to be removed by particulate traps. As DP emissions decline, so the gaseous component would increase, and traps may not be so efficient. The TDCS process would be enhanced if the exhausts were designed to reduce the exhaust gas temperature, e.g. using cooling fins. The predicted change towards more aromatic fuels will enhance DP formation and thus aid this strategy.

### 5.3 FURTHER WORK

1) The filter system should be coupled to TESSA to obtain a definitive exhaust sampling system capable of sampling the gaseous, mesoporous and microporous UHC fractions of the exhaust. This could be easily applied to a variety of modern DI engines.

2) The DP from the modern DI engines should be studied. The higher relative quantities of % FES would suggest that the microporous PAH in these particulate would be very high, over a wide range of conditions and might pose an chronic environmental risk.

3) The soot from radio-labelled TESSA studies should be examined to determine whether this solvent technique has scrubbed microporous bound FES. It is hypothesised that some radio-labelled UHC's (pyrolysis products etc) would become trapped in the micropores and thus not extracted by TESSA. This could be assessed to give a clearer understanding of combustion processes.

4) The TD method, if developed non-gravimetrically would be cheap, simple to operate and could be coupled directly to a GC instrument. The gravimetric instrument used in this work allowed better understanding of the sample degassing behaviour and thus aided sample handling.

5) The microporous FES should be further characterised by GC-MS and fractionation to determine it's detailed composition and it's significance to the total FES. The PAH fraction, it's mutagenicity and bioavailability could thus be investigated.

## REFERENCES

- ABBASS, M.K.; ANDREWS, G.E.; WILLIAMS, P.T. & BARTLE, K.D. 1989.  
Diesel particulate composition changes along an air cooled  
exhaust pipe and dilution tunnel.  
SAE Paper 890789.
- ABRAHAMSON, J. 1977.  
Saturated platelets are new intermediates in hydrocarbon  
pyrolysis and carbon formation.  
Nature, 226, p323-327.
- ADAMS, K.E. 1988.  
The structure and reactivity of some metallurgical carbons.  
Ph.D. Thesis, Plymouth Polytechnic. 304pp.
- ADAMSON, A.W. 1976.  
Physical Chemistry of Surfaces. 3rd Edition.  
Wiley-Interscience. 698pp.
- AGAR, A.W. 1971.  
Principles and Practise of Electron Microscopy Operation  
Glavert, A.M. (Ed).  
N.Holland Publish Co. 306pp.
- AKHTER, M.S.; CHUGHTAI, A.R. & SMITH, D.M. 1984.  
The structure of hexane soot.  
I. Spectroscopic Studies. Appl. Spectros.  
In: Goldberg, E.D. Black Carbon in the Environment: Properties  
and Distribution.  
J. Wiley & Sons. 197pp.
- AMANN, C.A.; STIVENDER, D.L.; PLEE, S.L. & MACDONALD, J.S. 1980.  
Some rudiments of diesel particulate emissions.  
SAE Paper 800251.
- AMES, B.N.; McCANN, J. & JAMASAKI, E. 1975.  
Methods for detecting carcinogenics and mutagens with the  
salmonella/mammalian - microsome mutagenicity test.  
Mutat. Res. 31, p347-346.
- ANDREWS, G.E.; IHEOZOR-EJIOFOR, I.E.; PANG, S.W. &  
OEAPIPATANAKUL, S. 1983.  
Unburnt hydrocarbon and polynuclear aromatic hydrocarbon  
emissions and their relationship to diesel fuel composition.  
IMEchE, C73/83.

- BALL, D.J. 1984  
Environmental implications of increasing particulate emissions resulting from diesel engine penetration of the European automotive market.  
Sci. Total Environ., 33, p15-20.
- BARRER, R.M.; MACKENZIE, N. & REAY, J.S.S. 1956.  
Capillary condensation in single pores.  
J. Colloid Sci., 11, p479-486.
- BEER, J.A. 1988.  
Stationary combustion: the environmental leitmotiv.  
22nd Symposium (International) on Combustion,  
The Combustion Institute, p1-15.
- BITTNER, J.D. & HOWARD, J.B. 1980.  
Pre-particle chemistry in soot formation.  
Proc of the General Motors Symposium Oct 1980. p109-137.
- BJORSETH, A. 1983 (Ed).  
Handbook of Polycyclic Aromatic Hydrocarbons. 250pp.  
Academic Press. 265pp.
- BOEHN, H.P.; TERCZKI, B. & SCHANZ, K. 1982  
Blocking of pores in porous carbons by chemisorption.  
Stud. Surf. Sci. Catal., 10, p395-401.
- BRADDOCK, J.N. & GABELLE, 1977.  
Emission patterns of diesel powered passenger cars, Part 2.  
SAE Paper 770168.
- BRORSTROM-LUNDEN, E. & LINDSKOG, A. 1985.  
Degradation of polycyclic aromatic hydrocarbons during simulated stack gas sampling.  
Environ. Sci. Technol., 19, p313-316.
- BRUNAUER, S.; EMMETT, P.H. & TELLER, E. 1938.  
Adsorption of gases in multimolecular layers.  
J. Amer. Chem. Soc., 60, p309-322.

CALCOTE, H.F. 1981.

Mechanisms of soot nucleation in flames, a critical review.  
Combust. Flame, 42, p215-242.

CARTELLIERI, W. & TRITTHART, P. 1984.

Particulate analysis of light duty diesel engines (IDI & DI)  
with particular reference to the lube oil particulate fraction.  
SAE Paper 840418.

CARTER, M.A. 1983.

Carbon and coke reactivity in zinc-lead blast furnace practice.  
Ph.D. Thesis, Plymouth Polytechnic, 365pp.

CASQUERO-RUIZ, J.D.; GUIL, J.M.; LOPEZ-GONZALEZ, J.D. &  
RUIZ-PANIEGO, A. 1988.

Study of the porous structure of active carbons by nitrogen  
adsorption and n-nonane preadsorption.  
Carbon, 26, p647-652.

CHAN, T.L.; LEE, P.S. & SIAK, J-S. 1981.

Diesel particulate collection for biological testing.  
Comparison of electrostatic precipitation and filtration.  
Environ. Sci. Technol., 15, p89-95.

CHUI, J. 1968.

Polymer characterisation by coupled thermogravimetry-gas  
chromatography.  
Anal. Chem., 40, p1516-1523.

CLERC, J.C. & JOHNSON, 1980.

A computer heat transfer and hydrocarbon adsorption model for  
predicting diesel particulate emissions in dilution tunnels.  
SAE Paper 821218.

CRANSTON, R.W. & INKLEY, F.A. 1957.

The determination of pore structures from nitrogen adsorption  
isotherms.  
Adv. Cat., 9, p143-154.

CRC, 1972.

Handbook of Chemistry and Physics.  
53rd Edition, CRC Press. 2427pp.

CRC, 1980.

Informational report on the measurement and characterisation of diesel exhaust emissions.

CRC Report N° 517.

CUDDIHY, R.C.; GRIFFITH, W.C. & McCLELLAN, R.O. 1984.

Health risks from light duty diesel vehicles.

Environ. Sci. Technol., 18, p1-5.

CUTHBERTSON, R.D.; STINTON, H.C. & WHEELER, R.W. 1979.

The use of a thermogravimetric analyser for the investigation of particulates and hydrocarbons in diesel engine exhaust.

SAE Paper 790814.

DAISEY, J.M.; LOW, M.J.D. & TASCAN, J.M.D. 1984.

The nature of surface interactions of adsorbed pyrene on several types of particles.

In: Cooke, M. & Dennis, A.J. (eds), Polynuclear Aromatic Hydrocarbons: Formation, Metabolism and Measurement.

Battelle Press. p307-315.

DE BOER, J.H. 1958.

The shapes of capillaries.

In: Everett, D.H. & Stone, F. (eds), The Structure and Properties of Porous Materials.

Butterworth, p68-79.

DENNEY, D.W.; KARASEK, F.W. & BOWERS, W.D. 1978.

Detection and identification of contaminants from foil-lined screw-cap sample vials.

J. Chrom., 151, p75-80.

EEC Directive. 1970. 70/220/EEC.

EEC Directive. 1972. 72/306/EEC.

EEC Directive. 1988. 88/76/EEC.

EEC Directive. 1988. 88/77/EEC.

FRISCH, L.E. 1979.

Effect of fuel and dilution ratio on diesel particulate emissions.

SAE Paper 790417.

FUJIWARA, Y. & FUKAZAWA, S. 1980.

Growth and combustion of soot particles in the exhaust of diesel engines.

SAE Paper 800984.

GALLAGHER, P.K. 1978.  
Evolved gas analysis system.  
Thermochim. Acta., 26, p175.

GLASSMAN, I. 1988.  
Soot formation in combustion processes.  
22nd Symposium (International) on Combustion Institute,  
The Combustion Institute. p295-311.

Glasson, D.R. 1988.  
Personal communication.

GLASSON, D.R. & LINDSTEAD-SMITH, D.E.B. 1973.  
Vacuum microbalance studies on the formation and reactivity of  
some synthetic and natural phosphates.  
In: Bevan, S.C., Gregg, S.J. & Parkyns, N.D. (Eds), Progress in  
Vacuum Microbalance Techniques, Vol 2. Heyden, p209-217.

GLASSON, D.R.; SEEBOLD, C.R.; HORN, N.J. & MILLWARD, G.E. 1988.  
The microstructures of carbon soots from diesel engine exhausts.  
In: McEnaney, B. & Mays, T.J. (Eds), Proc. Conf. (Int.) Carbon.  
Institute of Physics.  
IOP Publishing Ltd. p31-35.

GLEGG, G.A. 1987.  
Estuarine chemical reactivity at the particle-water interface.  
Ph.D. Thesis, Plymouth Polytechnic. 264pp.

GOLDSTEIN, J.I. 1981.  
Scanning Electron Microscopy and X-ray Microanalysis: a text for  
biologists, materials scientist and geologists.  
Plenum Press. 673pp.

GREGG, S.J. & SING, K.S.W. 1967.  
Adsorption, Surface Area and Porosity.  
Academic Press. 303pp.

GREGG, S.J. & SING, K.S.W. 1982.  
Adsorption, Surface Area and Porosity.  
Academic Press, 2nd Edition. 303pp.

- GREEVES, G. & WANG, C.H.T. 1981.  
Origins of diesel particulate mass emission.  
SAE Paper 810260.
- GRIEST, W.H. & CATON, J.E. 1983.  
Extraction of polycyclic aromatic hydrocarbons for quantitative analysis.  
In: BJORSETH, A. (Ed). Handbook of Polycyclic Aromatic Hydrocarbons.  
Academic Press. p95-127.
- GRIMMER, G., HILDEBRANDT, A. & BOHNKE, H., 1973.  
Investigation on the carcinogenic burden by air pollution in man.  
III. Sampling And analytics of polycyclic aromatic hydrocarbons in automobile exhaust gas, 2. Enrichment of the PNA and separation of the mixture of all PNA.  
Zbl. Bakt. Hyg. I. Abt. Orig. B. p35-49.
- GROB, R.E. (Ed), 1985.  
Modern Practice of Gas Chromatography. 2nd Edition.  
Wiley Interscience Publishers. 425pp.
- HADDAD, S.D. 1984.  
Combustion and heat release in diesel engines.  
In: Haddad, S.D. & Watson, N. (Eds) Principles and Performance of Diesel Engineering.  
Ellis Horwood Ltd. 223pp.
- HARE, L.T. 1976.  
Fuel and additive effects on diesel particulate developments and demonstration of methodology.  
SAE Paper 760130.
- HARKER, A.; RICHARDS, L. & CLARK, W. 1977.  
Effect of atmospheric SO photochemistry upon observed nitrate concentrations.  
Atmos. Environ., 2, p87-91.
- HAYNES, B.S. & WAGNER, H.Gg. 1981.  
Soot formation.  
Prog. Energy Combust. Sci., 7, p229-273.
- HILDEN, D.L. & MAYER, W.J. 1984.  
The contribution of engine oil to particulate exhaust emissions from light duty, diesel powered vehicles.  
SAE Paper 841395.



- HOMANN, K.H. 1978.  
Soot formation.  
FVM Frankfurt, 327, p137.
- IKEGAMI, M.; LI, X-H.; NAKAYAMA, Y.; MIWA, K. 1983.  
Trend and origins of particulate and hydrocarbon emissions from  
a direct-injection diesel engine.  
SAE Paper 831290.
- KAMIMOTO, K. & YAGITA, M. 1989.  
Particulate formation and flame structure in diesel engines.  
SAE Paper 890436.
- KHATIN, N.J. 1978.  
The characteristion of the hydrocarbon and sulphate fractions  
of diesel particulate matter.  
SAE Paper 780111.
- KITTLESON, D.B.; MOON, K.C. & LIU, B.Y.H. 1984.  
Filtration of diesel particles  
Sci. Total Environ., 36, p153-158.
- KRAFT, J.; HARTUNG, A.; SCHULZE, J. & LIES, K-H. 1982.  
Determination of polycyclic aromatic hydrocarbons in diluted  
and undiluted exhaust gas of diesel engines.  
SAE Paper 821219.
- LAHAYE, J. & PRADO, G. 1981.  
Morphology & internal structure of soot and carbon blacks.  
In: Particulate Carbon: Formation During Combustion.  
SIEGLA, D.C. & SMITH, G.W. (Eds),  
Plenum. 300pp.
- LATER, D.W.; WILSON, B.W. & LEE, M.L. 1985.  
Standardization of alumina and silica adsorbents used for  
chemical class separations of polycyclic aromatic hydrocarbons.  
Anal. Chem., 57, p2979-2984.
- LEE, M.L.; VASSILAROS, D.L.; WHITE, C.M.; NOVONTNY, M. 1979.  
Retention indicies for programmed-temperature capillary column  
gas chromatography of polycyclic aromatic hydrocarbons.  
Anal. Chem., 51, p768-773.
- LEE, M.L.; NOVOTNY, M.V. & BARTLE, K.D. 1981.  
Analytical Chemistry of Polycyclic Aromatic Compounds  
Academic Press. 462pp.

- LEE, F.S-C.; HARVEY, T.M.; PRATER, T.S.; PAPITA, M.C. & SCHUETZLE, D. 1980.  
Chemical analysis of diesel particulate matter and evaluation of artefact formation.  
In: Sampling and Analysis of Toxic Atmospheric Organics.  
American Society for Testing and Materials. STP. 721. p92-110.
- LEE, F.S-C. & SCHUETZLE, D. 1983.  
Sampling, extraction and analysis of polycyclic aromatic hydrocarbons from internal combustion engines.  
In: Bjorseth, A. (Ed). Handbook of Polycyclic Aromatic Hydrocarbons.  
Academic Press, p27-94.
- LEVINE, S.P.; SKEWES, L.M.; ABRAMS, L.D. & PALMER, A.G. 1982.  
High performance semi-preparative liquid chromatography and liquid chromatography-mass spectrometry of diesel engine emission particulate extracts.  
In: Cooke, M. & Dennis, A.J. (eds), The Structure and Properties of Porous Materials.  
Butterworths, p439-447.
- LILLY, L.C.R. (Ed), 1984.  
Diesel Engine Reference Book.  
Butterworth. 700pp.
- LIN, C. & FRIEDLANDER, S.K. 1988.  
A note on the use of glass fibre filters in the thermal analysis of carbon containing aerosols.  
Atmos. Environ., 22, p605-607.
- LINDSKOG, A. 1983.  
Transformation of polycyclic aromatic hydrocarbons during sampling.  
Environ. Health Perspect., 47, p8-84.
- LINDSKOG, A.; BRORSTROM-LUNDEN, E.; ALFHEIM, I. & HAGEN, I. 1987.  
Chemical transformation of PAH on airborne particles by exposure to nitrogen dioxide during sampling: a comparison between two filter media.  
Sci. Total Environ., 61, p51-57.
- LONGWELL, J.P. 1982.  
Polycyclic aromatic hydrocarbons and soot from practical combustion systems.  
In: Soot in Combustion Systems and its Toxic Properties.  
LAHAYE, J. & PRADO, G. (Eds),  
NATO Conference Series, Series 6, Materials Science; v.7.  
Plenum Press. 433pp.

- LOW, G.K-C. & BATLEY, G.E. 1988.  
Comparative studies of adsorption of polycyclic aromatic hydrocarbons by fly ashes from the combustion of some Australian coals.  
Environ. Sci. Technol., 22, p322-327.
- MAUDERLY, J.L.; JONES, R.K.; MCCLELLAN, R.O.; HENDERSON, R.F. & GRIFFITH, W.C. 1986.  
Carcinogenicity of diesel exhaust inhaled chronically by rats.  
In: Ishinishi, N.; Koizumi, A.; McClellan, R.O. & Stöber, W. (Eds), Carcinogenic and Mutagenic Effects of Diesel Engine Exhausts, Proc. International Satellite Symposium on Toxicological Effects of Emissions from Diesel Engines.  
Elsevier Science Publishers, p397-409.
- MAYER, W.J.; LECHMAN, D.C. & HILDEN, D.L. 1980.  
The contribution of engine oil to diesel exhaust particulate emission.  
SAE Paper 800256.
- MCCLELLAN, R.O. 1986.  
Toxicological effects of emissions from diesel engines.  
In: Ishinishi, N.; Koizumi, A.; McClellan, R.O. & Stöber, W. (Eds). Carcinogenic and Mutagenic Effects of Diesel Engine Exhausts, Proc. International Satellite Symposium on Toxicological Effects of Emissions from Diesel Engines.  
Elsevier Science Publishers, p529-534.
- MEDALIA, A.I. & RIVIN, D. 1982.  
Particulate carbon and other components of soot and carbon black.  
Carbon, 20, p481-492.
- McENANEY, B. & MASTERS, K.J. 1983.  
Assessment of adsorption in microporous carbons.  
In: Jayaweera, S.A.A. (Ed) 20th International Vacuum Microbalance Techniques Conference.  
Thermochim. Acta. 82. p157-163.
- McENANEY, B. 1988.  
Adsorption and structure in microporous carbons.  
Carbon, 26, p267-274.
- MIKAIL, R.S. & ROBENS, E. 1983.  
Microstructure and Thermal Analysis of Solid Surfaces.  
John Wiley. 496pp.

- MILLS, G.A. 1983.  
Polynuclear aromatic hydrocarbon emissions from diesel engines.  
Ph.D. Thesis, University of Southampton. 152pp.
- MILLS, G.A.; HOWARTH, J.S. & HOWARD, A.J. 1984  
The effect of diesel aromaticity on polynuclear aromatic  
hydrocarbon exhaust emissions.  
J. Inst. Energy, 3, p275-286.
- OBUCHI, A.; AOYAMA, H.; OHI, A, & OHUCHI, H. 1984.  
Determination of polycyclic aromatic hydrocarbons in diesel  
exhaust particulate matter and diesel fuel oil.  
J. Chrom., 312, p247-259.
- ONODERA, S. 1977  
Gas chromatographic studies of thermal decompositions of  
Hexaammine Chloropentaamine Cobalt (III) and Transdichloro  
Tetraammine cobalt (III) Chloride in solid state.  
Bull. Chem. Soc. Japan., 50, p123-137.
- PALLFLEX, 1988.  
Filters for air quality sampling.  
Pallflex, Inc.
- PEAKE, E. & PARKER, K. 1980.  
PAH and the mutagenicity of used crankcase oils.  
In: Bjorseth, A. & Dennis, A.J., Polycyclic Aromatic  
Hydrocarbon Chemistry and Biological Effect,  
Academic Press, p1025-1039.
- PELLIZZARI, E.D.; BUNCH, J.E.; CARPENTER, B.H. &  
SANWICKI, E.B.H. 1975.  
Collection and analysis of trace organic vapour pollutants in  
ambient atmospheres - thermal desorption of organic vapors from  
sorbent media.  
Environ. Sci. Technol., 9, p556-560.
- PEREZ, J.M.; LIPARI, F. & SEIZINGER, D.E. 1984.  
Cooperative development of analytical methods for diesel  
emissions and particulates - solvent extractables, aldehydes and  
sulfate methods.  
SAE Paper 840413.
- Perkins Technology Business, 1987.  
Personal communication.
- Perkins Technology Business, 1989.  
Personal communication.

- PETCH, G.S.; TRIER, C.J.; RHEAD, M.M.; FUSSEY, D.E.  
& MILLWARD, G.E. 1987.  
The development of a novel exhaust sampling technique with particular relevance to polycyclic aromatic hydrocarbons.  
In: Vehicle Emissions and Their Impact on European Air Quality, Proc. IMechE, C340/87.
- PETCH, G.S.; RHEAD, M.M. & FUSSEY, D.E. 1988.  
The use of radiolabelled polycyclic aromatic hydrocarbon fuel components to investigate diesel engine emissions.  
In: Combustion in Engines - Technology and Application. Proc. IMechE, C65/88.
- PITTS, J.N.Jr.; VAN CAUWENBERGHE, K.A.; GROSJEAN, D.; SCHMID, J.P.; FITZ, D.R.; BELSER, W.L. KNUDSEN, G.B. & HYNDS, P.M. 1978.  
Atmospheric reactions of polycyclic aromatic hydrocarbons: facile formation of mutagenic nitro-derivatives.  
Science, 202, p515-519.
- PLEE, S.L. & MACDONALD, J.S. 1980.  
Some mechanisms affecting the mass of diesel exhaust particulate collected following a dilution process.  
SAE Paper 800186.
- PRADO, G. & LAHAYE, J. 1983.  
Mechanisms of PAH formation and destruction in flames related to organic particulate matter.  
In: Rondia, D.; Cooke, M. & Haroz, R.K. (Eds). Mobile Source Emissions including Polycyclic Organic Species, D. Reidel Publishing Co. p259-276.
- PURI, B.R. 1970.  
In: Walker, P.L. (Ed), Chemistry and Physics of Carbon. vol 6, Marcel Dekker. p191-282.
- RIGBY, M.; SMITH, B.E.; WAKEHAM, W.A. & MAITLAND, G.C. 1986.  
The Forces Between Molecules.  
Clarendon Press. 252pp.
- ROBENS, E. 1980.  
Physical adsorption studies with the vacuum microbalance,  
In: Wolsky, S.P. Microweighing in vacuum controlled environments. Elsevier Scientific. 496pp.

- ROBBINS, W.K. & McELROY, F.C. 1982,  
Rational selection of sample preparation techniques for the  
measurement of polynuclear aromatics.  
In: Cooke, M.; Dennis, A.J. & Fisher, G.L. (Eds). PAH's Physical  
and Biological Chemistry.  
Academic Press, p673-686.
- ROSS. M.M., 1981.  
Physicochemical properties of diesel particulate matter.  
Ph.D Thesis. The Pennsylvania State University. 162pp.
- ROSS, M.M.; RISBY, T.H.; STEELE, W.A.; LESTZ, S.S. & YASBIN, R.E.  
1982.  
Physicochemical properties of diesel particulate matter.  
Colloids Surf., 5, p17-31.
- SCHUETZLE, D. 1983.  
Sampling of vehicle emissions for chemical analysis and  
biological testing.  
Environ. Health Perspect., 47, p65-80.
- SCHWARTZ, D.P. 1978.  
Glass wool as a potential source of artefacts in chromatography.  
J. Chrom., 152, p514-516.
- SEEBOLD, C.R.; GLASSON, D.R.; MILLWARD, G.E. & GRAHAM, M.A. 1989.  
Diesel particulate characterisation by vacuum microbalance  
techniques.  
In: Jayawerra, S.A.A. (Ed), 23rd International Vacuum Microbalance  
Techniques Conference,  
Thermochim. Acta., (In Press).  
Elsevier.
- SHAW, R.W.; DZUBAY, T.G. & STEVENS, R.K. 1979.  
The denuder difference experiment.  
EPA Report 600-2-79-051.
- SMITH, O.I. 1981.  
Fundamentals of soot formation in flames with application to  
diesel engine particulate emissions.  
Prog. Energy Combust. Sci., 7, p274-291.

- STENBERG, U.; ALSBERG, T. & WESTERHOLM, R. 1983.  
Applicability of a cryogradient technique for the enrichment of PAH from automobile exhausts: demonstration of methodology and evaluation experiments.  
Environ. Health Perspect., 47, p43-51.
- STENBURG, U. & ALSBERG, T. 1981.  
Vacuum sublimation and solvent extraction of polycyclic aromatic compounds adsorbed on carbonaceous materials.  
Anal. Chem., 53, p2967-2070.
- STEVENS, R.K. (Ed) 1979.  
Current methods to measure atmospheric nitric acid and nitrate artifacts.  
EPA Report 600-2-79-051.
- STOBER, W. 1987.  
On the health hazards of particulate diesel engine exhaust emissions.  
SAE Paper 871988.
- SVAROVSKY, L. 1981.  
Solid-liquid Separation. 2nd Edition.  
Butterworth. 364pp.
- TITLEY, J.G. 1988.  
The microstructures of estuarine particles.  
Ph.D. Thesis. Plymouth Polytechnic. 250pp.
- TOSAKA, S.; FUJIWARA, Y. & MURAYAMA, T. 1989.  
The effect of fuel properties on diesel engine exhaust particulate.  
SAE Paper 890421.
- TRIER, C.J.; PETCH, G.S.; RHEAD, G.S.; FUSSEY, D.E. & SHORE, P.R. 1987.  
Assessing the contribution of lubricating oil to diesel exhaust particulates using geochemical markers.  
In: Vehicle Emissions and Their Impact on European Air Quality.  
Proc. IMechE, C341/87.

- TRIER, C.J. 1988.  
The origins of the organic fraction in diesel exhaust emissions.  
Ph.D. Thesis, Plymouth Polytechnic. 171pp.
- TRIER, C.J.; FUSSEY, D.E.; PETCH, G.S.; & RHEAD, M.M. 1988.  
A comparison of diesel engine exhaust emissions collected by an  
EPA recommended dilution tunnel/filter with the sample from a new  
solvent scrubbing system.  
In: Combustion in Engines - Technology and Applications.  
Proc. IMechE, C64/88.
- VAN DELL, R.D. & BOGGS, G.U. 1987.  
Particulate associated partial combustion products of  
dichlorobenzene.  
Chemosphere, 16, p973-982.
- VAN den HUL, H.J. & LYKEMA, J. 1968.  
Determination of specific surface areas of dispersed materials of  
the negative adsorption method with some other methods.  
J. Amer. Chem. Soc., 90, p3010-3015.
- VOGEL, A.I. 1956  
A Textbook of Practical Organic Chemistry.  
3rd Edition, 412pp.
- VUK, C.T.; JONES, M.A.; JOHNSON, J.H. 1976.  
The measurement and analysis of the physical character of diesel  
particulate emissions.  
SAE Paper 760131.
- WALKER, E.A. 1979.  
Solvents: purity and purification .  
In: Egan, H.; Castegnaro, M; Bogovski, P.; Kunte, H.  
& Walker, E.A. (Eds).  
Environmental Carcinogens: Selected Methods of Analysis, vol 3,  
International Agency for Research on Cancer. p73-78.
- WALLER, E.A. 1986.  
The toxicity of diesel emissions.  
Warren Spring Laboratory Investigation of Air Pollution.  
Standing Conference of Co-operating Bodies, SCCB 106/5.
- WALL, J.C. & HOEKMAN, S.K. 1984.  
Fuel composition effects on heavy duty diesel particulate  
emission.  
SAE Paper 841364.



- WARNE, T.M. & HALDER, C.A. 1986.  
Toxicity of Lubricating Oils.  
J. Am. Soc. Lub. Engineers, 2, p97-103.
- WENDLANDT, W.W.M. 1986.  
Thermal Analysis. 3rd Edition.  
J. Wiley & Sons, 813pp.
- WERSBORG, B.L. 1975.  
Soot concentration and adsorption coefficient in a low-pressure flame.  
Combust. Flame, 24, p1-10.
- WILLIAMS, R.L. 1985.  
A review of sampling condition effects on polynuclear aromatic hydrocarbons from heavy duty diesel engines.  
SAE Paper 852081.
- WHATMAN, 1988.  
Filtration and Chromatography Catalog.  
Whatman LabSales Ltd.
- WHEELER, R.W. 1984  
Diesel exhaust emissions.  
In: Haddad, S. & Watson, N. Principles and Performance in Diesel Engineering.  
J. Wiley & Sons. p205-234.
- WOLFF, R.K.; HENDERSON, R.F.; SNIPES, M.B.; SUN, J.D.;  
BOND, J.A.; MITCHELL, C.E.; MAUDERLY, J.L.; McCLELLAN, R.O. 1986.  
Lung retention of diesel soot and associated compounds.  
In: Ishinishi, N.; Koizumi, A.; McClellan, R.O. & Stober, W.  
(Eds), Carcinogenic and Mutagenic Effects of Diesel Engine Exhaust, Proc. International Satellite Symposium on Toxicological Effects of Emissions from Diesel Engines.  
Elsevier Science Publishers, p199-211.
- YU, R.C.; WONG, V.W. & SHAHED, S.M. 1980.  
Sources of hydrocarbon emissions from direct injection diesel engines.  
SAE Paper 800048.
- ZITOMER, F. 1968.  
Thermogravimetric-mass spectrometric analysis.  
Anal. Chem., 40, p1091.

## APPENDIX I

### PUBLISHED WORK

During the period of registration a number of relevant scientific meetings were attended. A number of conference papers were also presented and three papers were published as listed below:

GLASSON, D.R.; SEEBOLD, C.R.; HORN, N.J. & MILLWARD, G.E. 1988.  
The microstructures of carbon soots from diesel engine exhausts.  
In: McEnaney, B. & Mays, T.J. (eds), Proc. Conf. (Int.) Carbon.  
Institute of Physics, 34-36.  
IOP Publishing Ltd.

SEEBOLD, C.R.; GLASSON, D.R.; MILLWARD, G.E. & GRAHAM, M.A. 1989.  
Diesel particulate characterisation by vacuum microbalance techniques.  
In: Jayawerra, S.A.A. (ed), 23rd International Vacuum  
Microbalance Techniques Conference, (In Press).

SEEBOLD, C.R.; GLASSON, D.R.; MILLWARD, G.E. & GRAHAM, M.A. 1989.  
E.G.A. of diesel engine exhaust particles.  
In: Applications of Evolved Gas Analysis.  
Thermal Methods Group of the Royal Society of Chemistry,  
(In Press).

## THE MICROSTRUCTURES OF CARBON SOOTS FROM DIESEL ENGINE EXHAUSTS

Douglas R. Glasson, Christopher Seebold\*, Nicholas J. Horn\* and Geoffrey E. Millward\*\*

Department of Environmental Science, Plymouth Polytechnic, Plymouth PL4 8AA

\* Department of Mechanical Engineering, Plymouth Polytechnic

\*\*Institute of Marine Studies, Plymouth Polytechnic.

Key Words: Microstructure, Carbon soots, Diesel engine.

### 1. INTRODUCTION

Diesel particles (DP) and unburnt hydrocarbons (UHC) are the emission products of diesel engine combustion, which is controlled by air/fuel ratio (AFR) and engine stoichiometry. High AFR (from low load on engine) results in fuel "lean" combustion, giving high UHC and low soot emissions. Low AFR (at high engine loads) gives fuel "rich" combustion with low UHC and high soot emissions.

DP consist of carbonaceous particles with a density of 1600-2000 kg/m<sup>3</sup>. The microstructure is thought to be composed of 10<sup>6</sup> turbostratically arranged crystallites, each having 2-5 platelets of carbon atoms in a hexagonal face-centred array (1). The formation mechanism of DP is poorly understood but consists of overlapping stages:- Pyrolysis, nucleation, surface growth, aggregation (2). The amount of soot formed in a combustion system is usually very small compared to the total carbon of the fuel.

UHC is composed of unburnt fuel and lubricating oil, which as the exhaust temperature declines may condense or adsorb on the DP. Condensation is favoured in low dilution ratio environments with low filter temperatures and high hydrocarbon concentrations and only likely with lubricating oil. Adsorption is the adherence of UHC to DP by either chemical or physical (van der Waal) forces (3). Adsorption has been found to be the most dominant exhaust process (4-6). Adsorbed UHC may amount to 75 wt-% of DP.

In the present research, the physico-chemical relationship between DP and UHC has been studied and the effect of UHC adsorption on DP microstructure.

### 2. EXPERIMENTAL

The engine used was a Ricardo E6/T with Comet Mk V IDI head and a compression ratio of 22:1. Before each sampling session it was pre-conditioned and then stabilised to the required engine state. The filter unit was preheated by the exhaust gas and a pre-extracted by ultrasonication (5 min) in dichloromethane (DCM) to remove buried soot from the filters. Electron micrographs were taken of the fresh soot-laden filters. Specific surface area (SSA) and porosity were determined by a gravimetric BET nitrogen gas sorption technique (7). Then thermal degassing of the soots was undertaken in vacuo at 350°C (90 min) to remove adsorbed UHC, before the SSA was redetermined. The engine was run at 1500 and 1750 rpm speed (13.4 and 27.9 Nm load) and filters were taken at two positions down in the exhaust:- CLOSE (30 cm) and FAR (230 cm) from engine.

### 3. RESULTS AND DISCUSSION

The filter loading of UHC and DP reflected the classical AFR relationship:-  
 High AFR causes high UHC and low soot (Fuel "lean" at low loads)  
 Low AFR causes low UHC and high soot (Fuel "rich" at high loads).  
 As Table 1 shows, the mean particle diameter was greater at high loads when more soot was produced. Additionally, the higher speed gave smaller particles probably because of higher temperatures enhancing carbon oxidation after initial formation. However, the SSA of these soots do not

Table 1 Particle Size and Specific Surface Area against Engine Condition.

ENGINE CONDITION		FILTER POSITION CLOSE	
Speed	Load	Particle Size (E.N. nm)	Specific Surface Area (SSA m <sup>2</sup> /g)
1500rpm	13.7Nm	10.2nm	66.6m <sup>2</sup> /g
	27.4Nm	11.7nm	113m <sup>2</sup> /g
1750rpm	14.2Nm	9.1nm	64m <sup>2</sup> /g
	27.9Nm	10.4nm	84.7m <sup>2</sup> /g

Particle Size from mean diameters of 20 samples

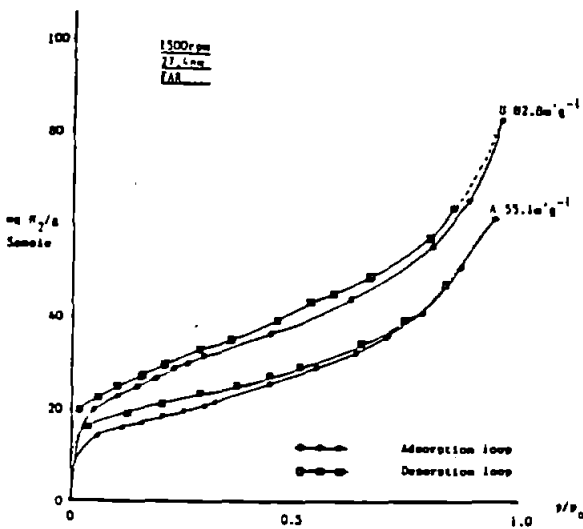
Table 2 SSA Data and Exhaust Temperature against Engine Condition and Filter Position.

ENGINE CONDITION		FILTER POSITION	
Speed	Load	Close	Far
		A / B	A / B
1500rpm	13.7Nm	51.4 / 66.6 (+23%) (130°C)	70.5 / 106.3 (+34%) (100°C)
	27.4Nm	103.5 / 113 (+8%) (335°C)	55.1 / 82.8 (+33%) (150°C)
1750rpm	14.2Nm	47.3 / 64 (+26%) (190°C)	46.5 / 80.3 (+42%) (145°C)
	27.9Nm	80.6 / 84.7 (+5%) (340°C)	99 / 110 (+10%) (260°C)

Extra Sample (Brushed, Unextracted)

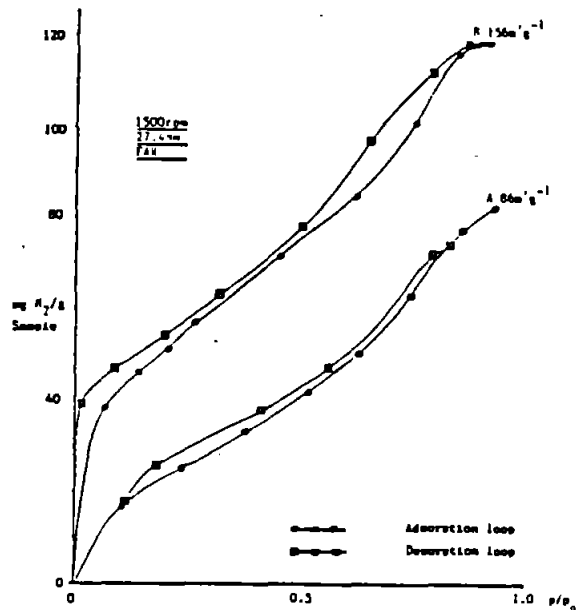
1500rpm	27.4Nm	86 / 156 (+44%) (150°C)
---------	--------	----------------------------

SSA data in m<sup>2</sup>g<sup>-1</sup>  
 'A' refers to normal SSA Determination data.  
 'B' refers to Thermal Outgassed SSA data.  
 Temperature of Exhaust Gas in Parenthesis.



Particles Extracted by UDCM from Feilflex Filters

Fig 1



Particles Extracted by Brushing from Feilflex Filters

Fig 2

Hysteresis Loops for Diesel Soots collected and extracted by UDCM and Brushed methods.

'A' refers to normal SSA data.

'B' refers to Thermal Outgassed SSA data.

# DIESEL PARTICULATE CHARACTERISATION BY VACUUM MICROBALANCE TECHNIQUES

C.R. SEEBOLD<sup>1</sup>, D.R. GLASSON<sup>2</sup>, G.E. MILLWARD<sup>3</sup> and M.A. GRAHAM<sup>4</sup>.

<sup>1</sup>Department of Mechanical Engineering.

<sup>2</sup>Department of Environmental Sciences.

<sup>3</sup>Institute of Marine Studies.

Polytechnic South-West, Plymouth, Devon, PL4 8AA, U.K.

<sup>4</sup>Perkins Technology Business, Peterborough, Cambridgeshire, PE1 5NA, U.K.

## SUMMARY

The physical and chemical character of Diesel Particulate (DP) has been determined. Electron Microscopy (EM) and a gravimetric BET method (BET) determined particle size and specific surface area (SSA). Two different diesel engine types (direct injection (DI) and indirect injection (IDI)) were run at similar operating conditions and DP collected by filtration of the exhaust gas at temperature without dilution.

An in-vacuo gravimetric thermal degassing (TD) apparatus has been constructed to extract adsorbed hydrocarbon volatiles from the DP, during a slow heating program. The desorbed volatiles were trapped and analysed by gas chromatography (GC). The carbons were fuel and oil derived unburnt hydrocarbons (UHC), trapped within the slit-shaped micropores and 'ink-bottle' shaped mesopores/surface of the aggregated diesel particles.

## INTRODUCTION

Diesel engine combustion produces emission products, which include partially pyrolysed or unburnt hydrocarbons (UHC) which may adsorb onto diesel particulate (DP) which is co-formed. The UHC include some potentially carcinogenic hydrocarbon species (eg polyaromatic hydrocarbons (PAH's))(1). The physico-chemical interaction between DP and UHC was studied, so that engine manufacturers, environmental scientists and emission legislators might further understand exhaust processes and assess health risks.

The character of DP and UHC has been reported previously (2). DP are carbonaceous particles, varying in size from 5 to 100nm in diameter (for incipient to aggregated particles) and possess a complex microporous and aggregate structure. UHC adsorption during formation depends on engine load. Low engine load produces 'fuel rich' conditions and the DP formed is 'saturated' with UHC trapped in the slit-shaped micropores (<2nm diameter) thus giving soots of low SSA (<20m<sup>2</sup>/g). High load conditions, have high DP production and 'fuel lean' conditions and therefore less UHC is trapped in the micropores and SSA values are higher (upto 100m<sup>2</sup>/g). In the exhaust, temperature controls UHC adsorption to the 'ink-bottle' mesopores (2-50nm diameter) and macropore/surface (>50nm). This UHC adsorption only slightly decreases SSA but enlarges particle size and

encourages particle aggregation to form large fluffy structures (3). The UHC collected by the filter, at temperature and extracted by any method is termed filter extracted sample (FES).

A previous study (2) identified the exhaust process, termed temperature dependent chemical scavenging (TDCS) and examined how DP SSA varies between engine conditions, for ultrasonicated soots. These were then subjected to TD which desorbed the FES, opened the pores and increased SSA. Unfortunately, the volatiles could not be collected. Thus an in-vacuo evolved gas analysis (EGA) system has been constructed to trap the desorbing FES for analysis by gas chromatography. This method offers the advantages of a fast solvent-free extraction without fibre contamination (4).

## EXPERIMENTAL

The engines used were a single cylinder Ricardo E6/T with Comet Mk 5 IDI head (compression ratio 22:1, cylinder volume 0.5l) and a pre-production four cylinder Ford DI (compression ratio 19:1, cylinder volume 2.5l) engine. The engines were preconditioned for 1 hour (full speed and load) before being stabilised to the required engine state of 1500rpm and full load (27.4Nm and 84.2Nm respectively). Filter samples were taken at 3.3m down an exhaust of 4.2cm I.D. DP, filtered using a specifically designed unit was collected on Pallflex TX-40, teflon/borosilicate glass fibre filters. The mass loading was determined by the filter weight gain measured after equilibration in an humidity box (Rh 60%). The exhaust gas volume of the DI engine limited the filter to  $\frac{3}{4}$  full exhaust flow.

Electron micrographs were taken of the fresh DP. Specific surface area (SSA) and pore character were determined on-filter by a gravimetric BET  $N_2$  adsorption technique (5). The TD apparatus (Fig. 1.) degassed DP on-filter. A CI Electronics Mk II balance head used for the BET method, was adapted to accept a glass sample envelope (with Pt/Rh 13% thermocouple to monitor temperature), around which a heating furnace could be raised. The filter sample was suspended, and a cold trap filled to be within 4cm of the sample. The apparatus was evacuated to 1mm Hg pressure to remove those volatiles with an appreciable vapour pressure at room temperature (mainly water). Liquid  $N_2$  was added to the cold trap dewar and the temperature program initiated (approx 5°C/min to 320°C). Weight and temperature changes were recorded on a coupled chart recorder. Samples could be degassed at preset temperatures, the volatiles collected and microstructure re-examined.

A Carlo Erba HRGC 5360 equipped with cold on-column injection and an FID, was employed to analyse the volatiles removed from the trap with dichloromethane (DCM). The DCM soluble FES was reduced in volume (rotary evaporation, 30°C) and transferred quantitatively to a preweighed vial (1.75ml) and  $N_2$  used to blow down

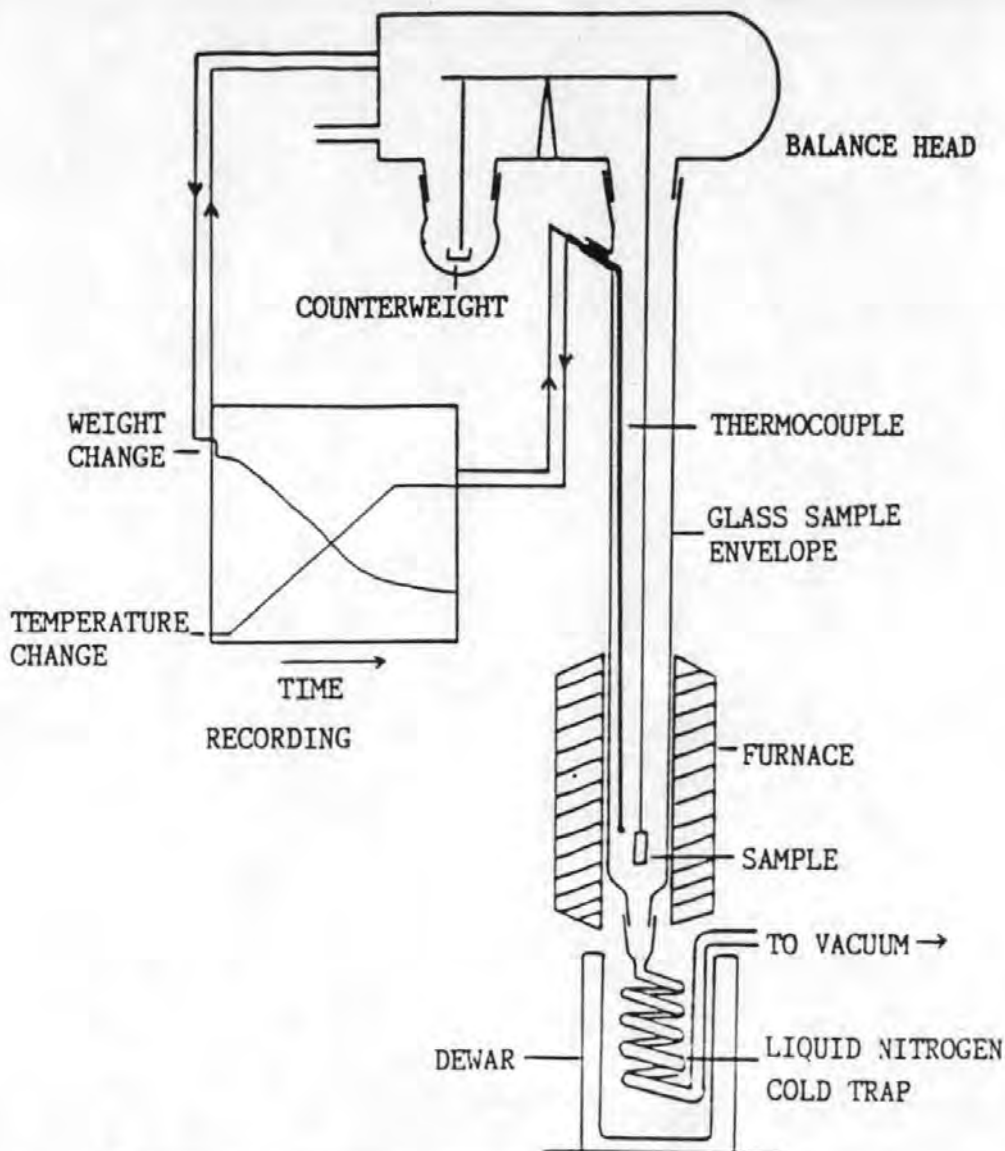


Fig. 1. The Thermal Degassing Apparatus for Extracting Volatile FES from Diesel Particulate (DP). The Apparatus was Operated at 1mm Hg Pressure and Samples were Thermally Degassed (TD) to 320°C.

to dryness, thereby giving a dry FES mass. Injection volume was 0.1ul and sample concentration 10mg/ml.

## RESULTS AND DISCUSSION

### 1. Filtration and Filter Influences.

During this investigation, we attempted to obtain for all engine conditions, a DP mass loading sufficient for mechanical removal from the filter. With the exception of the sample in Fig. 2, which was an over-fuelled, high load sample (thus giving exceptional DP production), this was found to be impossible. This was due to filter matrix burial and low DP mass loadings, so therefore on-filter techniques were developed.

Fig. 2, shows a DP structure which is characteristic of a non-compacted exhaust soot, showing a cross between an IUPAC Type II and Type IV isotherm (6), suggesting a semi-porous solid. The hysteresis profile is largely H3, typical of slit-shaped platelet microstructure, but with some H1 influence ( $>0.3P/P_0$ ).

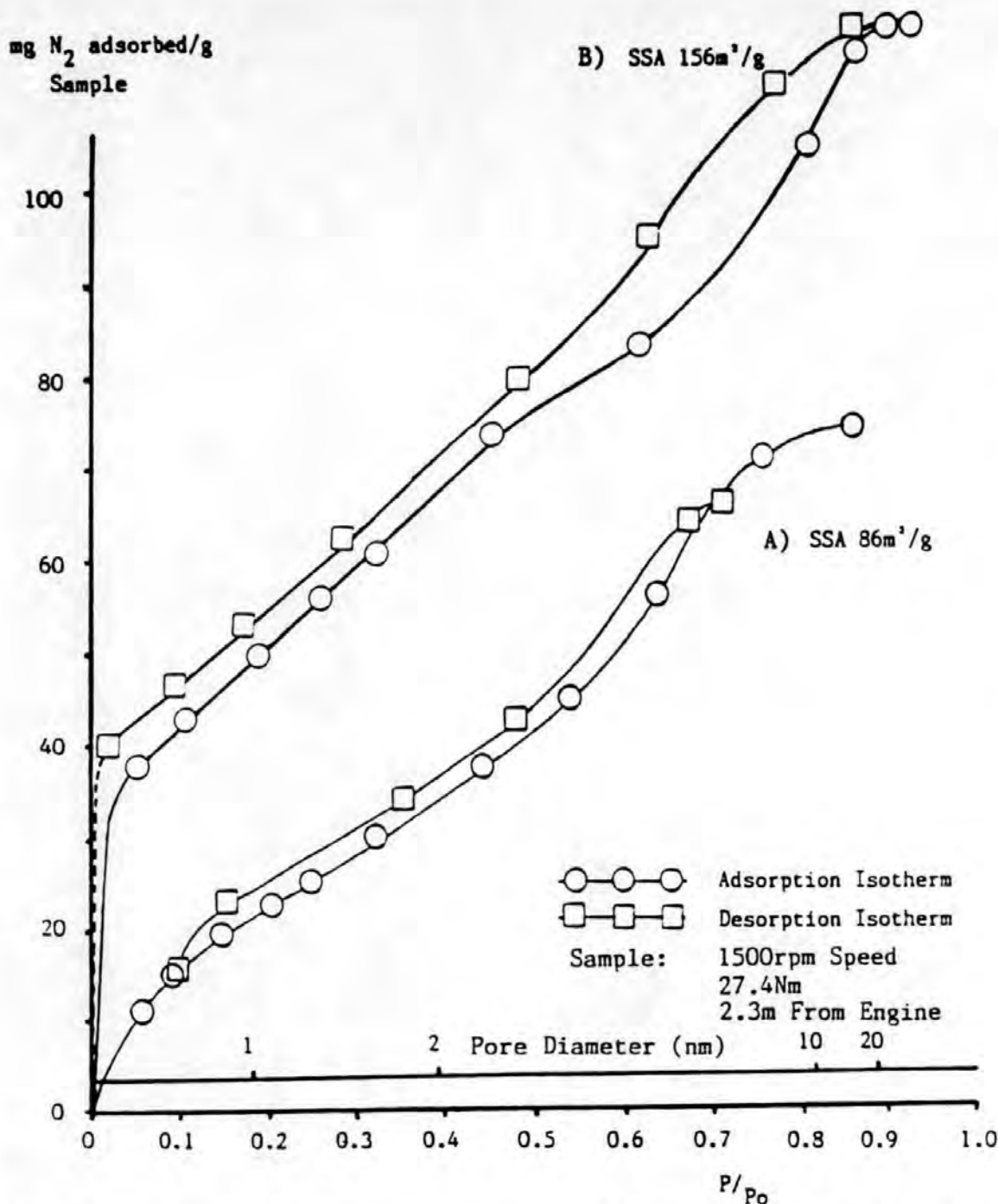


Fig. 2. Adsorption/Desorption Isotherms and Hysteresis Loops of a DP Brushed from a Filter Exposed to the Exhaust of the Ricardo IDI Engine. The Figure shows the sample Before 'A' and After 'B' Thermal Degassing.

This suggested that the aggregate particles produced 'ink-bottle' pores between them. The EM particle size analysis showed a mean particle size distribution of 30–40nm which nearly correlated with the HI point of influence ( $>0.93 P/P_0$ ). TD opened the micropores ( $<1\text{nm}$ ) and mesopores ( $>8\text{nm}$ ) with the SSA increased from  $86\text{m}^2/\text{g}$  to  $156\text{m}^2/\text{g}$ . Unfortunately, this sample was analysed before the trapping system had been developed and no FES was collected.

The mass and density of buried DP and filter must be accounted for in the assessment of SSA. The SSA value, calculated using the BET method (5) and used



for carbons by Carter (7), was corrected using Equation 1, assuming a filter x-ray density of 2.08g/cm<sup>3</sup> and a filter SSA of 2.47m<sup>2</sup>/g ±5%.

$$DP\ SSA = \frac{S_1 - (S_2 \cdot M_2)}{M_1} \quad (1)$$

where S<sub>1</sub> is the SSA value calculated from the BET equation.

S<sub>2</sub> is the SSA of the filter (2.24m<sup>2</sup>/g).

M<sub>1</sub> is the particulate dry mass divided by dry sample mass.

M<sub>2</sub> is the filter dry mass divided by dry sample mass.

Sample mass is the sum of filter and DP mass.

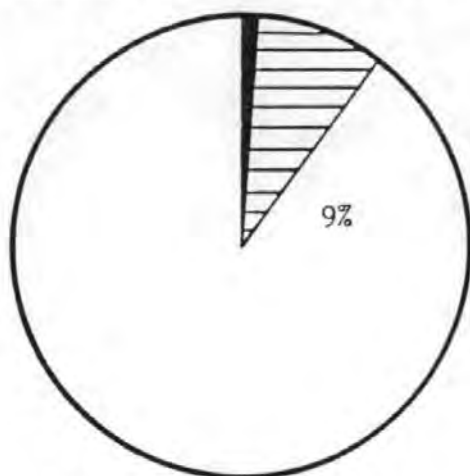
The filter showed hysteresis in all pore ranges. The influence of this on DP isotherms was to 'flatten' the isotherm profile and to give a permanent open microstructure; thus on-filter samples never show micropore closure, even when significant soot was present and microporous gain was noted.

## 2. Compositional Analysis of DP On-Filter

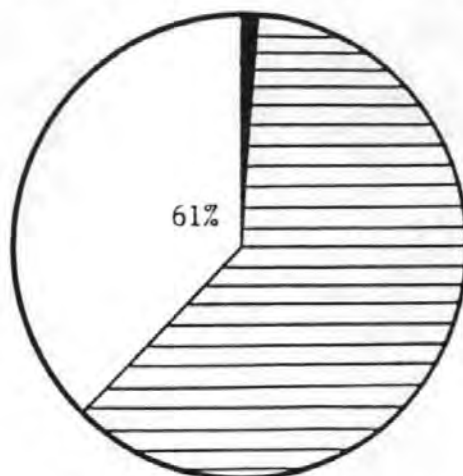
DP, from the two engines showed characteristic differences (Fig. 3.). The influence of engine type on DP emission but not UHC output (8). The IDI engine produced high DP emissions due to its relatively inefficient design and prechamber 'fuel rich' combustion. Thus FES represented 9% of DP

RICARDO IDI ENGINE - 1 CYLINDER

FORD DI ENGINE - 4 CYLINDERS



0.55mg/sec DP Mass Emission  
(Whole Exhaust)  
SSA 109m<sup>2</sup>/g → 147m<sup>2</sup>/g



0.29mg/sec DP Mass Emission  
(75% Split Flow Exhaust)  
SSA 1m<sup>2</sup>/g → 110m<sup>2</sup>/g

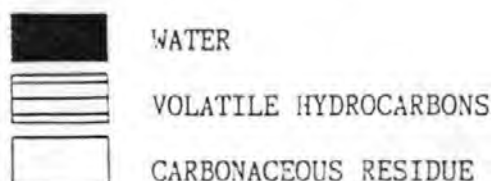


Fig 3. Pie Graphs of Composition of DP Collected from the Exhausts of the two Engines. Also shown is the Specific Surface Area (SSA) before and after Thermal Degassing (TD).

mass and gave an initial SSA of 109m<sup>2</sup>/g. The DI engine produced less DP from its four cylinders, as one would expect from a modern DI engine but had low SSA (1m<sup>2</sup>/g) and 61% FES of DP mass. This was higher than expected, reflecting that the SSA of the DP was more suppressed when the low DP mass adsorbed the high quantity of UHC present.

### 3. EGA and Microstructural Characterisation of DP On-Filter.

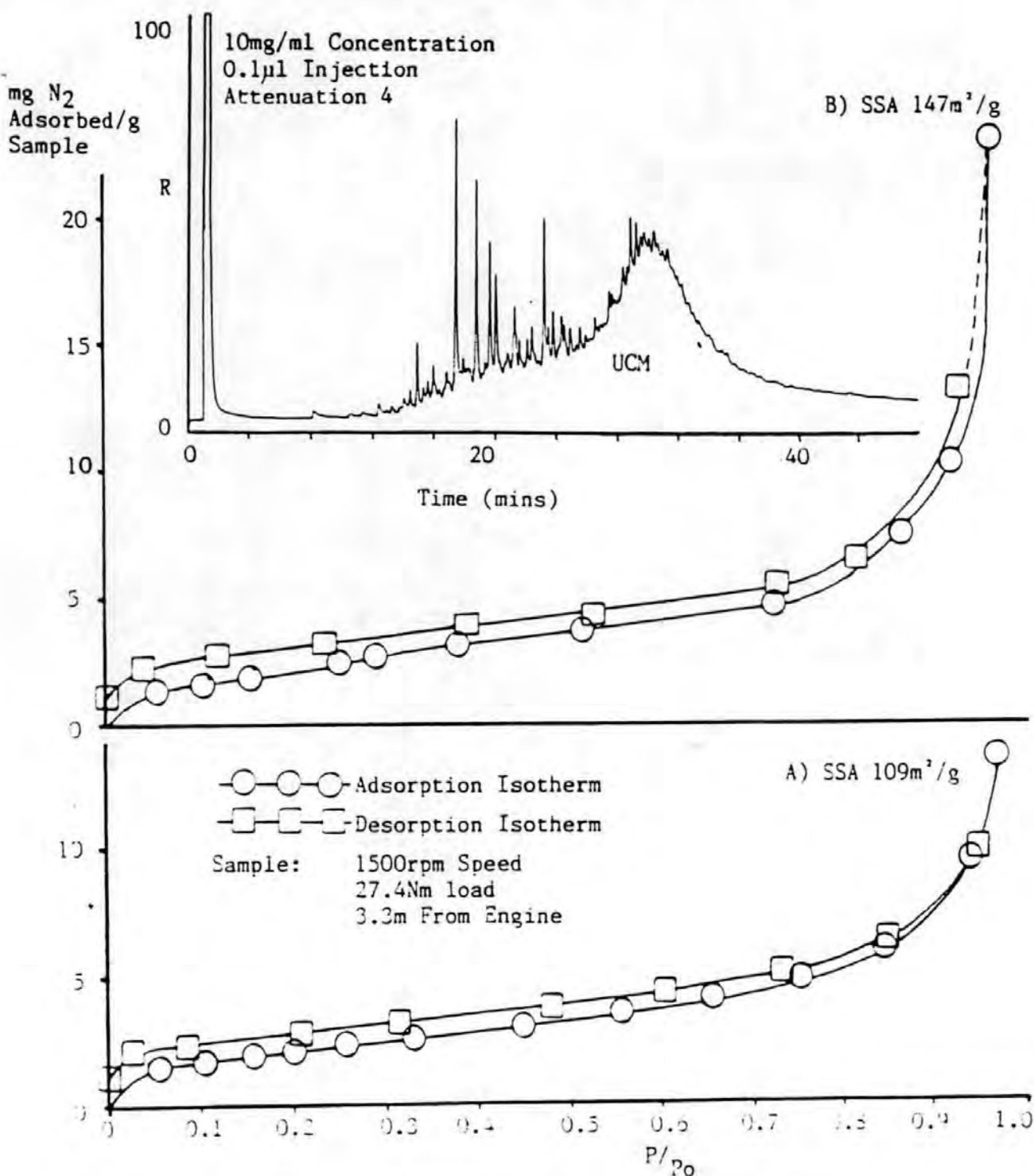


Fig. 4. Adsorption/Desorption Isotherms and Hysteresis Loops of a DP Collected from the Exhaust of the Ricardo IDI Engine. The Figure shows the Chromatogram of the Volatile FES and the Microstructure Before 'A' and After 'B' Thermal Degassing.

The microstructure, before 'A' and after 'B' TD, and degassed volatile FES chromatograms are shown in Fig. 4 and 5, for the IDI and DI engines respectively. Both samples showed H3 slit-shaped pore character (modified by filter hysteresis with a 'flatter' profile and no closed micropores), but no H1 influence because compaction and filter burial had destroyed the 'open' agglomerate structure. TD of DP, opened the pores with a gain in SSA, greatest for the DI sample

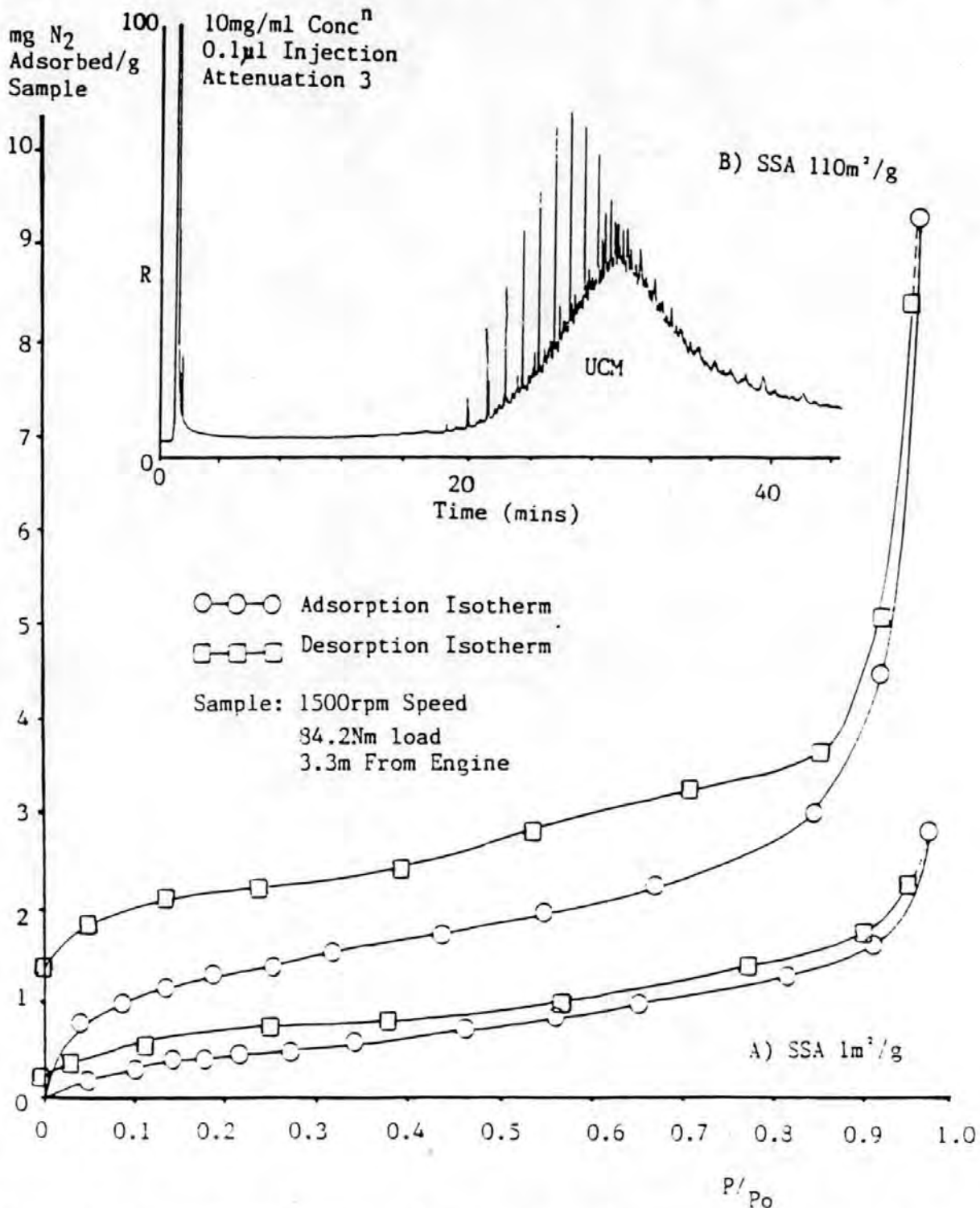


Fig. 5. Adsorption/Desorption Isotherms and Hysteresis Loops of a DP Collected from the Exhaust of the Ford DI Engine. The Figure shows the Chromatogram of the Volatile FES and the Microstructure Before 'A' and After 'B' Thermal Degassing.

because of its high FES content. Analysis of the chromatograms showed that both samples contained an unknown complex mixture (UCM) of branched hydrocarbons and polar compounds, which correlated with the retention time of lubricating oil. An n-alkane series of peaks was also evident (identified by co-injection of standards) which corresponded to the higher molecular weight hydrocarbons left after combustion of the fuel.

## CONCLUSIONS

The vacuum microbalance techniques is advantageous over conventional carrier gas methods by more efficiently removing higher boiling point UHC quantitatively at lower temperatures. This reduces the possibility of decomposing the volatiles and changes of the DP through microstructural thermal swelling. The technique also permits determination of the changes in surface area and porosity of the DP on progressive removal of volatiles.

## REFERENCES

- 1 F.S-C. Lee and D. Schuetzle, The Sampling, Extraction, and Analysis of Polycyclic Aromatic Hydrocarbons from Internal Combustion Engines, in: A. Bjorseth (Ed.), Handbook of Polycyclic Aromatic Hydrocarbons, Marcel Dekker Inc, 1983.
- 2 D.R. Glasson, C.R. Seebold, N.J. Horn and G.E. Millward, The Microstructures of Carbon Soots from Diesel Engine Exhausts, Proc. Int. Conf. Carbon, Newcastle upon Tyne, U.K. 1988.
- 3 C.R. Seebold, PhD. Thesis, The Interaction between UHC and DP in Diesel Exhausts, Polytechnic South-West, Plymouth, Devon, PL4 8AA. U.K. 1989.
- 4 V. Stenburg and T. Alsberg, Vacuum Sublimation and Solvent Extraction of Polycyclic Aromatic Compounds Adsorbed on Carbonaceous Materials. Anal. Chem. 53, 2067-2072, 1981.
- 5 D.R. Glasson, Production of Active Solids by Thermal Decomposition, Part 8, J.chem. Soc. 1506-1510, 1956.
- 6 S.J. Gregg and K.S.W. Sing, Adsorption, Surface Area and Porosity, Academic Press, London, 1982.
- 7 M.A. Carter, PhD Thesis, Carbon and Coke Reactivity in Zinc-Lead Blast Furnace Practice, Plymouth Polytechnic, Plymouth, Devon, U.K. 1983.
- 8 L.R.C. Lilly, Diesel Engine Reference Book, Butterworths, London, 1984.

## EGA OF DIESEL ENGINE EXHAUST PARTICLES

C.R. SEEBOLD<sup>1</sup>, D.R. GLASSON<sup>2</sup>, G.E. MILLWARD<sup>3</sup> and M.A. GRAHAM<sup>4</sup>.

<sup>1</sup>Department of Mechanical Engineering.

<sup>2</sup>Department of Environmental Sciences.

<sup>3</sup>Institute of Marine Studies.

Polytechnic South-West, Plymouth, Devon, PL4 8AA, U.K.

<sup>4</sup>Perkins Technology Business.

Peterborough, Cambridgeshire, PE1 5NA, U.K.

### Key Words:

Evolved Gas Analysis, Diesel Particles, GC, BET, Adsorption.

### INTRODUCTION.

Diesel engine combustion produces emission products, which include partially pyrolysed or unburnt hydrocarbons (UHC) which are found adsorbed onto diesel particles (DP) which are co-formed. The UHC include some potentially carcinogenic hydrocarbon species (e.g. polyaromatic hydrocarbons (PAH's))(1). The physico-chemical interaction between DP and UHC was studied, so that engine manufacturers, environmental scientists and emission legislators might further understand combustion and exhaust processes to assess potential health risks.

The character of DP and UHC has been reported previously (2,3). DP are carbonaceous aggregates, which possess a complex microstructure (similar to graphite) and a high specific surface area (SSA). The relative quantities of UHC and DP depend on

engine condition which control in-cylinder combustion temperatures. Low engine load produces 'fuel rich' conditions and the DP formed is 'saturated' with UHC trapped in slit-shaped micropores (<2nm diameter) thus giving soots of low SSA (<20m<sup>2</sup>/g). High load conditions, have high DP production and 'fuel lean' combustion, and therefore less UHC are trapped and SSA values are higher (upto 100m<sup>2</sup>/g). A previous study (2) identified the exhaust process, termed temperature dependent chemical scavenging (TDCS), when UHC adsorbs and/or condenses to the 'ink-bottle' mesopores of 2-50nm diameter (formed between particles) and onto the soot surface. TDCS slightly decreases SSA and enlarges particle size, encouraging particle aggregation and the formation of large fluffly soot structures.

## EXPERIMENTAL

The experimental details of the engine and sample collection process have been reported previously (3,5). The exhaust filtration method produces a soot laden filter from which a filter extractable sample (FES) may be extracted. Specific surface area (SSA) and pore character were determined on-filter by a gravimetric BET N<sub>2</sub> adsorption technique (4). The SSA of the collected soot was deduced after allowing for the SSA of the filter (5). The BET apparatus was adapted for evolved gas analysis (EGA) of the thermally extracted volatiles, with

analysis by gas chromatography. Fig. 1. shows the thermal degassing apparatus which efficiently (<95%) extracted high molecular mass volatiles at low pressure (1mm Hg) and at temperatures <340°C. This apparatus was advantageous over nitrogen gas flow methods because it reduced the potential for volatile condensation during transfer to the trap, minimised buoyancy and gas vibration problems and reduced the potential for thermal changes in the solid matrix. This paper describes a set of experiments when a low load diesel soot sample was progressively degassed at successively higher temperatures in vacuo, with the changes in microstructure and SSA compared with the released volatiles. The sample was successively heated at 120, 190, 290 and 340°C, and each volatile fraction collected. The SSA and pore character was determined before and after each heating stage. This technique was also compared to standard methods of UHC extraction: ultrasonication and soxhlet extraction (6).

## RESULTS AND DISCUSSION

### 1. SEQUENTIAL DEGASSING OF DIESEL SOOT

The sample (Fig. 2.) initially showed a low surface area (<7.5m<sup>2</sup>/g) because the UHC were blocking the pores of the soot matrix. The soot had blocked upper mesopores (>8nm pore diameter) which unblocked when degassed, releasing a range of

weakly adsorbed hydrocarbons and increasing the SSA by  $8\text{m}^2/\text{g}$ . Further degassing (to  $190^\circ\text{C}$ ) released a significant quantity of high molecular mass volatiles (which corresponded to the lubricating oil retention window, 24-38minutes) producing a significant gain in SSA (to  $43\text{m}^2/\text{g}$ ) and all pore ranges were seen to open. At  $290^\circ\text{C}$  (Fig. 3.), significantly more oil derived hydrocarbons were released, as the pores continued to release high molecular mass hydrocarbons but with only a small SSA increase (to  $54\text{m}^2/\text{g}$ ). At  $340^\circ\text{C}$  (Fig. 4.), the structure of the DP began to change as the last volatiles are released. The SSA increased to  $519\text{m}^2/\text{g}$ , as the micropores released highly adsorbed low molecular mass hydrocarbons which corresponded with the fuel retention window (8-24minutes).

The fuel species were presumably trapped during the initial formation of the crystallite layers and tightly held by the overlapping van der Waal field's. Oil appeared to be more weakly adsorbed in larger pores trapped after soot formation in mesopores and on the particle surface and this may be strongly linked to the process of TDCS.

## 2. COMPARISON BETWEEN EXTRACTION METHODS

Thermal degassing (TD) (2hrs) was compared to the standard solvent extraction techniques of soxhlet (24hrs) and ultrasonication (0.5hrs) (dichloromethane (DCM), 150ml). Changes in microstructure, SSA and FES were noted and full details have



been reported (3). The isotherms were all similar.

Table 1. and Fig. 5. illustrate how the extraction technique affects the soots and their composition. In the solvent methods, DCM molecules penetrated the pores, extracting the weakly-bound mesoporous/surface UHC but not the highly adsorbed microporous hydrocarbons. The DCM did however, become permanently adsorbed and reduced the SSA by 17-24m<sup>2</sup>/g. The more energetic ultrasonication method enabled DCM molecules to penetrate more deeply and reduce the SSA to 74m<sup>2</sup>/g. The soots pre-extracted by the solvent methods were then re-extracted by thermal degassing, and further volatiles were released. The chromatograms revealed the release of straight-chain n-alkane species presumably highly adsorbed in the slit-shaped micropores. The release of highly adsorbed FES also results in a dramatic gain in SSA to the values reported in Table 1, as the DCM and FES is released.

The thermally degassed control sample gave poor results. The initial SSA after the first extraction was only slightly higher (it was expected to be around 150m<sup>2</sup>/g) than the starting SSA, despite a definite release of volatiles. Further degassing released fuel molecules from the micropores but the SSA declined. This was determined to due to reordering of the lattice microstructure after removal of all FES.

The FES chromatograms showed the effectiveness of each method with TD being the most efficient extracting both fuel and

oil-derived hydrocarbon species from all pore ranges. The solvent methods were less efficient (only 85% by mass for this sample) and the solvent was permanently adsorbed within the micropores, reducing SSA.

#### SUMMARY.

An EGA technique was employed to study the interaction between diesel particles (DP) and unburnt hydrocarbons (UHC) in a diesel exhaust. A gravimetric BET method for specific surface area was used before and after thermal degassing, in a vacuum microbalance system, at preset temperatures to simulate the exhaust system. Desorbed volatile UHC were trapped and analysed by gas chromatography.

Characterisation of UHC showed them to be derived from fuel and lubricating oil from within the cylinder. Two UHC fractions existed; a largely fuel-derived microporous-bound fraction, trapped during DP growth, and a meso-porous fuel/oil-derived fraction presumably adsorbed after DP formation. TD proved more efficient for the extraction of FES than standard ultrasonic or soxhlet methods.

## REFERENCES.

- 1) LEE, F.S-C, & SCHUETZLE, D. 1983. Sampling, extraction and analysis of polycyclic aromatic hydrocarbons from internal combustion engines.  
In: Bjorseth, A. (ed). Handbook of Polycyclic Aromatic Hydrocarbons. Academic Press, p27-94.
- 2) GLASSON, D.R.; SEEBOLD, C.R.; HORN, N.J. & MILLWARD, G.E. 1988. The microstructures of carbon soots from diesel engine exhausts. In: McEnaney, B. & Mays, T.J. (eds), Proc. Conf. (Int.) Carbon. Institute of Physics.  
IOP Publishing Ltd. p31-34.
- 3) SEEBOLD, C.R. 1989. The interaction between UHC and soot in diesel exhausts. Ph.D. Thesis. Polytechnic South-West. pp250
- 4) GLASSON, D.R. 1956. Production of active soids by thermal decomposition, Part 8, J. Chem. Soc. 1506-1510.
- 5) SEEBOLD, C.R.; GLASSON, D.R.; MILLWARD, G.E. & GRAHAM, M.A. 1989. Diesel particulate characterisation by vacuum microbalance techniques.  
In: Jayawerra, S.A.A. (ed), 23rd International Vacuum Microbalance Techniques Conference, (in Press).
- 6) GRIEST, W.H. & CATON, J.E. 1983. Extraction of polycyclic aromatic hydrocarbons for quantitative analysis.  
In: Bjorseth, A. (ed). Handbook of Polycyclic Aromatic Hydrocarbons.  
Academic Press. p95-135.

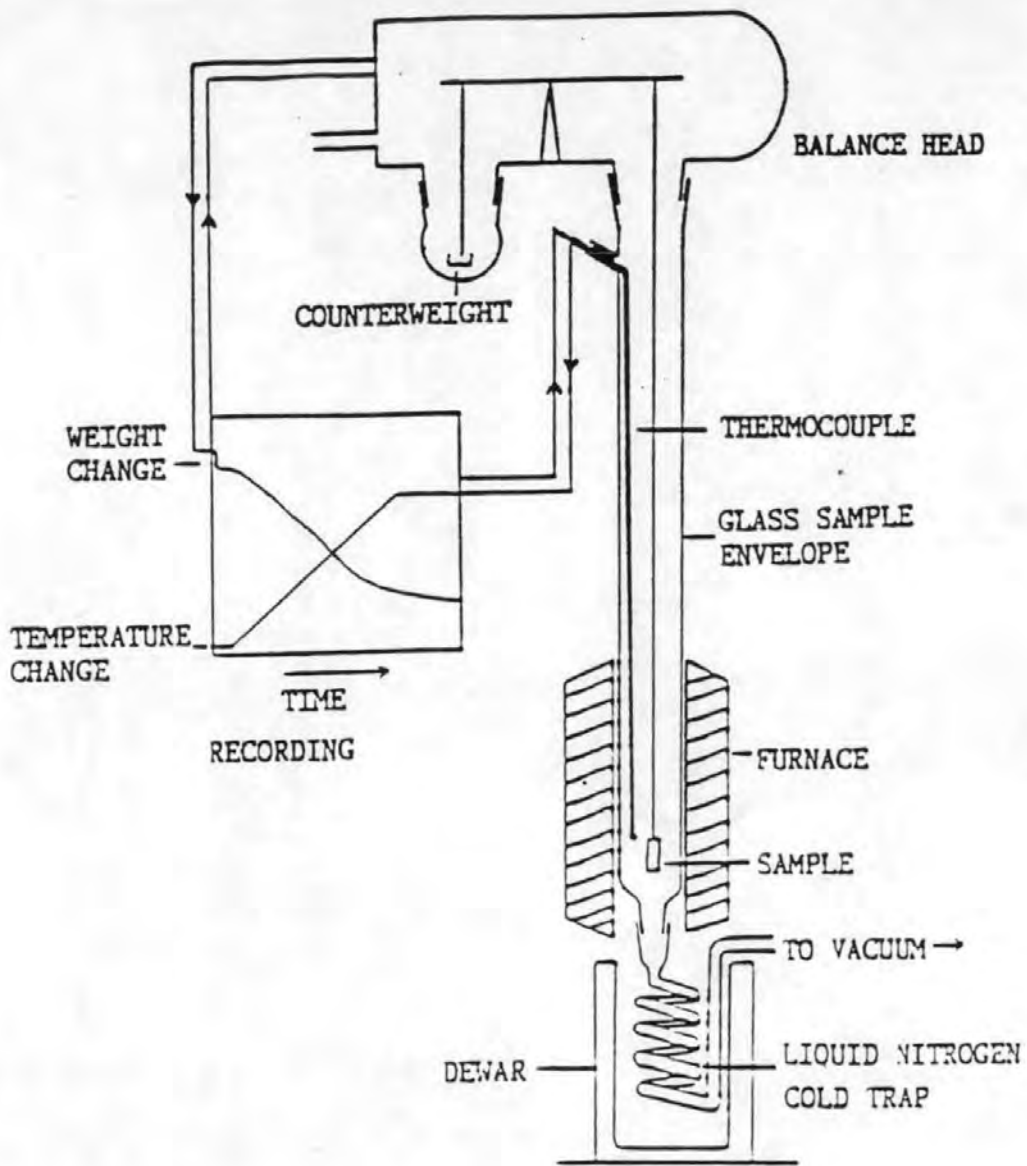


Fig. 1. The Thermal Degassing Apparatus for Extraction of Volatile Hydrocarbons from Diesel Soots.  
 Operating Conditions: 1mm Hg Pressure  
 340°C Maximum Temperature

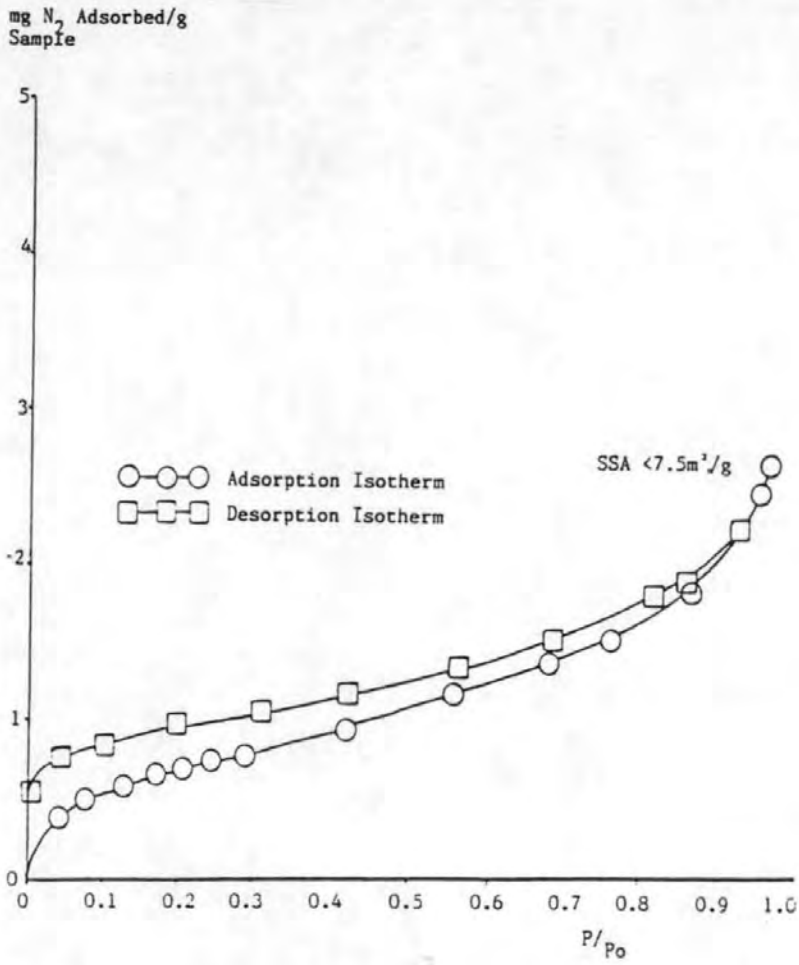


Fig. 2. Adsorption/Desorption Isotherm of a Diesel Particulate Sample Analysed On-Filter.  
 Sample: 1500r/min Engine Speed  
 13.7Nm Engine Load  
 Sampled 3.3m from Engine  
 SSA 7.5m<sup>2</sup>/g

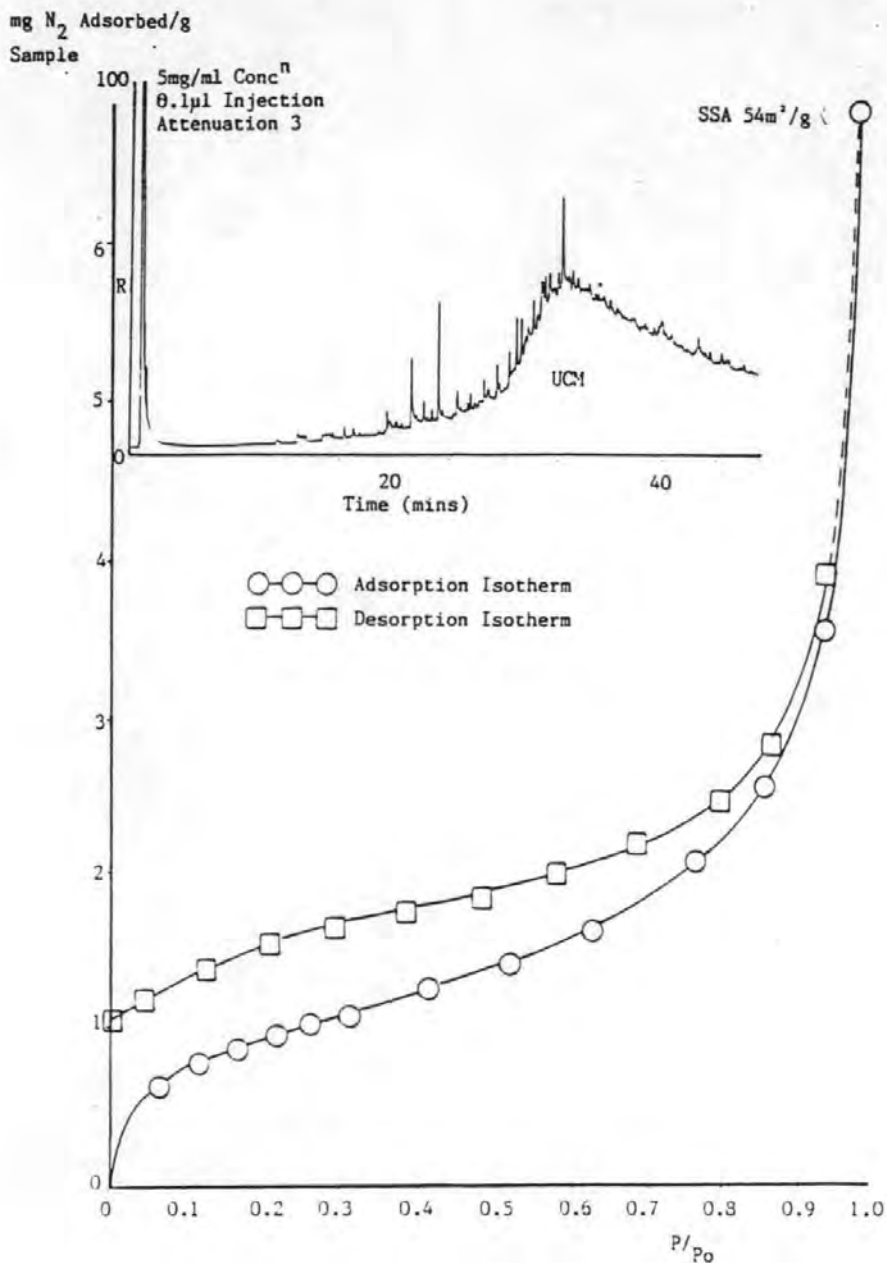


Fig. 3. Adsorption/Desorption Isotherm of a Diesel Particulate Sample Analysed On-Filter.

The Sample has been Thermally Degassed to 290°C and the Released Volatiles Analysed by Gas Chromatography is Shown.

Sample: 1500r/min Engine Speed  
13.7Nm Engine Load  
Sampled 3.3m from Engine  
SSA 54m<sup>2</sup>/g

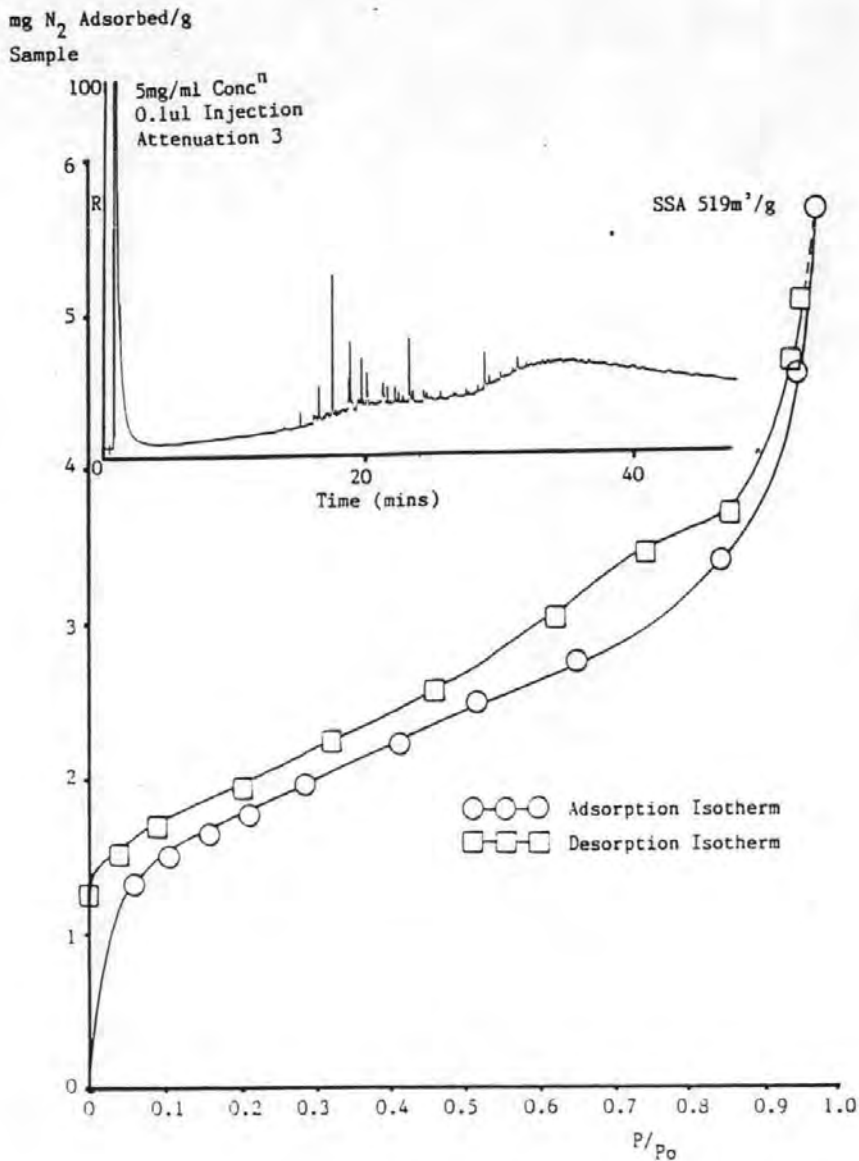


Fig. 4. Adsorption/Desorption Isotherm of a Diesel Particulate Sample Analysed On-Filter.

The Sample has been Thermally Degassed to 340°C and the Released Volatiles Analysed by Gas Chromatography is Shown.

Sample: 1500r/min Engine Speed  
13.7Nm Engine Load  
Sampled 3.3m from Engine  
SSA 519m<sup>2</sup>/g

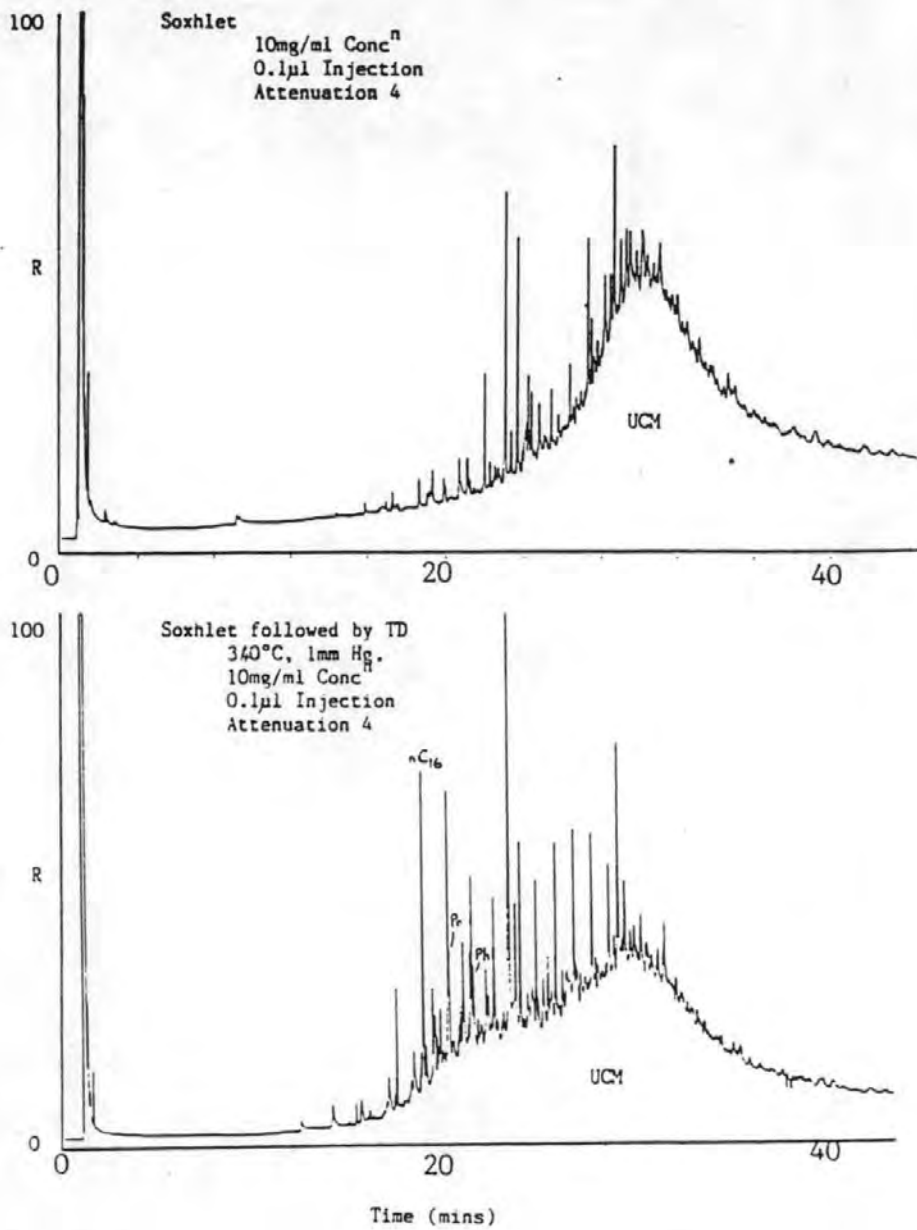


Fig. 5. Gas Chromatographs of FES Extracted by Soxhlet Extraction followed by Thermal Degassing at the Typical Operating Conditions. The TD Sample Shows the Additional Release of Hydrocarbons not Extracted by the Other Method.